Tetraspanins as Biomarkers and Causative Proteins in Prostate Cancer

Ben Troy Copeland
B.Biotech (Hons)

A thesis submitted in fulfilment of the requirements for the degree of Doctor of Philosophy

School of Biomedical Sciences and Pharmacy
University of Newcastle

July 2013

Declaration

This work contains no material which has been accepted for the award of any other degree or diploma in any university or other tertiary institution and, to the best of my knowledge and belief, contains no material previously published or written by another person, except where due reference has been made in the text. I give consent to this copy of my thesis, when deposited in the University Library, being made available for loan and photocopying subject to the provisions of the Copyright Act 1968.

Signature: …… Date: ……

ACKNOWLEDGMENTS

Like all PhD candidates I have too many people to thank than I can express here. But of course there are few people who deserve special mention. When I initially had a motorbike accident it was my recently passed Grandmother, Marjorie Copeland who took me in and suggested I attend University to find another career path. I remember openly laughing at the thought of going to University instead of working on a job site, but I did it, one step at a time as she suggested. I thank her for that initial catalyst that has led me on this wonderful and exciting new journey in my life.

My Mother (Marie) and Father (John) gave me a great free spirited, wonderful upbringing that gave me the resilience and strength of character to achieve this PhD. They still guide and support me to this day more than either of them realise and for that I thank them.

A huge thank you to all my supervisors Judith Weidenhofer, Severine Roselli and (unofficially) Nikki Verrills for all their support and help, in particular Professor Leonie Ashman. Leonie was consistently available to me and her ability to call a spade a spade to get me back on track when needed was exactly the supervision I required. Her willingness to help others (with no personal benefit), her enthusiasm and encouragement for collaborations and translational research was inspiring. When I see much of the scientific community being proactively insular, it was very refreshing and I will endeavour to promote these ideas in my subsequent career. Now this thesis is done, I sincerely wish her the all best in her well-deserved retirement (that started over a year ago!!).

In and around the labs, special mention has to go to Matthew Bowman for all the hard work he put in to help me trudge through the seemingly never ending pile of work that had to be done in the lab. Especially when we were holding over 200 animals at some stages that all needed constant monitoring!! All the staff and

students on level 3 LSB were always willing to help me out. Cheers to Dani and Jude for proof reading final copies of this thesis, when all the words started blurring into one to me. Thanks to the research support unit staff who were never too busy to help out even when they were swamped. Karen Chiam at the Garvan was a huge help with the patient data under trying circumstances. Thanks also to Ricardo Vilian at H.A.P.S who was always very helpful and extremely patient explaining anatomical pathology to a researcher.

Finally this work would not have been carried out without financial support from the University of Newcastle, the Prostate Cancer Foundation of Australia and the Mary Minto Sawyer scholarship.

TABLE OF CONTENTS

List of Figures

List of Tables

Abstract

Prostate cancer (PCa) is the most commonly diagnosed solid cancer and the cause of the second highest mortality rates in men in the majority of western counties. There are two major unmet needs in dealing with prostate cancer. Firstly, since the majority of deaths from prostate cancer are attributed to the largely untreatable late stage metastatic forms of the disease, understanding molecules involved in the metastatic cascade of PCa may prove beneficial in regards to therapeutic options. Secondly, PCa is a very heterogeneous disease and in many cases follows an indolent course. There are currently no reliable biomarkers to gauge which patients will progress on to advanced disease. Hence, biomarkers that can be implemented into the diagnostic process to stratify patients diagnosed with PCa in regards to their likely outcome allowing the assignment of the most effective and less invasive treatment options are urgently needed.

Tetraspanins are membrane bound proteins that associate with motility related molecules such as integrins. *In vivo* and *in vitro* experimental studies have indicated tetraspanins may be important regulators of tumour invasion and metastasis in a number of cancers. Furthermore clinical studies have shown that high expression levels of the tetraspanins CD82 and CD9 have been correlated to good prognosis, while in contrast increased expression of the tetraspanins CD151 and Tspan8 have been correlated with more aggressive cancers and poor outcomes. In this study, for the first time the effects of gene ablation of the pro- and anti-tumourigenic/metastatic tetraspanins, *Cd151* and *Cd9* respectively, have been evaluated in a *de novo* developing and spontaneously metastasising murine model of prostate cancer. In addition analysis of clinical tissue microarrays containing a cohort of various prostate tissue samples have been assessed by immunohistochemistry for CD151, Tspan8, CD82 and CD9 expression levels.

The *Cd9* and *Cd151* knock-out mouse models were independently crossed onto the TRansgenic Adenocarcinoma of Mouse Prostate (TRAMP) mouse model. We report here for the first time that development of primary prostate tumours was not affected by ablation of either *Cd9* or *Cd151*. However ablation of *Cd9* resulted in an increase of metastatic lesions (number of foci and total area) to the liver. Conversely ablation of *Cd151* resulted in a decrease of metastatic lesion (number of foci and total area) to the lungs. No change in average area of individual metastases was observed in either case.

Normal and matched PCa tissue samples on tissue micro-arrays obtained from the Australian Prostate Cancer Consortium (APCC) were analysed by IHC. The expression of CD151 and Tspan8 was shown to be positively correlated to PCa progression. In contrast, CD9 and CD82 expression was shown to be negatively correlated to cancer progression. Our results showed weaker correlation with prognosis than previous reports and possible reasons are discussed. In adjunct to the classical pathological IHC manual scoring method, automated digital pathology (Aperio) systems were evaluated in an attempt to standardise IHC scoring. The automated scoring showed similar trends with manual scoring, in regards to tetraspanin expression and cancer progression, however resulted in less significant associations.

In summary, the tetraspanins *Cd9* had anti-metastatic effects while conversely *Cd151* had pro-metastatic effects. Both *Cd9* and *Cd151* had no effect on the development of primary prostate tumours in the TRAMP model. These molecules may be beneficial therapeutic options as metastatic modulators. More extensive evaluation the tetraspanins CD151, Tspan8, CD9 and CD82 as prognostic markers that can delineate PCa patients whose disease may remain indolent and those who will progress is needed.

Papers published

Copeland B.T, Bowman M.J and Ashman L.K. (2013a). "Genetic Ablation of the Tetraspanin *Cd151* Reduces Spontaneous Metastatic Spread of Prostate Cancer in the TRAMP Model." Molecular Cancer Research. 11(1), 95-105.

Copeland B.T, Bowman M.J, Boucheix C and Ashman L.K. (2013b) Knockout of the tetraspanin *Cd9* in the TRAMP model of *de novo* prostate cancer increases spontaneous metastases in an organ specific manner. International Journal of Cancer. DOI: 10.1002/ijc.28204.

Conference Presentations

Oral presentations

Ben T Copeland, Matthew J Bowman, Claude Boucheix and Leonie K Ashman. *The Genetic Ablation of Tetraspanins Cd9 and Cd151 and its effects on Prostate Cancer Progression in the TRAMP Model*. Early Career Researchers Day Symposium, November 2012. Newcastle, Australia.

Ben T Copeland, Matthew J Bowman, Claude Boucheix and Leonie K Ashman. *The Effects of the Genetic Ablation of Tetraspanins Cd9 and Cd151 on Prostate Cancer Development and Progression in the TRAMP Model.* Hunter Medical Research Institute Cancer Research Symposium, November 2012. Newcastle, Australia.

Ben T Copeland, Matthew J Bowman and Leonie K Ashman. *Tetraspanins Influence on Initiation and Progress of Prostate Cancer*. Hunter Medical Research Institute Cancer Research Symposium, November 2011. Newcastle, Australia. ***Awarded best talk from selected abstracts.***

Ben T Copeland Matthew J Bowman and Leonie K Ashman. *Tetraspanins CD151 and CD9 and their effect on Prostate Cancer and Initiation and Progression.* School of Biomedical Sciences and Pharmacy Seminar, September 2011. University of Newcastle, Newcastle, Australia.

Ben T Copeland Matthew J Bowman, Claude Boucheix and Leonie K Ashman. *Tetraspanins CD151 and CD9: Metastatic Regulators in Prostate Cancer.* FASEB Summer Research Conference, Membrane Organization by Molecular Scaffolds, July 2011. Vermont, United States. ***Awarded travel grant from abstract***.

Ben T Copeland, Matthew J Bowman and Leonie K Ashman.
CD151 and CD9: Opposing Roles in Prostate Cancer? Hunter Medical Research Institute Cancer Research Symposium, November 2010. Newcastle, Australia.

Ben T Copeland, Ricardo Vilain, Leonie Ashman.
Tetraspanins as Biomarkers and Causative Proteins in Prostate Cancer. Hunter Medical Research Institute Cancer Research Symposium, November 2009. Newcastle, Australia.

Poster presentations

Ben T Copeland and Leonie K Ashman.
Tetraspanins as Potential Biomarkers in Prostate Cancer. The 13th Australian Prostate Cancer Conference, August 2013. Melbourne, Australia. (Abstract accepted).

Ben T Copeland, Matthew J Bowman, Claude Boucheix and Leonie K Ashman.
The Effects of the Genetic Ablation of Tetraspanins Cd9 and Cd151 on de novo Forming and Spontaneously Metastasising Prostate Cancer in the TRAMP Model. The 5th European Conference on Tetraspanins, September 2012. Nijmegen, The Netherlands.

Ben T Copeland, Matthew J Bowman, Claude Boucheix and Leonie K Ashman.
Tetraspanins as Regulators of Metastasis in Prostate Cancer. 14th International Biennial Congress of the Metastasis Research Society, September 2012. Brisbane, Australia. ***Awarded travel grant from abstract***.

Ben T Copeland, Matthew J Bowman, Claude Boucheix and Leonie K Ashman. *The Effect of Tetraspanins on Prostate Cancer Progression*. The Australian Medical Research Society Research Week, June 2012. Sydney, Australia.

Ben T Copeland, Matthew J Bowman, Claude Boucheix and Leonie K Ashman. *Tetraspanins and their Effects on Prostate Cancer Initiation and Progression*. 24th Lorne Cancer Conference, February 2012, Lorne, Victoria, Australia. ***Awarded travel grant from abstract***.

Ben T Copeland, Matthew J Bowman, Claude Boucheix and Leonie K Ashman. *Tetraspanins Influence Prostate Cancer Metastases but not Primary Tumour Growth*. Hunter Medical Research Institute Cancer Research Symposium, November 2011. Newcastle, Australia.

Ben T Copeland, Matthew J Bowman, Claude Boucheix and Leonie K Ashman. *Tetraspanins role in Prostate Cancer Progression.* Early Career Researchers Group Poster Competition, The University of Newcastle, October 2011. Newcastle, Australia. ***Awarded silver prize***.

Ben T Copeland Matthew J Bowman, Claude Boucheix and Leonie K Ashman. *Tetraspanins CD151 and CD9 and their Effects on Prostate Cancer Initiation and Progression.* FASEB Summer Research Conference, Membrane Organization by Molecular Scaffolds, July 2011. Vermont, United States. ***Awarded travel grant from abstract***.

Ben T Copeland, Matthew J Bowman, Judith Weidenhofer, Claude Boucheix and Leonie K Ashman.
Tetraspanins CD151 and CD9 and their effects on Prostate Cancer Initiation and Progression. 12th Annual Prostate Cancer Conference, July 2011. Melbourne, Australia.

Ben T Copeland, Mark Formby, Ricardo Vilain and Leonie K Ashman.
Evaluation of Tetraspanin Expression in Prostate Cancer Tissue Microarrays.
Hunter Medical Research Institute Cancer Research Symposium, November 2010.
Newcastle, Australia.

Ben T Copeland, Ricardo Vilain, Leonie Ashman
Tetraspanins as Biomarkers and Causative Proteins in Prostate Cancer. The 10th
Hunter Cellular Biology Meeting, March 2010. Pokolbin, Australia.

Ben T Copeland, Ricardo Vilain, Leonie Ashman.
Tetraspanins as Biomarkers in Prostate Cancer. 10 of the Best Research
Showcase, The University of Newcastle, September 2009. Newcastle, Australia.

Ben T Copeland, Ricardo Vilain, Leonie Ashman.
Tetraspanins as Prognostic Indicators in Prostate Cancer. The Beatson
International Cancer Conference, July 2009. Glasgow, Scotland. ***Awarded travel grant from abstract***.

Ben T Copeland, Ricardo Vilain, Leonie Ashman.
Tetraspanins as Prognostic Biomarkers in Prostate Cancer. The Australian Medical
Research Society Research Week, June 2009. Sydney, Australia.

Media releases

From the Copeland et al. (2013b) paper published in the International Journal of Cancer, figure 4 was chosen to grace the cover.

Scientific photo with accompanying plaque outlining project details. The *HMRI through the lens* competition. Displayed at Wallsend District Library; May-July 2010, John Hunter Hospital; July-September 2010, Waiting hall of the chief scientific advisor office, Canberra; ongoing. University of Newcastle, ongoing; Hunter Medical Research Institute, ongoing. Electronically displayed on the ABC website http://www.abc.net.au/local/photos/2010/05/28/2912341.htm.

Newspaper article in the *Newcastle Herald* outlining the research project and importance to the community. November 2008. Fairfax Media Limited, Sydney, Australia.

Abbreviations

1°	Primary
2°	Secondary
A.B.R	Australian Bio Resource
A.P.C.C	Australian Prostate Cancer Collaboration
AP	Anterior prostate
AR	Androgen receptor
ARBS	Androgen receptor binding site
B6	C57BL/6
bp	Base pair
BPH	Benign prostatic hyperplasia
CCG	Cysteine-cysteine-glycine
CO_2	Carbon dioxide
DAB	Diaminobenzidine
ddH2O	Double distilled water/Milli Q water
DNA	Deoxyribonucleic acid
DP	Dorsal prostate
DRE	Digital rectal examination
EC1	Extracellular loop 1
EC2	Extracellular loop 2
ECM	Extracellular matrix
FFPE	Formalin fixed paraffin embedded
FVB	FVB/n
GEMMs	Genetically engineered mouse models
H&E	hematoxylin and eosin
het	Heterozygous
HIER	Heat induced antigen epitope retrieval
HRP	Horse radish peroxidase
HRPC	Hormone refractory prostate cancer
IF	Immunofluorescence
IgG	Immunoglobulin G
IHC	Immunohistochemistry
KO	Knockout
LEL	Large extracellular loop
LP	Lateral prostate
mAb	Monoclonal antibody
mCRPC	Metastatic castrate resistant prostate cancer
MD	Moderately differentiated
MMPs	Matrix metalloproteinases
n	Number

O/N	Overnight
OCT	Optimal cutting temperature
PAP	Prostatic acid phosphatase
PBS	Phosphate buffered saline
PCa	Prostate cancer
PCR	Polymerase chain reaction
PD	Poorly differentiated
PIN	Prostatic intraepithelial neoplasia
PSA	Prostate specific antigen
Rab	Rabbit
ROI	Regions of interest
rPB	Minimal rat probasin promoter
SD	Standard deviation
SEL	Small extracellular loop
SEM	Standard error of the mean
SV	Seminal vesicle
SV40	Simian virus 40
T/N/M	Tumour/node/metastases
Tag	Early tumour antigen
TEM	Tetraspanin enriched micro-domain
TMA	Tissue microarray
TRAMP	Transgenic adenocarcinoma of the mouse prostate
TURP	Transurethral resection of the prostate
UoN	University of Newcastle
UT	Urogenital tract
v/v	Volume/volume
VP	Ventral prostate
w	Watts
w/v	Weight/volume
WD	Well differentiated
wt	Wild type

Chapter 1

Introduction

1.1 *The prostate*

1.1.1 Gross anatomy of the human prostate

The prostate is an organ common throughout male mammals (Figure 1). In humans the prostate begins to enlarge upon puberty under the stimulus of testosterone. In adult males, the healthy prostate is typically the size of a walnut and located directly below the bladder, between the pubic bone and lower rectum. The prostate consists of three distinct anatomical zones, the transitional, central and peripheral zones. The urethra passes through the apex of the prostate, in the transitional zone and passes out the anterior side of the peripheral zone connecting with the penis. The seminal vesicles also pass through the sides of the prostate, through the central zone, and eventually connect to either side of the urethra (McNeal 1997, reviewed by Stephens 2000).

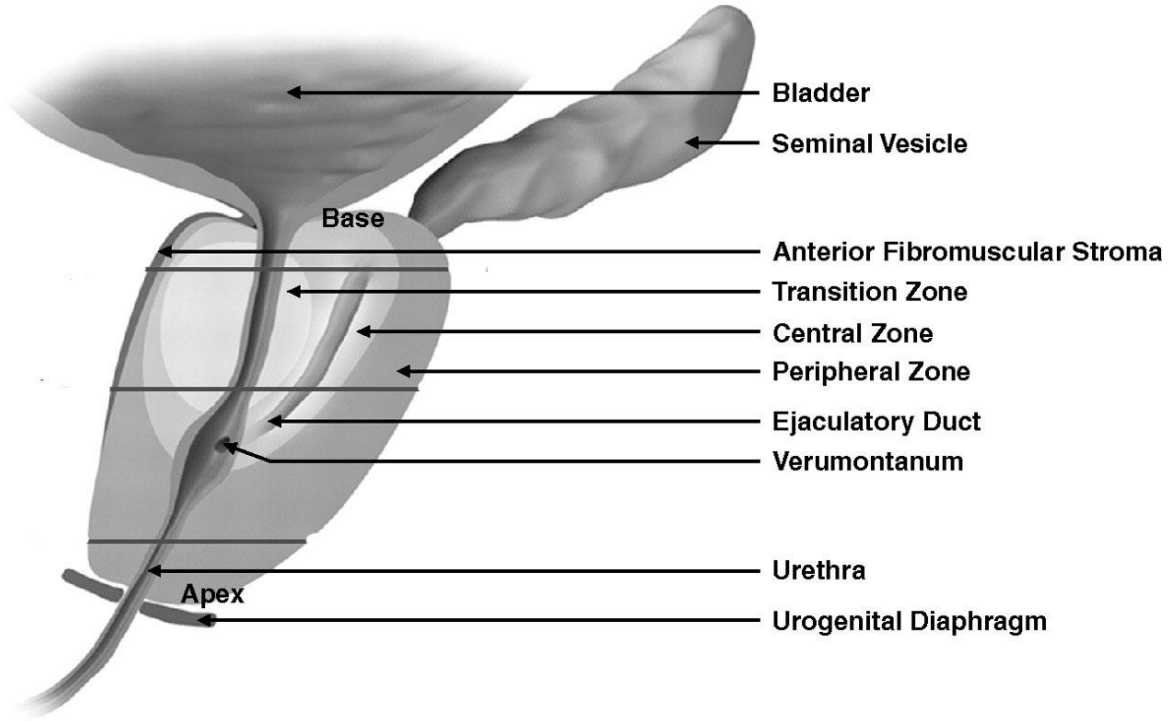

Figure 1: Schematic of the normal human prostate.
A representation of the normal human urogenital tract, highlighting main features. Reproduced with permission (Kundra, Silverman et al. 2007).

1.1.2 Cellular anatomy of the prostate gland

The two main cell types of the prostate are epithelial and mesenchymal cells which originate from the Wolffian ducts and urogenital sinus (reviewed by McNeal 1997). The epithelial cells make up the basal and luminal layer of the secretory glands within the prostate. The luminal cells express high levels of androgen receptors (AR), prostate specific antigen (PSA) and prostatic acid phosphatase (PAP) and are androgen dependent for survival (Collins and Maitland 2006), while the basal cells express low to undetectable levels of AR and are androgen independent (Kyprianou and Isaacs 1988). It should be noted that the basal cells of the prostate glands are not strictly myoepithelial cells as is common in other glandular organs as it has been shown that they contain no muscle filaments, however they still do mature into the secretory luminal cells (reviewed by McNeal 1997). The second main type of cells in the prostate, the mesenchymal cells along with muscular filament cells make up the stroma which surround the glands (Collins and Maitland 2006). Lastly, prostatic stem cells and neuroendocrine cells are intermittently spread throughout the prostate, but to a much lesser extent. The stem cells seem randomly scattered through the prostate (Collins and Maitland 2006), while the neuroendocrine cells are positioned between the basal and secretory luminal cells of healthy tissue, however do not extend into the lumen (reviewed by McNeal 1997). The only known biological function of the prostate is to excrete prostatic fluids into semen during ejaculation. The prostatic fluids liquefy semen to help cell motility and also help mature the sperm cells, increasing fertility, discussed in more detail in section 1.4.2.1.

1.2 *Benign prostate ailments*

There are three main non-cancerous problems that can develop in the prostate, prostatitis, prostatodynia and benign prostate hyperplasia (BPH); all three are treatable and considered non-life threatening (reviewed by Stephens 2000). Some symptoms are common through the benign diseases and unfortunately can also be

symptoms of prostate cancer adding complexity to diagnosis of urogenital complaints. These include any combination of the following; pain in the pelvic region, difficulty in urinating, pain with urinating, blood in the urine, urgency to urinate, pain with ejaculation, loss of libido and impotence (reviewed by McNeal 1988).Prostatitis is an inflammation of the prostate while prostatodynia is a chronic disease of the prostate that has no associated signs of inflammation or infection; treatment of both involves antibiotics and/or steroid treatments (reviewed by Stephens 2000, Ramakrishnan and Salinas 2010).

BPH is a non-cancerous enlargement of the prostate. Due to the enlargement of the prostate surrounding the urethra, difficulty and pain are often associated with urination and/or ejaculation. If the enlargement is severe, a transurethral resection of the prostate (TURP) is preformed to remove excess prostate tissue and unblock the urethra. Newer therapies are becoming common for BPH such as the anti-androgenic 5-alpha-reductase inhibitors, which are very effective in inhibiting disease progression and reducing the need for surgery (reviewed by Barkin 2008). BPH is exclusively found in the transitional zone while the peripheral zone is the major site of adenocarcinoma (cancer of the epithelial cells). Due to the physical separation of the zones and the fact that recent reports have found no direct evidence to date, it is generally thought that BPH is not a precursor for prostate adenocarcinoma (Alcaraz, Hammerer et al. 2009, De Nunzio, Kramer et al. 2011).

1.3 *Prostate cancer (PCa)*

1.3.1 PCa epidemiology

The latest published report from the American Cancer Society predicted that in 2012 241,740 new cases of PCa will be diagnosed and 28,179 deaths will occur from PCa in the United States (Siegel, Naishadham et al. 2012). To put these numbers in context, PCa is the most commonly diagnosed cancer, behind lung (1

in 6 men) and one of the leading causes of cancer related deaths (1 in 36 men) in males in the United States.

In the New South Wales Cancer Council's most recent report, the incidence of PCa diagnosis and deaths follow a very similar pattern to the United States with PCa being the most frequently diagnosed cancer in all cancer patients and the second highest cause of mortality in males (Tracey, Baker et al. 2007, AIHW 2010). The diagnosis of PCa has steadily risen over the last decade, while the mortality rate has only reduced slightly, which is discussed in section 1.4.2.2.

1.3.2 PCa progression

Cancer of the prostate follows a well characterised pattern of progression (reviewed by Bono 2004, Damber and Aus 2008). Prostatic intraepithelial neoplasia (PIN) is widely accepted as the precursor to PCa; briefly it is defined as encroachment of the epithelial cells of the prostate glands into the luminal interior. Prostate adenocarcinoma *in situ* is the first stage where clearly defined cancer cells are located within the gland and includes loss of basal cells surrounding the lumen, with associated pleomorphic nuclear and general atypia. Locally invasive adenocarcinoma is defined by the spreading of the cancer cells out of the prostate capsule into adjacent tissues with an obvious increase in the nuclear to cytoplasmic ratio of the cancerous cells. The most severe stage (disregarding receptor status, detailed in 1.5.3) is metastatic cancer, where the adenocarcinoma has disseminated from the primary tumour through the surrounding extracellular matrix (ECM), undergoes intravasation to either the blood or lymph circulatory system, with subsequent extravasation to distant sites to form secondary tumours. Bone metastases are the most common secondary site of PCa, which also represents the major cause of pain and mortality, while liver and lung are also frequent secondary sites (Gittes 1991, reviewed by Jin, Dayyani et al. 2011, Suva, Washam et al. 2011).

1.4 *Current diagnostic and prognostic measures for PCa*

The current diagnostic and prognostic measures used with prostate cancer are arguably the most controversial of all cancers and therefore could fill an entire literature review. This section of the review will briefly summarise the main current diagnostic modalities and highlight controversial areas and other published extensive reviews on the subject.

In Australia there are currently no population based screening programs, however the Prostate Cancer Foundation of Australia (PCFA) recommends yearly prostate specific antigen (PSA) testing along with a digital rectal (DRE) examination of men over 50 years of age and 40 years of age if a family history of PCa exist (Giles 2006).

1.4.1 Digital Rectal Examination (DRE)

DRE's are used as a diagnostic measure for prostate cancer in males over 50 and younger men with symptoms of PCa and/or with familiar history of PCa (reviewed by Stephens 2000, Jones and Koeneman 2008). The healthy prostate should feel smooth and rubbery, while a lump or uneven texture would warrant further investigation, however the diagnosis is far from definitive. Firstly, only a limited amount of the prostate can be felt due to physical barriers, which may result in underdiagnoses. Secondly, non-malignant inflammations or BPH may explain abnormalities in the prostate possibly leading to over diagnoses (reviewed by McNeal 1988). Interestingly the DRE was dropped as a screening measure from a large scale European Randomized Study of Screening for Prostate Cancer (ERSPC) (Schröder 2008). This was due to the previous findings that it had low diagnostic and prognostic performance in patients with low levels of prostate specific antigen (<3.9 ng/ml) (Schroder, van der Maas et al. 1998).

1.4.2 Prostate Specific Antigen (PSA)

1.4.2.1 Biology of PSA

Prostate specific antigen (PSA), a 34 KD serine protease, is a member of the kallikrein like peptidases and is also known in the literature as kallikrein 3 or KLK3. PSA is androgen regulated, expressed exclusively within the epithelial cells of the prostate and released into the seminal vesicles. Here it is thought to fulfil its biological role of liquefying, coagulated post-ejaculated seminal fluid, by chymotrypsin like breakdown of proteins, rendering sperm actively fertile (reviewed by Linton and Hamdy 2003, Lilja, Ulmert et al. 2008, Jin, Dayyani et al. 2011).

1.4.2.2 PSA as a biomarker in PCa

Stamey *et al*. (1987) first correlated PSA blood levels to PCa clinical stage and tumour volume. The hypothesis behind the correlation of increased serum PSA levels with PCa development results from both an increase in PSA production by the epithelial cells coupled with the prostate glands being unable to contain PSA that is usually secreted into the lumen, as a result of loss of prostate gland architecture (reviewed by Lilja, Ulmert et al. 2008, O'Rourke 2011). Serum PSA levels were originally used as a marker for PCa recurrence after treatment. However during the late 1980's and early 1990's its use was rapidly established as a PCa screening tool. Since then PSA has arguably become one of the most important clinically relevant and at the same time one of the most contentious cancer biomarkers.

The increased incidence and early detection of PCa seen in the early 1990's has been attributed at least in part to the advent of PSA testing. However mortality rates from PCa have only modestly decreased over the same time frame, as seen in Figure 1-2. As a result the U.S. preventive services task group released a report stating that they did not recommend regular PSA screening of males in any age

group, due to the lack of a net benefit (Harris and Lohr 2002). Lin *et al.* (2008) from the same task force, updated the report in 2007 and again did not recommend population based routine PSA screening. To date The National Health and Medical Research Council (NHMRC 2002) has similar guidelines in Australia.

Recently two large ongoing randomised trials, the ERSPC and the Prostate, Lung, Colorectal and Ovary (PLCO) trial have published, long awaited, interim results looking specifically at PSA screening and effects on mortality. The ERSPC trial involved over 180, 000 men. The interim report concluded that PSA screening only modestly reduced the mortality rates in a specific subset of men (ages 55-69) and that to prevent a single death, 1410 men would need to be screened and 48 men would need to be treated (Schroder, Hugosson et al. 2009). More recently at the ERSPC 11 year follow up point it was reported that the PSA screened cohort did see a 21% reduction in mortality but this was at the cost of significant over diagnosis. Resulting in morbidity due to over-treatment and stress associated with diagnosis of an indolent disease (Schröder, Hugosson et al. 2012). At 10 and also 13 years follow up, the PLCO trial which involved over 78,000 men in the US, concluded that no significant difference was seen in mortality as a result of screening men for PSA serum levels (Andriole, Crawford et al. 2009, Andriole, Crawford et al. 2012).

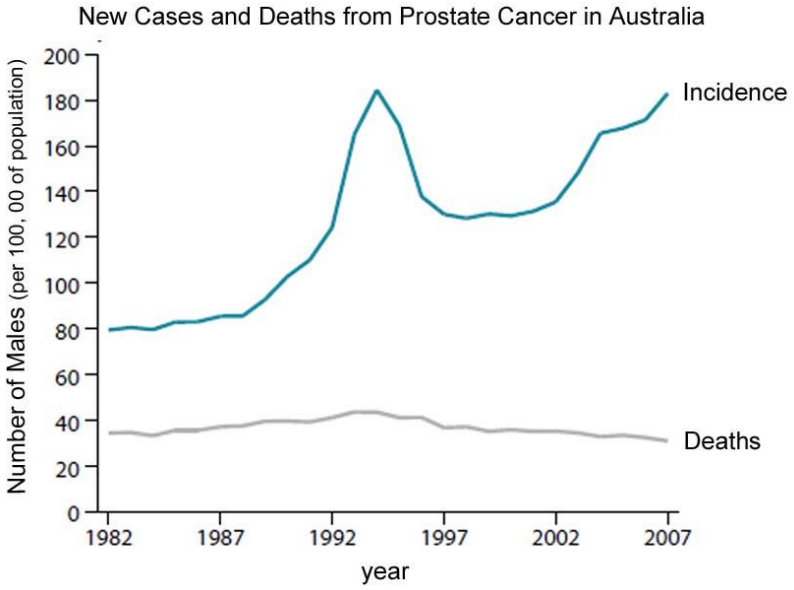

Figure 1-2: Prevalence of incidence and deaths from PCa.
Graphical representation showing the trends in age standardised new cases and deaths, per 100, 000 males, from PCa in Australia from 1982 to 2007. The lack of correlation between the rise in incidence and modest decrease in deaths is clearly shown. Figure modified from the Australian National Cancer Statistics Clearing House (AIHW 2010).

Sensitivity and specificity of PSA tests are extremely controversial issues that have created a dichotomy in views in the field. This is exemplified by a simple search on the PubMed.gov ejournal database site (on 24/4/2013) for “PSA prostate cancer screening” which resulted in 11, 309 matches of published papers.

Normal serum PSA levels in a healthy male are approximately 0.6 ng/ml and the raised PSA cut-off amount is still very contentious, however the generally accepted PSA threshold limit is 4 ng/ml, to warrant further investigation of the patient’s prostate. The controversial issues of sensitivity and specificity arise because normal serum PSA levels can also be raised by non-cancerous issues such as increased age, race, BPH, prostate manipulation (DRE), biopsy and even recent ejaculation (reviewed by Stricker 2001). These issues have been extensively reviewed elsewhere (Lilja, Ulmert et al. 2008, O'Rourke 2011). The concern is that too low a threshold limit will result in over diagnosis in males, while too high a threshold limit could increase the risk of missing early stage PCa. PSA testing

especially in the so called 4-10 ng/ml “grey area” range lacks specificity to discriminate between PCa that will remain indolent and PCa that will progress to malignancy (Magklara, Scorilas et al. 1999). This leads to the very important issue of over diagnosis, where the patient may be put through painful, invasive and physiologically stressful biopsy and treatment procedures, with possible side-effects, for cancers that would not have caused a problem in the patients’ natural life (reviewed by Stricker 2001, Gillatt, Klotz et al. 2007, Lilja, Ulmert et al. 2008, Lin, Lipsitz et al. 2008). Furthermore given that reports have stated a nearly 100% five year survival rate for men that are diagnosed with PCa still confined within the gland compared to only 31% five year survival for men with metastatic PCa at diagnosis (N.H.S 2009), if the PSA threshold limits were raised some of the earlier stage cancers would presumably be missed and lead to men presenting with later stage cancer with associated reduced survival.

These issues highlight the need to find biomarkers that are not only robust but definitive in stratifying which patients warrant further investigation but also markers that have prognostic values to stratify the treatment modalities that can be invasive and carry unwanted side effects (further explained in 1.7).

1.4.3 Needle biopsy

If a patient does present with elevated PSA levels, obtaining a tissue sample via biopsy is recommended. Controversies in obtaining a needle biopsy revolve around the number of needle biopsies that should be taken from the prostate to make sure the biopsy recapitulates the *in-vivo* environment (reviewed by de la Taille, Jones et al. 2008). Once the biopsy is taken it is viewed and graded via histopathology by a pathologist, detailed below.

1.4.4 Gleason score

Since the early 1900's there have been over forty histological grading systems introduced to stratify the various stages of prostate cancer (reviewed by Humphrey 2003). During the late 1960's and early 1970's, Donald. F Gleason and members of the Veterans Administration Cooperative Urological Research Group developed the Gleason histological grading system (Gleason and Mellinger 1974). To this date it is still the most common prostate grading system worldwide (Humphrey 2004). The Gleason grading system has been shown to be an independent indicator of PCa prognosis, while also being used in decisions for treatment modalities (Humphrey 2004, Gelmann 2008).

The Gleason grading system is based solely on the architecture of the biopsy sample, viewed by a pathologist, under a light microscope after hematoxylin and eosin (H&E) staining (Gleason and Mellinger 1974). The system consists of five grades of increasing severity, from normal glandular characteristics, to invasive adenocarcinoma (Figure 1-3). The two most prominent histological patterns are included to give a Gleason score, allowing varying histological patterns to be included in the system (reviewed by Humphrey 2004). However many PCa display more than two histological patterns; for example Ruijter *et al*. (1996) reported up to 4 different histological patterns in 3% of cases.

The Gleason grading system was subjected to a review in 2005 by the International Society of Urological Pathology (Epstein, Allsbrook et al. 2005). Some changes were implemented, such as the addition of cribriform structures and ill-defined luminal glands into stage 4 (up from stage 3) and the capability of allowing tertiary patterns into the system (Billis, Guimaraes et al. 2008). A review on the updates to the Gleason grading system has shown that several post-update reports had confirmed the positive impact of the changes to the Gleason classification system to patient care (Epstein 2010). A recent publication on the

past, present and future of the Gleason system reviews the subject concisely (Delahunt, Miller et al. 2012).

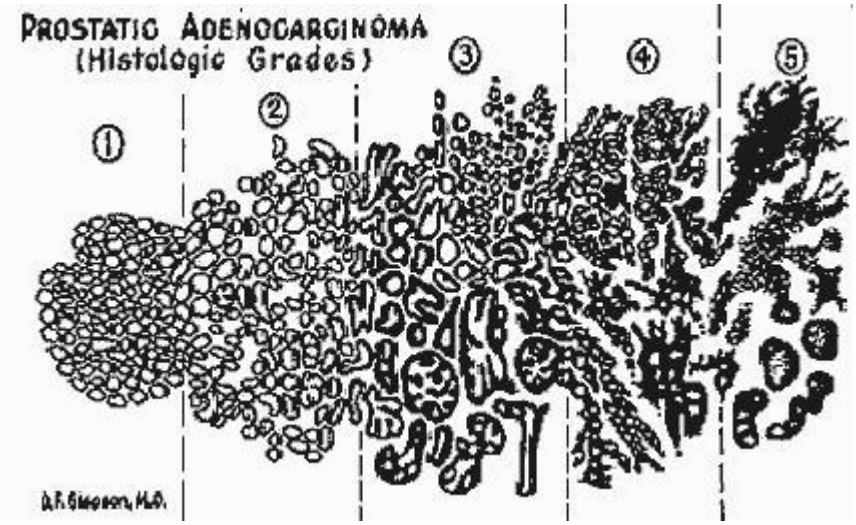

Figure 1-3 Gleason histological scoring system.
Gleason's original drawing describing the five histological grades of PCa (Gleason and Mellinger 1974). Reproduced with permission (Delahunt, Miller et al. 2012).

1.4.5 Clinical staging (TNM)

The tumour/node/metastases (TNM) staging system can also provide valuable information to the clinician either as an adjuvant to the Gleason score or independently. Factors that are involved are the extent of the primary tumour (T), absence or presence of metastasis to nearby lymph nodes (N) and the existence of distal metastases (M). There are four stages of the primary tumour (T) classifications, while the lymph node involvement and distant metastases are simply present or absent and abbreviated as 0 or X respectively (reviewed by Stricker 2001). The TNM system is widely used in conjunction with the Gleason system for clearer diagnosis and greater prognostic value.

1.5 *Treatment of PCa*

As with the diagnostic and prognostic measures for PCa (1.4), treatment modalities for PCa are very controversial. Specifically the controversy surrounds which and

when to use primary treatments with the added complexities of if and when to use adjuvant therapies. Many factors play in the choice of treatment modalities; these include the already mentioned parameters of PSA levels, Gleason score and clinical stage. However the age of the patient, family history, patient's sentiment about complications and related side effects and finally the presence of clear surgical margins for surgical removal (if viable) are also usually factored in to personalise the treatment for each patient There are many extensive published reviews on these controversies, therefore this section will briefly highlight some of the treatment modalities and associated controversies (reviewed by Bono 2004, Gillatt, Klotz et al. 2007). Furthermore, a review describing recent and on-going clinical trials targeting prostate biomarkers and explaining the relevant therapeutic mechanisms has recently been published (Detchokul and Frauman 2011).

1.5.1 Localised PCa

PCa which is localised within the prostatic gland, is the most commonly diagnosed stage of PCa (reviewed by Bono 2004, Damber and Aus 2008). The primary treatment options are surgery (radical prostatectomy) and/or radiotherapy (Brachytherapy or external Beam Therapy) all with curative intent (Gnanapragasam, Mason et al. 2012). The third option is active surveillance, sometimes referred to as watchful waiting where the patient receives no immediate treatment but continues to be intently monitored for any changes in the prostate by DRE and PSA testing (Damber and Aus 2008). The recently published American Prostate Cancer Intervention Versus Observation Trial (PIVOT) of 731 men reported that at the 10 year follow up mark there was no significant difference in overall survival between active surveillance and radical prostatectomy (Wilt 2012). Controversies surround the use of adjuvant and neoadjuvant hormonal treatments in localised PCa. Martinez-Pineiro (2008) reviewed 17 studies by meta-analysis and found no overall survival benefit in adjuvant or neoadjuvant hormonal therapies with radical prostatectomy in localised PCa. However they did see a 10 year survival increase with adjuvant hormonal treatment post primary radiotherapy.

Another group performed meta-analysis of results from more recently published randomised trials for the use of radical prostatectomy with or without adjuvant radiotherapy to treat patients with localised disease. They reported conflicting results in regards to which single or combination therapies result in the best outcomes for patients (Gnanapragasam, Mason et al. 2012). Highlighting this controversy was a report from the 2011 Genitourinary Cancer Conference, which stated that there is still a debate about the best treatment options for these patients, especially in the case of high risk localised PCa. (Bellmunt, Attard et al. 2012).

1.5.2 Locally advanced PCa

Locally advanced PCa is defined as cancer which has progressed beyond the prostatic gland, excluding lymph node involvement (reviewed by Van Poppel, Joniau et al. 2005). Primarily, treatment for locally advanced PCa is radiotherapy, which may include dosage escalation and/or neo-adjuvant or adjuvant hormonal therapy (Gillatt, Klotz et al. 2007, Hsu, Joniau et al. 2007). Controversies in locally advanced PCa that revolve around the time to administer hormonal therapies and radiotherapy and for how long are widely debated as the side effects are extensive and vary with patient and treatment modality with varying beneficial patient outcomes (Steigler, Denham et al. 2012). To reduce the effects of androgen ablation the non-steroidal anti-androgens, such as bicalutamide have been utilised with modest results (McLeod, Iversen et al. 2006). Adjuvant surgical resection may also be an option if there are reasonably clear surgical margins (reviewed by Hsu, Joniau et al. 2007, Soulie 2008).

1.5.3 Advanced PCa

Treatment options in advanced (metastatic) androgen receptor positive PCa are unfortunately, mostly palliative. Since the ground breaking work by Charles Huggins (1941) the predominant treatment modality has been hormone reduction

therapy either through surgery (orchidectomy) or more commonly these days by chemical castration techniques such as anti-androgens and gonadotropin releasing hormone analogues to control testicular and pituitary testosterone (reviewed by Beekman and Hussain 2008, Sartor 2011). The initial response to androgen ablation is a profound reduction in tumour volume and symptomatic relief in about 70-80% of patients (Huggins and Hodges 1941). However the effect is transient as over time most patients relapse with a more aggressive form of PCa, discussed below. A vast amount of research and many trials have looked at the effects of combined treatment modalities as adjuvant, delayed adjuvant and neo-adjuvant modalities, that has sparked a lot of controversy and debate about the benefits to patients (Dayyani, Gallick et al. 2011, Sartor 2011).

1.5.4 Androgen independent metastatic PCa

As explained above most PCa treated with hormone withdrawal will progress and develop into an aggressive form of the disease, known as either hormone refractory prostate cancer (HRPC) or the more recently coined term metastatic castrate resistant prostate cancer (mCRPC), which will be used in this review. This stage of the disease represents the most advanced stage of PCa and is responsible for the majority of deaths from PCa (Bono 2004, Damber and Aus 2008, Sartor 2011). Patients with mCRPC are considered incurable and even chemotherapeutic treatment was traditionally thought to be ineffective until two landmark trials showed an increase in survival, albeit modest, when docetaxel was utilised (Petrylak, Tangen et al. 2004, Tannock, de Wit et al. 2004). Docetaxel is still the first line anti-mitogenic chemotherapeutic agent for mCRPC, however patients will eventually develop resistance to Docetaxel. A recent report from has shown patient benefits with the use of the microtubule inhibitor Cabazitaxel as a second line chemotherapeutic, which along with other such drugs as Sipuleucel-T (personalised inmmuno-stimulant) and Abiraterone (which reduces circulating testosterone) have now been approved by the food and drug administration in the United States for treatment of patients with mCRPC (Agarwal, Sonpavde et al.

2011, Bahl, Bellmunt et al. 2012). Due to the dismal 18-20 month median life expectancy of patients with mCRPC, there has been vigorous research into treatments of mCRPC with some interesting and novel therapies emerging, such as inhibitors of angiogenesis, antisense molecules, small molecule inhibitors, monoclonal antibodies and vaccines (reviewed by Risbridger, Davis et al. 2010, Dayyani, Gallick et al. 2011, George and Moul 2012, Osanto and Van Poppel 2012, Sala-Valdés, Ailane et al. 2012).

1.6 *Cancer initiation: The stochastic and hierarchy theories*

The theory behind cancer initiation is that a progressive series of genetic changes gives rise to a cancerous cell phenotype. The genes that can be altered can be broadly classified as either tumour promoter, tumour suppressor or stability (site of mutations) genes (Vogelstein and Kinzler 2004).

Two hypotheses have been proposed for the cells involved in cancer initiation, the stochastic model and the hierarchy model (reviewed by Collins and Maitland 2006, Maitland and Collins 2008, Wang and Shen 2011). The stochastic model proposes that all cells have the ability to acquire the genetic changes to initiate tumours. The hierarchy model suggests that only small subsets of cells have the ability to progress to the cancerous phenotype, these cells are hypothesised to be stem cells. Since stem cells last the hosts' lifetime, the theory is that they are more susceptible to progressive mutations. It should be noted that to date PCa stem cells have not definitively been identified, so the more common and correct term for the cells found able to give rise to PCa, is tumour initiating cells. A review has been recently published that was specific to identifying the originating cell in PCa (Risbridger and Taylor 2011).

1.7 *Molecular biomarkers in PCa*

The genetic changes aforementioned have been the focus of a vast amount of research trying to correlate the detectable genetic or subsequent protein expression changes to cancer diagnostic and/or prognostic parameters.

In PCa many biomarkers have been studied for diagnostic and prognostic significance, amid varying success (reviewed by Bradford, Tomlins et al. 2006, Mazzola, Ghoneim et al. 2011). Among the plethora of published reports of emerging biomarkers for PCa, some of the more promising ones, which importantly have clinical relevance include PCa antigen 3 (PCA3) (Roobol, Schroder et al. 2010), the TMPRSS2:ERG gene fusion (Salagierski and Schalken 2012), prostate-specific membrane antigen (PMSA) (Murphy, Kenny et al. 1998), prostate stem cell antigen (PSCA) (Han, Seligson et al. 2004), human glandular 2 (hK2) (Darson, Pacelli et al. 1997), kallikrein 14 (Lose, Lawrence et al. 2012), α-methyl-CoA racemase (AMACR) (Jiang, Wu et al. 2004) along with the tetraspanins CD82 (Dong, Lamb et al. 1994) and in a small study that we hope to confirm and expand upon in this study, CD151 (Ang, Lijovic et al. 2004). Various genetic studies that cover vast amounts of data are currently being analysed for their potential to identify biomarkers in PCa (Taylor, Schultz et al. 2010, Kote-Jarai, Olama et al. 2011, Eeles, Olama et al. 2013). Despite this there are still no markers besides PSA which are currently used in clinical settings for PCa.

The need for more specific and sensitive biomarkers not only for diagnostic evaluation of men at risk of PCa, but also importantly prognostic markers that allow the stratification of men once diagnosed with PCa into treatment groups is currently still a major focus of the scientific community. Specifically, markers to identify which men will have indolent PCa and therefore can avoid the invasive treatments and associated side effects and which men will have aggressive PCa, allowing better classification of treatment modalities and better survival outcomes are

needed. (reviewed by Lilja, Ulmert et al. 2008, Rubin 2008, Mazzola, Ghoneim et al. 2011).

1.8 *Tetraspanins*

1.8.1 Overview

The tetraspanin super family, also recognised in the literature as the transmembrane-4 superfamily (TMSF-4) was discovered through sequence homology in 1990. These proteins, characterised by very conserved sequence motifs have an extensive evolutionary span across species from *Caenorhabditis elegans* through to 33 members identified in humans (Table 1-1) (Oren, Takahashi et al. 1990, Wright, Henkle et al. 1990, reviewed by Wright and Tomlinson 1994, Zoller 2009, Romanska and Berditchevski 2011). Given the large number of tetraspanins, this review, will focus on the tetraspanins directly involved with this project that also represent some of the best characterised tetraspanins within the family, Cluster of Differentiation 151 (CD151), CD9, CD82 and Tspan8 with focus on the relevance to PCa. These are highlighted in Table 1-1. Recently a book entitled “Tetraspanins” has been published that is written by a wide range of long-standing experts in the field. This book eloquently covers the field of tetraspanins and due its scope and depth is highly recommended as a reference source (Berditchevski and Rubinstein 2013).

Table 1-1: List of known human tetraspanins and associated information.
The tetraspanins CD151, Tspan8, CD9 and CD82 which were investigated in this study are highlighted. Adapted and extended from (Miranti 2009, Romanska and Berditchevski 2011).

Tetraspanin (Tspan)	Alternative Name(s)	Chromosome	Entrez Gene ID	DNA #	Protein ID
1	NET-1	1p34.1	10103	NM_005727.2	NP_005718
2	FLJ12082	1p13.1	10100	NM_005725	NP_005716
3 (2 isoforms)	TM4SF8.1/2, OAP-1	15q24.3	10099	NM_198902.1 NM_005724	NP_005715, NP_944492
4	TM4SF7, NAG-2	11p15.5	7106	NM_003271.3	NP_003262
5	TM4SF9, NET-4	4q23	10098	NM_005723.2	NP_005714
6	TM4SF6, T245	Xq22	7105	NM_003270.2	NP_003261
7	TM4SF2, Talla-1, A15, CD231	Xp11.4	7102	NM_004615.2	NP_004606
8	**TM4SF3, CO-029, D6.1A (rat)**	**12q14.1-q21.1**	**7103**	**NM_004616**	**NP_004607**
9	NET-5	12p13.33-32	10867	NM_006675.3	NP_006666
10	Oculospanin (OCSP)	17q25.3	83882	NM_031945.2	NP_114151
11	Possibly mouse only (CD151 like)	12p11.21	441631	XM_497334	XP_497334
12	NET-2, TM4SF12	7q31.31	23554	NM_012338.3	NP_036470
13	NET-6, TM4SF13	7p21.1	27075	NM_014399	NP_055214
14	TM4SF14, NEW2	10q22.3	81619	NM_030927.1	NP_112189
15	NET-7	10q22.1	23555	NM_012339.3	NP_036471
16	TM-8, TM4-B	19p13.2	26526	NM_012466.2	NP_036598
17	TM4SF17, NEW3	5q35.3	26262	NM_130465.3	NP_569732
18	Neurospanin	11p11.2	90139	NM_130783.2	NP_570139
19	XP_084868	12q21.31	144448	XM_084868	XP_084868
20	Uroplakin1b	3q13.3-q21	7348	NM_006952.3	NP_008883
21	Uroplakin1a	19q13.13	11045	NM_007000.2	NP_008931
22	RDS/peripherin	6p21.2-p12.3	5961	NM_000322.2	NP_000313
23	ROM1	11q13	6094	NM_000327	NP_000318
24 (2 variants; UTR)	**CD151, PETA-3, SFA-1**	**11p15.5**	**977**	**NM_6205999 NM_139030**	**NP_004348, NM_004357.3**
25	CD53/OX44	1p13	963	NM_000560.2	NP_000551
26	CD37	19p13-q13.4	951	NM_001774.1	NP_001765
27	**CD82, *kang* ai, KAI1, R2, C33**	**11p11.2**	**3732**	**NM_002231.3**	**NP_002222**
28	CD81, TAPA-1	11p15.5	975	NM_004356.3	NP_004347
29	**CD9, MRP-1**	**12p13.3**	**928**	**NM_001769.2**	**NP_001760**
30	CD63, LIMP-1	12q12-q13	967	NM_001780.3	NP_001771
31	SAS	12q13.3	6302	NM_005981.3	NP_005972
32 (3 variants; UTR)	TSSC6	11p15.5	10077	NM 139024 NM_005705 NM_139024	NP_620593, NP_620591, NP_005696
33	Penumbra, NEW7	7q32.3	340348	NM_178562	NP_848657

The structures of most tetraspanins are predicted from sequence analysis coupled with modelling based on the 3D crystal structural of the large extracellular loop of CD81 (Kitadokoro, Bordo et al. 2001). Typically tetraspanins proteins are between 160-350 amino acids in length. There are a number of requirements for a molecule to be included in the tetraspanin superfamily such as four hydrophobic transmembrane domains (TM1-TM4; Figure 1-4). They must also possess two extracellular regions, a small and large extracellular loop (SEL and LEL respectively) of which the LEL has a constant region and a variable region. The constant region has highly conserved a, b and e helices, while the variable region has c and d helices juxtaposed by cysteine-cysteine-glycine (CCG) motifs and conserved cysteine residues. The variable region has been shown to be the site for specific protein interactions (Seigneuret, Delaguillaumie et al. 2001) (detailed in 1.8.3). Tetraspanins also possess short carboxyl and amino terminal intracellular terminal tails that have conserved cysteine residues which can be palmitoylated (Boucheix and Rubinstein 2001, Hemler 2005, Levy and Shoham 2005, Rubinstein 2011), again detailed in 1.8.3.

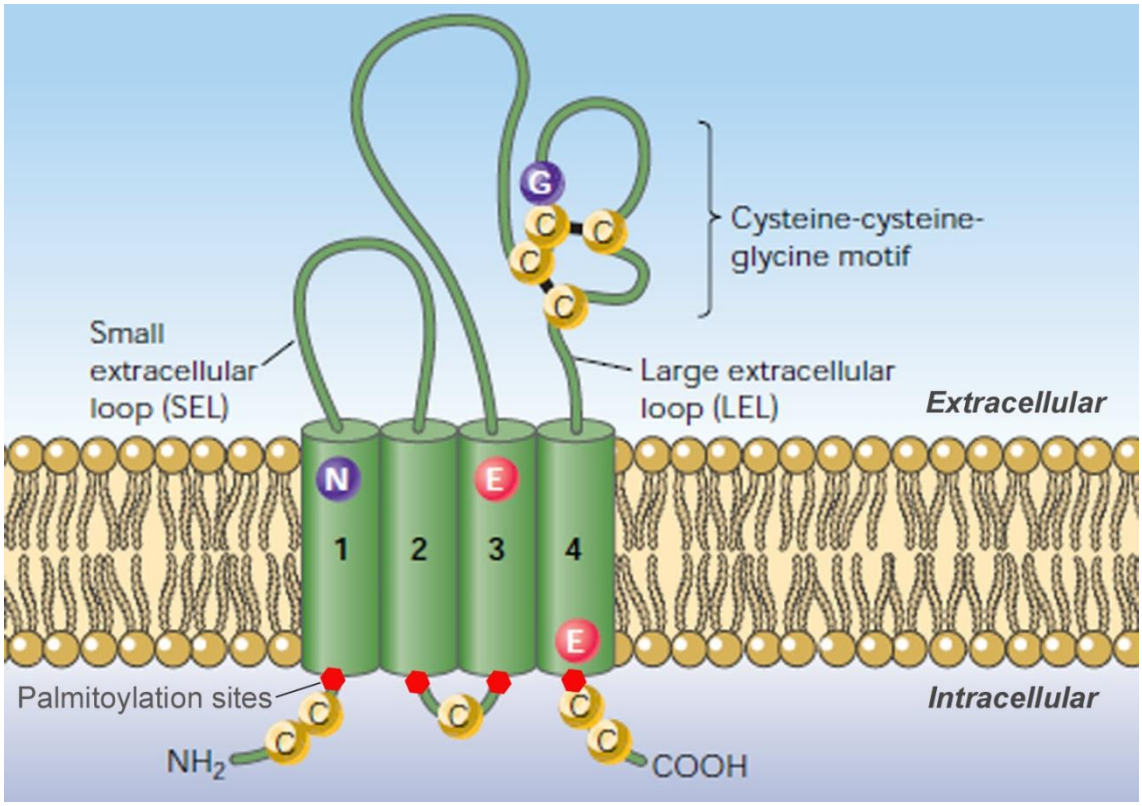

Figure 1-4: Structure of a typical tetraspanin.
The predicted topology of the tetraspanin based on sequence homology. General features include the four transmembrane domains, two extra cellular loops and two cytoplasmic tails (Adapted from Levy and Shoham 2005).

1.8.2 The tetraspanins CD151, Tspan8, CD9 and CD82

1.8.2.1 Discovery and nomenclature

CD151 (also known as PETA-3, SFA-1, glycoprotein 27 (GP27), and tetraspanin-24) has been mapped to human chromosome 11p15.5 and was first discovered by the platelet and endothelial cell binding capability of the monoclonal antibody (mAb), 14A2 (Ashman, Aylett et al. 1991) and in 1995 the cDNA was cloned by Fitter *et al*. (1995). Subsequently the cDNA was independently cloned from human T-cell leukaemia virus type 1 (HTLV-1) infected T-cells and termed SF-HT-activated gene 1 (SFA-1) (Hasegawa, Utsunomiya et al. 1996). The most up-to-

date official nomenclature, CD151, was assigned at the VIth International Leukocyte Typing Workshop (Ashman, Fitter et al. 1997). It should be noted that even though all the tetraspanins have been assigned a number as displayed in Table 1-1, these are not commonly used in the literature, with referral to the CD classification mostly taking precedent.

Tspan8 is also known as transmembrane-4-super family-3 (TM4SF3) and CO-029 due to the antibody it was originally identified with on colon cancer cells (Szala, Kasai et al. 1990). It is also referred to in papers as D6.1A, however should only be correctly called this when referring to the *Tspan8* gene or protein in rodents, again the moniker was derived from the name of the antibody (D6.1) used to identify it. D6.1 was found in metastatic rat cell lines, that later showed sequence homology to the earlier discovered human Tspan8 (Claas, Herrmann et al. 1996). *Tspan8* is located on chromosome12p71.

CD9 is also cited in the literature as motility related protein 1 (MRP-1) and is located on human chromosome 12p13.3 (Boucheix, Nguyen-van et al. 1985). Sequence data published by three different groups in 1991 was found to be homologous for the MRP-1 and CD9 clones (Boucheix, Benoit et al. 1991, Lanza, Wolf et al. 1991, Miyake, Kovama et al. 1991).

CD82 was originally identified as a novel cDNA clone through hybridisation techniques of stimulated Jurkat and lymphoid cell cDNA libraries and termed R2 (Gaugitsch, Hofer et al. 1991). Liu and Zhang (2006) have published a very elegant review of CD82 which includes extensive details on the origins of the molecule. CD82 is located on human chromosome 11p11.2. Dong *et al*. (1994) termed this gene that had anticancer and metastatic properties, *KAI1* (an abbreviation of *kang* ai; Chinese for anticancer). A search in Genebank by the group found multiple homologous sequences entered through 1991 and 1992. It was entered as a member in the Cluster of Differentiation antigens in 1994 (Engel and Tedder 1994).

1.8.2.2 Expression of tetraspanins

Most tetraspanins in mammals are heterogeneously expressed with nearly all cell types expressing multiple tetraspanins at various levels. CD151 and CD9 have been shown to be expressed in platelets and megakaryocytes, endothelial, epithelial, smooth muscle, Schwann and dendritic cells (Sincock, Mayrhofer et al. 1997, Geary, Cambareri et al. 2001) in addition to erythrocytes (Karamatic-Crew, Burton et al. 2004). Epithelial expression of CD151 has been shown to be high at the basal surface and in membrane junctions, while CD9 was also detected at the apical luminal membrane. Furthermore some expression patterns were found to be tissue specific such as CD151 but not CD9 being expressed in cardiac muscle while CD9 and not CD151 is expressed in white and grey brain matter and fibroblasts (Sincock, Mayrhofer et al. 1997, Yanez-Mo, Tejedor et al. 2001). CD82 has been shown to be widely expressed in epithelial and endothelial cells, fibroblasts, platelets, skeletal and smooth muscle cells and unspecified brain matter (Dong, Lamb et al. 1994, Kawana, Komiya et al. 1997). Much less has been published on Tspan8, however its expression has been shown in epithelial, endothelial (capillary), muscle (striated and smooth) as well as nerve cells (Sela, Stwplewski et al. 1989, Gesierich, Paret et al. 2005, Greco, Bralet et al. 2010). Interestingly, a small number of tetraspanins show restricted expression, such as uroplakins which are expressed only on urothelial cells, while peripherin and ROM-1 are only found in the rod and cone cells (photoreceptors) of the retina (Boucheix and Rubinstein 2001, Berditchevski and Rubinstein 2013).

1.8.3 Molecular interactions of tetraspanins

The cellular plasma membrane is classically portrayed by the fluid mosaic model where molecules freely diffuse along the lipid bi-layer (Singer and Nicolson 1972). Over the years the fluid mosaic model has been constantly revised; one such revision was the incorporation of ordered structural micro-domains within the membrane, called lipid rafts (reviewed by Staubach and Hanisch 2011). The two

sub-classes of lipid rafts, planar and caveolae are proposed to spatially orientate partner molecules to facilitate subsequent cellular process. More recently another class of structured membrane micro-domains, distinct from lipid rafts (Israels and McMillian-Ward 2007), that involve the tetraspanin proteins has been reported (Rubinstein, Le Naour et al. 1996). These structures are known interchangeably in the literature as tetraspanin webs (Boucheix and Rubinstein 2001) or tetraspanin enriched micro-domains, which can be abbreviated to TEMs (Hemler 2003) or TERMs (Berditchevski, Odintsova et al. 2002). TEMs are ordered structures that are formed through tetraspanins interacting with other tetraspanins and many other non-tetraspanin molecules in a dynamic way to form multi-molecular complexes that can influence cellular processes, such as signalling, adhesion and motility. There has been an abundant amount of experimental studies trying to elucidate tetraspanin binding partners and the subject has been extensively reviewed elsewhere (Yunta and Lazo 2003, Levy and Shoham 2005, Charrin, Naour et al. 2009, Stipp 2010, Rubinstein 2011, Veenbergen and van Spriel 2011, Berditchevski and Rubinstein 2013). Hence, here a brief overview will be given on tetraspanin interactions and potential influences on cellular processes.

It is important to note at this point in the review, that some confusion arises in the literature surrounding tetraspanin binding partners due to the use of various terminologies in regards to tetraspanin interactions. Specifically the terms homo-interaction/clustering and hetero-interaction/clustering can mean various things in different contexts. For example, when discussing all molecules in a cell, a homo-interaction can be any tetraspanin-tetraspanin interaction, for example CD151-CD9 or if discussing tetraspanins exclusively, it can mean a specific tetraspanin-tetraspanin interaction like CD151-CD151. Furthermore in the same vein hetero-interactions can mean, for example a tetraspanin-integrin interaction; however it can also can mean an interaction between different tetraspanins, for instance CD151-CD9. The field would benefit from some consistency between published papers in the nomenclature. In this review, the interaction will always be put in

context, for example interaction such as CD151-CD9, will be classified as a tetraspanin hetero-interaction, or when appropriate the specific molecule names will be clearly stated, for example a CD151-CD151 tetraspanin homo-interaction.

The majority of work trying to elucidate tetraspanin partner molecules has utilised membrane detergent solubilisation techniques to fractionate the membrane, separate out and characterise the TEMs through immuno-precipitation, electrophoretic separation, immunoblotting or mass spectrometry, along with chemical cross linking, fluorescence resonance energy transfer, fluorescence correlation spectroscopy and single molecule tracking techniques (reviewed by Berditchevski and Rubinstein 2013). These techniques not only characterise the tetraspanin binding partners, but also can characterise their adhesion strength and stoichiometry to some degree. Homo and hetero tetraspanin-tetraspanin interactions have been demonstrated for a wide range of various tetraspanins (Kovalenko, Yang et al. 2004) along with other associations with non tetraspanin membrane molecules. These homo and hetero tetraspanin-tetraspanin/non tetraspanin complexes have been suggested to form the core of the TEMs which can then recruit other non tetraspanin binding partners to associate with the TEM complex.

A model has been proposed that has three levels of interactions between tetraspanin and partner molecules based on the detergent strength required to disrupt binding (reviewed by Hemler 2005, Zoller 2009). The most stringent interactions are direct primary associations that include homo/hetero tetraspanin-tetraspanin binding through the ECL2 and tetraspanins with other molecules such as integrins (e.g. CD151 and α3β1) and immunoglobulin super-family proteins (e.g. CD9 and EWI-F) explained more below. The less robust type 2 and type 3 interactions have been shown to be stabilised through palmitoylation of the cysteine residues proximal to the membrane on the tetraspanins (Berditchevski, Odintsova et al. 2002, Charrin, Maine et al. 2002). The palmitoylation of the

membrane proximal cysteines on the intracellular N and C tails are not strictly essential for tetraspanin interactions but do influence association-dissociation kinetics and can have subsequent functional implications (Yang, Claas et al. 2002, Yang, Kovalenko et al. 2004, reviewed by Lazo 2007, Stipp 2010). For instance, the disruption of CD151-tetraspanin binding by mutation of the CD151 palmitoylation sites was shown to affect α3β1 dependant adhesion and migration on laminin (Zevian, Winterwood et al. 2010).

The best characterised interactions of tetraspanins with non tetraspanin molecules are with integrins. Integrins are cell surface receptors that consist of two glycoprotein subunits. Currently 18 α subunits and 8 β subunits have been identified, which form 24 known functional integrins (van der Flier and Sonnenberg 2001, Hynes 2002). They form a family of integral membrane proteins, which transverse the membrane from the extracellular matrix to the cytoskeleton and are anchored to the membrane by a single hydrophobic transmembrane domain.

CD151, Tspan8, CD82 and CD9 have all been shown to interact with multiple integrins with various hierarchy and affinity in a dynamic way, highlighting the complex nature of these interactions. The main binding partners for these tetraspanins include integrins such as alpha3beta1 (α3β1), α6β1 and α6β4. In fact the relatively stable primary interaction that CD151 preferentially adopts with this laminin binding subset of integrins is arguably the best studied interaction of tetraspanins with partner molecules in the literature (reviewed by Stipp 2010). CD151, CD82 and CD9 also associate with α4β1, α5β1, while CD151 and CD9 also associate with α7β1 and αIIbβ3. Lastly, CD82 further associates with αLβ2 and αVβ3, highlighting that both the α and β subunits are important in the association complexes (Fitter, Sincock et al. 1999, Yauch, Kazarov et al. 2000, Berditchevski 2001, Sterk, Geuijen et al. 2002, Gesierich, Paret et al. 2005, Berditchevski and Rubinstein 2013).

Integrins have been identified as regulators of such cell functions as differentiation, survival, motility, growth, invasion, angiogenesis and proteinase expression (reviewed by Hynes 2002, Munshi and Stack 2006, Alam, Goel et al. 2007, Goel, Alam et al. 2009). Thus the aberrant expression of integrins can possibly lead to phenotypes that represent the specific defined stages of PCa, detailed in section 1.3.2. and a number of integrins have been shown to correlate with PCa disease progression (reviewed by Goel, Li et al. 2008, Goel, Alam et al. 2009). Furthermore due to the relevance of integrins in cellular adhesion, motility, invasiveness and angiogenesis, the tetraspanin regulated, tetraspanin-integrin complexes have been suggested to have direct relevance to tumour metastatic potential (Hood and Cheresh 2002, Zhang, Kazarov et al. 2002, Janes and Watt 2006, King, Pawar et al. 2008, Stipp 2010).

Multiple tetraspanins including CD151, CD9 and Tspan8 have also been shown to associate with other intracellular signalling molecules such as phosphatidylinositol 4-kinase and protein kinase C (Yauch and Hemler 2000, Zhang, Bontrager et al. 2001, Class, Wahl et al. 2005). Tetraspanin associations with growth factor receptors have been moderately investigated with CD9 and CD82 reported to interact with the hepatocyte growth factor receptor (HGF-R) (Trusolino and Comoglio 2002, Zhang, Lane et al. 2003) and CD82 with the epidermal growth factor receptor (EGFR) (Odintsova, Sugiura et al. 2000). In prostate tissue CD82 has been shown to have a primary interaction with the epithelial membrane protein, duffy antigen of receptor chemokines (DARC/CD234; 1.8.4.2) (Bandyopadhyay, Zhan et al. 2006). CD9 and Tspan8 have been shown to interact with the epithelial cell adhesion molecule (EpCam) (Le Naour, Andre et al. 2006) and the IgG superfamily protein EWI-F (Stipp, Orlicky et al. 2001, Class, Wahl et al. 2005). CD9 also associates with EWI-F related EWI-2 (Stipp, Kolesnikova et al. 2001) and with transforming growth factor (TGF) (Shi, Fan et al. 2000) and, along with CD82, to the antigen presenting major histocompatibility complex (MHC; with MHC type II being more common) (Unternaehrer, Chow et al. 2007). Adhesion related

molecules such as E-Cadherin associate with CD151 and Tspan8 (Chattopadhyay, Wang et al. 2003, Greco, Bralet et al. 2010), while intracellular adhesion molecule (ICAM-1) and vasculature cell adhesion molecule (VCAM-1) interact with CD9 and CD151 respectively (Barreiro, Zamai et al. 2008). This once again highlights the potential effects tetraspanins may have on cellular processes, proposed to be from the lateral organisation and spatial orientation of molecules such as these growth factors, signalling, IgG and adhesion related molecules. Furthermore, CD9 is one of the only tetraspanins reported to directly bind ligands, specifically pregnancy-specific glycoprotein 17 (Waterhouse, Ha et al. 2002) and more relevant to cancer progression, fibronectin (Longhurst, Jacobs et al. 2002)..

Tetraspanins have also been shown to associate with matrix metalloproteinases (MMPs). MMPs are a class of endopeptidases that degrade various components of the ECM and have been strongly correlated to metastatic potential in a number of cancers (Rundhaug 2003). A number of tetraspanins have been reported to associate with various MMPs. For example, CD151 has been shown to co-localise with MMP-7, with increased CD151 expression correlated to increased expression of MMP-7, MMP-2 and MMP-9 (Hong, Jin et al. 2006, Hasegawa, Furuya et al. 2007). Furthermore, the secreted proenzyme version of MMP-7, proMMP-7 has been suggested to be a possible ligand for CD151 (Shiomi, Inoki et al. 2005). Conversely increased CD82 and CD9 expression was shown to down regulate MMP-9 (Hong, Jin et al. 2006) and MMP-26 (Yamamoto, Vinitketkumnuen et al. 2004) expression respectively.

Along with direct and indirect lateral binding and subsequent “outside-in signalling” effects of the tetraspanins on cellular processes, tetraspanins and TEMs in exosomes may also be involved in proximal and distal cross-talk between cells. Exosomes, first identified by Johnstone *et al.* (1987) are 30-100nm multivesicular bodies that originate within a cell. The basic functional mechanism of the exosome is to facilitate movement of biologically active intracellular substances across the

plasma membrane to release to the extracellular environment. A number of tetraspanins including CD151, CD82, CD9 and Tspan8 have been shown to be highly enriched in exosomes. Interestingly, a group showed that transfer of exosomes from highly metastatic cell lines to low-metastasising cell lines can induce the recipient cells to display the highly metastatic phenotype (Hao, Ye et al. 2006). Furthermore, an animal model grafted with exosomes enriched with CD151 and Tspan8, was shown to form pre-metastatic niches, which resulted in a normally non-metastasising cell line forming metastatic lesions in the model (Jung, Castellana et al. 2006, Klingbeil, Marhaba et al. 2009).

The overall picture of tetraspanin interactions and subsequent functional effects is still in its relative infancy, the role of tetraspanins seems to be as so called “molecular facilitators”. It has been proposed that tetraspanins transverse the plasma membrane in transient association with other tetraspanins and/or other non-tetraspanin partner molecules. These small transient complexes can be evoked by cellular stimuli to cluster forming larger functional TEMs to facilitate functional effects. Furthermore, TEMS also have the ability to communicate with distant cells through exosomal trafficking routes (Rana, Yue et al. 2012). Due to the highly dynamic, diverse multi-molecular composition of the TEM that is also influenced by palmitoylation and glycosylation, along with the exosomal cell communication possibilities that are all, presumably constantly influenced by the cells rapidly changing dynamic state, it is not so surprising that the molecular biochemical role of tetraspanins is still not fully elucidated.

1.8.4 Tetraspanins and cancer

Tetraspanins expression levels have been correlated with cancer stage, patient outcome and metastatic potential in a number of cancers as detailed below.

1.8.4.1 Clinical studies

1.8.4.1.1 ***CD151***

Using immunohistochemistry (IHC) and polymerase chain reaction (PCR) methods, increased expression of CD151 was shown be associated with a poor survival in non-small lung cancer patients (Tokuhara, Hasegawa et al. 2001). This study also analysed expression levels of CD9 and CD82 (see relevant sections below). The group subsequently reported a correlation between increased CD151 expression and poor survival in colon cancer patients (Hashida, Takabayashi et al. 2003). In prostate cancer CD151 was shown, by IHC to be up-regulated in tumours compared to BPH and also had prognostic significance (overall survival) that surpassed the traditional Gleason grading system, especially in well and moderately differentiated tumours (Ang, Lijovic et al. 2004).

In breast cancer IHC analysis showed CD151 to be upregulated in patients with hormone receptor negative and advanced cancer (Kwon, Park et al. 2012), correlated to higher tumour grade (Yang, Richardson et al. 2008) and to high grade ductal *in situ* carcinoma (Novitskaya, Romanska et al. 2010). Increased CD151 expression was also correlated with reduced survival and shown to have prognostic significance in breast cancer (Sadej, Romanska et al. 2009).

Up-regulated CD151 expression also showed prognostic significance in advanced renal cell carcinoma (Yoo, Lee et al. 2011), endometrial cancer, when comparing early to late stage disease (Voss, Gordon et al. 2011), squamous cell carcinoma (Suzuki, Miyazaki et al. 2010), resected gastric cancer (Yang, Zhang et al. 2013)

and non-small cell lung cancer (Kwon, Seo et al. 2013). Huang *et al.* (2010) and Devbhandari *et al*. (2011) showed CD151 was up-regulated in intrahepatic cholangiocarcinoma and hepatocellular tumour samples, respectively, compared to matched normal samples. Both studies reported that increased CD151 expression correlated to poor survival. IHC analysis showed CD151 was over-expressed in pancreatic cancer compared to normal tissue (Gesierich, Paret et al. 2005). A more recent study also showed expression of CD151 to have clinical prognostic significance in pancreatic adenocarcinoma (Zhu, Huang et al. 2010). In a relatively small study, IHC confirmed CD151 was upregulated in primary osteosarcoma in comparison to adjacent non-tumour tissue (Zhang, Zhang et al. 2010). Other studies have looked at tetraspanin mRNA levels in cancers. One study using cDNA microarrays showed that CD151 mRNA expression levels were upregulated in glioblastoma in comparison to normal brain tissue (Bredel, Bredel et al. 2005). Another study using qPCR reported that CD151 mRNA expression was correlated with poor survival in gingival squamous carcinoma (Hirano, Nagata et al. 2009). Also using qPCR another group found they could delineate metastatic potential in clear cell renal carcinoma using an array of genes including the upregulation of CD151 (Sanjmyatav, Steiner et al. 2011). To date only one IHC study has shown a significant reduction in CD151 expression in cancer (colon) compared to adjacent normal tissue (Chien, Lin et al. 2008). Collectively these results show that in general increased CD151 expression is associated with an advanced stage and correlates with poor prognosis in a variety of cancers.

1.8.4.1.2 ***Tspan8***

Analysis of Tspan8 expression by PCR and western blot showed Tspan8 to be upregulated in two primary metastatic cell lines of colon cancer compared to a normal primary cell line, all created from a single patient (Le Naour, Andre et al. 2006). Another study of colon cancer found Tspan8 expression was upregulated in

tumours compared to adjacent normal tissues and correlated to poorer prognosis (relapse) (Greco, Bralet et al. 2010).

A more recent study a performed meta-analysis from 11 publically available datasets, consisting of 829 patient samples. They reported that upregulation of Tspan8 was correlated to advanced ovarian cancer (Fekete, Raso et al. 2012). The findings were confirmed by qPCR in a further 64 collected patient samples. Tspan8 expression was shown to not be correlated to survival outcomes in this meta-analysis study. Tspan8 has been less studied than CD151, CD9 and CD82 however the available published data suggest that increased expression of Tspan8 is associated with advanced cancer and possibly poorer prognosis.

1.8.4.1.3 ***CD82***

In direct contrast to CD151 and Tspan8, decreased CD82 mRNA and protein expression has been associated with cancer progression and/or poorer prognosis of various cancers. CD82 is one of the best studied tetraspanins and reviews have extensively covered clinical studies involving it (Tonoli and Barrett 2005, Liu and Zhang 2006, Malik, Sanders et al. 2009, Miranti 2009, Zoller 2009, Tsai and Weissman 2011).

Briefly, Tonoli and Barrett (2005) have provided the most extensive review on CD82 to date with 64 clinical studies included. These included bladder, bone and soft tissues, breast, cervix, endometrial, gastrointestinal, head and neck, leukaemia, liver, lung, brain, oral, ovary, pancreas, prostate, skin and thyroid cancer. They reported a negative correlation of CD82 expression and cancer progression in 83% of the studies. Since the review by Tonoli, many clinical studies involving CD82 on a wide range of cancers have been published. Huang *et al.* (2005) reported that CD82 and CD9 were downregulated in breast tumours. Another study found similar results by IHC and RT-PCR (Christgen, Bruchhardt et al. 2008). Both studies showed surprisingly, that CD82 was still expressed in the

metastasis associated, estrogen receptor (ER) negative metastatic tumour samples. A more recent review by Malik *et al*. (2009) reviewed a further 15 clinical studies not included in the earlier Tonoli and Barrett review. They reported that all studies showed varying levels of CD82 protein and/or mRNA downregulation in correlation with cancer progression and poorer patient outcome.

From the majority of the large number of clinical studies to date it is widely accepted that reduced expression of CD82 is associated with advanced cancer and a poor prognosis in patients.

1.8.4.1.4 ***CD9***

Following in the trend of CD82, decreased CD9 expression has mainly been associated with progression and/or poorer prognosis in a variety of cancers including prostate (Chuan, Pang et al. 2005, Wang, Begin et al. 2007), breast (Miyake, Nakano et al. 1995, Miyake, Nakano et al. 1996), lung (Higashiyama, Taki et al. 1995, Higashiyama, Doi et al. 1997), colon (Cajot, Sordat et al. 1997, Mori, Mimori et al. 1998, Hashida, Takabayashi et al. 2002), oral squamous cell carcinoma (Kusukawa, Ryu et al. 2001), head and neck (Erovic, Pammer et al. 2003, Mhawech, Dulguerov et al. 2004), urothelial bladder (Mhawech, Herrmann et al. 2003), multiple myeloma (De Bruyne, Bos et al. 2008) and gall bladder (Zou, Xiong et al. 2012). One study that found an inverse correlation of CD9 expression with progressive cervical cancer, also reported strong CD9 expression within specific regions of tumour invasion into lymphovascular spaces (Sauer, Windisch et al. 2003). This suggests that CD9 may differentially affect particular aspects of tumour growth and progression. In contrast to the majority of findings reporting inverse correlations of CD9 expression and cancer progression there have been two independent reports showing a correlation between increased CD9 expression and progression in gastric cancers (Hori, Yano et al. 2004, Soyuer, Soyuer et al. 2010). Another study saw no correlation of CD9 expression with prognosis in progressive osteosarcoma (Kubista, Erovic et al. 2004). As with CD82, the majority

of the clinical studies to date show that decreased CD9 expression is associated with advanced cancer and a poor prognosis in patients.

1.8.4.1.5 ***Summary***

Clinical studies mainly show that increased CD151 and Tspan8 expression are associated with advanced cancer grade and poor prognosis in patients. In direct contrast to this, decreased expression of CD9 and CD82 are mostly associated with advanced cancer grade and poor prognosis in patients. There are some conflicting reports in the clinical studies in a variety of cancers. This is especially interesting surrounding gastrointestinal cancer where some studies have seen a shift from the normal trend. Specifically four studies involving CD82 and two studies involving CD9, which are normally downregulated in correlation with advanced cancers, have reported a positive correlation with gastrointestinal cancers. Similarly, one study also showed the usually upregulated CD151 to be downregulated in advanced colon cancer. The correlation of these tetraspanins with tumour progression in a variety of cancers warrants further investigation into their role as possible prognostic markers in PCa. As previously stated, better prognostic markers are required that can indicate patients prognosis once diagnosed with PCa. This would allow better stratification of the somewhat invasive treatment modalities reducing unnecessary possible side-effects.

1.8.4.2 In-vitro and in-vivo studies

Results from *in-vitro* and *in-vivo* work involving tetraspanins has recapitulated results from the human clinical studies, where increased expression of CD151 and Tspan8 correlate to a more invasive phenotype and conversely increased expression of CD82 and CD9 reduced the invasive phenotype. Since this topic has been reviewed in detail within the discussion sections of chapters 4 and 5, some examples briefly highlighting the salient results are summarised here.

In vitro studies have repeatedly shown that CD151 is involved with cell migration and adhesion (reviewed by Zoller 2009, Stipp 2010, Berditchevski and Rubinstein 2013). For example, knockdown of CD151 in the MCF-10A breast cancer cell line was shown to reduce motility but did not affect proliferation (Deng, Li et al. 2012). KD of CD151 in epidermal carcinoma cell lines also resulted in reduced migration and adhesion on laminin-5, through associations of CD151 with laminin binding integrins (Winterwood, Varzavand et al. 2006). Studies involving *Cd151* knockout (KO) animals have reported reduced angiogenesis in *in vivo* functional assays and reduced primary tumour growth in subcutaneous grafts (Takeda, Kazarov et al. 2007). The same group later showed reduced metastatic potential in experiments involving subcutaneous transplants of melanoma and lung cancer cells into *Cd151* KO animals. Notably in contrast to their earlier study, this study showed no effect on primary tumour growth (Takeda, Li et al. 2011). Another *in-vivo* grafting study using a CD151 blocking mAb showed a reduction in tumour metastatic potential, also without effecting primary tumour growth (Zijlstra, Lewis et al. 2008).

Much less has been reported on Tspan8. However, antibody mediated blocking of Tspan8, in conjunction with E-cadherin downregulation, reduced cell migration in colon cancer cell lines (Greco, Bralet et al. 2010).

Even though the *Cd9* KO mouse model has been developed, the majority of experimental studies involving CD9 have focused on *in vitro* systems. These have mostly shown that CD9 expression is negatively correlated to the metastatic related functions of motility, migration, adhesion and platelet activation (Zoller 2009, Powner, Kopp et al. 2011). On the point of platelet activation, several reports have recently focused on the role of tetraspanins in immunological surveillance of tumour cells (reviewed by Veenbergen and van Spriel 2011).

The aforementioned association of CD9 and CD82 with HGF-R (1.8.3) is noteworthy in regards to cancer as HGF-R is involved with the epithelial-mesenchymal transition that is thought to be a preliminary step in tumour dissemination (Trusolino and Comoglio 2002). Furthermore CD82 acting as a binding partner with DARC in PCa has ramifications in tumour progression as loss of CD82-DARC prohibits cells entering into senescence, allowing them to take on a cancerous like phenotype of unhindered growth (Bandyopadhyay, Zhan et al. 2006). CD82 has been extensively studied and is widely considered as a metastatic suppressor (Liu and Zhang 2006, Malik, Sanders et al. 2009, Zoller 2009).

As previously mentioned the *in vivo* and *in vitro* studies involving CD151 and CD9 are extensively detailed in context of the results of this thesis in chapters 4 and 5.

1.8.5 Association of tetraspanins to other diseases

Tetraspanins have also been linked to a wide range of diseases other than cancer, highlighting their heterogeneous emerging role in human pathology. In humans deleted or mutated *CD151* has been associated to sensorineural deafness, pretibial bullosa skin blistering, end stage kidney failure and thalassemia minor (Kagan, Feld et al. 1988, Karamatic-Crew, Burton et al. 2004). In murine models the KO of *Cd151* has so-far recapitulated some of the human CD151 phenotypes, such as reduced wound healing capabilities, due to diminished keratinocyte proliferation, laminin 5 disruption in the basement membrane and the impairment of the normal upregulation of α6β4 in the wound area (Wright, Geary et al. 2004, Cowin, Adams et al. 2006). Strain dependant proteinuria and glomerular basement disruption which leads to progressive kidney failure has also been observed (Sachs, Kreft et al. 2006, Baleato, Guthrie et al. 2008) while abnormal platelet function was also reported in the *Cd151* KO model (Lau, Wee et al. 2004). In a chick embryo model *Cd151* has been shown to affect specialisation of cranial

sensory ganglia, which control sensory transmissions to the majority of the face (McCabe and Bronner-Fraser 2011).

The knockdown of *Cd9* has been shown to impair oocyte fertilization by inhibiting downstream sperm egg fusion events in murine models (not recapitulated in humans) (Le Naour, Rubinstein et al. 2000, Rubinstein, Ziyyat et al. 2006). Also CD9 and to a lesser extent CD82 have also been shown to be upregulated, and associated with the FC receptors in antigen presenting cells from patients with atopic dermatitis (Peng, Yu et al. 2010).

Tetraspanins have also been implicated in viral fusion and entry mechanisms. Specifically, CD9, CD82 and CD81 have been shown to be involved with the infection process of HIV-1 virus particles to $CD4^+$ cells, while CD81 is also involved in hepatitis C virus and malaria infection (Silvie, Rubinstein et al. 2003, Flint, von Hahn et al. 2006, Gordon-Alonso, Yañez-Mó et al. 2006). CD9 has been shown to be a co-receptor for the diphtheria toxin and a regulator of canine distemper disorder (Iwamoto 1994, Singethan, Topfstedt et al. 2006). Furthermore, CD151 and more specifically the association of CD151 with its partner integrins in TEMs has been shown to be required for the endocytic entry of human papilloma virus, types 16 (Scheffer, Gawlitza et al. 2013) 18 and 31 (Spoden, Kühling et al. 2013) into cells.

Other tetraspanin abnormalities linked to human diseases include an X-linked mutation in the *Talla-1/TM4SF2* gene that is associated with mental retardation (Zemni, Bienvenu et al. 2000). Loss of CD53 expression was reported in one family resulting in an increase of multiple heterogeneous infections (Mollinedo, Fontan et al. 1997), while mutations in the *peripherin/RDS* (*ROM-; tetraspanin 22*) gene results in patients with retinal degradation (van Soest, Westerveld et al. 1999).

1.9 *Models of PCa*

1.9.1 Overview

Many cell culture (reviewed in a two part series by Sobel and Sadar 2005, Sobel and Sadar 2005) and grafting systems (reviewed by Valkenburg and Williams 2011) have been developed and provided invaluable insights into the development and progression of PCa. However these do not recapitulate the extensive, dynamic biological interactions of the developing prostate tumours with the *in-vivo* environment. Dogs and rats are the only animals that develop spontaneous prostate cancer as in humans; however both have inherent disadvantages for use as models of PCa. Long and heterogeneous latency periods, with experimental obstacles such as difficulty of genetic manipulation coupled with general high cost from housing and long gestation periods effectively rule out dogs as feasible models. The rat has been used as an experimental model for PCa, however it also has limitations, specifically the long latency and infrequency of primary tumours and general lack of metastases (reviewed by Jeet, Russell et al. 2010, Valkenburg and Williams 2011).

1.9.2 Genetically engineered mouse models of PCa

Genetically engineered mouse models (GEMMs) of PCa have the potential allow the study of the total course of the disease from initiation, primary tumour growth and subsequent invasion right through to distant metastasis. The mouse models also have functioning immune systems, interacting microenvironments and transgenes that can be temporally and spatially expressed. The use of inbred strains also allows the genetics to be controlled while housing the experimental animals as litter mates controls the environmental variables.

The basic biology and genetics that underpin the development of the transgenic mouse models is that a transgene linked to a tissue specific promoter is introduced

into the inheritable mouse genome. Expression of the transgene can either down-regulate another gene (usually a tumour suppressor gene) or act as a dominant oncogene, to induce PCa.

1.9.2.1 TRansgenic Adenocarcinoma of Mouse Prostate (TRAMP) Model

The TRAMP model that was used in this project was developed by Greenberg *et al*. (1995) and to date it is the best characterised murine model of PCa available (reviewed by Ahmad, Sansom et al. 2008, Hensley and Kyprianou 2011). The model has a transgene consisting of 426bp of the rat probasin promoter (rPB) and 28bp of the 5' untranslated region to drive expression of the fused simian virus 40 large and small tumour antigen (SV40 T-ag) coding region. The *SV40 T-ag* transgene was microinjected into the pronucleus of C57BL/6 (B6) male mouse embryos, incorporated into the genome which set up an animal line that passed the transgene to offspring in a Mendelian manner.

The biological mechanism of the *SV40 T-ag* transgene is in that the rPB promoter restricts expression specifically to the epithelial cells of the dorsal ventral and lateral lobes of the mouse prostate (Greenberg, DeMayo et al. 1994). Importantly, due to two androgen receptor binding sites, ARBS-1 and ARBS on the promoter, the transgene is only expressed upon commencement of androgen synthesis which coincides with puberty. The expressed SV40 large and small T proteins have the ability to act as oncoproteins. Specifically, large T exerts a suppression effect on the tumour suppressor p53 and retinoblastoma proteins, which under normal circumstances regulate epithelial cell growth, while small t antigen interacts with the tumour suppressor PP2A protein. The resultant transgenic animals exhibit spontaneous autochthonous PCa which resembles the progressive pathology of human PCa, from PIN and adenocarcinoma by 8-14 weeks, right through to distant metastases to the lung, lymph nodes and importantly, to bone as is common in humans by 22-35 weeks (Greenberg, DeMayo et al. 1994, Gingrich, Barrios et al. 1996). Furthermore the TRAMP model was the first to display androgen

independent PCa when subjected to androgen ablation, via castration (Kaplan-Lefko, Chen et al. 2003).

TRAMP mice on a FVB/n (FVB) background develop tumours that progress to metastases much more rapidly than the original TRAMP on the pure B6 strain, however, importantly a subset of these tumours have been reported to display a mainly neuroendocrine phenotype rather than epithelial as in the case of human PCa (Huss, Grayy et al. 2007, Chiaverotti, Couto et al. 2008). The background strain of mouse models can have striking effects on the phenotype (Taft, Davisson et al. 2006, Huss, Grayy et al. 2007, Baleato, Guthrie et al. 2008). In regards to TRAMP mice, only mice on the B6/FVB F_1 background develop bone metastases, unlike the TRAMP on the pure B6 background (Gingrich, Barrios et al. 1996). It has also been shown that PCa therapies such as castration and/or chemotherapy can dramatically increase the expansion of cells with a neuroendocrine tumour phenotype in the TRAMP model on the B6/FVB F_1 (Tang, Wang et al. 2008). The same group later reported that on the B6/FVB F_1 background by 36 weeks of age 100% of animals had carcinomas with none having a neuroendocrine phenotype. However a large proportion of F_1 mice that were treated by hormone therapy did present with neuroendocrine tumours at 36 weeks (Tang, Wang et al. 2009). These findings recapitulate the increased neuroendocrine differentiation in patients treated with adjuvant hormonal ablation therapy (Ahlgren, Pedersen et al. 2000).

In another study involving TRAMP mice on the B6/FVB F_1 background, very low frequencies of neuroendocrine phenotype tumours were seen. Importantly the neuroendocrine phenotype markers were not seen in early stage tumours, only in advanced tumours. This suggests the tumours did not arise from progenitor neuroendocrine cells (Kaplan-Lefko, Chen et al. 2003) and again recapitulates human PCa where neuroendocrine differentiation correlates to higher grade tumours (Segawa, Mori et al. 2001). Furthermore the late stage neuroendocrine differentiation (which may be terminal) in advanced TRAMP tumours is also

supported by the fact that the neuroendocrine tumour cells are not androgen dependant and do not display proliferative markers such as ki67 (Chiaverotti, Couto et al. 2008). With this strain specific phenotype in mind many researchers have opted to use the TRAMP model on the B6/FVB F_1 background strain. Furthermore, it should be noted that although background strain does seem to have an effect in TRAMP animals, time to onset of adenocarcinoma does not show as much variation between B6, FVB and B6/FVB F_1 (Chiaverotti, Couto et al. 2008). Given that between 30% to 100% of human prostate cancers involve at least some neuroendocrine cells (Abrahamsson 1999, Sagnak, Topaloglu et al. 2011) and prostatic epithelial cells are extremely plastic and are capable of differentiating into neuroendocrine cells (Nelson, Cambio et al. 2007), the role of neuroendocrine cells in human PCa is unclear. Furthermore clinical studies have shown neuroendocrine differentiation to be correlated with Gleason grade (Segawa, Mori et al. 2001) and more recent reports have stated that the amounts of neuroendocrine cells in PCa may have prognostic value (reviewed by Sagnak, Topaloglu et al. 2011).

Many reports have been published utilising the TRAMP model. The majority of the studies have used the TRAMP model to test preventative agents of PCa. These various agents range from traditional extracts such as bitter lemon extract (Ru, Steele et al. 2011) and green tea (Adhami, Siddiqui et al. 2009) through to more rationally designed potential therapeutics such as finasteride, selenium, vitamin E, and carotenes along with a large raft of chemopreventatives such as genistein, alpha-difluoromethylornithine, toremifene, R-flurbiprofen and celecoxib, all with varying degrees of success (reviewed by Nguewa and Calve 2010). A report in *Cell* used the TRAMP model crossed with an IKKα KO transgenic model to show a link between inflammation and PCa through a pathway associated with the IKKα gene (Luo, Tan et al. 2007). The group also showed a reduction in PCa onset and a reduction in mortality that was associated with reduced metastatic incidence in the IKKα null animals in comparisons to wt. Another study published in *Nature* utilised

the TRAMP models' ability to progress to metastatic castration resistant prostate cancer (mCRPC) and analysed associations of inflammation and PCa specifically through B-cell derived lymphotoxin and its effects on PCa progression to mCRPC (Ammirante, Luo et al. 2010).

1.9.2.2 Other mouse models of PCa

Many other mouse models have been developed for research into PCa that have various genetic modifications, such as transgenic and gene KO, both stable and conditional. These have been extensively reviewed elsewhere (Abate-Shen and Shen 2002, Ahmad, Sansom et al. 2008, Hensley and Kyprianou 2011, Valkenburg and Williams 2011) and therefore only a few of the more commonly used mouse models used in PCa research are briefly reviewed here.

One of the most common transgenic mouse models, the LADY (12T-7f) model (Kasper, Sheppard et al. 1998) is related to the TRAMP model used in this project (detailed in 1.9.2.1) Unlike the minimal prostate specific rat probasin promoter (rPB) in the TRAMP model the LADY model uses a longer version of the promoter (LPB) that results in increased expression in comparison. The second main difference in the LADY model is that the attached transgene, based on the TRAMP *SV40* oncogenic transgene that expresses the large and small T/t antigens, only expressed the large T antigen, eliminating the subsequent small t antigen suppression of the tumour suppressor PP2a. However, even with the increased transgene expression, the LADY model displays extended latency, reduced frequency and increased variability of primary prostate tumours, along with reduced metastatic incidence compared to the TRAMP model. The LADY model also did not reliably progress on to castrate resistant prostate cancer subsequent to androgen ablation. The deletion of the small t antigen in the transgene has been suggested as the reason for these variations; however given that the background strains of models can have dramatic effects on models (see 1.9.2.1) and the differing background strains of the TRAMP to the LADY models may also influence

the onset and progression PCa in the models. To overcome the lack of metastatic potential the next generation of the LADY model was developed with an even stronger expressing promoter. The hepsin transgene was introduced along with the large T transgene, due to hepsin being shown to be associated with motility in conjunction with laminin-332 (Klezovitch, Chevillet et al. 2004). The double transgenic LADY model was shown to progress to distant liver and lymph metastases in about 50 % of experimental animals; however these were later shown to be neuroendocrine in nature and not epithelial as in human PCa. The LADY model is still widely utilised and very beneficial for research into early stage PCa, however for research involving analysis of metastases other murine models are more suited.

The phosphatase and tensin homologue deleted on chromosome 10 (*Pten)* model is characterised by inactivation of *Pten* tumour suppressor gene, which usually downregulates the Akt-mTOR signalling pathway (Trotman, Niki et al. 2003). The model progressed to PIN, however did not reliably develop invasive carcinomas and no metastases were reported. The *Nkx3.1* KO model has the *Nkx3.1* tumour suppressing transcription factor deleted (Bhatia-Gaur, Donjacour et al. 1999). The Nkx3.1 model developed hyperplasia in the prostate epithelial cells; however no further PCa progression was detected. Since these models somewhat recapitulate the early stages of PCa, they are still widely used and valuable to address specific relative questions to early PCa. Furthermore double KOs involving both *Pten* and *Nkx3.1* together and with other KO gene combinations have been developed that display a more aggressive phenotype. However these KO models still lack frequent, reproducible incidences of distant metastases.

The next major advance in mouse models was development of the conditional KO models with the cre-loxP system (Sauer and Henderson 1989). The molecular biology that underpins how these models function is reviewed elsewhere (Ahmad, Sansom et al. 2008) and specifically the suite of PCa conditional KO models

developed using the cre-loxP system are reviewed in detail by Valkenburg (2011). Briefly when this system is used in conjunction with a tissue specific promoter, there is the ability to spatial and temporally KO a gene, or conversely by excising an upstream stop codon of a transgene, can cause constitutive expression of the transgene, to induce carcinogenesis.

The conditional KO models are very sophisticated and as previously stated the temporal and spatial gene deletion can be very useful to researchers. However like all models the specific characteristics of each conditional KO models need to be evaluated to make sure they are best model to fulfil the experimental approach to answer specific research aims. Furthermore, specific to PCa research when tamoxifen is used as the inducer in the cre-loxP system, the exogenous tamoxifen can down regulate endogenous androgen. This can then cause the reduction of proliferation of the androgen dependent prostatic epithelial cells, causing secondary unwanted uncontrollable experimental effects in the models.

There are some exciting new developments taking place in regards to the use of transgenic mouse models that are reviewed in detail by Miller (2011), such as analysis of molecular and biochemical pathways, tumour growth and angiogenesis by real time *in vivo* imaging of fluorescent or bioluminescent tagged proteins and/or cells.

Most of the existing mouse models of PCa have inherent flaws such as that they are not strictly prostate specific, are androgen independent, have low frequencies and highly variable forms of PCa or do not progress to invasive adenocarcinoma and/or metastasis. Furthermore only the TRAMP model on the B6/FVB F_1 background has shown metastases to the bone as is common in human PCa metastases (reviewed by Ahmad, Sansom et al. 2008).

1.9.2.3 Cd151 and Cd9 knockout (KO) murine models

Our lab has generated a *Cd151* KO murine model on the B6 (Wright, Geary et al. 2004). We have also acquired a B6 *Cd9* KO strain from collaborators Drs E. Rubinstein and C Boucheix in France at INSERM 268, Villejuif, France and imported to Australia via the European Mouse Mutant Archive (www.emmanet.org, Heidelberg, Germany). We have extensively backcrossed both these models onto the FVB background as well. Characterisation of the models has revealed some pathology associated with CD151 and CD9 deletion as detailed in section 1.8.5. Briefly, the *Cd151* KO mice develop kidney disease on the FVB background while remaining healthy on both the B6 and B6/FVB F_1 backgrounds (Sachs, Kreft et al. 2006, Baleato, Guthrie et al. 2008). *Cd151* null mice have also been shown to have defective wound healing capabilities and impaired platelet function (Wright, Geary et al. 2004, Cowin, Adams et al. 2006, Geary, Cowin et al. 2008). The female CD9 KO is infertile but otherwise the strain displays a normal healthy phenotype (Le Naour, Rubinstein et al. 2000).

1.9.3 Normal mouse prostate histology

The various lobes of the normal mouse prostate have been well characterised and can be distinguished by histology (Gingrich, Barrios et al. 1999, Kaplan-Lefko, Chen et al. 2003, Shappell, Thomas et al. 2004). The dorsal prostate histology is notable for its columnar epithelial lumen cells, moderate infolding and homogenous and eosinophilic luminal secretions (Figure 1-5, A and B).The lateral lobes are distinguished by the cuboidal epithelial cells of the lumen, that have relatively little infolding and the secretions are notably particulate, as well as being eosinophilic (Figure 1-5, C and D). The ventral lobes share some histological characteristics with the lateral lobes in that there is very little infolding, however the cells are columnar and the secretions are pale, non-particulate and serious in nature (Figure 1-5, E and F). The anterior lobe also has columnar epithelial cells and is defined by

the finger like projection protruding into the lumen with homogenous secretions (Figure 1-5, G and H).

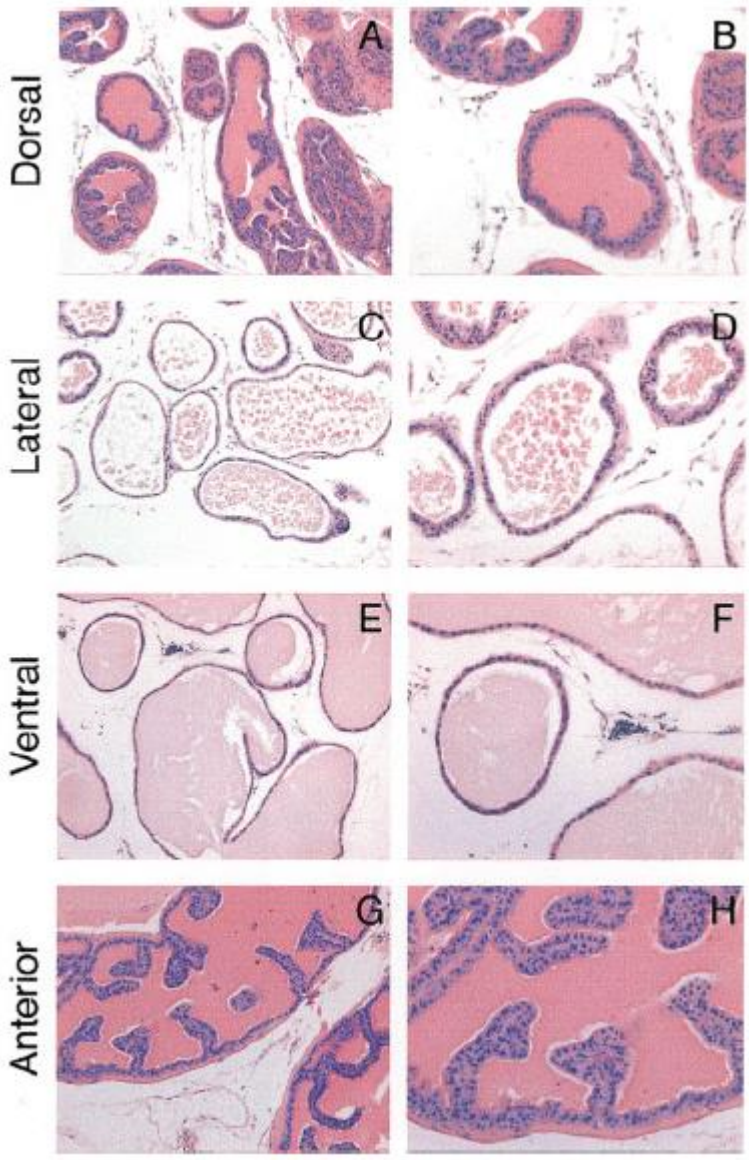

Figure 1-5: Histological representation of the four lobes of the mouse prostate.
The four lobes of the mouse prostate are represented here by H&E sections (modified from Kaplan-Lefko, Chen et al. 2003). Panels A and B represent the dorsal lobe at 100x and 200x magnification respectively. Panels C (100x) and D (200x) represent the lateral lobe. Panels E and F represent the ventral lobe at 100x and 200x magnification respectively, while panels G (100x) and H (200x) represent the anterior lobe. Reproduced with permission (Kaplan-Lefko, Chen et al. 2003).

1.9.4 TRAMP prostate pathology

The Gleason grading system used to grade human PCa is based on pathological and clinical parameters specific to the human disease and is not applicable to the mouse models due to the different anatomy. A pathology grading classification for tumour progression specific to the TRAMP model was devised by Greenberg's team who developed the model (Gingrich, Barrios et al. 1999). This original classification system has been revised and updated over the years by the same team (Kaplan-Lefko, Chen et al. 2003) and others, Shappel *et al.* (2004), Chiaverotti *et al*. (2008) and most recently by Berman-Booty *et al.* (2011) who also briefly reviewed the pre-existing grading classifications systems. The original grading system developed in Greenberg's lab and the much aligned updated grading system by the same group, devised specifically for the B6/FVB F_1 mice (Kaplan-Lefko, Chen et al. 2003) are still the most widely used systems. The systems mainly differ in that the updated system does not separate the presumed cancer precursor, PIN to low and high grades and includes the additional cancer grading subset of phyllodes-like lesions. With this in mind experimental research not specifically focused on PIN and using F_1 animals tend to use the updated Greenberg system, as is the case in this study. This classification system has been reviewed in detail many times (Kaplan-Lefko, Chen et al. 2003, Berman-Booty, Sargeant et al. 2011). Briefly the system classifies PIN as having elongated, hyperchromatic nuclei with associated stratification (represented in Figure 1-6). Epithelial cells are tufted, stratified and form micropapillary structures into the lumen of the prostate glands that can may have cribriform structures, with increased mitotic and apoptotic events. Well differentiated (WD) carcinomas in comparison to PIN have reduced nuclei atypia that are smaller and rounded, mitotic and apoptotic events are increased with overall smaller sized glands. Moderately differentiated (MD) carcinomas contain mostly anaplastic sheets of cells with dispersed remnants of prostate glandular structures. Poorly differentiated carcinomas (PD) are made up of solid sheets of pleomorphic cells that have high

nuclear to cytoplasmic ratios, can be highly vascularised and contain necrotic regions.

The subsequent revised classification systems vary little from one another in regards to descriptive terminology and seem more to address needs specific to the research being undertaking by the revising authors, such as assigning numerical scores for quantification. The Bar Harbour system (Shappell, Thomas et al. 2004) should be mentioned as it is by far the most detailed classification system to date. It was created from a culmination of three meetings attended by members of the Prostate Pathology Committee of the Mouse Models of Human Cancer Consortium. However the classifications system's strong points are also its hindrance for acceptance to the wider research community as it requires a pathologist to decipher the sometimes minute details, which are far beyond the scope of many research questions.

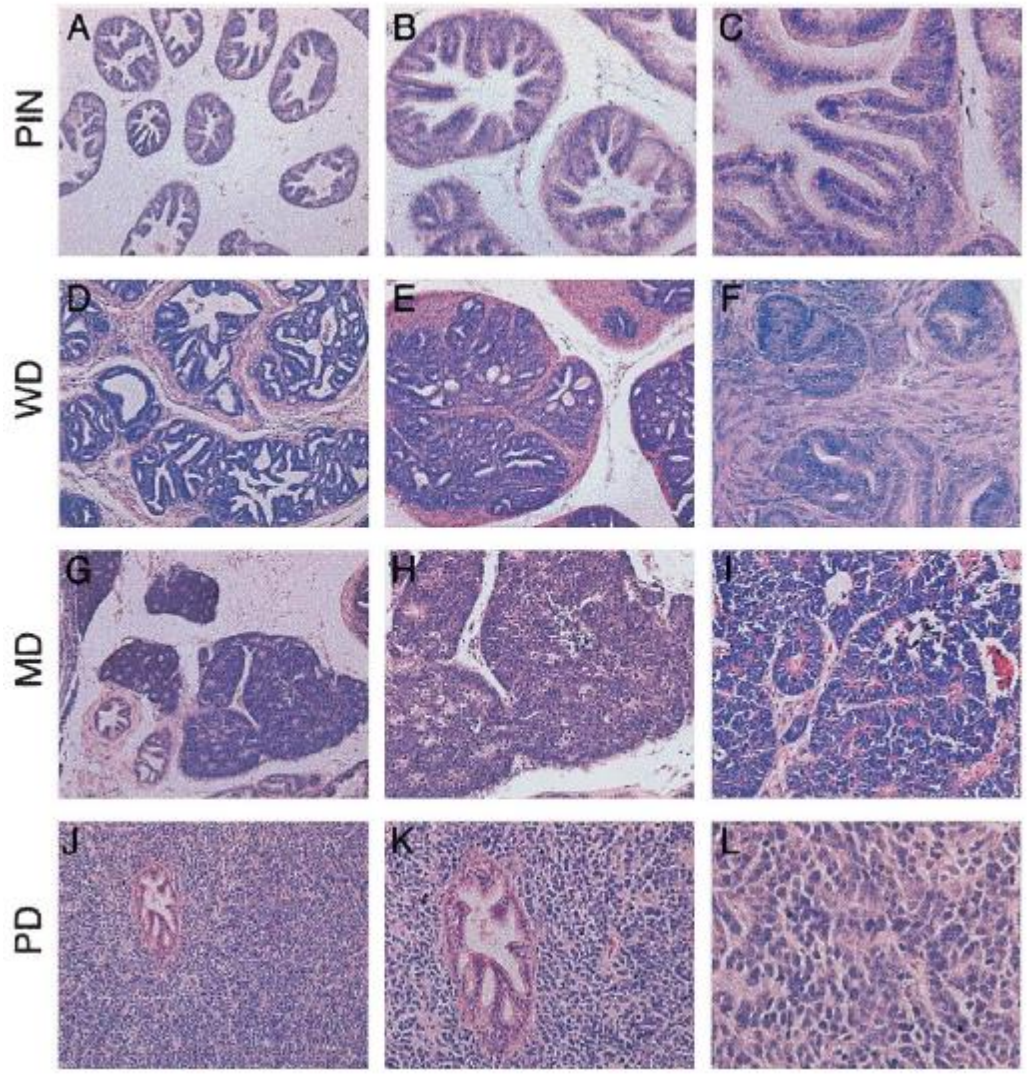

Figure 1-6: Representation of the TRAMP histopathology.
Prostatic intraepithelial neoplasia (PIN) is represented in panels A, B and C at 100x, 200x and 400x magnification respectively. Well differentiated (WD) PCa is represented in panels D, E and F (100 x, 200x and 400x magnification respectively). Moderately differentiated (MD) PCa is represented in panels G, H and I (100x, 200x and 400x). Poorly differentiated (PD) PCa is represented in panels J, K and L (100x, 200x and 400x magnification respectively). Reproduced with permission (Kaplan-Lefko, Chen et al. 2003).

1.9.4.1 Differences in mouse and human prostate anatomy

There are many compelling arguments validating the use of animal models in PCa research; however there are some anatomical differences between the mouse and human prostate that need to be addressed and fully understood to allow the

scientific data to be interpreted and translated across species. The differences between human and mouse prostate anatomy have been extensively reviewed elsewhere (Kaplan-Lefko, Chen et al. 2003, Ahmad, Sansom et al. 2008).

As previously explained (1.1.1) the human prostate is spatially contained as a single organ with three zones, whereas the mouse prostate has 4 distinct lobes ventral, dorsal, lateral and anterior, with each lobe containing a left and right segment as shown in Figure 1-7. The lobes do not fully surround the urethra as in the human prostate and smooth muscle is much sparser in the surrounding stroma of the mouse prostate. The mouse dorsal and lateral lobes, where the *SV40 T-ag* oncogene is expressed, are most analogous to the peripheral zone of the human prostate, where 68% of human PCa initiates (McNeal 1988). The anterior lobe corresponds to the central zone of the human prostate due to the spatial alignment with the seminal vesicles and ejaculatory ducts, and in both cases has very low incidence of PCa. The ventral lobe of the mouse prostate, also a site of *SV40 T-ag* expression and the transitional zone of the human prostate have no cross species counterparts. Both are intermediate in terms of disease showing lower incidence of PCa than the dorsal/lateral lobes and peripheral zones, however the transitional zone is the sole site of BPH in humans. In both humans and mice the urogenital tract originates from the urogenital sinuses and Wolffian ducts. They similarly contain prostatic lumen in both species consisting of epithelial cells which are androgen responsive for growth, basal and neuroendocrine cells (Szmulewitz and Posadas 2007, Tang, Wang et al. 2008).

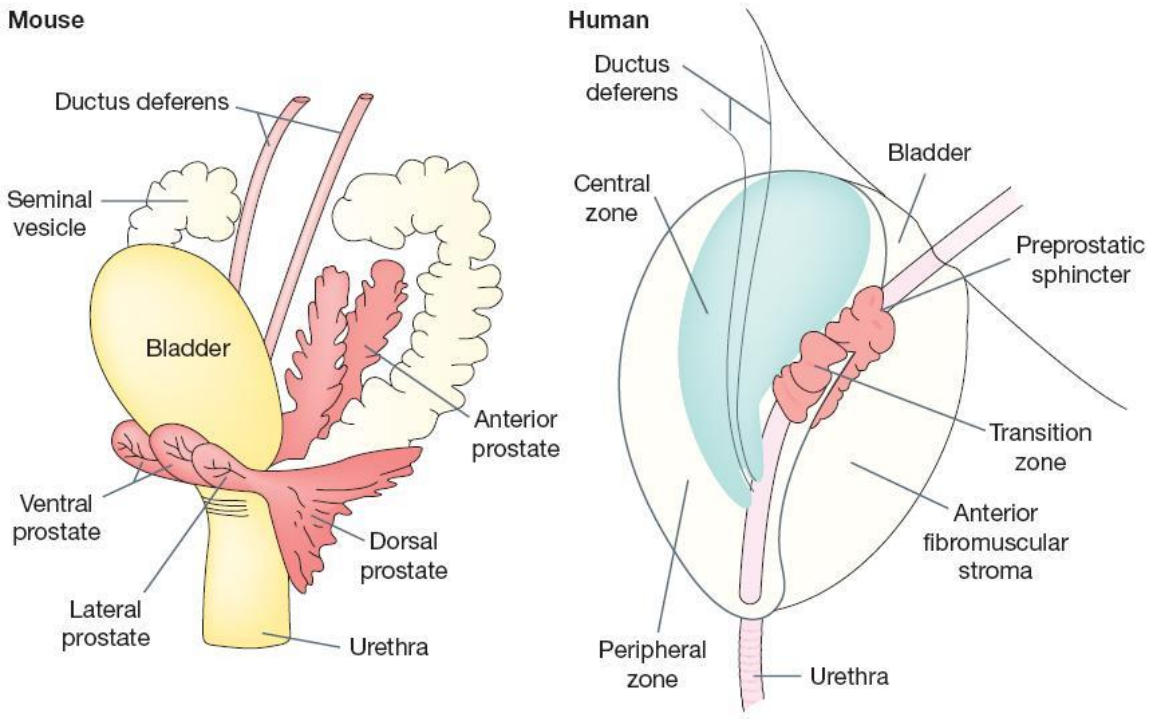

Figure 1-7: Comparison of mouse and human prostate anatomy.
Representatives of the different anatomies between the mouse and human lower urogenital tract. Reproduced with permission (Ahmad, Sansom et al. 2008).

1.10 *Summary and project outline*

Two major unmet needs in prostate cancer are firstly, understanding the molecular mechanisms of the metastatic cascade and secondly, the stratification of patients diagnosed with PCa in regards to their outcome and treatment modalities. This thesis addresses both these issues through the hypothesis that *Tetraspanin proteins influence prostate cancer progression and also can be used as an adjunct to classical grading methods to predict the outcome of treatment and, ultimately to determine which patients require adjuvant therapy*.

The project approaches this through two specific aims; firstly to determine whether the tetraspanins CD151 and CD9 directly influence PCa initiation and/or progression in a transgenic mouse model. In PCa the metastatic disease state confers a very poor prognosis. Given that reports have stated a nearly 100% five

year survival rate for men that are diagnosed with PCa still confined within the gland compared to only 31% five year survival for men with metastatic PCa at diagnosis (N.H.S 2009), knowledge of the molecular mechanisms behind the metastatic process may be of great benefit to patients of PCa. As previously mentioned, CD151 and CD9 have been implicated in progression and metastatic potential of PCa. The *Cd151* and *Cd9* KO murine models have been crossed with the TRAMP prostate cancer model, to create two distinct new transgenic models of PCa, the CD151/TRAMP and CD9/TRAMP KO models. Characterisation of the two new models is discussed in chapter 3 and then for the first time, the direct effects of *Cd151* and *Cd9* on onset of *de-novo* primary PCa and subsequent spontaneous metastasis are detailed in chapters 4 and 5 respectively. We report here that the ablation of *Cd151* and *Cd9* did not affect the development of primary PCa. However ablation of *Cd151* did reduce metastatic incidence to the lungs while ablation of *Cd9* increased metastatic incidence to the liver in the TRAMP model. These studies confirm that *Cd151* and *Cd9* principally act to regulate metastasis.

The second aim of the project was to undertake clinical studies analysing the prognostic significance of tetraspanins CD151, CD9, CD82 and Tspan8 in PCa Currently no one marker is specific and sensitive enough to be used alone to diagnose PCa or determine which tumours will progress to cause morbidity and which will remain indolent (reviewed by Stricker 2001, Rubin 2008, Schröder 2008). The National Health and Medical Research Council in Australia (2002) highlighted the problem with PCa markers in their most recent guidelines on treatment of localised PCa, by stating “The refinement and application of markers (either individual or combined) to predict outcome in prostate cancer remains one of the most important tasks for molecular biologists and epidemiologists”. More recently Lilja *et al*. (2008) stated “There is great need for more accurate markers of response to treatment”. Also recently Rubin (2008) has opened a paper with “The clinical dilemma today in the management of PCa is to distinguish men who need definitive treatment from men who have indolent disease” .

CD151 has shown promise in a small cohort of PCa patients (Ang, Lijovic et al. 2004). This will be expanded on, with a larger cohort of human PCa samples with matched normal samples and include other promising tetraspanins CD9, CD82 and Tspan8. Expression of the tetraspanins CD151 and Tspan 8 was shown to be positively correlated with PCa progression, while CD9 and CD82 expression was negatively correlated with PCa progression. The tetraspanins showed limited prognostic values compared to previous studies and possible explanations for this are discussed in chapter 6.

Chapter 2: Materials and Methods

2.1 *Overview*

For clarity, this chapter has been set out into two separate sections that represent the two main aims of the project. Firstly, methods that deal with the animal experiments are described in section 2.3 and secondly methods that deal with the human TMA biomarker experiments are described in section 2.4.

2.2 *General chemicals and reagents*

All chemicals and reagents were research or molecular biology grade, and purchased from Sigma Aldrich (St Louis, MO) or Merck Pty Ltd (Kilsyth, VIC) unless otherwise stated. Buffers and stock solutions are detailed in appendix 1.

2.3 *Methods relating to animal experiments*

2.3.1 Breeding of transgenic mice

2.3.1.1 General

To address the research question of whether the tetraspanins CD151 and CD9 influence PCa, the TRAMP (PCa model) mice (Greenberg, DeMayo et al. 1995) were crossed, independently with both the *Cd151* KO mice (Wright, Geary et al. 2004) and *Cd9* KO mice (Le Naour, Rubinstein et al. 2000). This resulted in two new models, the CD151/TRAMP and CD9/TRAMP models.

Mice were bred at the Australian Bio Resource (ABR) specific pathogen free animal facility (Moss Vale, NSW). All animal work was covered by the University of Newcastle ethics approval A-2008-130 and Biosafety approval 247-2008.

2.3.1.2 TRAMP mice

TRAMP mice originally produced in the Greenberg lab (Greenberg, DeMayo et al. 1995) were a kind gift from Dr Matt Naylor of the Garvan Institute NSW. The *SV40* transgene in the TRAMP mice (detailed in 1.9.2.1) was maintained in heterozygous female mice on the B6 background to prevent the initiation of prostate cancer in the breeder mice and to avoid genetic drift.

2.3.2 CD151/TRAMP breeding scheme

Breeding of the CD151/TRAMP experimental animals involved two constraints. Firstly, homozygous *Cd151* KO mice on the FVB/N (FVB) background develop kidney disease requiring the use of *Cd151* heterozygous FVB breeders (Baleato, Guthrie et al. 2008). Secondly it was required that the final experimental animals were bred to consist of a 50% B6 and 50% FVB (F_1) background to eliminate the possibility of unwanted tumour pathologies as detailed in section 1.9.2.1 and importantly, to eliminate random re-assortment of alleles from the two strains.

Accordingly the breeding schedule involved the B6 TRAMP females being crossed with the B6 male *Cd151* KO mice. Then, to achieve the generation of truly homogenous (B6/FVB) background F_1 hybrid KO with a single, final cross, the B6 TRAMP, *Cd151* heterozygous female progeny were crossed with the FVB *Cd151* heterozygous males to produce the CD151/TRAMP F_1 animals as in Figure 2-1.

It should be noted that the FVB/N *Cd151* null mice used in the final cross had previously been generated by backcrossing the original inbred C56BL/6 *Cd151* null mice onto the FVB strain for no less than 10 generations (Baleato, Guthrie et al. 2008). The breeding strategy used in this project allowed the use of littermate *Cd151* wt, heterozygous and KO controls in all experiments. The experimental animals only consist of male mice due to only male mice developing prostate

tumours in the models. Expected frequencies of the male experimental animals are displayed next to the genotypes in Figure 2-1.

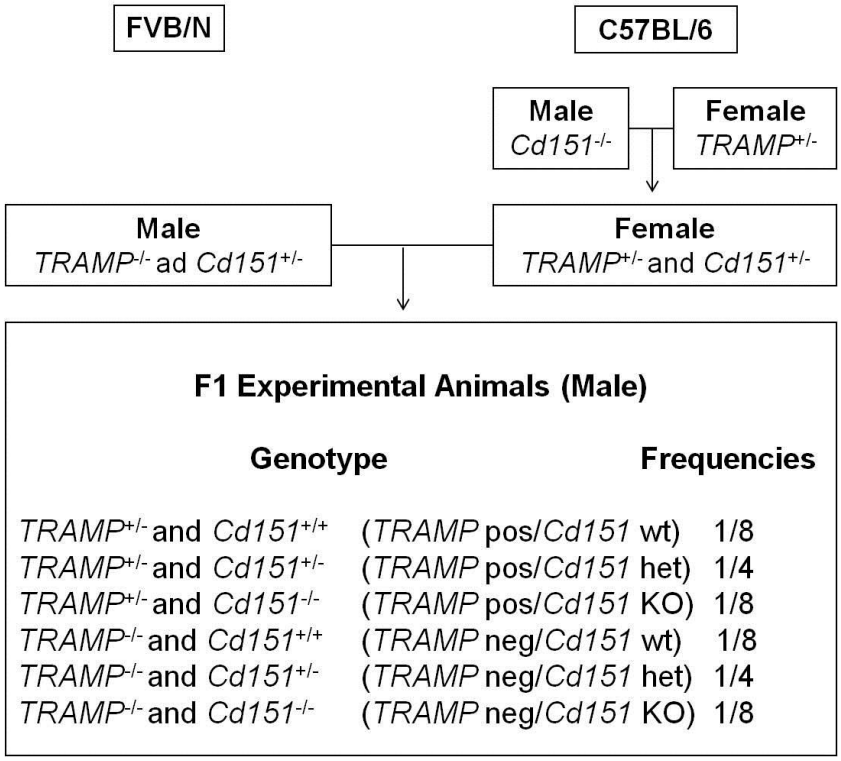

Figure 2-1: Breeding strategy to produce the CD151/TRAMP experimental animals.
To produce the required CD151/TRAMP F_1 experimental animals, TRAMP B6 females were crossed with *Cd151* KO B6 males. The resultant *Cd151* het B6 TRAMP females were then crossed with *Cd151* heterozygous FVB males. Genetic frequencies shown are specific for the male experimental animals.

2.3.3 CD9/TRAMP breeding scheme

The *Cd9*$^{+/-}$ mice were originally generated on the C57BL/6 background at INSERM 268, Villejuif, France and imported to Australia via the European Mouse Mutant Archive (www.emmanet.org, Heidelberg, Germany). To produce the CD9/TRAMP experimental animals the breeding schedule as with the CD151/TRAMP also had constraints. Specifically the *Cd9* homozygous null females are infertile (Le Naour, Rubinstein et al. 2000) and again the B6/FVB F_1 experimental animals were required. Accordingly the breeding schedule followed a similar format to that for the CD151/TRAMP animals, as in Figure 2-2. Briefly, the B6 TRAMP females were

crossed with the B6 male *Cd9* KO mice. Then the B6 TRAMP, *Cd9* heterozygous female progeny were crossed with FVB *Cd9* heterozygous males to produce the CD9/TRAMP F_1 experimental male animals. As with the CD151/TRAMP breeding strategy, littermate controls were used throughout, and the FVB/N *Cd9* null mice used in the final cross had previously been generated by backcrossing the original inbred B6 *Cd9* null mice onto the FVB strain for no less than 10 generations.

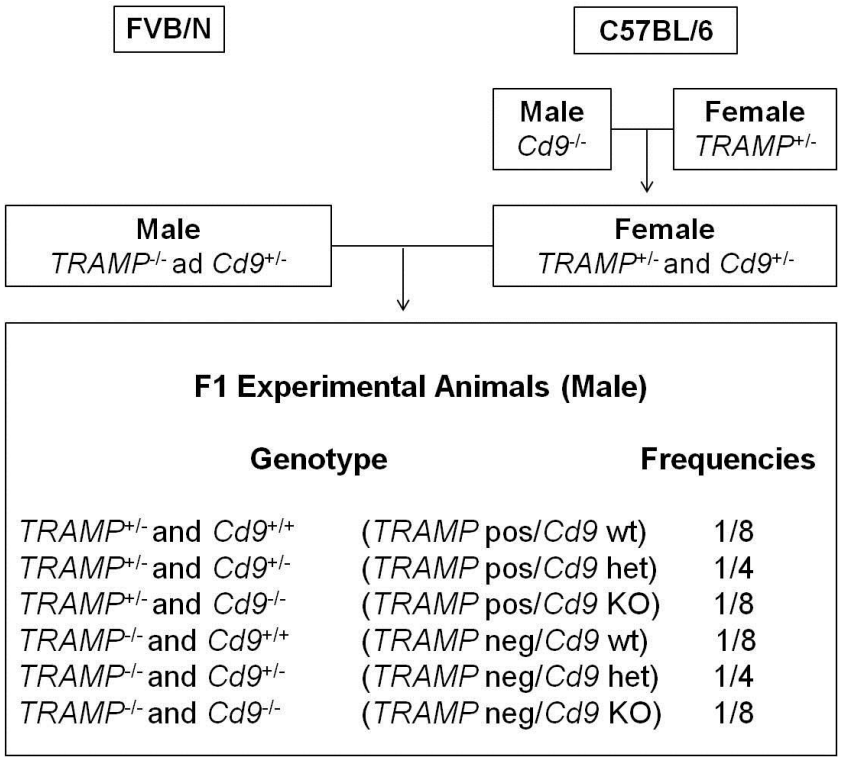

Figure 2-2: Breeding strategy to produce the CD9/TRAMP experimental animals.
To produce the required CD9/TRAMP F_1 experimental animals, TRAMP B6 females were crossed with *Cd9* KO B6 males. The resultant *Cd9* het B6 TRAMP females were then crossed with *Cd9* het FVB males. Genetic frequencies shown are specific for the male experimental animals.

2.3.3.1 Husbandry of Experimental Animals

Ear punches were collected at weaning and sent to the University of Newcastle (UoN) for genotyping (2.3.4). The animals were then allocated to the appropriate experimental groups (see Table 2-4 and Table 2-5) and surplus animals of unwanted genotypes were culled. The required experimental animals were

exported from the ABR to either UoN between 8 and 12 weeks of age for general monitoring of tumour development or to the University of New South Wales (UNSW) at 4 weeks of age for bioluminescence experiments (section 2.3.5.2) and housed in PC2 animal housing facilities. At UoN, since the facility is not specific pathogen free (SPF), the animals were housed in individually ventilated cages (IVC) (Airlaw, Smithfield, NSW) with “igloos” for shelter. Bedding of 1/8 inch corn cob (Shepherd speciality paper Inc., Rydalmere, NSW) was changed twice a week. Diet consisted of a formulated pellet diet (Specialty Feeds, Glen Forest, WA) that was autoclaved prior to dispensing and tap water mixed with 0.1% sodium hypochlorite, both provided *ad libitum*. The animal rooms were controlled for temperature (21ºC), humidity (40-50%) and light cycle (12h/12h). Housing conditions were similar at ABR and UNSW except feed at ABR was Gordon’s premium irradiated mouse pellets (Gordon's Specialty Stockfeed, Yanderra, NSW)

2.3.4 Genotyping of Mice

2.3.4.1 DNA extraction

Tissue samples were collected in the form of ear punches. The “High Speed Easy DNA Extraction” kit (HiSpEx; Fisher Biotech, Subiaco, WA) was used as per the manufacturer’s instructions. Briefly, the lysis reagent and buffer were added directly to the sample in an eppendorf tube and incubated at 95ºC in a dry heat block for 20 min. The lysis reaction was terminated by addition of a stop reagent and the digested DNA stored at -20ºC.

2.3.4.2 Polymerase chain reaction (PCR)

PCR mastermixes were prepared in a still-air box that had been irradiated with UV light for 20 min prior to use to reduce the risk of contamination. All PCR kit reagents (Promega, Madison, WI) and primers (Table 2-1) were kept on ice and aliquoted in quantities as stated Table 2-2. Samples were mixed thoroughly and

centrifuged briefly before being loaded into a Mastercycler ProS™ thermocycler (Eppendorf, Hamburg, Germany). Thermocycler PCR conditions for each primer set were as in Table 2-3. Each PCR experiment contained both PCR negative and positive controls, while the *TRAMP* PCR also included an internal run control which was specific for *casein*. The internal control was not included in the *Cd151* or *Cd9* PCR, due to competitive primers and bands being of similar sizes. PCR products were stored at 4ºC prior to electrophoresis. The primer sets in Table 2-1 were optimised from previously described original primer sets, specifically *Cd151* (Wright, Geary et al. 2004), *Cd9* (Claude Boucheix and Francois LeNaour, INSERM U602, France, personal communication), *SV40* (Greenberg, DeMayo et al. 1994) and the internal control casein primer sequences were obtained from N.Greenberg's now defunct website, URL http://128.249.134.198.

Table 2-1: PCR primer sets.
Primer sequences for genotyping experimental animals.

Oligonucleotide	Sequence 5' to 3'	Product size (~bp)
Cd151 wt Fwd	CAGCTTAGGACCTCTTCTCA	420
Cd151 wt Rev	GCTCCATGTTCCTGTACACT	
Cd151 KO Fwd	CAGCTTAGGACCTCTTCTCA	440
Cd151 KO Rev	ATGATAACCCACCATGTGTC	
Cd9 wt Fwd	TGCAGGCATGGAGGCGCAGC	450
Cd9 wt Rev	GTGCCGGCCTCGCCTTTCCC	
Cd9 KO Fwd	CTGGTCACACCCCCTAACGGAG	600
Cd9 KO Rev	AGAGCTTGGCGGCGAATGGGCT	
SV40 (*TRAMP*) Fwd	CCGGTCGACCGGAAGCTTCCACAAGTGCATTTA	600
SV40 (*TRAMP*) Rev	CTCCTTTCAAGACCTAGAAGGTCCA	
Casein (control) Fwd	GATGTGCTCCAGGCTAAAGTT	500
Casein (control) Rev	AGAAACGGAATGTTGTGGAGT	

Table 2-2: PCR mastermixes.
Reagent amounts for PCR master mixes for each primer set (total volume is 25µl).

Target gene	Reagents							
	5X Buffer	MgCl2 (mM)	DNTPs (µM)	Target Primer (ng per Fwd & Rev)	Control Primer (ng per Fwd & Rev)	DNA (µl)	Taq (U)	Water (µl)
Cd151	1X	1.5	200	50	0	1.25	5	16.15
Cd9	1X	1.5	200	50	0	1.25	5	16.15
SV40 (TRAMP)	1X	3	200	120	120	1.25	10	12.6

Table 2-3: PCR thermocycler conditions.
Cycling conditions for each primer set

Cycle repeats	**1 X**	**30 X**		
Target gene	Initial denaturation	Denaturation	Annealing	Elongation
Cd151	5 min at 94ºC	1 min at 94ºC	1 min at 55ºC	1 min at 72ºC
Cd9	5 min at 94ºC	1 min at 94ºC	1 min at 62ºC	1 min at 72ºC
SV40 (TRAMP)	2 min at 94ºC	1 min at 94ºC	1 min at 60ºC	1 min at 72ºC

2.3.4.3 DNA electrophoresis

PCR products were separated in a horizontal electrophoresis apparatus (Biorad, Hercules, CA) on 1.5% agarose gels (Applichem, Darmstadt, Germany) in 1X sodium borate buffer and 1 % ethidium bromide. 10 µl of the PCR product was loaded into the preformed wells and gels were run in 1X sodium borate running buffer at 250 volts (V) for 5 min for Cd151 and Cd9 PCR products and 25 min for TRAMP products. The stained DNA was visualized by fluorescence using the LAS-1000 imager (Fuji, Tokyo, Japan).

2.3.5 Experimental groups of mice

There were three experimental animal groups, firstly, the basic tumour progression characterisation group (house at UoN) which involved small numbers of animals culled at earlier time points of 10 or 20 weeks to validate and characterise the onset of PCa and metastasis in the models. Secondly, the palpable tumour burden endpoint study group (also housed at UoN) which analysed the effects of the tetraspanins *Cd151* and *Cd9* on PCa tumour onset and metastatic incidence. Lastly, the bioluminescence study group, housed at UNSW which involved *Cd151* wt and *Cd151* KO animals being given intra-cardiac injection of bioluminescence tagged TRAMP cell lines that were *Cd151* wt. These animals were analysed in regards to metastatic burden to see effects of the *Cd151* KO in the environment (animal) only, as opposed to the ablation of *Cd151* in both the animal and developing tumour in the endpoint group. This was designed to allow analysis of the effects of the *Cd151* KO in the environment on the metastatic incidence rates.

Once genotyped, animals were allocated to appropriate experimental groups in a sequential manner based on date of birth. Mice were allocated firstly, to the tumour onset characterisation groups, followed by the endpoint study groups and finally the bioluminescence study groups. Table 2-4 shows the number of CD151/TRAMP animals of specific genotypes allocated to the experimental groups and Table 2-5 shows experimental groups for the *Cd9* animals. Note that the bioluminescence studies only comprised of *Cd151* animals. The number of animals allocated to each group was in slight excess in regards to statistical advice to compensate for any attrition, and therefore may differ slightly from the number of mice stated in the results. All experimental animals were co-housed and compared with littermate controls.

Table 2-4: Experimental groups of CD151 animals based on genotype.
Table headings show which group animals were allocated to and at what age they were culled in parenthesis, with number of animals and genotypes in the body of the table.

Genotype	Endpoint study (40 weeks)	Bioluminescence study (8-9 weeks)
TRAMP$^{+/-}$ and *Cd151*$^{+/+}$	29	-
TRAMP$^{+/-}$ and *Cd151*$^{+/-}$	25	-
TRAMP$^{+/-}$ and *Cd151*$^{-/-}$	31	-
TRAMP$^{-/-}$ and *Cd151*$^{+/+}$	13	8
TRAMP$^{-/-}$ and *Cd151*$^{+/-}$	-	-
TRAMP$^{-/-}$ and *Cd151*$^{-/-}$	15	11

Table 2-5: Experimental groups of CD9 animals based on genotype.
Table headings show which group animals were allocated to and at what age they were culled in parenthesis, with number of animals and genotypes in the body of the table.

Genotype	PCa onset (10 weeks)	PCa onset (20 weeks)	Endpoint study (40 weeks)
TRAMP$^{+/-}$ and *Cd9*$^{+/+}$	7	10	33
TRAMP$^{+/-}$ and *Cd9*$^{+/-}$			28
TRAMP$^{+/-}$ and *Cd9*$^{-/-}$		3	35
TRAMP$^{-/-}$ and *Cd9*$^{+/+}$			10
TRAMP$^{-/-}$ and *Cd9*$^{+/-}$			-
TRAMP$^{-/-}$ and *Cd9*$^{-/-}$			10

2.3.5.1 Endpoint study group

2.3.5.1.1 ***Palpation of mice***

Mice in the endpoint group (UoN) were palpated blind with respect to genotype, every 2-3 days for primary tumour development. Animals were held firmly by the

scruff and the tail held in place between the 4th and 5th finger to stretch out the abdomen. The thumb and forefinger palpated both ventral and lateral areas surrounding the urogenital region for any irregularities. If a tumour was detected the mouse was immediately culled, autopsied and the time to palpable tumour recorded. Tumour, liver, lungs and any other overtly abnormal organs were harvested and fixed for subsequent analysis. The presence of lung and liver tumour metastatic lesions was determined as described in section 2.3.14.3.
We initially aimed to follow the tumour onset and progression by crossing in a luciferase reporter gene driven by a prostate specific promoter to the mouse model and monitoring by non-invasive *in-vivo* bioluminescence imaging as reported by Hsieh *et al.* (2007). However we were unable to obtain the necessary transgenic strain, due to the commercial company being unable to revive the mouse line from frozen embryos. We did try to image tumour growth in the TRAMP model with fluorescent probes that are activated by the tumour associated proteases, cathespin and matrix metalloproteinases (ProSense 750, CatB 750 and MMPSense 680 respectively; PerkinElmer, Waltham, MA) using the MSFxPro small animal imager (Carestream Health, Rochester, NY). However we were unsuccessful due to non-specificity of the probes and poor localisation to the tumour sites.

2.3.5.1.2 ***Euthanasia and dissection of mice***

2.3.5.1.2.1 ***General***

Surgical instruments were washed in 7X detergent (MP Biomedicals, Seven Hills, NSW) followed by spraying with DNA exitus (AppliChem, Darmstadt, Germany). Mice were euthanased in a clean plastic container via asphyxiation with increasing amounts of carbon dioxide gas (CO_2) for 60 s, followed by immediate cervical dislocation. Absence of breathing, pedal and corneal reflexes were monitored for confirmation of death. If multiple mice were to be euthanased consecutively, they were housed in a separate room until time of euthanasia. Once euthanased, total

body weights were determined and recorded. Mice were then fastened by tape to sterile benchcloth to reduce movement during dissection. A ~2mm x 2 mm section of ear from each experimental animal was excised and placed in an eppendorf tube for reconfirmation of genotype. Each carcass was sealed in a plastic zip lock bag and stored at -80ºC until reconfirmation, in case of a discrepancy in which case another tissue sample could be harvested from the original source. In the rare cases that the two subsequent PCR genotyping results from the two post mortem tissue samples did not match the animals were excluded from the study.

2.3.5.1.2.2 ***Gross removal of urogenital/reproductive tract***

Mice were sprayed with 70% ethanol to reduce tissue contamination with body hair. A midline ventral incision was made to the outside skin layer just anterior to the penis to expose the peritoneal muscle wall and preputial gland. The semi-transparent peritoneal muscle wall was then carefully incised along the ventral midline just cranial to the preputial gland to expose the urogenital tract. Both layers of skin were then incised from the initial incision laterally towards both hind legs creating a “Y” flap revealing the urogenital tract. At this point photos were taken with a digital camera (Olympus, Tokyo, Japan). The testes and associated fat pads were removed by gripping the testes and pulling away from the peritoneal cavity until encountering resistance from the attached pairs of ductus deferens and internal spermatic veins and arteries, which were cut as close as possible to the prostate. The urogenital tract was moved by holding only either the bladder or urethra, to minimise damage to the prostate. While gently lifting the prostate, by the bladder, away from the peritoneal cavity the urethra and prostatic ramus (prostate blood supply) were cut as dorsally as possible without damaging the underlying femoral vein as its blood flow impeded further dissection. The entire urogenital tract containing seminal vesicles, bladder, urethra, ampullary gland, dorsal, ventral, lateral and anterior prostate lobes was pulled away from the peritoneal cavity until the set of ureters became stretched and visible allowing them to be cut close to the

prostate. The bladder was purged of urine by a small incision and the whole urogenital tract was weighed and photographed.

2.3.5.1.2.3 ***Partial and full micro-dissection of prostate lobes***

Under a dissecting microscope any associated fat and visceral tissue was removed. The anterior prostate was gently removed along with the seminal vesicles by grasping them at the point of insertion on the urethra with tweezers and gently tearing them away. The deferens and any associated veins and arteries were trimmed back and discarded. The bladder was removed by carefully stretching it out from the urethra with tweezers and cutting around the circular connection that joins it to the urethra.

When required, the prostate was further dissected into the eight individual lobes that make up the full mouse prostate. The prostate lobes (two of each) were removed in the order of ventral, lateral, dorsal and anterior by gripping the prostate lobe proximal to the urethra at the point of insertion and gently pulling it away from the urethra. Once all lobes had been removed the seminal vesicles were removed from their point of insertion to the urethra. Finally the urethra was inspected to make sure the ampullary gland was still attached to the urethra to eliminate any contamination to the removed prostatic lobes.

2.3.5.1.2.4 ***Collection of tumours and other organs***

The collection of prostatic tumour tissue was achieved by following the protocols above for removing the urogenital tract, however once placed in the petri dish and weighed, a sample of the tumour, approximately 10mm x 5mm x 3mm (L x B x D) was sliced away from the seminal vesicles and bladder (as best as possible) and immediately placed into 10% neutral buffered formalin (Clinipure, Middlesex, United Kingdom) or liquid nitrogen. A sample of liver tissue of approximately the same size as the tumour sample was taken from the bottom left side of the median lobe. For collection of the lungs the original ventral incision was extended right

through to the chin of the mouse and the diaphragm and rib cage were trimmed away to expose the lungs. The tracheal sheath was removed to expose the trachea and a 26 gauge needle attached to 10 ml syringe (Terumo, Elkton, MD) containing 10% neutral buffered formalin (Clinipure) was inserted into the trachea to inflate and fill the lungs with the formalin (1-2 ml). The trachea was cut and lungs removed from the chest cavity. The heart and excess trachea were cut away as close as possible to the lungs. Any other organs with irregularities were also collected.

2.3.5.2 Bioluminescence study group

As previously explained (2.3.5) we undertook preliminary animal experiments to determine the effects that the environment (animal) alone had on metastatic incidence rates of PCa tumour cells. Briefly, *Cd151* wt and *Cd151* KO F_1 male litter mate mice were injected with the TM2-Luc15 bioluminescence tagged prostate cancer cell line and metastatic incidence rates were analysed by *in-vivo* bioluminescence imaging and histopathology. The work was done with collaborators, Dr Carl Power and Dr Tzong-Tyng Hung, at the University of New South Wales (UNSW) and was covered by the UNSW animal ethics number ACEC11/107B.

2.3.5.3 Development of the TRAMP TM2-Luc15 cell line

The PCa cells that were used for the injections into the animals were developed by Dr Carl Power at the U.N.S.W. Cells, originally isolated from a metastatic liver lesion in a B6 male TRAMP mouse were cultured in DMEM supplemented with 10% fetal calf serum (FCS) and L-Glutamine under standard conditions of 37ºC and 5% CO_2, to expand the line. Then $1x10^6$ cells/ml in PBS were injected into the tibia of a B6 animal and the cells from the tumour lesions once again harvested and cultured as per previous conditions. The spontaneously immortalised cultured cells were then transfected with a luciferase tag, specifically pCMVLuc-FSR

(Genlantis, San Diego, CA), utilising Lipofectamine 2000 (Invitrogen) as the transfection agent. Resistance to Neomycin (418) was used to select stably transfected cells, and single colonies of the TM2-Luc15 cells were isolated for expansion with cell culture conditions as described above.

2.3.5.3.1 ***Intra-cardiac injections***

Once exported from ABR to the UNSW mice were acclimatised for one week as per UNSW ethics requirements. Mice were shaved with an electric shaver from abdomen to diaphragm prior to the intra-cardiac injections for sterility and ease, and then shaved again as needed prior to imaging to prevent signal reduction from the bioluminescence.

Mice were anesthetised with 2-3 % isoflurane with oxygen flow rate of 0.9 L/min. Mice were immobilised with tape tightly fixed across the abdomen to allow access for the needle to be inserted at 90º angle to the rib cage. 150 µl of the TM2-Luc15 cell suspension (at $1x10^7$ cells/ml in PBS) was drawn into a 1 ml syringe with 26 gauge needle. Importantly an air bubble was left between the fluid and the plunger; explained below. The needle was inserted ~5mm left of the sternum perpendicular to the ribcage through the thoracic cavity into the left ventricle. The back flow of bright red blood in to the needle and the pulsing movement in the air bubble between plunger and fluid confirmed positioning in the heart, then 100 µl of the cell suspension was injected directly into the heart (~$1x10^6$ cells injected).

2.3.5.3.2 ***In-vivo bioluminescence imaging of mice***

The TM2-Luc15 cells that were injected into the mice have a luciferase tag that can be utilised to non-invasively image the cells in the mice *in-vivo*. The mice were imaged 14 days post intracardiac injection and every subsequent seven days up to four weeks post injection on the IVIS Lumina imager (Caliper Life Sciences, Hopkinton, MA). The mice were given an intraperitoneal injection of D-Luciferin (150 mg/kg; Goldbio, St Louis, MO), anesthetised with 2-3 % isoflurane with

oxygen flow rate of 0.9 L/min and placed into the IVIS Lumina ventral side up on nose cones for further anaesthetic delivery. Mice were imaged 9 min post D-Luciferin injection for 1 min at medium binning, and then the animal was immediately rotated to image the dorsal surface.

2.3.5.3.3 ***In-vivo bioluminescence imaging end point and tissue collection***

At the 4 weeks post intracardiac injection the mice were imaged as previously described above. The mice were then skinned and the urogenital tract, kidneys, liver, lungs, heart, spleen and digestive tract removed and imaged *ex-vivo* along with the carcass separately. The carcass and other organs were fixed in 10% neutral buffered formalin for 24 h, then transferred to 70% ethanol and stored until processed (2.3.6) and analysed (2.3.14). A section of the liver was placed in cryomoulds (Tissue-Tek) and filled with optimal cutting temperature compound (OCT; Tissue-Tek), snap frozen in liquid nitrogen and stored at -80 ºC until processed (2.3.9.2).

2.3.5.3.4 ***In-vivo bio-imaging analysis***

The number of metastatic tumours was quantified visually from the *in-vivo* and *ex-vivo* images using the Living Image software (Caliper Life Sciences). Analysis was achieved by counting the bioluminescent “hotspots” from the images obtained. Due to the vast amount of metastases in the livers, compared to other sites in the animals, the counts from the liver bioluminescence are semi-quantitive due to the foci counted not always being totally separated by bioluminescence, thus histology was used to provide a better comparison between the groups (2.3.14.3).

2.3.6 Processing of formalin fixed paraffin embedded (FFPE) tissue samples

All procedures were carried out, and storage conditions were, at room temperature unless otherwise stated.

2.3.6.1 Tissue fixation

Dissected tissue was placed into biopsy cassettes (ProSciTech) and fixed in 10% neutral buffered formalin for 6 h, then transferred to 70% ethanol and stored until processed.

2.3.6.2 Tissue processing

The biopsy cassettes with the tissue inside were placed into a cassette jig in a Lynx II tissue processor (Electron Microscopy Sciences, Hatfield, PA). The processor was set up with an automated programme (Table 2-6)

Table 2-6: Conditions for processing of formalin fixed tissue in the LYNX II tissue processor.

Station #	Reagent	Time (min)	Sample arm	Temp (ºC)
1	70% Ethanol	20	Agitation	25
2	95% Ethanol	20	Agitation	25
3	95% Ethanol	20	Agitation	25
4	95% Ethanol	20	Agitation	25
5	100% Ethanol	20	Agitation	25
6	100% Ethanol	20	Agitation	25
7	100% Ethanol	20	Agitation	25
8	100% Xylene	20	Agitation	25
9	100% Xylene	60	Agitation	35
10	100% Paraffin	60	Agitation and vacuum	60
11	100% Paraffin	20	Agitation and vacuum	60

2.3.7 Tissue embedding

All procedures were carried out, and storage conditions were, at room temperature unless otherwise stated.

2.3.7.1 Formalin fixed paraffin embedded (FFPE)

Tissue was immediately transferred from the processor to the tissue embedding apparatus (Tissue-Tek, Tokyo, Japan). Cassettes were opened while submerged in paraffin and tissue segments transferred to 10 mm x 10 mm plastic disposable base moulds (ProSciTech) and filled with paraffin from a dispenser (Tissue-Tek). Backless cassettes (ProSciTech) were pre-soaked in the heated paraffin and placed on top of the moulds to serve as a fixture point for subsequent sectioning in the microtome. Once blocks were set they were popped from the moulds and stored for an indefinite period.
If required, prior to embedding the urogenital tracts dissected *en bloc* were cut transversally across the midline of the prostate on a slight posterior angle to reveal a cross sectional sample of ventral, dorsal and lateral lobes along with seminal vesicles, urethra, deferens and ampullary gland as described by Suwa *et al*. (2002).

2.3.7.2 Frozen tissue sections

Freshly dissected tissue was immediately placed in cryomoulds (Tissue-Tek) and filled with optimal cutting temperature compound (OCT; Tissue-Tek), snap frozen in liquid nitrogen and stored at -80 ºC.

2.3.8 Silanisation of glass microscope slides

Slides that were used to mount the FFPE tissue sections were coated with, 3-aminopropyltriethoxysilane (silane) to form a positively charged layer on the surface of the glass slides. The negatively charged tissue section readily adheres

to the slide and prevents sloughing during the sometimes rigorous IHC process, particularly the heat induced antigen epitope retrieval (HIER) step. Slide racks and trays were thoroughly washed in 7X detergent (MP Biomedicals), rinsed with ddH_20 and rinsed with small amounts of acetone (Chem Suppy, Gillman, SA) to remove any residual organic materials. Glass slides of standard dimensions (26mm x 76mm x 1mm; Livingstone, NSW) were placed into the horizontal metal slide holders (ProSciTech), incubated in a 2% silane/acetone solution for 5 min, followed by 3 consecutive washes in ddH_20 for 5 min each and dried at 60 ºC overnight. Treated slides were stored in their original slide boxes sealed in airtight plastic bags for a maximum of 6 months.

2.3.9 Sectioning of tissue blocks

2.3.9.1 FFPE

FFPE blocks were sectioned in a rotary microtome (ProSciTech) with a low profile blade (C.L Sturkley, Lebanon, PA). Blocks were trimmed at 10 µm to create a surface that consisted of a full section of tissue then sectioned at 5µm. Sections were “floated” on the surface of a 40ºC water bath, positioned onto silanised slides then incubated at 60 ºC for 2 min and used within 2 weeks for IHC.

2.3.9.2 Fresh frozen

Sections were cut on a Leica CM1900 cryostat (Leica, Wetzlar, Germany) with an arm temperature of -28 ºC and chamber temperature of -20 ºC. Blocks were kept on dry ice until fixed onto a pre-cooled chuck using the OCT as the bonding solution. Blocks were trimmed at 10 µm to create a surface that consisted of a full section of tissue. Sections were cut at 5µm and placed on poly- L- lysine coated slides (Knittel, Braunschweig, Germany). Sectioned slides were kept on dry ice then stored at -80 ºC.

2.3.10 Hematoxylin and eosin (H&E) staining of FFPE sections

All steps for the H&Es were performed at room temperature unless stated otherwise. Sections were heated at 60ºC for 2 min, deparaffinised in 2 x 5 min washes in 100% xylene, rehydrated in 1 x 5 min 100% alcohol and 1 x 5 min 80% alcohol, followed by 2 x 5 min in PBS. From here on the sections were never allowed to dry out. Sections were stained with Gill's 2 hematoxylin (ProSciTech) for 2 min, washed in 4 x ddH_20, "blued" with Scott's tap water substitute for 2 min and counterstained with eosin for 1 min. Sections were then washed four times in 100% alcohol, cleared in 2 x 5 min xylene washes, mounted with cytoseal 60 (Richard-Allan Scientific, Kalamazoo, MI) and cover slips applied.

2.3.11 Immunohistochemistry (IHC) staining of FFPE sections

For all IHC experiments the indirect peroxidise detection system was utilised through the use of the Avidin Biotin Complex (ABC) elite kit (Vector laboratories, Burlingame, CA) with diaminobenzidine (DAB) as the chromagen for visualisation. All experiments contained controls as described in 2.3.13 and all steps were performed at room temperature unless stated otherwise. Sections were deparaffinised and rehydrated as in section 2.3.10 above and then subjected to a heat induced antigen epitope retrieval (HIER) in 250ml of 10 mM citrate buffer, pH 6.0 (Vector laboratories, Burlingame, CA). Buffer was preheated at 1000 w for 3 min in an inverter microwave oven, then slides submerged in the buffer and heated at 500 w for 10 min (except for Ki67 where slides were heated at 500 watts for 20 min). An inverter microwave oven was used for the HIER to provide a constant heating temperature between 95ºC and 98ºC while eliminating shear forces from violent intermittent boiling that occurs in regular microwave ovens. Slides were cooled for at least 30 min and washed 2 x 5 min in PBS. As per the manufacturer's instructions of the ABC Elite kit (Vector Laboratories), non-specific staining was blocked for 30 min using serum from the species the secondary antibody was raised in, then tapped off the slide (not washed). When using the anti-

synaptophysin and anti-SV40 large T mouse primary antibodies on mouse tissues, the mouse IgG blocking solution was used from the mouse on mouse (M.O.M; Vector Laboratories) kits as per the manufacturer's recommendations, to eliminate background staining caused by the anti-mouse secondary antibody labelling the endogenous mouse immunoglobulins on the tissue section.

The primary antibodies (Table 2-7) were diluted in PBT (1X PBS; 1% Bovine Serum Albumin (w/v) and 0.1% tween 20 (v/v) as per appendix 1) and incubated for 1 h, except for the anti-mouse primary antibodies which were diluted in the M.O.M diluents and incubated for 30 mins. All primary antibodies were washed off by a 2 x 5 min wash in PBS. Secondary antibody was made up as specified in the ABC Elite kit and sections incubated for 1 h, except for the anti-mouse secondary antibodies which were diluted in the M.O.M diluents and incubated for 10 mins. All secondary antibodies were washed off in 2 x 5 mins PBS washes. Endogenous peroxidase activity was quenched with 1% hydrogen peroxide (Ajax Finechem, Taren Point, NSW) in PBS for 5 min, and slides washed again in 2 x 5 min in PBS. Sections were then incubated with the biotinylated avidin enzyme complex reagents, as per the manufacturer's protocol, for I h. The avidin/biotin complex was detected with the liquid chromogen diaminobenzidine, (DAB ImPact™; Vector Laboratories). Sections were counterstained with Gill's double strength hematoxylin for 30 s, rinsed in dd$H_2$0 and blued with Scott's tap water substitute for 2 min. Sections were then dehydrated in consecutive 80% and 100% ethanol washes for 5 min, cleared in two 5 min baths of xylene and mounted with Cytoseal 60.

2.3.12 Immunofluorescent (IF) staining of fresh frozen sections

For all IF experiments fluorescently labelled secondary antibodies were used as the detection system. All experiments contained controls as described in 2.3.13 and all steps were performed at room temperature unless stated otherwise. Frozen sections were allowed to equilibrate to ambient temperature for 20 min, then fixed

in acetone for 10 min and air dried for 5 min. Sections were then rehydrated in three 5 min incubations in PBS. Non-specific staining was blocked with 7% serum (from the species in which the secondary antibody was made) in PBT (1X PBS; 1% Bovine Serum Albumin (w/v) and 0.1% tween 20 (v/v) for 30 min. The blocking reagent was tipped off the slides, but not washed; primary antibody was added and incubated for 1 h (Table 2-7). Slides were washed for two 5 min incubations in PBS then Alexa™ 594 or 555 fluorophore secondary antibody (Invitrogen, Carlsbad, CA), diluted at 1:400 in PBT was added and incubated for 1 h, then washed for 2 x 5 min in PBS. Once secondary antibody had been added slides were kept in dark as much as possible, to reduce fading of the conjugated fluorophore. Sections were counterstained with 4',6-diamidino-2-phenylindole (DAPI) at 1:5000, washed for 2 x 5 min in PBS, mounted with Prolong Gold™ (Invitrogen) and stored in the dark at 4ºC for a maximum of 4 weeks.

2.3.13 IHC and IF controls

Positive controls were used in each IF experiment, specifically they were a tissue section previously shown positive for the relevant antibody. Also when labelling for CD151 and CD9, sections of CD151 and CD9 KO tissue were used as negative controls for each of the antibodies. For all other antibodies used in IHC either an antibody matched isotype IgG or a species specific serum/IgG was used as the negative control (Table 2-8). Furthermore during optimisation the primary antibody, secondary antibody and the avidin/biotin complex were each excluded sequentially, along with titration of the primary antibody to confirm specificity of staining.

Table 2-7: Primary antibodies used for labelling mouse tissue.

Antibody	Clone	Isotype	Company	Dilution
Rabbit anti mouse CD151	LAI-2	polyclonal	In-house *	1:500
Rabbit anti-human CD82	C-16	polyclonal	Santa Cruz	1:800
Rat anti-mouse CD9	KMC8	IgG_{2a}	BD Biosciences	1:1000
Mouse anti- human E-Cadherin	36	IgG_{2a}	BD Biosciences	1:1000
Mouse anti- bovine synaptophysin	SY-38	IgG_1	Chemicon	as is
Mouse anti-SV-40 large T antigen	P101	IgG_{2a}	BD Biosciences	1:400
Rat anti-mouse CD31	SZ31	IgG_{2a}	Dianova	1:20
Rabbit anti-human Ki67	SP6	Rab IgG	Neomarkers	1:200
Rabbit anti-cleaved caspase-3	ASP175	polyclonal	Cell Signaling	1:800
* LAI-2 (Baleato, Guthrie et al. 2008)				

Table 2-8: IHC negative control.

Isotype	Antibody	Company
IgG_1	1B5	In house *
IgG2a	ID4.5	In house **
Mouse IgG	Mouse IgG	Vectorlabs
Rabbit IgG	Rabbit IgG	Vectorlabs
Rat IgG	Rat IgG	Vectorlabs
* 1B5; anti-*Giardia* (G. Mayrhofer, University of Adelaide; unpublished)		
** ID4.5; anti-*Salmonella* (O'Connor and Ashman 1982)		

2.3.14 Analysis of FFPE slides with the Aperio digital pathology system

2.3.14.1 General

The Aperio™ digital pathology system (Aperio, Vista, CA) was used for the analysis of stained FFPE slides. Workflow consisted of the stained glass slides being converted into virtual digital slides by scanning with the Scanscope™ scanner (GS model with single slide tray) and then uploaded in to the Spectrum™ server (version 11.1.1.765). Digital images were visualised using the ImageScope™ software (version 11.1.2.760).

2.3.14.2 Scanning of slides

Glass slides stained via IHC were converted into “virtual digital slides” by scanning with the Scanscope console. The console configurations were set to “IHC parameters” and scanned at 20x (not 40x) for efficiency. The manual workflow process was followed as according to manufacturer’s recommendations. Briefly, a “snapshot” was acquired to obtain a macro image, file name and description entered to save the image, the “scan area” adjusted as appropriate, and the white balance point positioned on a position on slide that consisted of slide, mountant and glass cover slip, but no tissue. Then “auto focus points” was used to place focus points across the slide at multiple points. A pre-scan calibration was performed previous to the actual scan of the slide being undertaken. Scanned images were automatically sent to the Spectrum server for storage. Images were reviewed in ImageScope to check the final quality.

2.3.14.3 Analysis of mouse liver and lung metastases

Mouse liver and lung sections were stained by H & E, scanned into Spectrum as above and viewed in ImageScope at high magnification to identify any metastatic lesions. Annotations were drawn freehand around any lesions generating automated data consisting of number and area of metastatic lesions per image (tissue section) which could be exported to Excel software (Microsoft Corporation™, Redmond WA) for further analysis.

2.3.14.4 Characterisation of endpoint point group tumours

All tumour sections from the endpoint study group were scanned into Spectrum as detailed in 2.3.14.2 and classified for tumour grade by histopathology (H&E). To allow comparison of the tumour sections across the wt, heterozygous and KO genotypic groups from the animals in the endpoint group, the tumour sections needed to be normalised. To achieve this only poorly differentiated tumours were

included due to the poorly differentiated tumour comprising of a homogenous sheet of cells in terms of cell distribution across the sections.

The tumour sections were characterised by indirect IHC (2.3.11) by labelling with a cell proliferation marker (Ki67), an apoptosis marker (active caspase-3), and a marker of vascular endothelium to assess the extent of angiogenesis (CD31); antibody details are listed in Table 2-7. Once labelled the stained slides were also scanned into Spectrum as above. Images were annotated on a homogenous representative and consistent segment of the section, in regards to IHC labelling and containing only poorly differentiated tumour cell sheets, with a fixed region of interest of 16000 μm^2 x 16000 μm^2. Then the appropriate algorithm was used to determine percentage positive staining in the annotated region of interest as detailed below in section 2.3.14.4.10. The algorithms were run in an antibody batch type manner over each slide through Spectrum™ with a pseudo colour mark-up image for visual representation of the algorithm output on each spot. Results were batch exported from Spectrum™ as comma-delimited file types (.csv) and subsequently imported into Excel spreadsheets for analysis.

2.3.14.4.1 *Nuclear staining algorithm*

The IHC labelling of Ki67 was specific to the nucleus of the poorly differentiated tumour cells. Thus the nuclear staining algorithm could be used to quantify the percentage of positively labelled nuclei to negatively labelled nuclei within the annotated region of interest. IHC labelling of active caspase-3 was cytoplasmic to cell however, again the nuclear algorithm could be utilised by not restricting the algorithm for a upper cut-off limit for nuclear size, therefore the algorithm would see the active caspase-3 cytoplasmic staining in each cell as a single identity and count number of cell positive as a percentage to number of cells negative for active caspase-3 labelling. Parameters were set to an average curvature threshold of 1, average radius of 1, minimum roundness of 0.1, minimum compactness of 0 and minimum elongation of 0.1. Staining intensity thresholds are listed in Table 2-9.

Weak and medium thresholds were set to zero to result only in a positive or negative outcome as determined by the strong staining intensity threshold for each antibody. Again this allowed a percentage positive output result of positively labelled nuclei as a percentage of negatively labelled nuclei in the annotated region of interest. The thresholds were determined for each antibody by using representative images of very strong and very weak staining and optimising the algorithm thresholds to correspond to the desired cut-off between negative and positive staining.

Table 2-9: Intensity threshold limits for the nuclear staining algorithms.

1º Antibody	Weak Positive Threshold	Medium Positive Threshold	Strong Positive Threshold
Ki67	0	0	232
Caspase-3	0	0	211

2.3.14.4.2 *Positive pixel count algorithm*

The IHC labelling of CD31 was specific to the vascular endothelium and therefore the positive pixel count algorithm could be used to analyse the extent of DAB chromogen labelling as compared to negative counterstain, resulting in a percentage positive pixels in the annotated region of interest. The variable parameters of hue value, hue width and colour saturation threshold were 0.16, 0.44 and 0.04 respectively. As with the nuclear staining algorithm the thresholds were set to result only in a positive or negative outcome as determined by the strong staining intensity threshold for each antibody, resulting in percentage of positive pixels to negative pixels in the annotated region of interest.

Table 2-10: Intensity threshold limits for the positive pixel count algorithm.

1º Antibody	Weak Positive Threshold	Positive Threshold	Strong Positive Threshold
CD31	162	162	162

2.3.15 Fluorescence microscopy

Immunofluorescent slides were viewed with a Zeiss Axioplan 2 upright fluorescence microscope (Carl Zeiss, Oberkochen, Germany) using the various preset channels to excite the Alexa 594 flurophore (Invitrogen) as required. Capture of the images was via a Zeiss Axioplan MRm3 camera mounted on the microscope and operating through the Axiovision LE imaging system software (V 4.8.1.0). The multidimensional acquisition functions were used at set exposure times for each individual experimental set of slides to allow comparisons (500 millisecs for the CD151 antibody and 80 millisecs for the CD9 antibody)

2.3.16 Statistical Analysis

Statistical analysis on the data was performed using Prism V6 (GraphPad Software Inc., La Jolla, CA). Initially data sets were analysed for frequency distribution patterns, to see if they fitted a Gaussian distribution to reveal whether a parametric or non-parametric statistical test would be most appropriate. Non-parametric analysis was appropriate for the data sets. The log rank (Mantel-Cox) test was used for analysis of Kaplan-Meier survival curves. To analyse the metastases incidence data, that was binomial the Fishers exact test was used. When the three genetic groups were analysed together the non-parametric one way analysis of variance (Kruskal-Wallis) test was employed, if a significant difference was found between the groups then a pair wise analysis was done with the Mann-Whitney test. A p value of <0.05 was considered statistically significant.

2.4 *Methods relating to human TMA biomarker experiments*

2.4.1 Tissue Microarrays (TMAs)

2.4.1.1 Overview

TMAs were received from the Australian Prostate Cancer Collaboration (APCC; Kelvin Grove, QLD; http://www.apccbioresource.org.au). TMAs were stained fresh or stored at -80ºC in slide mailers (ProSciTech) sealed with parafilm. All work on the TMAs which contained human tissue samples was covered by the University of Newcastle ethics approval H-2008-0056 and Biosafety approval 178-2008.

2.4.1.2 Pilot TMAs

The pilot TMAs (APCC) consisted of 10, 1mm x 1mm tissue samples of various stages of PCa, BPH and normal tissue samples. The pilot array was used to optimise antibodies (Table 2-11) and immunohistochemistry protocols (2.3.11) prior to staining the Gleason progression TMAs (2.4.1.3). Five serial sections from the pilot TMA block were obtained.

2.4.1.3 Gleason progression TMAs

The “Gleason progression” TMAs (APCC) consisted of over 150 human prostate tissue samples (1mm x 1mm) from patients with BPH, tumours of various stages with predetermined Gleason scores and some matched normal tissue samples. Ten serial sections from the Gleason progression TMA block were obtained.

2.4.2 IHC on TMAs

Prior to use TMAs were removed from -80ºC, left sealed and upright, to prevent condensation forming on the sections, at 4ºC for 2 h, then a further 10 min upright

on bench to equilibrate to ambient temperature. IHC protocols were performed as previously described in section 2.3.11, except that primary antibodies and concentrations were as in Table 2-11.

The CD151 (clone RLM30) staining was performed at the Garvan Institute (N.S.W). The protocol was similar to normal IHC protocols except once the slides were brought to water, the Dako target retrieval solution, pH 6.0 (Dako, Glostrup, Denmark) was used for antigen retrieval for 30 mins in a water bath and then cooled for 30 mins. Slides were transferred to a Dako autostainer, where the endogenous peroxidase activity was quenched with 3% hydrogen peroxide for 5 minutes and then washed. Then slides were incubated in the Dako Protein Block Serum Free (Dako) for 10 minutes and the liquid was then blown off by the machine. The CD151 (RML30) primary antibody was applied at 1:200 dilutions, incubation for 60 minutes at room temperature and rinsed. Slides were then incubated In the Envision Labelled polymer-HRP Anti-Mouse secondary antibody (Dako) for 30 minutes at room temperature and then washed. The slides were then incubated in the Dako DAB+ chromogen (Dako) for 10 minutes and rinsed. Counterstaining, dehydration, clearing and mounting was as previously described in section 2.3.11.

Table 2-11: Primary antibodies used for labelling antigens in TMAs.

Antibody	Clone	Isotype	Company	Dilution
Mouse anti-human CD151	11B1.G4	IgG_{2a}	In house *	4µg/ml
Mouse anti- human CD151	RLM30	IgG_{2b}	Novocastra	1:100
Mouse anti- human CD9	72F6	IgG_1	Novocastra	1:100
Mouse anti- human CD82	G-2	IgG_3	Santa Cruz	1:50
Mouse anti-human Tspan8	Ts29.1	IgG_1	Boucheix lab**	2µg/ml
* 11B1 (Sincock, Mayrhofer et al. 1997) **Ts29.1 (Greco, Bralet et al. 2010)				

2.4.3 Analysis of TMAs

2.4.3.1 General

The Aperio™ digital pathology system (Aperio, Vista, CA) was used for the analysis of TMAs as detailed in section 2.3.14.1.

2.4.3.2 Scanning of TMAs

TMAs were scanned as detailed in section 2.3.14.2 except the console configurations were set to “TMA” parameters” and images were scanned in at 40x magnification to obtain the highest resolution possible. Each TMA spot was allocated at least three focus points. The Aperio Digital Slide Studio software was used to rotate the TMA serial section sets to a correct and constant orientation to conform to the TMA core maps.

2.4.3.3 TMA Lab

The scanned images of the TMAs were manipulated with the TMA lab II software as per manufacturer’s recommendations. Briefly, each digital TMA was segmented and data associated with that individual core entered for later identification.

2.4.3.4 Automated analysis of TMAs

2.4.3.4.1 ***Annotations of TMAs***

Due to the heterogeneity of prostate tissue, the pre-determined pathological grading was rarely consistent across the whole spot. A graphics tablet and pen was used to annotate the regions of interest that corresponded to the pre-evaluated associated Gleason grade. These regions were checked by a pathologist, Dr Mark Formby (Hunter Area Pathology Services; H.A.P.S). The

pathologist also validated changes that needed to be made as a result of discrepancies between the TMA map and actual TMA spot.

2.4.3.4.2 ***Colour deconvolution algorithm***

For analysis of the antibody labelling on the human TMAs the colour deconvolution algorithm was chosen, above the positive pixel count algorithm. This was due to the colour deconvolution algorithm having more scope for flexibility in optimisation and also having more sensitivity and specificity in analysis due to the capacity, as the name suggests to separate colour channels from the brown DAB (the positive antibody labelling) to the purple hematoxylin (the counter stain) and score the labelling intensities separately for each stain. The colour deconvolution algorithm was optimised for each antibody, therefore creating a separate algorithm for each antibody. The thresholds for each antibody were determined by using representative images of very strong and very weak staining and optimising the algorithm thresholds to correspond to the desired proportion of negative, weak, moderate and strong staining (Table 2-12). The resultant “score” was used as the data output from each of the colour deconvolution algorithms. The score is derived from a simple equation involving the positive staining as a direct result of positive thresholds. The manufacturer defines it as “Score = 1 x (percentage weak positive) 2 x (percentage medium positive) 3 x (percentage strong positive)”. Some patients had multiple samples on the TMA for normal or specific tumour grades; in these cases the scores were averaged before analysis.

Table 2-12: Upper threshold limits for the colour deconvolution algorithms.

1º Antibody	Weak Positive Threshold	Medium Positive Threshold	Strong Positive Threshold
CD9	198	168	147
CD151 (11B1)	213	190	170
CD151 (RLM30)	211	185	153
CD82	204	175	140
Tspan8	226	219	211

2.4.3.5 Manual analysis of TMAs

The IHC labelling intensities of CD9, CD82, Tspan8 and both CD151 antibodies on the TMAs were also scored manually. This allowed for not only an independent scoring of the antibody labelling on the TMAs, but also allowed a comparison between automated and manual scoring results. The TMAs had previously been labelled by IHC (2.4.2), scanned into digital images through Scanscope (2.4.3.2) and regions of interest that correlated to the pre-evaluated Gleason grade were annotated under guidance of a pathologist (2.4.3.4.1). Initially a region of interest representative of negative, low, medium and high labelling intensity for each antibody was chosen and printed out in colour on a laser-jet printer to use as a visual reference guide for determining specific staining intensity cut-offs when scoring. Two scientists (B. T. Copeland and M. J. Bowman) viewed all of the cores for each antibody through Imagescope at 400 x magnification (on the same computer monitor with consistent settings) and scored each spot as either negative, low, medium or high (0, 1, 2 or 3) in regards to antibody labelling intensity of the epithelial cells within the region of interest. All spots were scored with no prior knowledge of the predetermined Gleason scores, which tissue samples were normal/tumour matched or the other scorer's results. Any spot scores that varied between both scorers were again viewed in Imagescope and a consensus was agreed upon. Some patients had multiple samples on the TMA for normal or specific tumour grades; in these cases the scores were averaged before analysis.

2.4.3.6 Statistical Analysis

All statistical analysis was performed using Prism V6 (GraphPad Software Inc., La Jolla, CA). For statistics on the human bio-marker TMA data, the non-parametric Spearman rank test was employed for analysis of correlation of staining by the different antibodies. The Mann-Whitney test was used to analyse differences pairwise between the various stages of disease, and the Wilcoxon signed-ranked test was used to analyse differences between groups of matched pairs. All

statistical analyses were considered statistically significant when a p value was <0.05.

Chapter 3: Characterisation of the CD151/TRAMP and CD9/TRAMP mouse models

3.1 *Introduction*

Following on from correlative studies of tetraspanin expression with clinical data in patients with various cancers (detailed in section 1.8.4) the majority of experimental research into tetraspanins to date has been *in vivo* and *in vitro* functional studies focusing on three main areas. Firstly, *in vitro* analysis of tetraspanin partner molecules by separating out tetraspanins by detergent induced membrane disruption and analysis via western blots and more recently mass spectrometry. Secondly, *in vitro* over-expression and knockdown experiments have been used in functional assays to study the effects of tetraspanins in cell lines. Lastly, *in vivo* grafting studies have shown a role for various tetraspanins in a number of diseases including PCa. These research modalities have proved valuable for gaining fundamental insights into the role of tetraspanins with CD151 and CD9 shown to be involved in cell signaling, motility and adhesion. These are all essential functions in the progression of PCa to metastatic disease, the leading cause of PCa mortalities (1.8.4). However in regards to the multifaceted dynamics of cancer initiation and progression these somewhat reductionist techniques do not accurately recapitulate the progressive development of human cancers in their unique microenvironments.

Mouse models that combine tissue specific transgenic expression of oncogenes with KO of specific genes have proved very valuable in determining the contribution of these genes to the development and progression of various cancers as detailed in section 1.9. These transgenic mouse models can recapitulate the multifaceted dynamics of human cancer in that they possess intact native functioning immune systems, have multi cellular paracrine signalling/interaction abilities in a complete tumour microenvironment with blood and lymph vessels that develop with the forming tumours and most importantly can recapitulate the various stages of human cancers. Furthermore, transgene expression can be temporally and spatially controlled.

Several sophisticated and elegant mouse models of PCa have been developed (reviewed by Ahmad, Sansom et al. 2008, Hensley and Kyprianou 2011). Given that developing and maintaining transgenic mouse colonies is expensive, time consuming and labour intensive, when choosing a model, careful consideration must be given to the specific characteristics of each individual model. In particular the unique phenotypic characteristics and limitations of the model and how it will best address the specific research question need to be considered. For example the *NKx3.1* KO model develops PIN (1.9.2) that significantly parallels human PIN development and has become the gold standard for research into early stage PCa (Kim, Bhatia-Gaur et al. 2002). However the model does not develop metastatic lesions (unless compounded with the *Pten* KO) so is of little significance when the research aims are analysis of metastatic events (Abate-Shen, Banach-Petrosky et al. 2003). Another example highlighting the need for careful model choice is the fact that in the TRAMP model the oncogenic *SV40* transgene expression is temporally controlled by two regulatory androgen receptor binding sites within the promoter. This may confound research results that involve hormone ablation in the animals as downregulation of androgens may reduce the expression of the *SV40* transgene, therefore resulting in a reduction in PCa development, as a secondary effect to the experimental variable being studied.

One of the aims of this project, which was built upon previous *in vitro* and *in-vivo* studies that showed CD151 to have pro-metastatic effects and CD9 to have anti-metastatic effects, was to analyse if the tetraspanins CD151 and CD9 have a direct effect on PCa initiation and progression in a transgenic mouse model that best recapitulates the human progression of PCa. The TRAMP model has recently been cited as the best characterised mouse model of PCa to date (Jeet, Ow et al. 2008, Hensley and Kyprianou 2011). It was chosen for this project due to general beneficial characteristics inherent to the model as explained in 1.9.2.1 along with advantageous traits specific to the proposed research questions. These beneficial

features revolve around the fact that the TRAMP model closely recapitulates human PCa progression in a number of ways. The onset of expression of the TRAMP's *SV40* transgene is temporally controlled by androgen binding to the promoter for activation, while in the human disease initial onset is also androgen regulated. The expression of the *SV40* transgene in the mouse is specific to the prostate and the subsequent TRAMP prostate carcinomas are multifocal and heterogeneous as in human PCa. Furthermore the TRAMP PCa progress closely parallels the multistep human disease progression from PIN to, most importantly, truly spontaneously developing, autochthonous *de novo* primary prostate carcinomas right through to development of spontaneous distant metastatic lesions at high and consistent frequencies. When the TRAMP model of PCa is crossed with the *Cd151* and *Cd9* KO models, these features allow analysis of the direct effects of the tetraspanins in the initiation and progression of PCa.

Along with the TRAMP model, both the *Cd151* and *Cd9* KO models have been very well characterised on the B6, FVB and B6/FVB F_1 backgrounds as previously explained in sections 1.9.2.1 and 1.9.2.3. However when crossing two genetically engineered mouse models such as the TRAMP and C*d151* KO or TRAMP and C*d9* KO models as in this project, it is essential to characterise the resultant new mouse models in terms of genetics, overall development, organogenesis and manifestation of the expected (PCa) and unexpected phenotypes (Shappell, Thomas et al. 2004).

This chapter, for the first time, outlines the basic characterisation of the CD151/TRAMP and CD9/TRAMP models which provide the framework for the subsequent experiments described in chapters 4 and 5. Specifically, it addresses the characterisation of the two models in regards to confirmation of genetic crosses, developmental progression, overview of the model's progression in terms of prostate tumour onset and metastatic incidence, expression patterns of the

tetraspanins CD9, CD151 and CD82, expression patterns of the SV40 protein, origin of the metastatic lesions and basic characterisation of the tumour lesions.

3.2 *Results*

Many of the results from this chapter have been published (Copeland, Bowman et al. 2013a, Copeland, Bowman et al. 2013b).

3.2.1 Confirmation of genetic modifications in the mouse models

Once breeding of the CD151/TRAMP and CD9/TRAMP models was undertaken (section 2.3.1) the genotype of each animal had to be determined. Ear-punches were taken as tissue samples for genotyping by PCR as described in section 2.3.4. Each animal was genotyped for the presence or absence of the *SV40* transgene which represented the *TRAMP* or *TRAMP-negative* genotype respectively, along with the *Cd151* or *Cd9* wt, heterozygous or KO genotypes. The PCR products were electrophoretically separated as in Figure 3-1 which shows the SV40 PCR product of ~600bp length along with an internal control of ~500bp. Examples of genotyping of experimental animals for *Cd151* and *Cd9* are shown in Figure 3-2 and Figure 3-3, respectively.

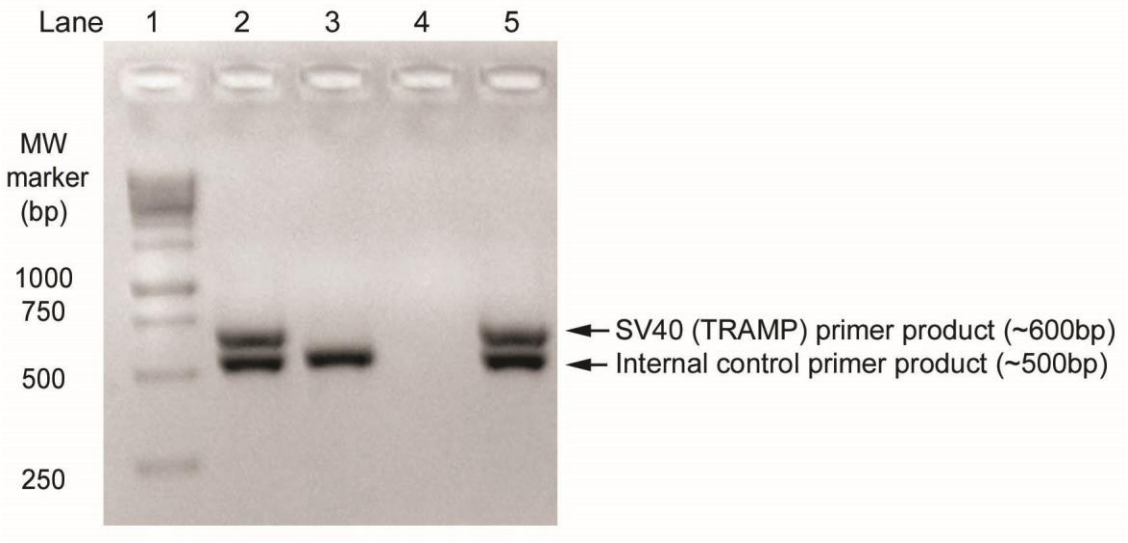

Figure 3-1: PCR of the *SV40* transgene was used to determine animals with the *TRAMP* genotype.
DNA extracted from ear punches was amplified by PCR using primers for the *SV40* transgene to determine if animals had a *TRAMP* or *TRAMP*-negative genotype (Table 2-1). PCR product size was determined relative to a 1 kb marker (lane 1). Samples with the *TRAMP* genotype appeared as two bands, the SV40 primer product band at ~600bp and an internal control (*Casein*) primer product band at ~500bp (lane 2), while *TRAMP* negative animals gave only the internal control band (lane3). The PCR negative control contained water in place of DNA and resulted in no PCR products (lane 4) while DNA from previously confirmed *TRAMP* animals was used as the PCR positive control (lane 5).

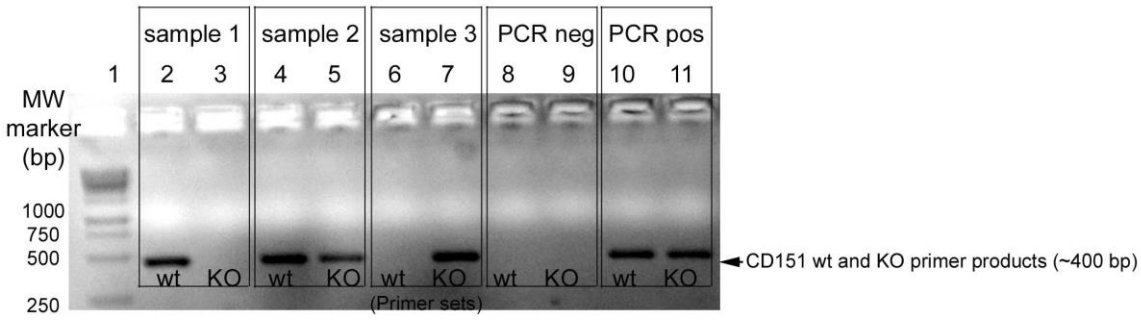

Figure 3-2: PCR determination of the *Cd151* wt, heterozygous and KO genotypes.
DNA extracted from ear punches was amplified by PCR using primers for the *Cd151* gene (Table 2-1). PCR product size was determined by reference to a 1 kb marker (lane 1). *Cd151* wt specimens gave rise to a single band (lane 2; sample1). *Cd151* heterozygous specimens gave bands with both wt and KO PCR primers (lanes 4 and 5; sample 2), while *Cd151* KO specimens yielded a single band for KO primers only (lane 7: sample 3). PCR negative control contained water in place of DNA and contained no PCR products (lanes 8 and 9) while DNA that had previously been confirmed as heterozygous for *Cd151* was used as the PCR positive control for both wt and KO primer pairs (lanes 10 and 11).

.

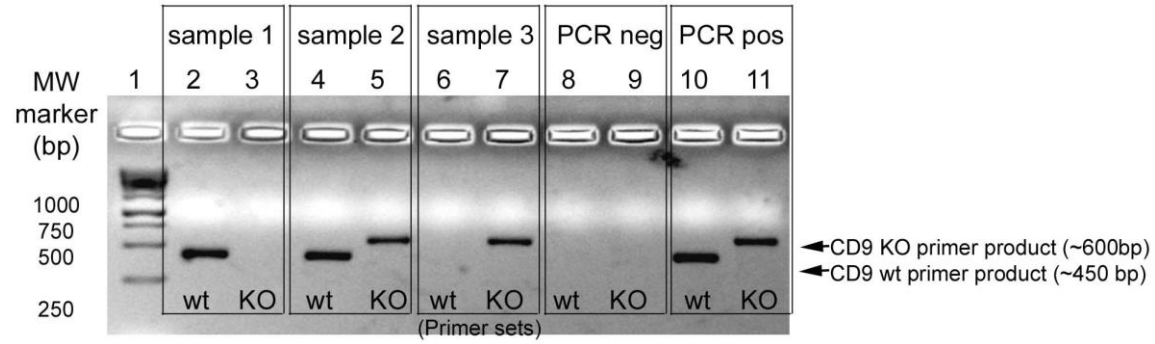

Figure 3-3: PCR determination of the *Cd9* wt, heterozygous and KO genotypes.
DNA extracted from ear punches was amplified by PCR using primers for the *Cd9* gene (Table 2-1). PCR product size was determined by reference to a 1 kb marker (lane 1). *Cd9* wt specimens gave rise to a single band from the wt primers (lane2; sample1). *Cd9* heterozygous specimens gave bands for both the wt and KO primers (lanes 4 and 5; sample 2), while *Cd9* KO specimens yielded a single band for the KO primers (lane 7: sample 3). The PCR negative control contained water in place of DNA and resulted in no PCR products (lanes 8 and 9) while DNA that had previously been confirmed as heterozygous for *Cd9* was used as the PCR positive control for both wt and KO primer pairs (lanes 10 and 11).

.

To eliminate any errors that arose during specimen handling, PCR and/or subsequent data entry, an additional ear punch was taken upon sacrifice to reconfirm each animal's genotype. If there was a discrepancy, the frozen corpse was retrieved and a third tissue sample was taken to get a consensus from a third PCR. Definitive genotypes were determined from agreement of the two PCR results obtained from the two post-mortem tissue samples. In the rare occasion that the two post-mortem PCR results were different the animal was excluded from the study. From this, overall error rates between the original and secondary genotyping PCR results could be determined (Table 3-1). Furthermore, Table 3-2 summarises the total numbers of male mice genotyped for the *SV40 T-ag* gene and *Cd151* or *Cd9*. It should be noted that no reproductive defects were seen in either of the CD151/TRAMP F_1 (n=187) or CD9/TRAMP F_1 (n=201) models as they followed the predicted Mendelian frequencies of 25% wt, 50% heterozygous and 25% KO with respect to each gene (data not shown).

Table 3-1: Error rates for genotyping of animals.
Error rates for genotyping of the experimental animals arising from PCR, data entry and specimen handling were determined by crosschecking each animal's genotype at weaning to a subsequent re-genotype at each animal's endpoint.

Primer set	Error rate (%)	Error rate
CD151	4.8%	6/123
CD9	3.5%	5/141
SV40 (Tramp)	4.1%	11/264

Table 3-2: Total male animals bred and genotyped.
Each male animal that was bred was genotyped for the *SV40* gene along with either the *Cd151* or *Cd9* wt and KO gene, to determine every male animal's genotype.

Model	Total male animals genotyped
CD151/TRAMP	463
CD9/TRAMP	501

3.2.2 Allocation of mice to study groups

Once mice had been genotyped (section 2.3.4) mice surplus to requirements for particular genotypes were culled. The rest of the animals were allocated to the required experimental groups as detailed in section 2.3.5. Briefly the three main experimental groups were, firstly, a tumour progression characterisation group, where animals were culled at 10 and 20 weeks of age (with no palpable tumour) for basic tumour progression characterisation of the model, secondly, the main endpoint study group (culled at tumour detection) to analyse the effects of CD151 and CD9 on tumour initiation and progression. Lastly, for CD151/TRAMP only, a bioluminescent study group (culled 4 weeks post intra-cardiac injection of tagged PCa cells) was used to look at effects of the host environment on tumour metastatic potential.

3.2.3 Developmental characterisation

3.2.3.1 Normal prostate development

It was vital to characterise the normal organ development of the *Cd151* and *Cd9* KO, TRAMP negative animals to make sure the ablation of the genes did not have

overt effects on normal organ development in particular the urogenital tracts and prostates. Groups of TRAMP negative mice were culled at 10, 20 and 40 weeks, autopsied for any overt organ defects and the prostates processed, sectioned, stained and examined for irregularities compared to their wt litter mates. As shown in Figure 3-4 no overt defects were seen between the wt and *Cd151* KO cohorts in general organ development or in the prostates upon microscopic analysis represented. Furthermore, no differences in normal prostate development were seen between the wt and *Cd9* KO groups or between the *Cd151* and *Cd9* KO groups (data not shown).

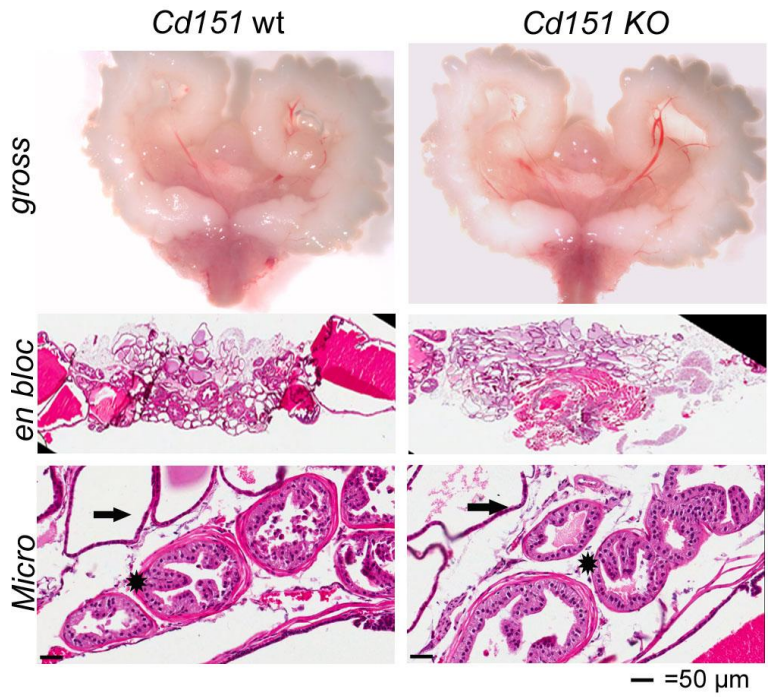

.

Figure 3-4: Representative of normal prostate development in the animals.
A number of *Cd151* and *Cd9* KO, TRAMP negative animals were culled at various time points (10, 20 and 40 weeks) to analyse normal prostate development. Prostates were examined at the gross level to view the lower urogenital tract. The urogenital tract was cross-sectionally dissected and stained by H&E, scanned into digital images and the tissues then viewed in Imagescope at 10 x magnification for en bloc and 200x magnification to view individual glands. Arrows highlight lateral prostate glands and the stars highlight dorsal prostate glands. No overt differences were seen in the *Cd151* KO (or *Cd9* KO; not shown) animals from their wt littermate controls.

3.2.3.2 Tumour progression in the model

Preliminary experiments were carried out to characterise the development of the prostate tumours in the TRAMP/KO model to determine if the tumour progression followed the expected patterns as previously seen in the TRAMP model (section 1.9.4) and therefore recapitulate the progression of human PCa.

To achieve this, two groups of TRAMP positive/*Cd9* wt animals were culled at earlier time points, specifically at 10 and 20 weeks, for characterisation of tumour onset and progression in the model. Animals from the *Cd9* cohort were chosen for these preliminary experiments as their breeding schedule was commenced earlier than the *Cd151* cohort. The urogenital tracts (UT) or prostate tumours, along with liver and lungs were harvested and histopathological analysis via H&E staining was undertaken. From the group of animals culled at 10 weeks, 6/7 animals (86%) had some form of primary prostate cancer, specifically 4 animals had PIN and 2 animals had well differentiated tumours in the prostate (Table 3-3). From the group of animals culled at 20 weeks 10/10 (100%) of animals had primary prostate cancer. Specifically, 3 animals had PIN, 2 animals had well differentiated tumours, 1 animal had a moderately differentiated tumour and 3 animals had poorly differentiated prostate tumours (Table 3-4). None of the animals in the group culled at 10 weeks (0/7) had either liver or lung metastases, however in the 20 week cull group 1/10 had liver metastases and 2/10 of animals had lung metastases.

Table 3-3: Tumour progression 10 week study group observations.
A group of animals were culled at 10 weeks and the prostates, liver and lungs were processed and FFPE blocks sectioned at 5 µm and analysed by histopathology to characterise tumour progression in the animals. Prostates were classed as being either normal tissue, prostatic intraepithelial neoplasia (PIN), well differentiated (WD), moderately differentiated (MD) or poorly differentiated (PD) tumours

Genotype (10 weeks)	Prostate pathology	Liver metastases	Lung metastases
TRAMP/ CD9 wt	Normal	no	no
TRAMP/ CD9 wt	PIN	no	no
TRAMP/ CD9 wt	PIN	no	no
TRAMP/ CD9 wt	PIN	no	no
TRAMP/ CD9 wt	PIN	no	no
TRAMP/ CD9 wt	WD	no	no
TRAMP/ CD9 wt	WD	no	no
total	6/7	0/7	0/7

Table 3-4: Tumour progression 20 week study group observations.
A group of animals were culled at 20 weeks and the prostates, liver and lungs were analysed by histopathology to characterise tumour progression in the model.

Genotype (20 weeks)	Prostate pathology	Liver metastases	Lung metastases
TRAMP/ CD9 wt	PIN	no	no
TRAMP/ CD9 wt	PIN	no	no
TRAMP/ CD9 wt	PIN	no	no
TRAMP/ CD9 wt	WD	no	no
TRAMP/ CD9 wt	WD	no	no
TRAMP/ CD9 wt	MD	no	no
TRAMP/ CD9 wt	PD	no	no
TRAMP/ CD9 wt	PD	no	no
TRAMP/ CD9 wt	PD	no	yes
TRAMP/ CD9 wt	PD	yes	yes
total	10/10	1/10	2/10

From all the animals in the 40 week endpoint groups (i.e. mice with palpable prostate tumours) both CD151/TRAMP and CD9/TRAMP models showed a range of tumour progression stages (specified in detail in section 1.9.4 and briefly here) from PIN (epithelial cells of glands displaying stratification, tufting with possible cribriform structures, elongated and hyperchromatic nuclei), well differentiated (reduced glandular structure size and invasion of epithelial cells into the stroma, increased cribriform structures and rounded nuclei compared to PIN), moderately

differentiated (increased sheets of cells with infrequent irregular glandular structures) through to poorly differentiated primary prostate tumours (solid sheets of cancerous cells with very high nuclear to cytoplasmic ratios) as illustrated in Figure 3-5. Specifically the number of animals in each cohort and different genetic group that had developed *de novo* primary prostate tumours were as follows; 25/27 (93%) of the *Cd151* wt animals, 19/21 (90%) of the *Cd151* heterozygous animals, 29/30 (97%) of the *Cd151* KO animals, 30/32 (94%) of the *Cd9* wt animals, 23/25 (92%) of the *Cd9* heterozygous animals and 32/35 (91%) of the *Cd9* KO animals. For detailed analysis on the incidence of metastases in the endpoint cohort of mice that developed palpable prostate tumours see sections 4.2.1.3 and 5.2.3.

Data from all the TRAMP endpoint experimental animals from both the CD151/TRAMP and CD9/TRAMP groups (wt, heterozygous and KO) was analysed to build up an overview of the progression of the two models as shown in Figure 3-6. Specifically, the CD151/TRAMP animals started to develop palpable primary prostate tumours by 16 weeks of age and metastatic lesions from 18 weeks of age, while CD9/TRAMP animals developed palpable primary prostate tumours from 18 weeks of age and metastatic lesions from 19 weeks of age. By 40 weeks of age 93% (73/78) of the CD151/TRAMP animals had primary prostate tumours and 38% had metastatic lesions. By comparison, 92% (85/92) of the CD9/TRAMP animals had primary tumours and 40% had distant metastases to either the liver or lungs. The incidence of primary prostate tumours and metastases are analysed in much greater detail for each of the *Cd151* and *Cd9* cohorts in the two following chapters. It should be noted that 100% (37/37) of the animals negative for the *TRAMP* transgene did not develop palpable prostate tumours, or present with any dysplasia in the prostate upon autopsy at 40 weeks; specifically 11 *Cd151* wt, 10 *Cd151* KO, 8 *Cd9* wt and 8 *Cd9* KO animals.

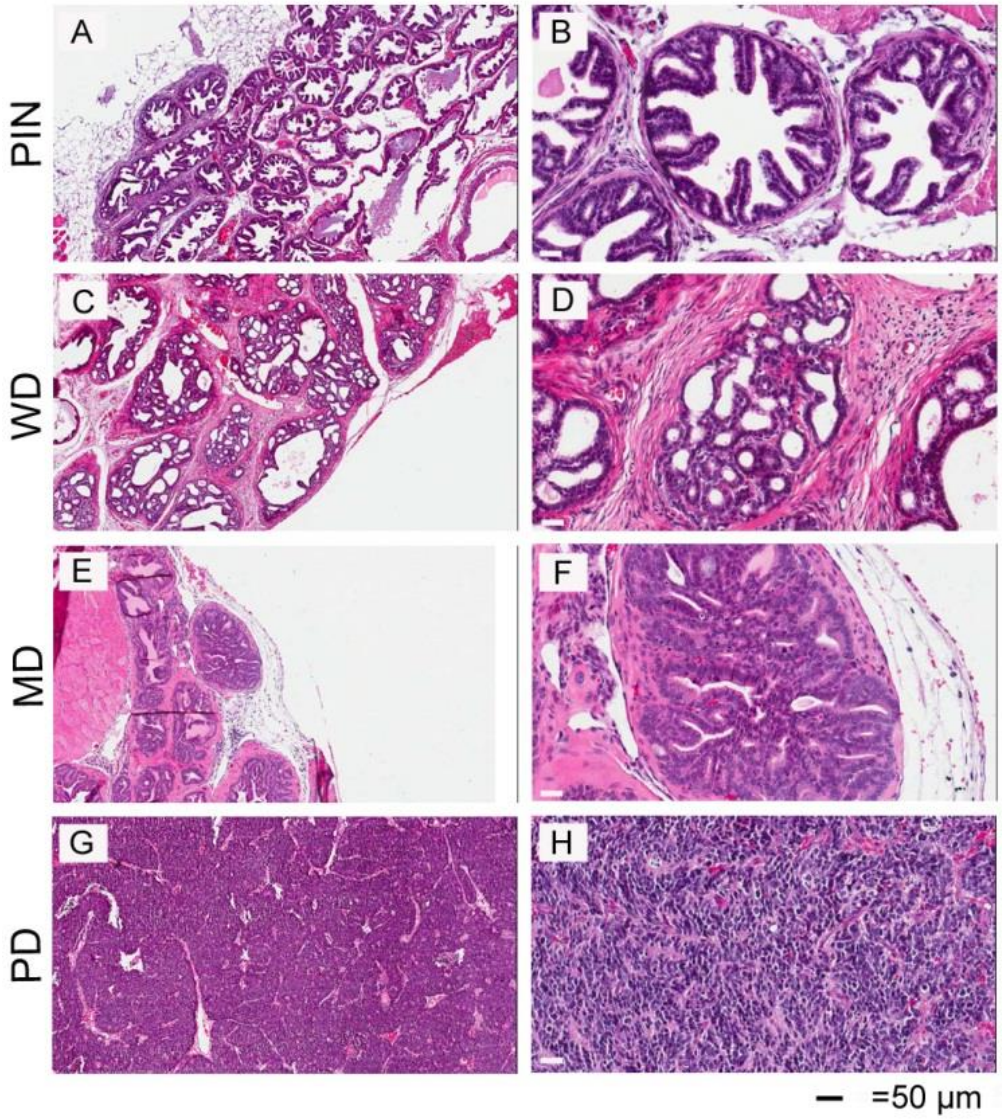

Figure 3-5: Tumours harvested from mouse models were analysed via histopathology. Once animals from the endpoint study group were sacrificed and the primary prostate tumours were harvested, 5 µm FFPE sections of the tumours were stained by H&E for analysis. The models presented with a range of PCa stages from PIN (A, 50xand B, 200x), well differentiated carcinoma (C, 50x and D, 200x), moderately differentiated carcinoma (E, 50x and F, 200x) and poorly differentiated carcinomas (G, 50x and H, 200x), as represented above from *Cd9* wt TRAMP positive animals.

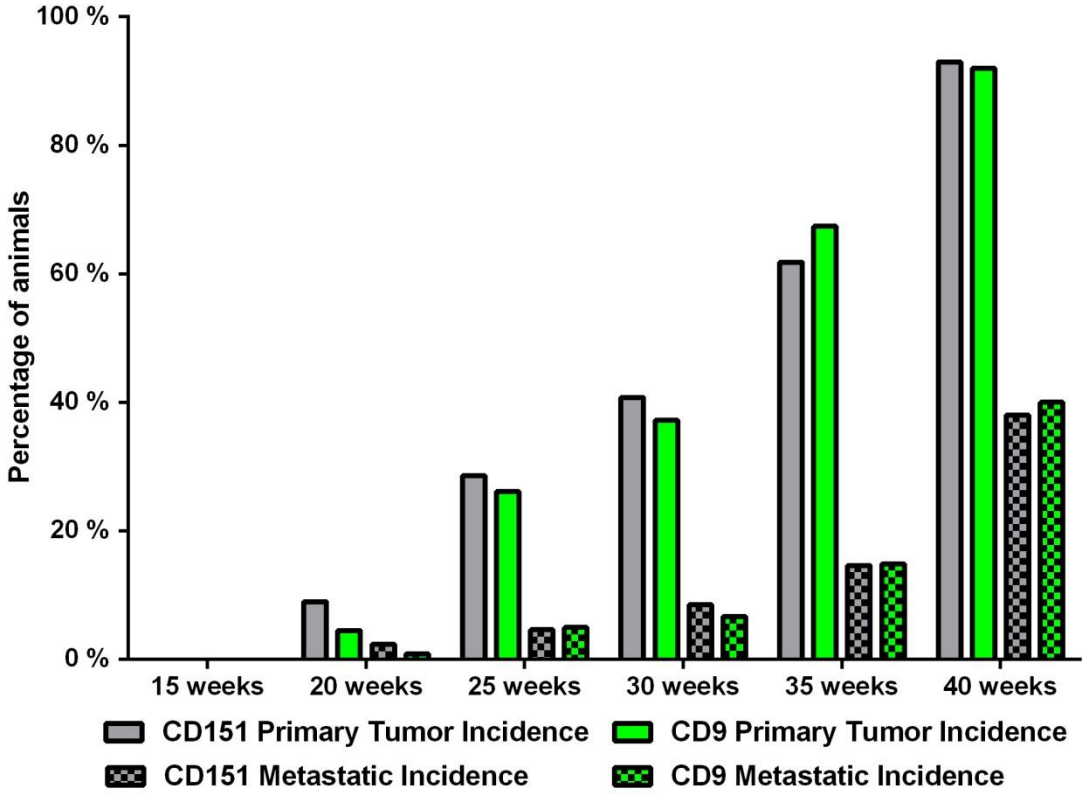

Figure 3-6: Cumulative incidence of palpable primary tumours and metastases, in the CD151/TRAMP and CD9/TRAMP animals from the endpoint group.
All TRAMP positive animals (*Cd151*/*Cd9* wt, heterozygous and KO) from the endpoint group were analysed in regards to time to palpable primary prostate tumour (tumour onset) and whether they displayed metastases in either the liver or lungs (metastatic incidence) at time of palpable prostate tumour to build up a general overview of disease progression in the model.

3.2.3.3 Seminal vesicle enlargement

Upon dissection of the experimental animals no overt developmental irregularities were noted in any of the organs other than the reproductive tract, as expected. However it was noted that all the *TRAMP* animals had grossly enlarged seminal vesicles in the comparison to *TRAMP* negative animals, regardless of whether the animals were *Cd151* or *Cd9* wt heterozygous or KO. A normal seminal vesicle from a 30 week old TRAMP negative animal can be seen in Figure 3-7 (A), while a seminal vesicle from a 30 week old *TRAMP* animal is clearly enlarged in comparison (B). Extremely enlarged seminal vesicles that also had some discolouration, due to necrosis were also seen in a few *TRAMP* animals (C).

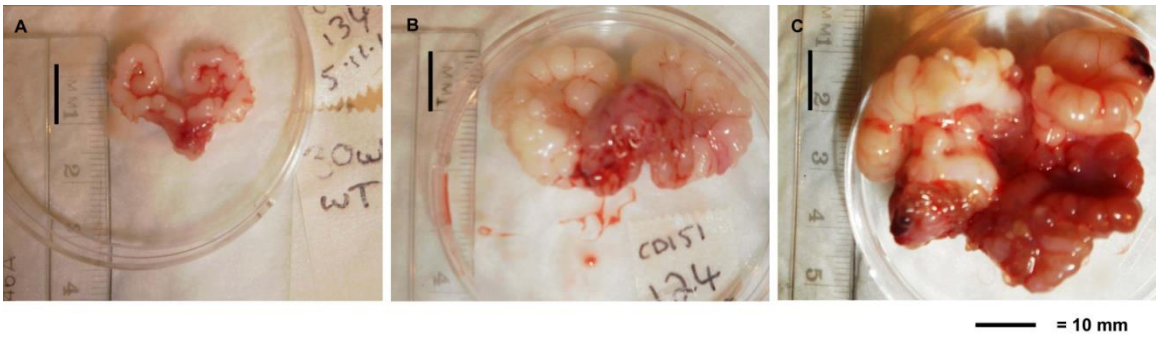

Figure 3-7: Seminal vesicles were enlarged in TRAMP animals.
Upon dissection, seminal vesicles from TRAMP animals were found to be overall grossly enlarged (B) compared to TRAMP negative animals (A). A small subset TRAMP positive animals had extremely enlarged seminal vesicles with associated necrosis (C).

3.2.4 Tetraspanin expression in mouse prostate tissue

As an initial step in the characterisation of the CD151/TRAMP and CD9/TRAMP mouse models, expression patterns of the tetraspanins proteins needed to be determined in terms of specificity, spatial orientation and intensity. The anti-CD151 and anti-CD9 antibodies would not label the antigens on FFPE sections so fresh frozen mouse tissue sections were used with IF. As an extension to the tetraspanin expression characterisation, CD82 was also labeled on FFPE mouse sections by IHC. The rationale for inclusion of CD82 was that CD82 was used in the human biomarker experiments in this thesis (chapter 6) and could allow some comparison of tetraspanin expression in mouse and human tissue. Furthermore CD82 is known to be down regulated in mouse and human cancerous tissue compared to normal tissue (1.8.2.2) and therefore could somewhat validate the tetraspanin expression patterns in the new mouse models.

3.2.4.1 Expression of Cd151 in mouse tissue

As part of the characterisation process, expression patterns of the tetraspanins were analysed by IF on FF mouse sections. To determine specificity of the CD151 antibody, sections of *Cd151* KO mouse prostate tissue were used as negative controls alongside *Cd151* wt mouse prostate tissue sections in all IF experiments. As shown in Figure 3-8 (panels A and B, 100x and 400x respectively) the KO

tissues did not express the Cd151 protein; furthermore the CD151 antibody resulted in no unspecific labeling in mouse prostate tissue, besides the secondary antibody infrequently sticking to the luminal secretions. Expression patterns of the Cd151 protein on *Cd151* wt mouse prostate tissue can be seen Figure 3-8. In normal mouse dorsal prostate tissue expression of Cd151 is predominantly on the membrane and cytoplasm of the basal cells, while the luminal epithelial cells express Cd151 on the basal and lateral membrane surfaces (panels C, 100x and D, 400x). In well/moderately differentiated prostate tumour tissue Cd151 expression is in the basal cells (where still present) and basal/lateral of the epithelial cells (panels E, 100x and F, 400x). In poorly differentiated prostate tumour tissue expression of CD151 expression is membranous in the tumour cells (panels G, 100x and H, 400 x).

Figure 3-8: Expression of Cd151 in mouse prostate normal and tumour tissue.
Cd151 protein expression was analysed via IF on 4µm fresh frozen mouse sections, from *Cd151* KO normal prostate glands (A, 100x and B, 400x), *Cd151* wt normal prostate glands (C, 100x and D, 400x), moderately differentiated tumours (E, 100x and F, 400x) and poorly differentiated tumour tissue (G, 100x and H, 400x). The anti CD151 primary antibody, clone LAI2 (Table 2-7) was used to label the Cd151 protein and visualised using the Alexa 594 conjugated secondary antibody and images captured on the Zeiss Axioplan fluorescence microscopy suite, using set exposure times of 500 milliseconds. The DAPI counterstain labels nuclear material in blue.

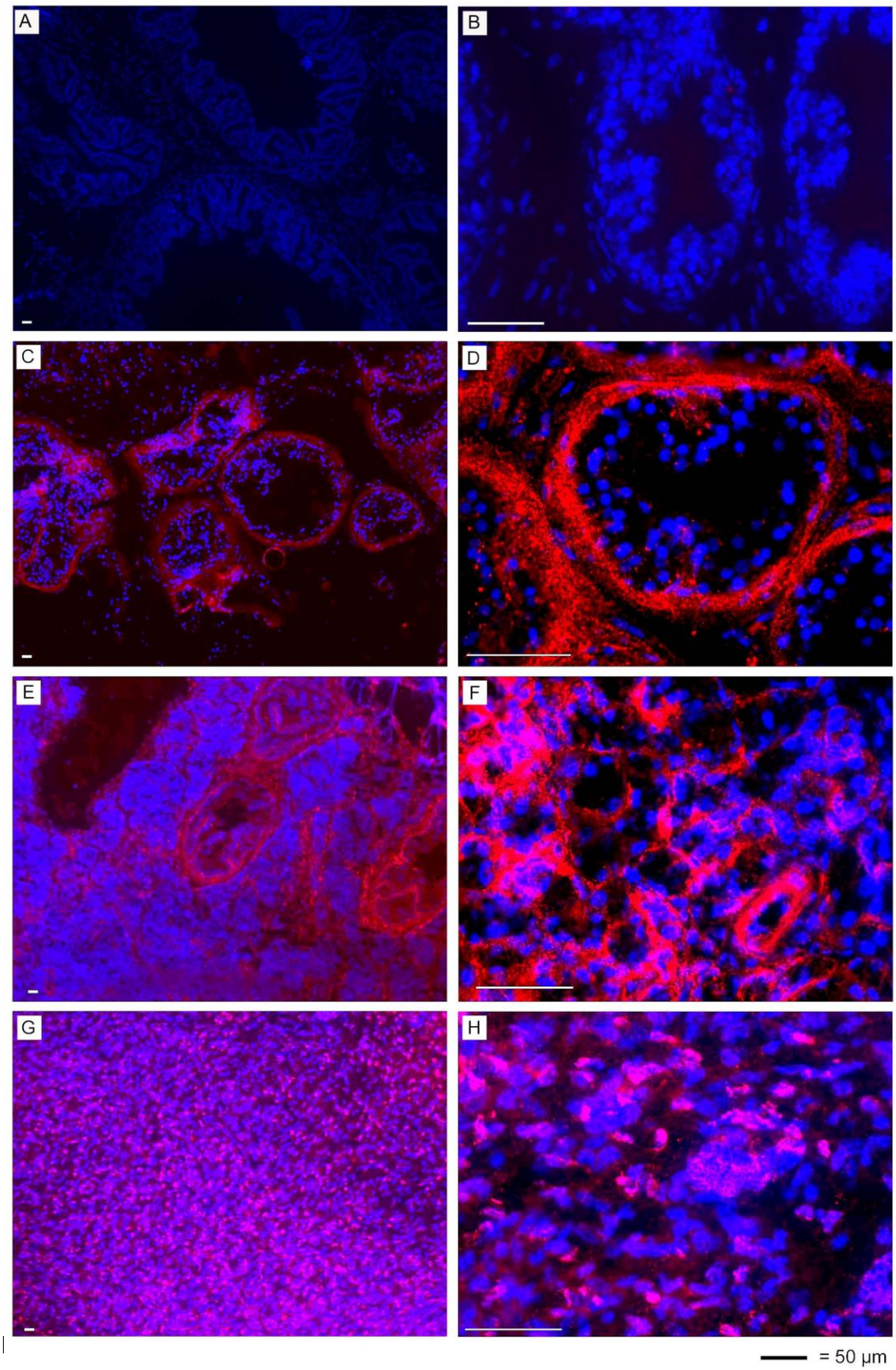
A
B
C
D
E
F
G
H
= 50 µm

3.2.4.2 Expression of Cd9 in mouse tissue

The analysis of the expression patterns of Cd9 on frozen mouse tissue, as with Cd151, was visualized by using IF labeling of the protein. To determine specificity of the CD9 antibody, sections of *Cd9* KO mouse prostate tissue were used as negative controls in all IF experiments. As shown in Figure 3-9 (panels A and B) the KO tissues did not express the Cd9 protein; furthermore the CD9 antibody resulted in no unspecific labeling in mouse prostate tissue, besides the secondary antibody infrequently sticking to the luminal secretions. In normal mouse dorsal prostate tissue expression of Cd9 is predominantly on the membrane and cytoplasm of the basal cells, while the luminal epithelial cells express Cd9 on the basal/lateral and apical membrane (panels C and D). Cd9 expression in well/moderately differentiated prostate tumour tissue is in basal/lateral and apical membrane of the epithelial cells (panels E and F). In poorly differentiated prostate tumour tissue expression of Cd9 expression is membranous around the tumour cells (panels G and H).

Figure 3-9: Expression of Cd9 in mouse normal prostate and prostate tumours.
Cd9 protein expression was analysed via IF on 4µm fresh frozen mouse sections from *Cd9* KO normal prostate glands (A, 100x and B, 400x), *Cd9* wt normal prostate glands (C, 100x and D, 400x), wt well differentiated tumours (E, 100x and F, 400x) and wt poorly differentiated tumour tissue (G, 100x and H, 400x). The anti CD9 primary antibody, clone KMC8 (Table 2-7) was used to label the Cd9 protein and visualised using the Alexa 594 conjugated secondary antibody and images captured on the Zeiss Axioplan fluorescence microscopy suite, using set exposure times of 62.4 milliseconds for 100 x magnification and 18.8 milliseconds for 400x magnification. The DAPI counterstain labels nuclear material in blue.

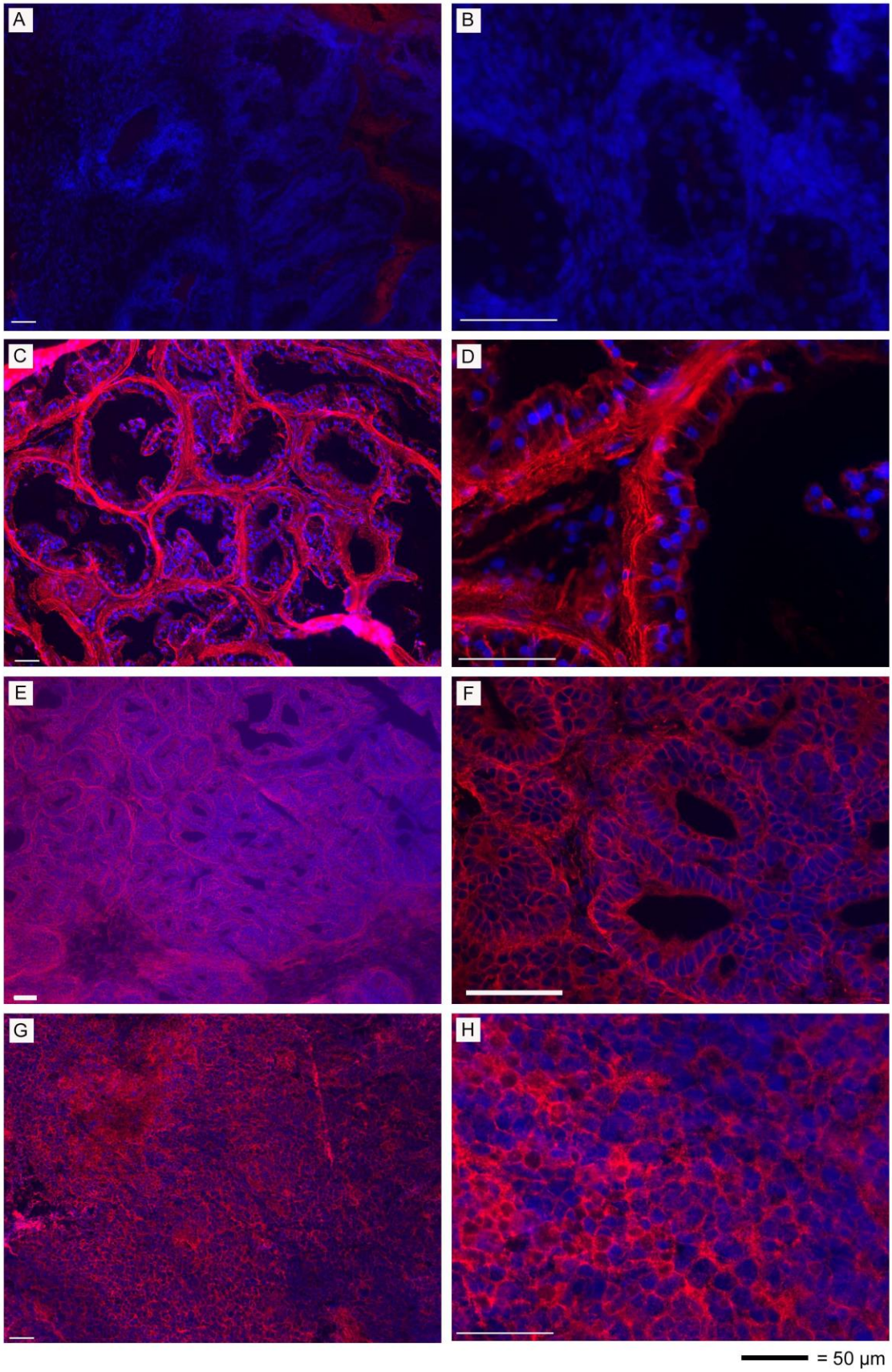
A
B
C
D
E
F
G
H
= 50 µm

3.2.4.3 Expression of Cd82 in mouse tissue

As part of the model characterisation process, expression of the Cd82 protein was analysed in the models. As previously stated the rationale for including Cd82 in the characterisation arises from Cd82 expression patterns being previously well characterized in models of PCa including the TRAMP, as detailed in section 1.8.4 as well as CD82 protein expression being investigated in human tissue in this project (chapter 6). Cd82 protein expression was visualised via IHC labelling of the protein on FFPE sections, as seen below in Figure 3-10. The isotype matched negative control did not label the luminal epithelial cells, however some unspecific staining throughout stroma, blood vessels and luminal secretions was present (panels A, 100x and B, 200x). Cd82 protein expression in normal mouse dorsal prostate tissue is specific to the basal and luminal epithelial cells (both membranous and cytoplasmic) (panels C, 100x and D, 200x). Expression in poorly differentiated tumour tissue was absent or extremely down-regulated, again some staining of the stroma, blood vessels and luminal secretions was present (panels E, 100x and F, 200x).

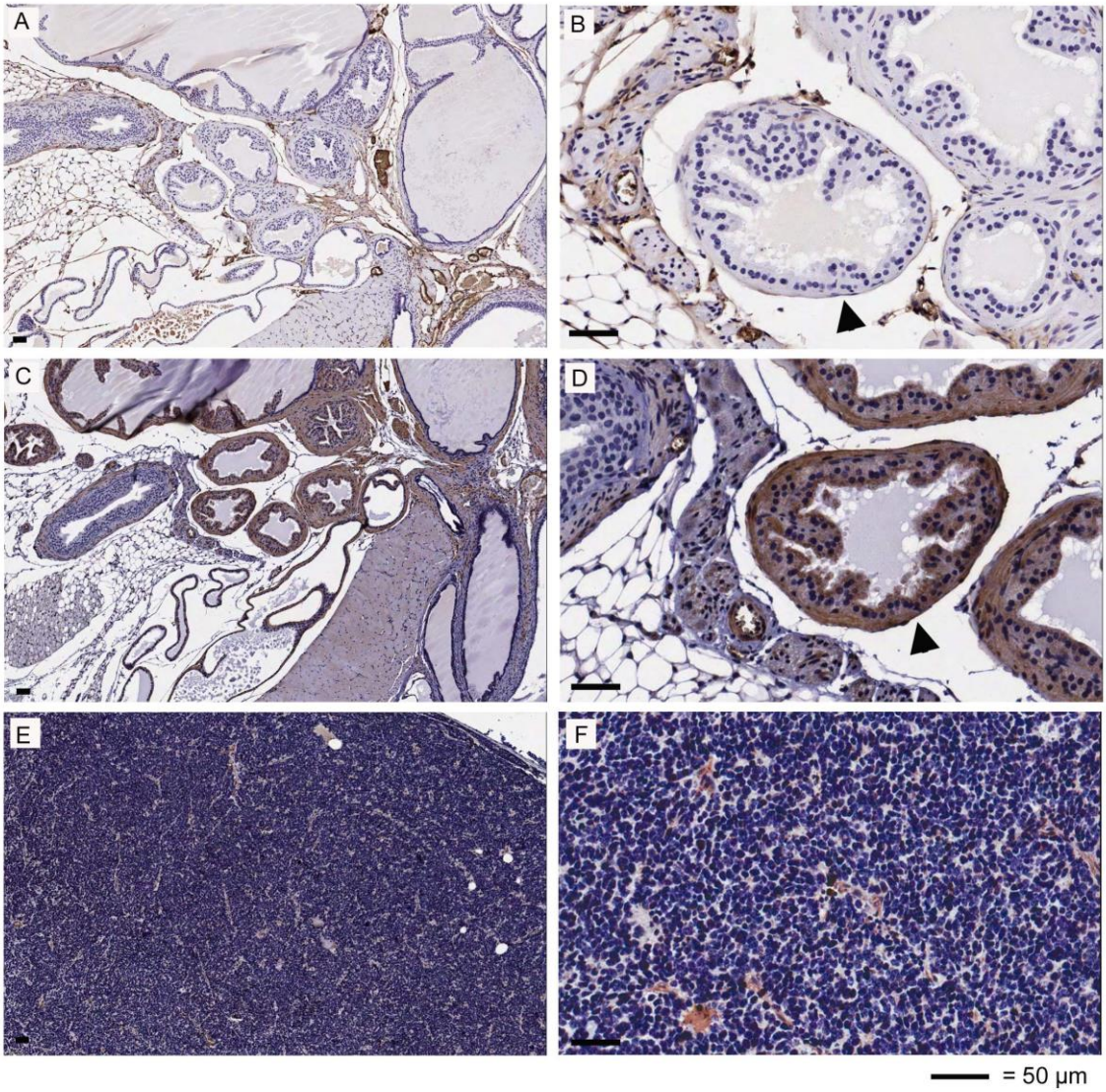

Figure 3-10: Expression of Cd82 in mouse prostate normal and tumour tissue.
Cd82 protein expression was analysed via indirect peroxidase IHC with DAB as the chromagen on 5µm FFPE mouse sections of normal prostate glands stained with an isotype matched antibody control did not label specifically for Cd82 (A, 50x and B, 200x). The normal glands did stain in the cytoplasm and membrane of the basal and epithelial cell of the prostate glands when the anti CD82 was used as the primary antibody, clone G2 (Table 2-7) (B, 50x and D, 200x). Very reduced (to absent) labeling was seen when the anti CD82 antibody was also used to label mouse poorly differentiated primary prostate tissue (E, 50x and F, 200x). The hematoxylin counter-stain labels nuclear material in blue.

3.2.5 Expression of the SV40 protein

By way of PCR it was shown that the *TRAMP SV40* transgene had successfully been crossed into the genome of the required experimental animals. However actual expression of the *TRAMP SV40* gene at the protein level must also be confirmed in the two new genetically engineered models. Using an antibody that specifically labels the SV40 large T antigen (T-ag) (Table 2-7) in the mouse tissue sections the expression of the SV40 T-ag protein could be determined in regards to spatial distribution and amount by IHC.

3.2.5.1 Expression of the SV40 protein in TRAMP and wt prostate tissue

Expression of the SV40 protein in 20 week old mouse prostate tissue was analysed by IHC. Figure 3-11 shows the SV40 protein was not present in the prostate glands from *TRAMP* negative animals, although there was some background staining of luminal secretions and stromal tissue (panels A; 50x and B; 200x) as is consistent with the negative control (panel F; 200x). The SV40 T-ag protein was expressed in the prostate glands tissue from *TRAMP* animals (panels C; 50x and D; 200x and E; 400x). Protein expression was specifically in the nucleus of the luminal epithelial cells of the prostate lobes in the *TRAMP* animals as indicated by the arrows in panel D.

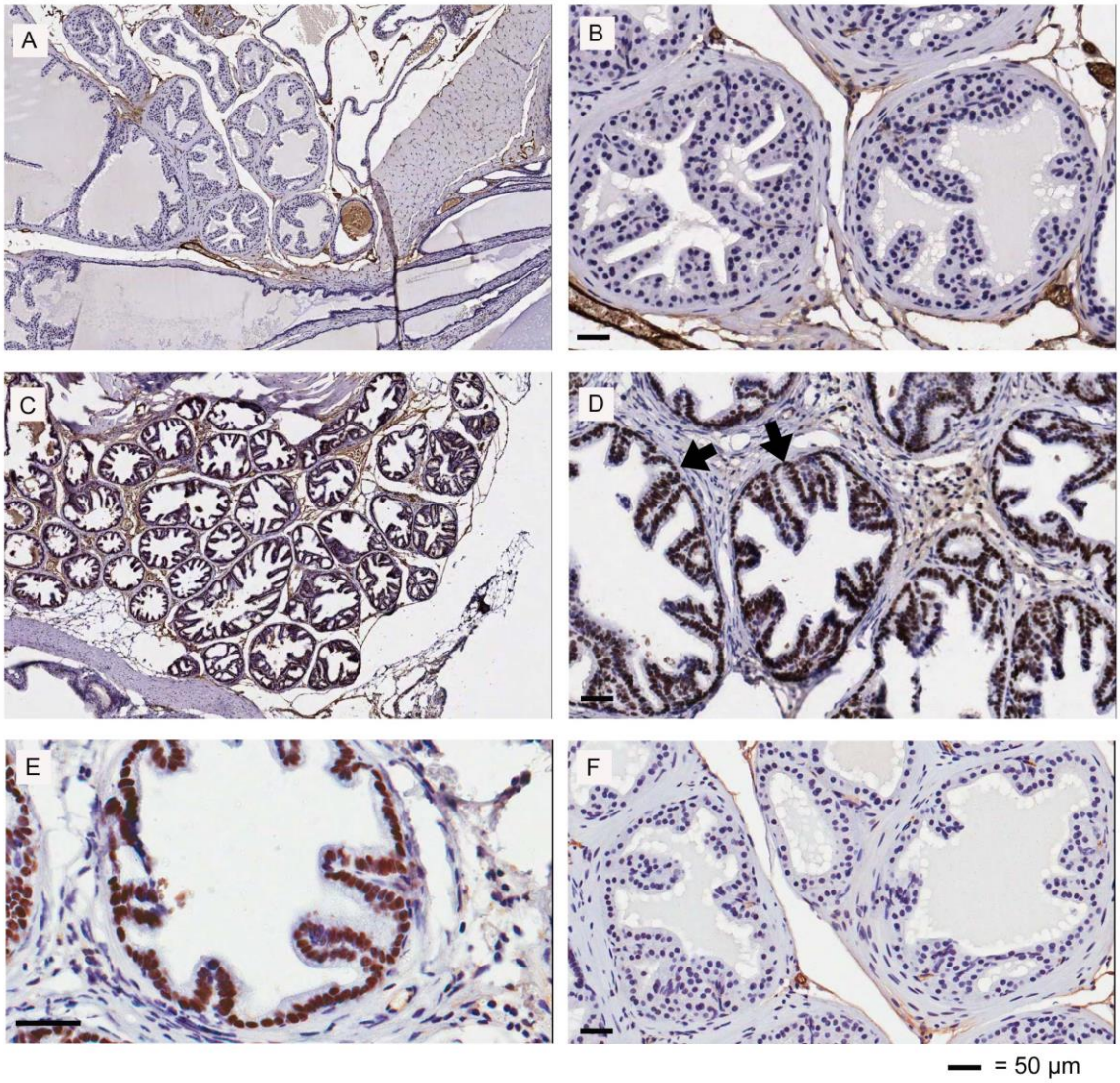

Figure 3-11: Expression of the SV40 T-ag protein in mouse prostate tissue.
Expression patterns of the SV40 T-ag protein was confirmed by indirect peroxidase IHC and DAB as the chromagen to label 5 µm FFPE mouse prostate tissues sections from 20 week old animals. The anti SV40 T-ag antibody, clone PAb100 was used use to label *TRAMP* negative tissues as a definitive negative control (A, 50x and B, 200x) and *TRAMP* prostate tissue (C, 100x and D, 200x and E, 400x). As a further negative control the isotype matched antibody was used to label normal prostate glands (F, 200x).

3.2.5.2 Expression of the SV40 protein in wt and Cd151 and Cd9 KO tissue

Expression of the SV40 protein in the prostate of the TRAMP model leads to PCa initiation and progression as previously explained in detail (1.9.2.1). Therefore to allow comparisons between the various genetically manipulated experimental

groups, expression of the SV40 protein must be consistent. IHC labeling patterns of the SV40 protein in terms of intensities and spatial distribution were consistent in the nuclei of luminal epithelial cells of non-cancerous TRAMP dorsal prostate tissue (Figure 3-12) and nuclei of cells in poorly differentiated TRAMP tumour tissue (Figure 3-13) from *Cd151* wt, KO and *Cd9* wt and KO animals (panels A, B, C and D respectively). Expression patterns of the SV40 protein were also comparable in the *Cd151* and *Cd9* heterozygous normal and tumour tissues (data not shown).

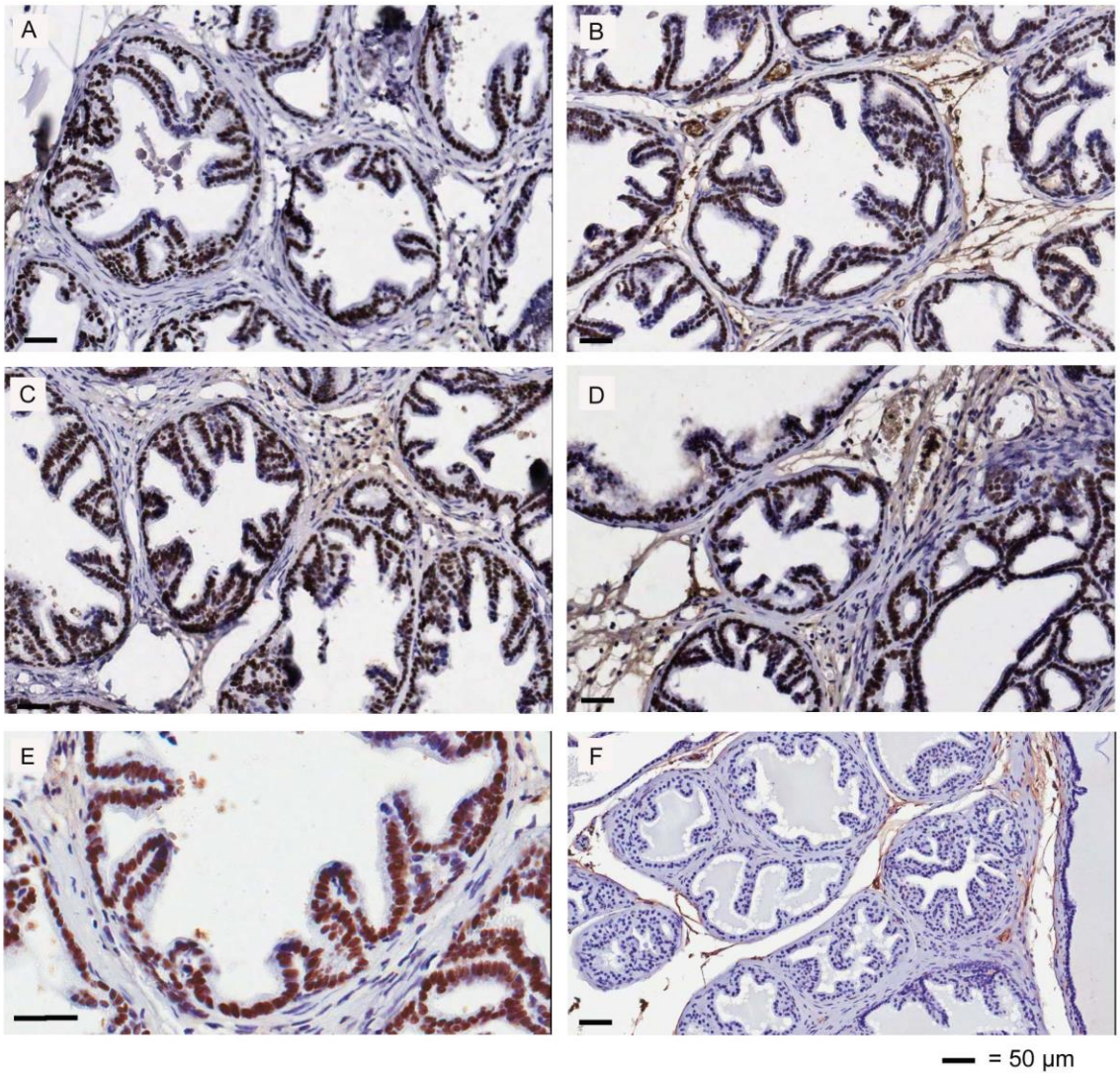

Figure 3-12: Expression of the SV40 protein in non-cancerous mouse prostate tissue of various genotypes.
Expression patterns of the SV40 T-ag protein was confirmed by indirect peroxidase IHC on 5 µm FFPE mouse prostate sections from *Cd151* and *Cd9* wt and KO dorsal prostate tissue sections from 20 week old mice using the anti SV40 T-ag antibody, clone PAb100. Intensity and distribution of the SV40 T-ag protein was consistent across the various genotypes. A; *Cd151* wt, B; *Cd151* KO, C; *Cd9* wt and D; *Cd9* KO at 200x magnification. Panel E represents SV40 expression in the nucleus of the epithelial cells in a dorsal prostate tissue sample at 400x magnification. As a negative control the isotype matched antibody control was used to label normal prostate glands (F, 200x).

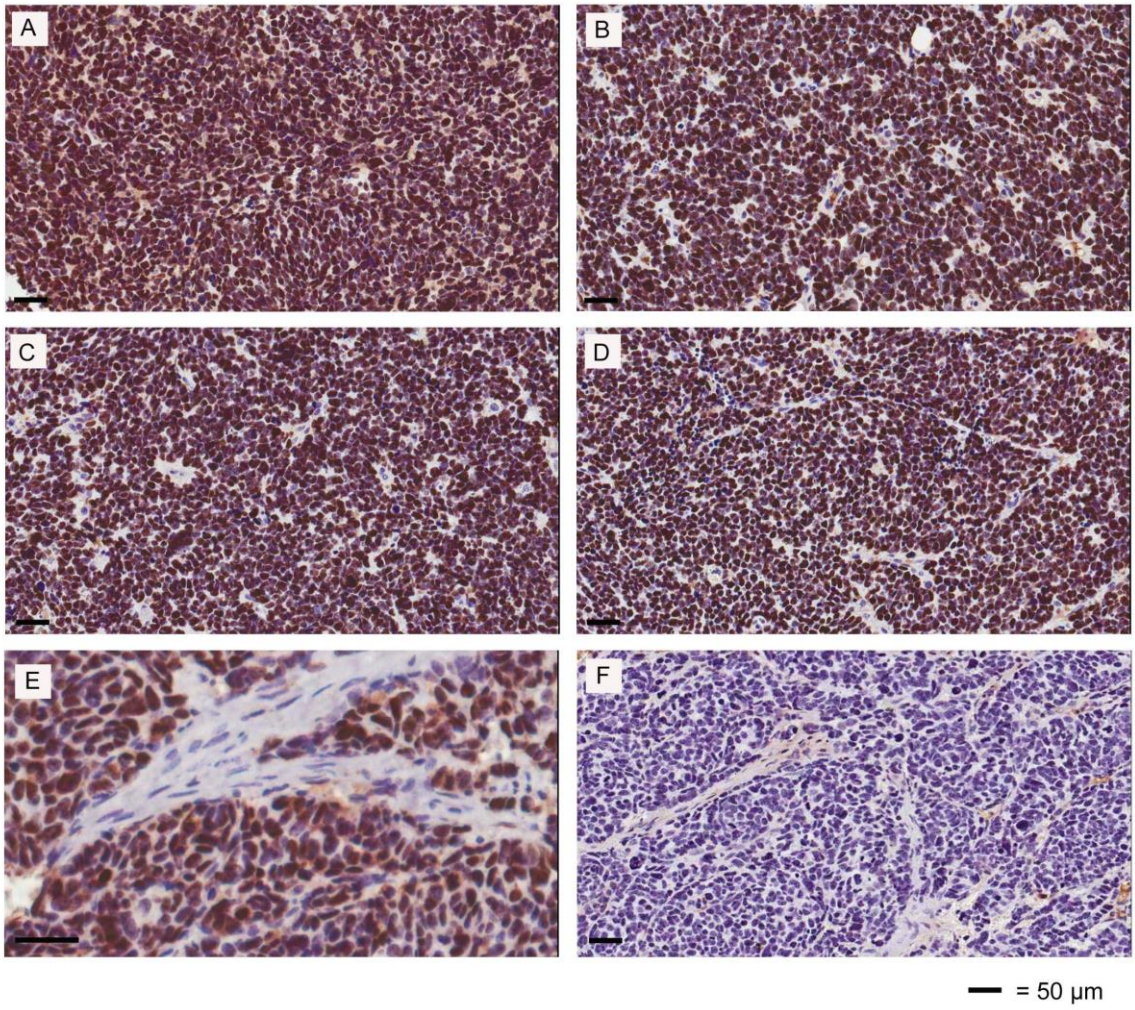

Figure 3-13: Expression of the SV40 protein in poorly differentiated mouse primary prostate tumour tissue of various genotypes.
Expression patterns of the SV40 T-ag protein was confirmed by indirect peroxidase IHC on 5 µm FFPE mouse poorly differentiated tumour sections from *Cd151* and *Cd9* wt and KO animals using the anti SV40 T-ag antibody, clone PAb100. Expression patterns in of the SV40 T-ag protein was analysed via IHC on FFPE. Intensity and spatial distribution of the SV40 protein was consistent across the various genotypes. A; *Cd151* wt, B; *Cd151* KO, C; *Cd9* wt and D; *Cd9* KO at 200x magnification. Panel E represents SV40 expression in the nucleus of the epithelial cells in a primary prostate poorly differentiated sample at 400x magnification. As a negative control the isotype matched antibody control was used to label poorly differentiated primary prostate tumour sections (F, 200x).

3.2.6 Characterisation of metastatic lesions

Once animals from the endpoint group had palpable prostate tumours they were sacrificed and the liver and lungs were collected, which revealed frequent visible cancerous lesions. As part of the characterisation it had to be determined if the lesions in the liver and lungs were metastases disseminated from the primary prostate tumour or in fact primary tumours formed in these organs.

The cancerous lesions in the liver and lungs were identified via H&E staining and serial sections were shown to label positively for the transgene protein SV40 T-ag as in Figure 3-14, A and B. The SV40 T-ag protein was present in the nuclei of the cells within the metastatic lesions of the liver and lungs, while completely absent from the surrounding normal tissue. Furthermore, two of the TRAMP positive animals were culled due to sickness (14 weeks and 18 weeks) and upon autopsy were found to have extensive cancer lesions in the lungs and/or liver while they were shown to have only very early stage prostate cancer, consisting of PIN. The liver and lung lesions from these animals did not stain for the SV40 T-ag (Figure 3-14, C and D). These finding imply that the SV40 T-ag positive tumours did not arise independently in the liver or lungs and are indeed derived from the primary prostate tumours.

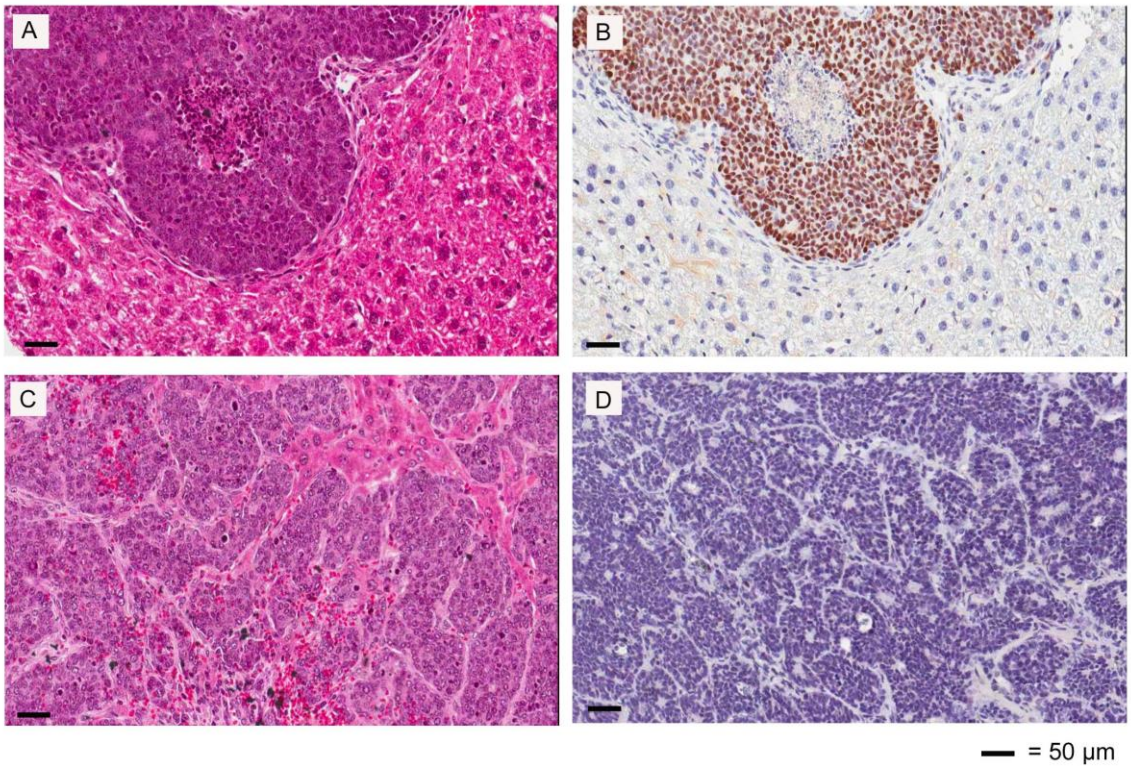

Figure 3-14: Determination of the origin of the metastatic lesions.
The origin of the cancerous lesions in the liver and lung were determined using 5µm FFPE sections via H&E staining techniques along with indirect peroxidase IHC using the anti SV40 T-ag antibody, clone PAb100. Cancerous regions in the liver and lungs animals culled for palpable prostate tumours were classified by H&E (A) and serial sections stained positive in the nucleus for the SV40 T-ag protein (B). TRAMP animals culled due to poor health with relatively normal prostates, had liver and lung cancerous regions identified by H & E (C) and serial sections were negative for SV40 T-ag (D), magnification 200 x.

3.2.7 Characterisation of cells in the primary tumour lesions

There have been previous reports raising issues that TRAMP animals in some previous studies have displayed tumours with a neuroendocrine type phenotype and not epithelial as expected, described in detailed in section 1.9.2.1. As part of the characterisation process a neuroendocrine phenotype of the cancerous lesions in early stage prostate tumours must be ruled out if the model is to recapitulate human PCa. The synaptophysin protein is the most widely used histopathological marker of neuroendocrine cells. IHC labeling of synaptophysin on a section of mouse brain tissue (Dendate gyrus) serves as both a positive and negative control due to the neuroendocrine rich and negative layers (Calhoun, Kurth et al. 1998,

King and Arendash 2002) as shown in Figure 3-15, panel A. Specifically, panel B shows positive staining marked with the star and negative specific staining marked with the arrow. PIN and well differentiated primary prostate tumour foci (panel C) and moderately differentiated metastatic lesions (panel D) were all negative for the neuroendocrine cell marker, except for some unspecific labeling of prostatic glandular secretions in panels B and C. Metastatic lesions in the lung and liver also did not express synaptophysin as represented in panel E.

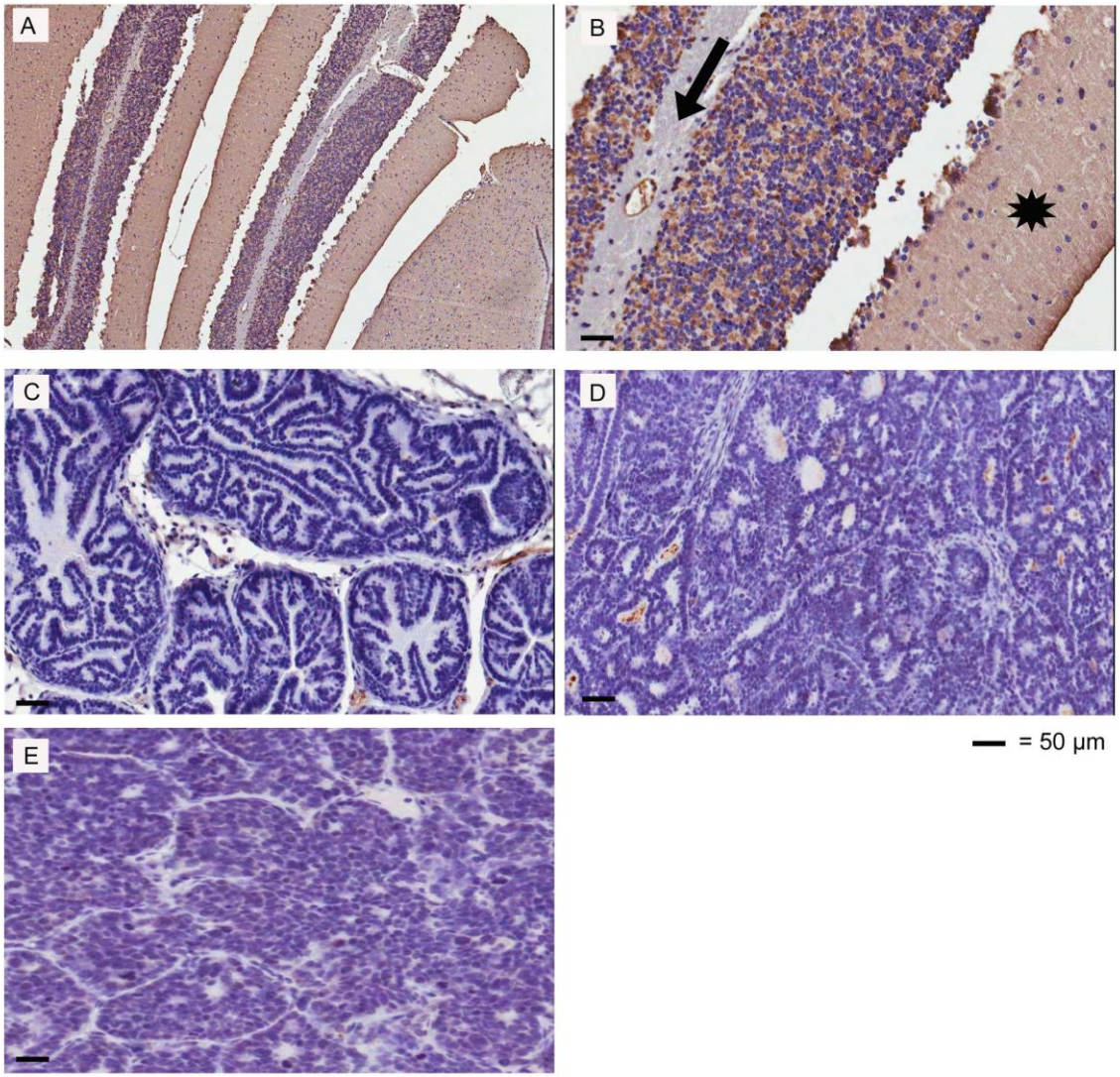

Figure 3-15: Characterisation of tumour lesions for expression of the neuroendocrine cell marker, synaptophysin.
5 µm FFPE sections of primary prostate tumours along with metastatic lesions in the lung and liver from TRAMP positive animals were characterised by indirect peroxidase IHC with DAB as the chromagen and the anti synaptophysin antibody (clone SY38, Table 2-7) that labels neuroendocrine cells as the primary antibody. Brain sections stained for neuroendocrine cells (panel A, 50 x and B 200x) show positive stained layers of the dendate gyrus indicated by the star in panel B while the arrow shows specificity as the layer is negative for synaptophysin labelling. PIN and well differentiated primary prostate tumours (C), moderately differentiated prostate tumour (D) along with lung and liver metastatic tumour lesion represented in E all did not express the synaptophysin protein (200x).

Furthermore in the cell characterisation process the epithelial cell marker E-cadherin was used to label normal glandular prostate and a range of early and advanced prostate tumour cells. E-cadherin was specifically expressed on the epithelial cells of the prostate glands (Figure 3-16; panels A, B and C) while E-cadherin labeling was negative in the surrounding poorly differentiated prostate tumour tissue. A serial section tissue sample from the same animal was labeled for the SV40 T-ag protein. The SV40 T-ag protein was expressed in the surrounding poorly differentiated tumour tissue while mostly negative in the luminal epithelial cells (panel D). Some of the epithelial cells of the normal prostate gland can be seen to be expressing SV40 T-ag protein as indicated by the arrows, which does correlate to the cells showing some dysplasia, such as cellular tufting and stratification (detailed in section 1.9.4).

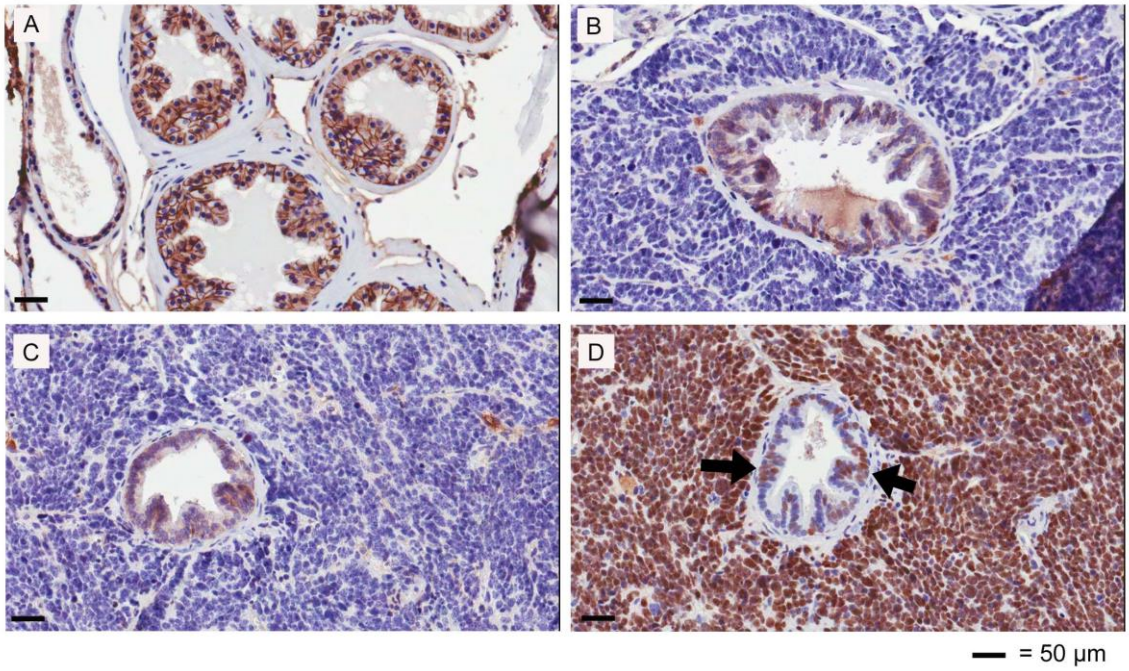

Figure 3-16: Characterisation of tumour lesions for the epithelial cell marker E-cadherin and the SV40 T-ag protein.
5 µm FFPE sections of normal prostate glands (panel A) and poorly differentiated primary prostate cancer cells surrounding normal glands (panels B, C and D) were labelled by indirect peroxidase IHC with DAB as the chromagen with either the epithelial cell marker E-cadherin (A, B and C; 200x) or the SV40 T-ag protein (D, 200x).
.

3.3 *Discussion*

Previous *in vitro* and *in-vivo* grafting studies involving tetraspanins have implied various roles in PCa cancer initiation and progression; however these previous methodologies do not recapitulate the tumour microenvironment or the multistep progression of the human disease. A major over aching aim of this project was to determine if the tetraspanins *Cd151* and *Cd9* directly affect PCa initiation and progression in a mouse model that best parallels the human form of PCa (chapters 4 and 5). To achieve this, the TRAMP model was chosen and crossed with the mouse *Cd151* and *Cd9* KO models. This chapter discusses the generation and characterisation of two new transgenic KO mouse models, the CD151/TRAMP and CD9/TRAMP models.

The models were generated by crossing the *Cd151* KO model on to the TRAMP model and also totally independently crossing the *Cd9* KO model onto the TRAMP model as detailed in 2.3.2 and 2.3.3. The approach of breeding the models separately resulted in a very extensive breeding program, however because the *Cd151* and *Cd9* KO models originated from different parental lineges, was essential to enable the use of co-house, littermate control animals for both the cohorts individually throughout the project. Furthermore both the KO models originally generated on the B6 background were extensively crossed onto the FVB backgrounds allowing a single final cross (individually for both KO models) to generate truly 50%/50% B6/FVB F_1 hybrid *Cd9* and *Cd151* KO's, eliminating any random re-assortment of alleles from the two strains as detailed in section (2.3.2).

Every experimental animal was genotyped at 3 weeks of age and the PCR products illustrated in Figure 3-1 to Figure 3-3 clearly discriminated between genotypes. Once genotyped the excess animals of unneeded genotypes were culled and remaining animals allocated to the appropriate experimental groups, with subsequent monitoring for tumour development of the co-housed experimental animals carried out blindly with regard to genotype. Secondary confirmation of

genotypes was achieved with an additional tissue sample taken from each experimental animal at sacrifice. This proved necessary as final analysis of the genotyping discrepancies showed error rates for each genotypic group were TRAMP; 4.9%, CD151; 6.5% and CD9; 3.5%, which would have influenced results if not rectified. Errors may have arisen not only as a result of PCR analysis but also from data entry and animal or sampling handling.

Since the two genetically engineered models were created for the first time specifically for this project, basic characterisation of the models had to be undertaken to validate subsequent results in chapters 4 and 5 (Shappell, Thomas et al. 2004). The *Cd151* and *Cd9* KO models have been characterized on both the B6, FVB and to some extent the B6/FVB F_1 backgrounds and have been found to develop certain pathologies as detailed in 1.9.2.3. Analysis of the *Cd151* and *Cd9* KO F_1 animals did not reveal any overt developmental defects, in agreement with published literature (Le Naour, Rubinstein et al. 2000, Baleato, Guthrie et al. 2008). The TRAMP model is the best characterized model of PCa to date and in this current study PCa development followed the generally expected pathways (Greenberg, DeMayo et al. 1995). When the TRAMP and *Cd151* and *Cd9* KO animals were cross bred to produce the CD151/TRAMP and CD9/TRAMP models on the B6/FVB F_1 background, again no unexpected overt developmental irregularities were seen in any of the organs (except the urogenital tract as expected). Furthermore reproduction in the two models was not effected in any detrimental way as litters were produced according to Mendelian frequencies (wt; 25%: het; 50% and KO; 25%).

As an early characterisation step to verify tumour development and determine tumour progression in the models, two groups of TRAMP positive/*Cd9* wt animals were culled at earlier time points (10 and 20 weeks). The animals in each group showed different stages of PCa development as displayed in Table 3-3 and Table 3-4. Even though the numbers were too small to allow statistical analysis, it did

allow us to verify tumour development and progress in the model is in agreement with other published reports (Gingrich, Barrios et al. 1996, Kaplan-Lefko, Chen et al. 2003, Tang, Wang et al. 2008).

The main groups of experimental animals were the endpoint study cohorts (explained in 2.3.5). Once the experimental animals had palpable prostate tumours or reached 40 weeks of age, they were culled as an endpoint, detailed in 2.3.5.1. The primary prostate tumours, liver and lungs were collected for subsequent analysis and the animals were subjected to a brief autopsy to determine any overt development irregularities were evident. As shown in Figure 3-5 both models presented with all the expected stages of PCa as previously reported in the TRAMP model (Gingrich, Barrios et al. 1999, Kaplan-Lefko, Chen et al. 2003, Shappell, Thomas et al. 2004) from PIN to well differentiated, moderately differentiated and poorly differentiated primary prostate lesions through to secondary metastatic lesions disseminated from the primary prostate tumours.

In contrast to the finding by Gingrich *et al* (1999) that the seminal vesicles were only enlarged in the TRAMP B6 animals and not the F_1 animals, we found all TRAMP F_1 animals to have enlarged seminal vesicles in comparison to the wt littermate control mice (Figure 3-7). This was in agreement with the findings of more recent studies (Matthew Naylor, Garvan Institute, NSW; unpublished data, personal communication). Due to the tissue collection method, where the tumour was dissected along with the bladder and seminal vesicles, because of the tumour frequently engulfing these organs, the seminal vesicle enlargement could not be quantified. No other developmental irregularities in any organs or tissues were identified.

The TRAMP model was chosen for its recapitulation of human prostate tumour progression. The results indicate that breeding the TRAMP with the two KO models to produce the experimental animals did not alter the characteristics of the

resultant prostate tumours or cause any other developmental effects and therefore validate their use in the project.

As an initial step in the characterisation of the two models, expression patterns for the tetraspanins had to be determined. This was especially pertinent since the aim of this part of the project was determining the specific effect of CD151 and CD9 on the initiation and progression of PCa in the models. Unfortunately there are currently no reliable antibodies for labeling of Cd151 and Cd9 in FFPE mouse tissue, so labeling the proteins in FF sections via IF was used instead. Firstly specificity of the two antibodies had to be determined by the use of appropriate negative controls. The project was in the fortunate position to have the *Cd151* and *Cd9* KO tissue sections to use as the definitive antibody negative controls. The CD151 and CD9 antibodies did not label the TRAMP *Cd151*/*Cd9* KO mouse prostate tissue sections in any specific manner and also did not give any unspecific background staining as represented in Figure 3-8 and Figure 3-9 (A and B). These results allow the conclusion that any labeling from these antibodies on mouse prostate tissue is specific and can be confidently interpreted.

Cd151 was expressed both in the membrane and cytoplasm of the basal cells of normal non-cancerous prostate glands, while expression of Cd151 in the luminal epithelial cells of the glands was mainly in the basolateral membrane with reduced cytoplasmic expression (Figure 3-8, C and D). In moderately differentiated tumour tissue where the basal cells were mostly absent, Cd151 expression was specific to the basolateral membranes of the epithelial cells of the glands (Figure 3-8, E and F). In poorly differentiated tumour tissue, where no prostate glandular structures were present, Cd151 expression was predominantly on the membrane of the individual tumour cells (Figure 3-8, G and H).

Cd9 expression showed similarities to expression of Cd151 in mouse prostate tissue. However unlike Cd151, Cd9 expression was also expressed on the apical

membrane of the epithelial cells in prostate glands along with reduced cytoplasmic expression (Figure 3-9, C and D). Protein expression patterns of Cd151 and Cd9 in the models were in agreement with other reports analysing mouse tissue samples (unpublished data from our lab; Severine Roselli *et al*, manuscript in preparation) and human tissue samples (Higashiyama, Doi et al. 1997, Sincock, Mayrhofer et al. 1997, Huang, Kohno et al. 1998, Geary, Cambareri et al. 2001, Chuan, Pang et al. 2005, Mosig, Lin et al. 2012) and therefore the Cd151 and Cd9 protein expression patterns in both the mouse models recapitulate the human expression of the proteins.

Cd82 protein expression patterns were also analysed in the mouse prostate tissues, however by IHC on FFPE tissue specimens. The reason for inclusion of Cd82 in the tetraspanin expression characterisation in the models was due to the tetraspanin Cd82 protein expression being previously characterised in various models including the TRAMP as detailed in 3.2.4, and furthermore it was used in this study to analyse CD82 protein expression in human tissue. In normal non-cancerous mouse prostate tissue Cd82 was expressed in the basal cells and the epithelial cells of the prostate glands, with the basal cells and epithelium apical membrane expression the strongest (Figure 3-10, C and D). The Cd82 expression was either severely down regulated or completely absent in poorly differentiated prostate tumour tissue (Figure 3-10, E and F). The down regulated expression pattern of CD82 in advanced PCa is in agreement with published work from human and mouse studies. (Dong, Lamb et al. 1994, Christgen, Bruchhardt et al. 2008, Protzel, Kakies et al. 2008). Therefore the Cd82 expression pattern in the two models recapitulates CD82 expression in human PCa.

Incorporation of the *TRAMP SV40* transgene in to the experimental animals was confirmed by way of PCR (3.2.1). However for the transgene to exert it's intended oncogenic effects it must express a biologically active, functioning protein. IHC labeling of the SV40 large T (T-ag) protein can be used as a way to analyse protein

expression of the SV40 protein, not only in terms of spatial distribution but also intensity, as indication of how strongly the protein is expressed. The *TRAMP* negative mouse prostate tissues did not express the SV40 T-ag protein (Figure 3-11, A and B), while the SV40 T-ag protein was strongly expressed in prostate tissues from *TRAMP* animals as can be seen in Figure 3-11 (C and D). Staining was specific to the nucleus of the epithelial cells of the prostate glands as expected due to the prostate specific promoter (detailed in section 1.9.2.1). Others organs were screened for SV40 T-ag however no endogenous expression was found in liver, lung or kidneys. This result allows determination that the oncogenic SV40 T-ag protein is being correctly expressed and that expression is specific only to the nucleus of the epithelial cells of the prostate glands in the TRAMP animals. Furthermore no expression of the SV40 protein was apparent (via IHC) in other tissues in the *TRAMP* animals that may exert any additional uncontrollable oncogenic stimulus.

The SV40 T-ag protein is the primary oncogenic stimulus for initiation and progression of PCa in the TRAMP model (1.9.2.1). With that in mind the next logical step in the characterisation process was to determine constant expression of the SV40 T-ag protein in the various genetic groups (wt, heterozygous and KO) of the two models. This allows any subsequent results to be interpreted as a direct result of the genetic modifications in the animals and not a secondary effect on SV40 T-ag expression. Expression of the SV40 T-ag protein in *Cd151* wt and KO and *Cd9* wt and KO normal dorsal prostates was consistent in terms of intensity and distribution as in Figure 3-12. Spatial distribution of the SV40 T-ag protein was also consistent in *Cd151* wt and KO and *Cd9* wt and KO poorly differentiated primary prostate tumour tissue (Figure 3-13). Tissues from *Cd151* heterozygous and *Cd9* heterozygous mice were also consistent for SV40 T-ag protein expression (data not shown). Therefore it can be concluded that any changes to the initiation and progression in PCa between the various genetic groups is a direct result of the effects of the differences in Cd151 or Cd9 protein expression.

Many of the animals upon dissection presented with macroscopically visible cancerous surface lesions on the lungs and liver. It should be noted here that original characterization of the TRAMP F_1 model showed that 25% (14/57) of animals developed lung metastases but only 3% (2/58) developed liver metastases (Gingrich, Barrios et al. 1999). Projects subsequent to this original published characterization of the TRAMP, involving the TRAMP animal have only analysed data from lung organ collection, based seemingly on the original characterization of the model. However in this project when dissection was taking place many of the animals had macroscopically visual cancerous surface lesions on not only the lungs but also the liver. Therefore we suggest that future metastasis studies using the TRAMP F_1 model include analysis of the liver as routine. This is justified when taking into consideration the fact that metastasis to the liver and lungs is also seen in the human form of the disease, albeit less than to bone (Gittes 1991).

The liver and lungs from every animal in the endpoint group were collected and analysed via histopathology to determine variations in the extent of metastases between the genotypic groups as in chapters 4 and 5. As a part of the characterisation process, to justify any subsequent results that arose from the analysis of the liver and lungs, the lesions had to be proven to be true secondary metastatic sites and not simply primary cancerous sites. This was essential as two young TRAMP mice had to be culled due to health complications and upon autopsy presented with either primary liver and/or lung carcinomas with mostly normal prostates. Histopathology (H & E) was used to identify cancerous regions in liver and lung sections from TRAMP animals with PCa (Figure 3-14, A), while a serial section was labeled for the SV40 T-ag protein (B). The cells in the identified liver tumour lesions did express the SV40 protein in the nucleus of the cells, while the surrounding normal liver tissue did not express the SV40 T-ag protein. Furthermore the cancerous liver lesions in the animals with normal prostates (C) did not express the SV40 T-ag protein (D). It is worthwhile reiterating the fact that

normal livers and lungs from TRAMP animals without prostate tumours also did not express the SV40 T-ag protein. Therefore it can be concluded that the cancerous lesions in the liver and lungs are in fact secondary metastatic sites that originate from the primary SV40 T-ag induced spontaneously from primary prostate tumours. Hence any variations in the incidence rates of tumour lesions in the liver and/or lungs in the different genotypic groups within the two models (wt, heterozygous and KO) can be interpreted to be an effect of the genetic modification on the metastatic cascade.

It should also be noted that lymph nodes have previously been reported to be a site of local tumour invasion in the TRAMP B6/FVB F_1 animals (Kaplan-Lefko, Chen et al. 2003, Tang, Wang et al. 2008). In this study lymph nodes were not routinely harvested since the majority of the animals did not have visibly enlarged pelvic lymph nodes, which are extremely difficult to locate unless significantly diseased. Furthermore this difficulty in locating lymph nodes is exacerbated with increasing age (up to 40 weeks in this study) due to the fat pads obscuring the nodes' visibility (Gingrich, Barrios et al. 1999, Kaplan-Lefko, Chen et al. 2003).

As described in detail in section 1.9.2.1, reports have been published about the TRAMP model on a pure FVB background developing a subset of aggressive cancerous lesions that display a neuroendocrine phenotype rather than epithelial as in human PCa (Huss, Grayy et al. 2007, Chiaverotti, Couto et al. 2008). As a part of the characterisation process this issue had to be addressed to rule out a neuroendocrine phenotype in prostate tumours in the two F_1 models. To achieve this objective the neuroendocrine cell marker, synaptophysin was labeled by IHC. The murine hippocampus, specifically the dentate gyrus has layers that are synaptophysin positive but also distinct synaptophysin negative layers (stratum pyramidal and granular cell layer) as seen in Figure 3-15 (Calhoun, Kurth et al. 1998, King and Arendash 2002). Therefore, these tissue sections were utilized as both experimental positive and negative controls. Well differentiated PCa was

consistently negative for synaptophysin expression as were liver and lung metastases disseminated from PCa. Our findings agree with the previously published report that the F_1 TRAMP model does not display an overt neuroendocrine cellular phenotype in the early stage prostate cancerous development (Gingrich, Barrios et al. 1996). Furthermore, consistent with previous reports in the TRAMP model (Gingrich, Barrios et al. 1999) and in the human disease (Tomita, van Bokhoven et al. 2000, van Oort, Tomita et al. 2007), E-cadherin was expressed in epithelial cells in prostate glands that showed signs of PIN, although the expression was reduced compared to epithelial cells in normal glands. Moreover expression of E-cadherin was absent or severely down regulated in poorly differentiated tumour tissue compared to normal prostate glands (Figure 3-16), which may suggest an epithelial to mesenchymal transition process occurring with tumour development. In a serial section it can be seen that SV40 T-ag protein was not highly expressed in the epithelial cells of the normal prostate glands although some minimal SV40 T-ag expression could be seen in distinct areas where PIN had started to develop. As expected, SV40 T-ag protein was highly expressed in the surrounding poorly differentiated tumour tissue.

These results show that the early stage primary prostate cancer foci and metastatic lesions in the two models are not composed of a neuroendocrine cell population. Furthermore cells showing signs of PIN (which represents early stage PCa) are epithelial. Taken together it can be concluded that the developing PCa tumours in the two models are not neuroendocrinal but do in fact develop from prostate cells that have an epithelial phenotype. Therefore the model does recapitulate the epithelial nature of PCa in the humans.

A graphical representation of the overall progress of the two models in the endpoint group with regards to prostate cancer onset and metastases is shown Figure 3-6. PCa initiation/onset in this project specifically refers to time to palpable prostate tumour. It should be noted that the original planned methodology in the project was

to track the tumour initiation and progress in the models through *in-vivo* bio-imaging as described by Hsieh *et al*. (2007), by crossing the models with an animal that had a prostate specific bioluminescent tag (PSA-luc; Caliper Life Sciences). However the supplier ultimately failed to supply the animal and it became necessary to monitor tumour progression manually. The result was an altered breeding schedule that used manual prostate palpation as a way to gauge prostate tumour initiation and then use that as an endpoint. The CD151/TRAMP animals started to developed palpable primary prostate tumours by 16 weeks of age while CD9/TRAMP animals developed palpable tumours by 18 weeks of age which is in agreement with other reports of the TRAMP F_1 model (Kaplan-Lefko, Chen et al. 2003, Tang, Wang et al. 2008). By 40 weeks of age 91% (68/75) of the CD151/TRAMP animals had primary palpable prostate tumours and 93% (80/86) of the CD9/TRAMP animals had palpable prostate tumours. Other studies have reported 100% of the experimental animal cohorts had PCa by earlier time points (Gingrich, Barrios et al. 1996, Kaplan-Lefko, Chen et al. 2003, Tang, Wang et al. 2008) This discrepancy is due to our end point being time to palpable tumour and while the other reports culled the cohorts at earlier cross sectional time points and classified every stage of PCa from PIN to invasive carcinoma as positive for PCa. However it should be noted that nearly all animals from the tumour progression groups culled at earlier time points (6/7 animals culled at ten weeks of age and 10/10 animals culled at 20 weeks of age) were found to have some form of neoplasia upon autopsy (3.2.3.2).Furthermore every TRAMP animal in the end-group experimental cohort was found to have some form of prostatic neoplasia when culled, in agreement with earlier published reports.

Once animals presented with a palpable tumour they were sacrificed and the liver and lungs of every animal in the experimental group were harvested to analyse for metastatic incidence. From this a broad overview of the metastatic incidence could be formulated for both models. The CD151/TRAMP model developed metastatic lesions from 18 weeks of age and by 40 weeks 26% had metastatic lesions while

the CD9/TRAMP model developed metastatic lesions from 19 weeks of age and 31% had distant metastases by 40 weeks. This is in agreement with other reports for metastatic incidence rates in the TRAMP F_1 model, specifically 30% (Tang, Wang et al. 2008) and 25% (Kaplan-Lefko, Chen et al. 2003).

Presented in this chapter, for the first time, is the basic characterisation of the CD151/TRAMP and CD9/TRAMP models. The models have no overt unexpected phenotypes or developmental irregularities and follow the expected PCa multistep progression that closely follows the progression of human PCa. The results presented in this chapter validate the use of the two models in the following two chapters to analyse the effects of the tetraspanins *Cd151* and *Cd9* on the initiation and progression of spontaneously developing PCa in a transgenic mouse model that, to date, best recapitulates human PCa.

Chapter 4: Effects of the genetic ablation of the tetraspanin *Cd151* on prostate cancer initiation and progression in the TRAMP model

4.1 *Introduction*

The two KO models used in this study (*Cd151* KO and *Cd9* KO) were obtained from different parental lineages and each crossed independently with the TRAMP model to create two distinct cohorts of experimental animals, allowing each cohort to have its own specific littermate controls (2.3.1). Accordingly, results from the two cohorts have been divided into separate chapters with results from the cohort from the *Cd151* KO crossed onto the TRAMP animals reported in this chapter and results pertaining to the cohort of *Cd9* KO model crossed on to the TRAMP model reported in the following chapter. The results from this chapter have been published in a peer reviewed scientific journal (Copeland, Bowman et al. 2013a).

The previous chapter reported on the characterisation of the CD151/TRAMP and CD9/TRAMP models and showed they recapitulate the human disease and validated their use as models for primary prostate tumour onset and subsequent metastasis. This chapter goes on to analyse the influence of endogenous CD151 on initiation and progression of prostate cancer by knocking out *Cd151* in the TRAMP model.

The tetraspanin CD151 (previously also known as PETA-3 and SFA-1) (Fitter, Tetaz et al. 1995, Ashman, Fitter et al. 1997) has been shown in the majority of clinical studies to have a positive correlation with cancer progression and poorer patient outcomes in a variety of cancers as previously described in section 1.8.4.1.1. Molecular studies involving CD151 with cancer progression and metastasis to date have focused on *in-vitro* and grafting models. These studies have mainly shown that knockdown/out or mutation of CD151 decreases cell motility (Gesierich, Paret et al. 2005, Winterwood, Varzavand et al. 2006, Takeda, Kazarov et al. 2007, Geary, Cowin et al. 2008, Ang, Fang et al. 2010, Tsujino, Takeda et al. 2012, Yang, Li et al. 2012) and/or decreases experimental metastasis (Testa, Brooks et al. 1999, Zijlstra, Lewis et al. 2008, Sadej, Romanska et al. 2010, Takeda, Li et al. 2011). Of all 33 known tetraspanins only two studies

to date have looked at the effects of tetraspanins in *de novo* models of cancer. Results from one recent study using the *Cd151* KO model in a *de novo* setting to show a reduction in tumourigenesis (Li, Yang et al. 2012) have been queried as detailed in a letter to Oncogene (Ashman 2013). Briefly, the chemically induced skin carcinogenesis model used in the study is heavily dependent on the strain used so the *Cd151* KO mice were backcrossed onto the more permissive FVB strain. The authors state the *Cd151* KO model was only backcrossed for 4 generations onto the FVB strain to avoid the known problem of kidney disease the *Cd151* animals develop on the FVB strain (Sachs, Kreft et al. 2006, Baleato, Guthrie et al. 2008). However, a study in our lab has shown that even as early as the second generation of backcross onto the FVB background a percentage of mice develop kidney disease, due to random allele distribution of the causative alleles (Naudin *et al*. manuscript in preparation). Potential kidney complications present in the skin carcinogenesis experimental animals may cause systemic stress and renal abnormalities that may confound results. In the letter to Oncogene it was suggested that simple proteinuria experiments should be carried out to exclude any confounding effects of the kidney failure. A recent paper has shown that the tissue specific ablation of *Cd151* in the epidermis of mice also resulted in a reduction of the two stage skin carcinogenesis, indicating that in that model no other *Cd151* dependant pathologies affected the result (Sachs, Secades et al. 2013). The potential issues regarding kidney pathology are present in another study by the same group using a *de novo* breast cancer model and again backcrossing the *Cd151* KO animals to the more susceptible FVB background for 4 generations (Deng, Li et al. 2012). We have overcome these issues in this study through intricate breeding strategies detailed previously (2.3.2). Briefly we have the *Cd151* KO model on the original BL6 background and also backcrossed for no less than 10 generations to the FVB background, through *Cd151* heterozygous breeders to avoid the kidney pathologies. This allowed us to do a final cross to produce F_1 (50 % BL6, 50 % FVB) experimental animals that have been previously shown to not develop any kidney defects (Baleato, Guthrie et al. 2008).

Furthermore, this final single cross also generates the experimental groups enabling co-housing of littermate controls and facilitates blind screening.

In light of these previous *in vitro* and *in vivo* studies *CD151* has been proposed as a potential metastatic enhancer gene. Here we progress the knowledge in this field by reporting for the first time the effects of ablation of *Cd151* in a *de novo* developing model of prostate cancer that also has subsequent spontaneously forming distant metastases. It was shown that the ablation of *Cd151* did not affect primary tumour initiation, however did significantly reduce the incidence of lung metastases.

4.2 *Results*

4.2.1 Results for the endpoint study group

4.2.1.1 Effects of Cd151 on primary prostate tumour development

As previously detailed the experimental animals were palpated blind with respect to genotype and once the animals had a palpable prostate tumour they were culled and lower urogenital tracts with associated tumour were removed and weighed (2.3.5.1.1 and 2.3.5.1.2). The time to palpable prostate tumour between the *Cd151* wt, heterozygous and KO animals was not significantly different as shown in Figure 4-1. Furthermore, as expected for this endpoint, there was no difference in the weights of the urogenital tracts/tumours between the experimental groups (Figure 4-2). By the 40 week endpoint the numbers of animals in each group that had developed *de novo* primary prostate tumours were as follows, 25/27 of the *Cd151* wt animals, 19/21 of the *Cd151* heterozygous animals and 29/30 of the *Cd151* KO animals. All TRAMP positive animals without a palpable tumour were culled at 40 weeks and all were found to have varying degrees of neoplasia of the prostate.

However, due to the experimental criteria of the development of a palpable prostate tumour they did not have their tumours weighed. In addition 4 animals that did develop palpable prostate tumours also did not have the tumours weighed as protocols were developed. However as appropriate, these 4 animals were included in the survival curves (Figure 4-1) and subsequent metastatic analysis as *n* reflects.

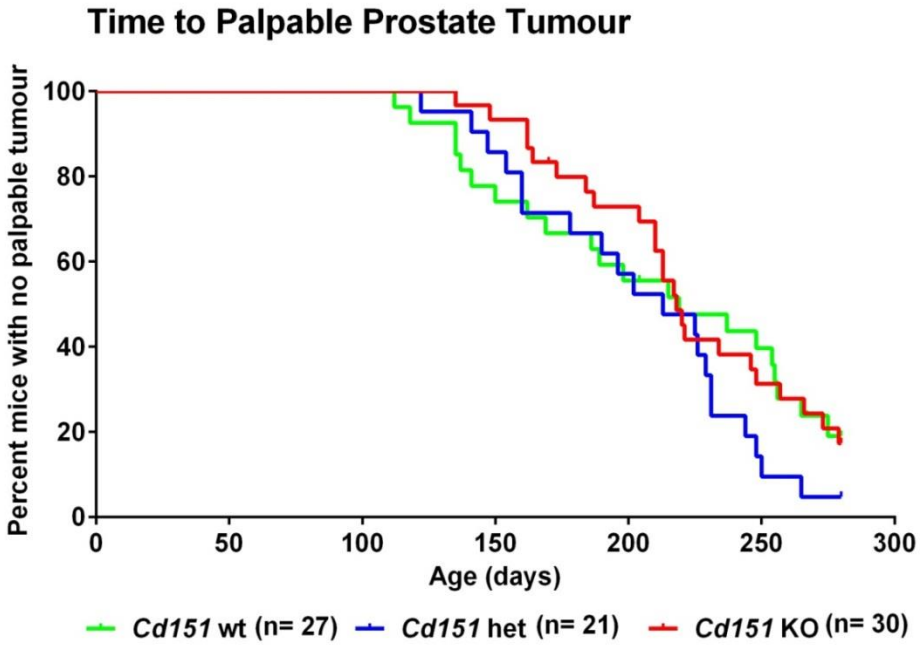

Figure 4-1: Survival curves of *Cd151* wt, heterozygous and KO animals.
CD151/TRAMP animals from the endpoint study group were monitored, blind with respect to their genotype, for onset of a palpable prostate tumour. Once animals had palpable prostate tumours they were culled and time to palpable tumour was plotted in Kaplan–Meier survival curves and found not to be statistically different through analysis carried out by the log-rank (Mantel–Cox) test (p=0.262).

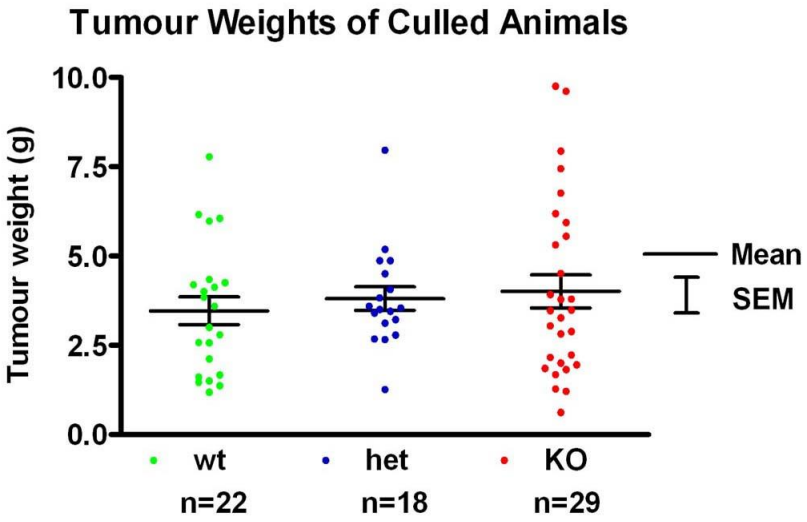

Figure 4-2: Tumour weights of *Cd151* wt, heterozygous and KO animals.
Once CD151/TRAMP animals from the endpoint study group had a palpable prostate tumour they were culled and urogenital tracts/prostate tumours were removed together with the seminal vesicles and bladder (drained) and weighed (as detailed 2.3.5.1.2). The weights of the tumours were not statistically different among the wt, heterozygous, or KO groups (Mann–Whitney rank sum test done individually between two groups at a time); the p value was lowest between the wt and heterozygous groups at 0.463.

4.2.1.2 Effects of Cd151 on proliferation, apoptosis and angiogenesis within the primary prostate tumour

The primary prostate tumours were further characterised by IHC for markers of proliferation (KI67), apoptosis (active caspase-3) and angiogenesis (CD31) as detailed in 2.3.14. Figure 4-3 (A, D and G) shows a representative of the IHC staining for each marker along with the pseudo markup of positive stained cells by the Aperio™ automated algorithms with positive cells in yellow and negative cells in blue (B, E and H). The automated analysis was used for graphical representation of the quantification (C, F and I). There were no significant differences between the *Cd151* wt, heterozygous and KO groups for any of the markers of proliferation, apoptosis or angiogenesis.

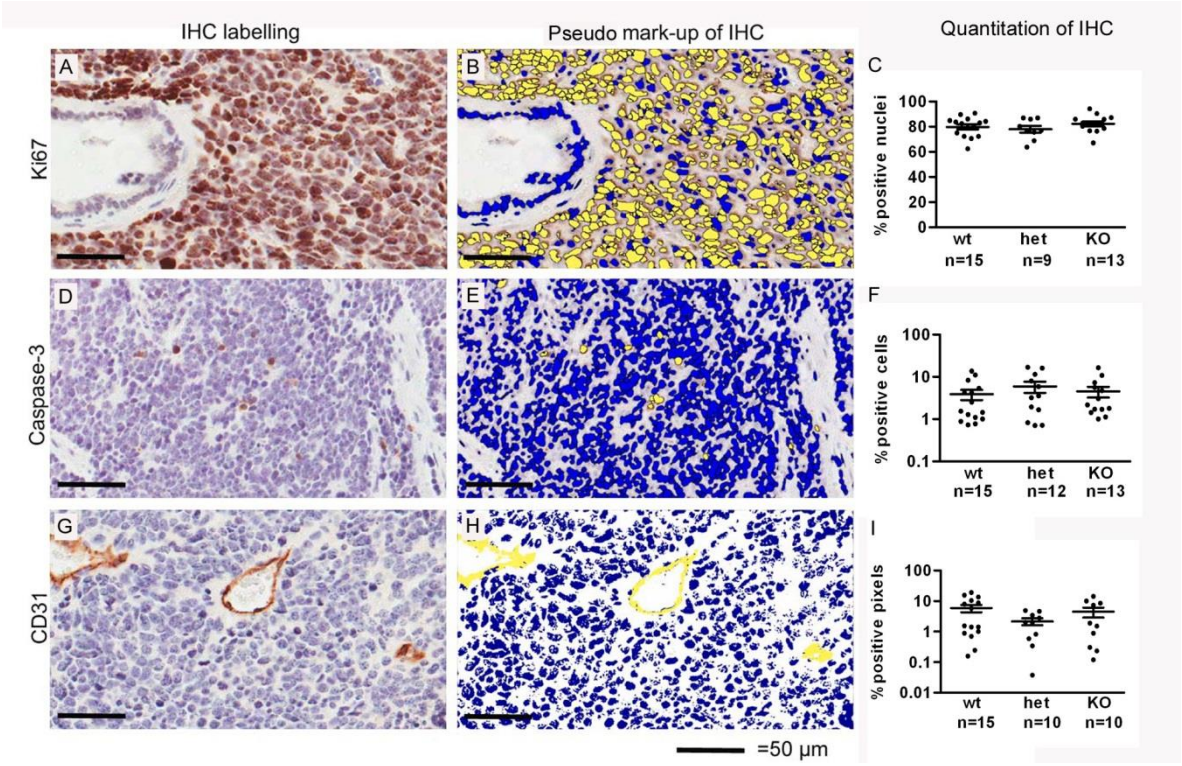

Figure 4-3: Representative IHC labelling and automated algorithm analysis of TMAs. 5um FFPE tumour sections from animals culled in the endpoint group were labelled by indirect peroxidase IHC using DAB as the chromagen using primary antibodies, anti-ki67 (clone SP6; Panel A), anti-active caspase-3 (clone ASP 175, panel D) and anti-CD31 (clone SZ31, Panel G) detailed in Table 2-7. KI67 and active caspase-3 staining was analysed for percentage positive staining to percentage negative staining using the Aperio nuclear algorithm (B and E respectively) where the positive cells are marked in a yellow and negative cells are blue. CD31 staining was analysed using the positive pixel algorithm for percentage positive pixels, marked in yellow to negative pixels, marked in blue (panel H), described in detail in section 2.3.14.4. The percentage of positive staining for each of the markers was not statistically different among the wt, heterozygous, or KO groups (Mann–Whitney rank sum test done individually between two groups at a time; Panels C, F and I respectively). Lowest p values for each of the markers were Ki67 p=0.229 (wt v's KO), active caspase-3 p=0.359 (wt v's KO) and CD31 p=0.276 (wt v's het).

4.2.1.3 Effects of Cd151 on metastasis in the CD151/TRAMP model

Mice that were culled due to development of primary prostate tumours also had the liver and lungs removed as described in section 2.3.5.1.2.4. The liver and lungs were processed and analysed for presence of metastatic foci, which were previously shown to be derived from the primary prostate tumours (section 3.2.6).

Since the metastatic incidence data was binominal, in that each animal either had metastases or not, the data were placed into two 2 x 2 contingency tables below as raw numbers and as a percentage of the total for that group in brackets. Table 4-1 shows metastatic incidence to the liver of the wt and KO animals and Table 4-2 shows lung metastatic incidence for the wt and KO animals. This allowed statistical analysis of the data via the stringent Fisher's exact test. Ablation of *Cd151* was shown to significantly reduce the incidence of metastatic disease in the lungs, but not in the liver as shown in Figure 4-4. *Cd151* heterozygous animals appeared to have an intermediate incidence of lung metastasis but the difference was not significant, p=0.495 for wt compared to heterozygous and p=0.225 for heterozygous compared to KO. For visual representation, the data was also graphed as the percentage of mice in each genetic group to develop metastases in the liver or lungs as seen in Figure 4-4. The statistics in the graph are from the Fisher's exact test gained from the contingency tables.

Table 4-1: Contingency tables showing incidence of metastatic lesions to the liver in wt and *Cd151* KO animals.
The binominal metastases data was placed in contingency tables and analysed for differences in metastatic incidences in the liver (Table 4-1) and lung (Table 4-2) between the different genetic groups.

Incidence of metastasis to the liver in *Cd151* wt and KO mice	Number of animals with NO metastases (Total number and % of mice)	Number of animals with metastases (Total number and % of mice)	**Total animals**
Cd151 wt animals	**17 (74%)**	**6 (26%)**	23
Cd151 KO animals	**21 (75%)**	**7 (25%)**	28
Total animals	37	14	51

Table 4-2: Contingency table showing incidence of metastatic lesions to the lung in wt and *Cd151* KO animals.

Incidence of metastasis to the lung in *Cd151* wt and KO mice	Number of animals with NO metastases (Total number and % of mice)	Number of animals with metastases (Total number and % of mice)	**Total animals**
Cd151 wt animals	**13 (56%)**	**10 (43%)**	23
Cd151 KO animals	**25 (89%)**	**3 (11%)**	28
Total animals	38	13	51

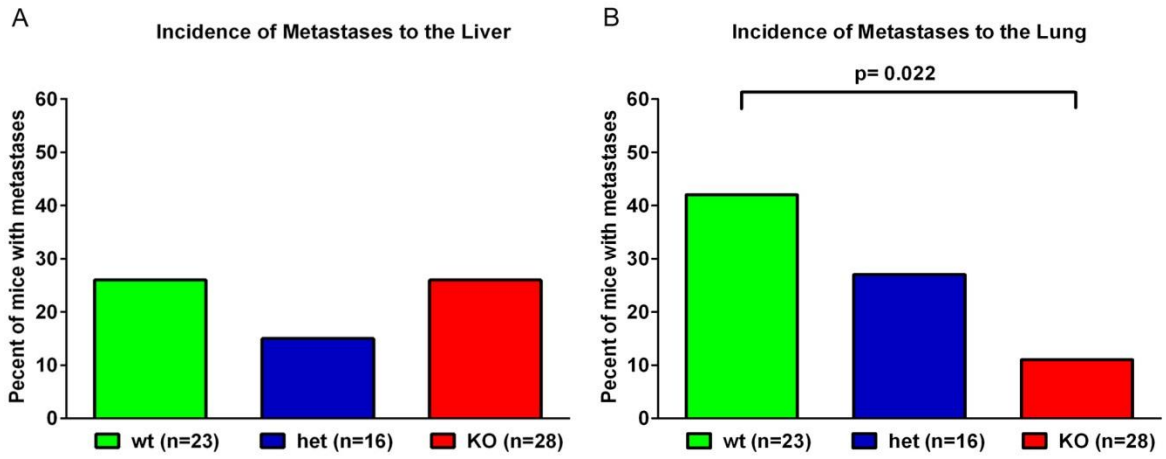

Figure 4-4: Incidence of metastasis in the *Cd151* animals.
Once animals from the endpoint study group were culled their liver and lungs were dissected and analysed by histopathology for presence of metastatic lesions. Incidence of metastases (graphed as a percentage of the total animals with metastases present for each genotype) in *Cd151* wt, heterozygous and KO animals to the liver, A; and to the lung, B; are shown. The p-values were determined by the Fishers exact test with the data in contingency tables (Table 4-1).Incidence of metastases to lung were significantly different in wt compared to the *Cd151* KO group. There was no significant differences between any groups in incidence to the liver, with all p values greater than 0.225.

The ablation of *Cd151* also significantly reduced the number and total area of metastatic foci to the lung with an intermediate effect seen in the *Cd151* heterozygous animals (Figure 4-5, B and D). In contrast there was no significant difference in number or total area of metastatic foci in the liver (Figure 4-5, A and C). The average areas of the individual metastatic foci in each organ in each animal were also analysed (Figure 4-6). Statistical analysis revealed no significant difference in the average foci area between wt, heterozygous and *Cd151* KO groups in the liver or the lung; p= 0.201 and p=0.994, respectively.

The discrepancy of *n* between number of animals that developed primary tumours as stated in 4.2.1.1 and total animals included here was due to technical difficulties in fixing, processing or sectioning of liver and/or lungs from a small number of animals for analysis of metastases. Exclusion was done with no knowledge of the donor animals' genotype or presence or absence of metastases within those samples.

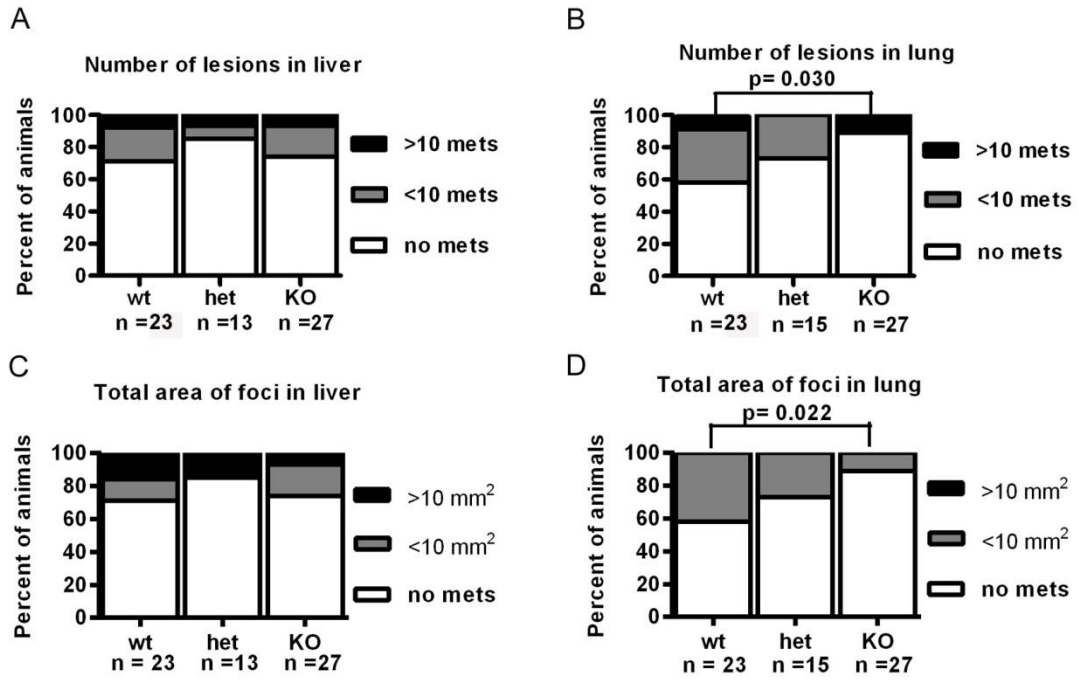

Figure 4-5: Total number and area of metastatic foci in *Cd151* wt, heterozygous and KO animals.

When animals from the endpoint study group were culled their liver and lungs were harvested and analysed by histopathology for presence of metastatic lesions. Images were viewed in Imagescope at 200x magnification and metastatic foci were manually annotated to produce an automated output of number of metastatic foci and total area of metastatic foci for each organ for each animal. The raw count data were statistically analysed using the Mann-Whitney-U (rank sum) test to obtain p values. Due to the data containing many zero counts (animals with no metastases) making the graphs difficult to distinguish, data were grouped arbitrarily into 3 subsets for graphing, animals with no metastases, less than 10 metastatic lesions and more than 10 metastatic lesions in the liver (**A**) and lungs (**B**) for each of the wt, heterozygous and KO genotype groups. Similarly data on the total area of metastatic lesions were grouped according to no lesions, less than 10 mm^2 total area of metastatic lesions and animals with more than 10 mm^2 total area of metastatic lesions in the liver (**C**) and lungs (**D**) for each of the wt, heterozygous and KO genotype groups. No statistical difference was seen between the wt, heterozygous or KO groups in the total number or area of metastatic lesions in the liver ($p>0.345$). Both the number of metastatic foci and total area of metastatic lesions in the lungs were significantly decreased between the wt and *Cd151* KO animals.

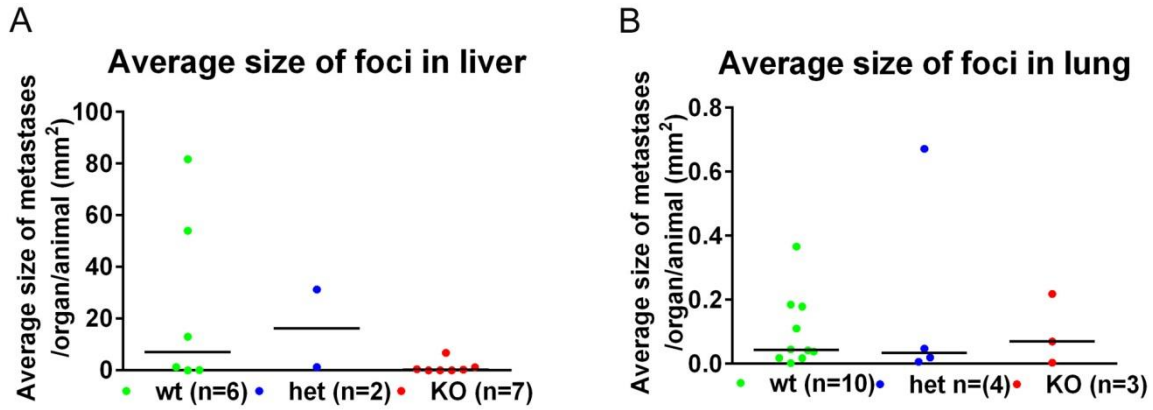

Figure 4-6: Average area of metastatic foci in each organ of each mouse.
When animals from the endpoint study group were culled their liver and lungs were harvested and analysed by histopathology for presence of metastatic lesions. Images were viewed in Imagescope at 200x magnification and metastatic foci were manually annotated to produce an automated output of number of metastatic foci and area of each metastatic foci for each organ for each animal. An average area for the metastatic foci was calculated and plotted for the wt, heterozygous and *Cd151* KO groups for both the liver and lung average metastatic area. Statistical analysis was performed by the non-parametric Kruskal-Wallis one way analysis of variance test. No significant differences in average metastatic foci in either the liver or lung were seen between the groups (p=0.201 for liver and p=0.994 for lung).

4.2.2 Results for the bioluminescence study group

In the endpoint experiments above, we found that the ablation of *Cd151* did have an effect on the incidence of spontaneous metastasis to lung but not the liver. In the *Cd151* KO animals, *Cd151* is ablated from all cells in both the tumour and host (surrounding environment). To try and delineate this, we went on to do a preliminary study to determine what the effect of *Cd151* ablation in the environment (host animal) had on metastatic incidence (detailed in 2.3.5.2). This was done in collaboration with Dr Carl Power and Dr Tzong-Tyng Hung, at the University of New South Wales (UNSW) imaging facility. Briefly we used another cohort of wt and *Cd151* KO experimental animals that did not have the TRAMP oncogenic transgene. Instead the (C57BL/6 x FVB/N) F_1 wt and *Cd151* KO mice animals were injected via the heart with cells from the TM2-Luc15 bioluminescence tagged TRAMP derived prostate cancer cell line (origin and culturing detailed in 2.3.5.3). For confirmation of bioluminescence they were titrated out in a 96 well plate as in Figure 4-7. Mice were monitored by *in vivo* bioluminescence for *in vivo* tumour

growth over 4 weeks (Figure 4-8). After 4 weeks the mice were culled and dissected to allow *ex vivo* imaging of the organs (Figure 4-9) as detailed in section 2.3.5.2). No significant differences for tumour foci growth were seen between the wt and *Cd151* KO groups (Figure 4-10) by *in vivo* bioluminescence over 4 weeks.

4.2.2.1 Bio imaging analysis of liver metastasis

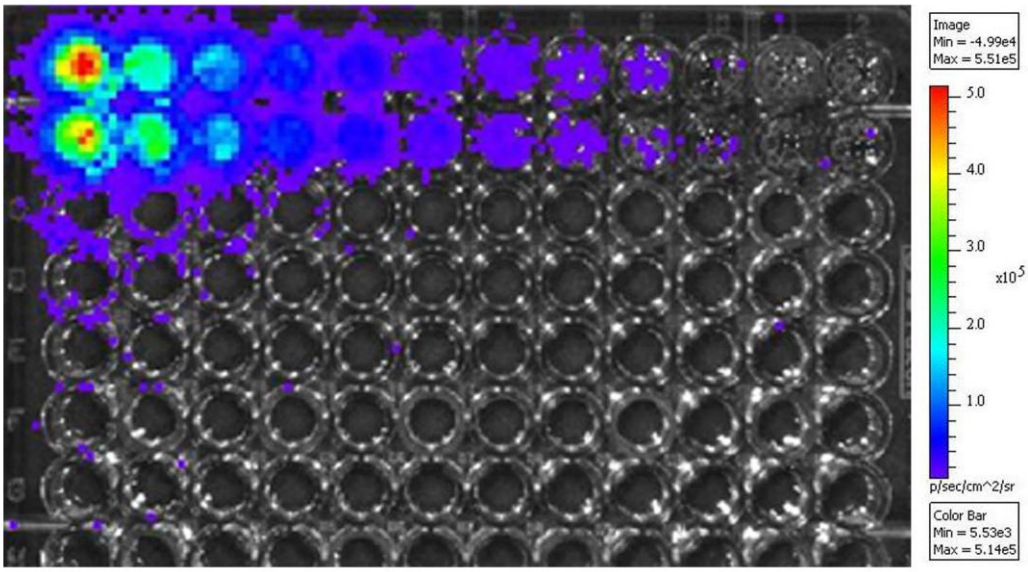

Figure 4-7: *In vitro* bioluminescence of TM2-luc15 cells.
To ascertain the bioluminescence and also to assess the *in vitro* sensitivity of the TM2-luc15 cells, they were plated out in a 2x serial dilution in PBS on a 96 well plate. Number of cells/well were (from left to right) ~ 10000, 5000, 2500, 1250, 625, 310, 150, 75, 35, 17 and 8, while the last well contained media only. The cells did express the bioluminescent tag and could reliably be seen *in vitro* at approximately 35 to 17 cells.

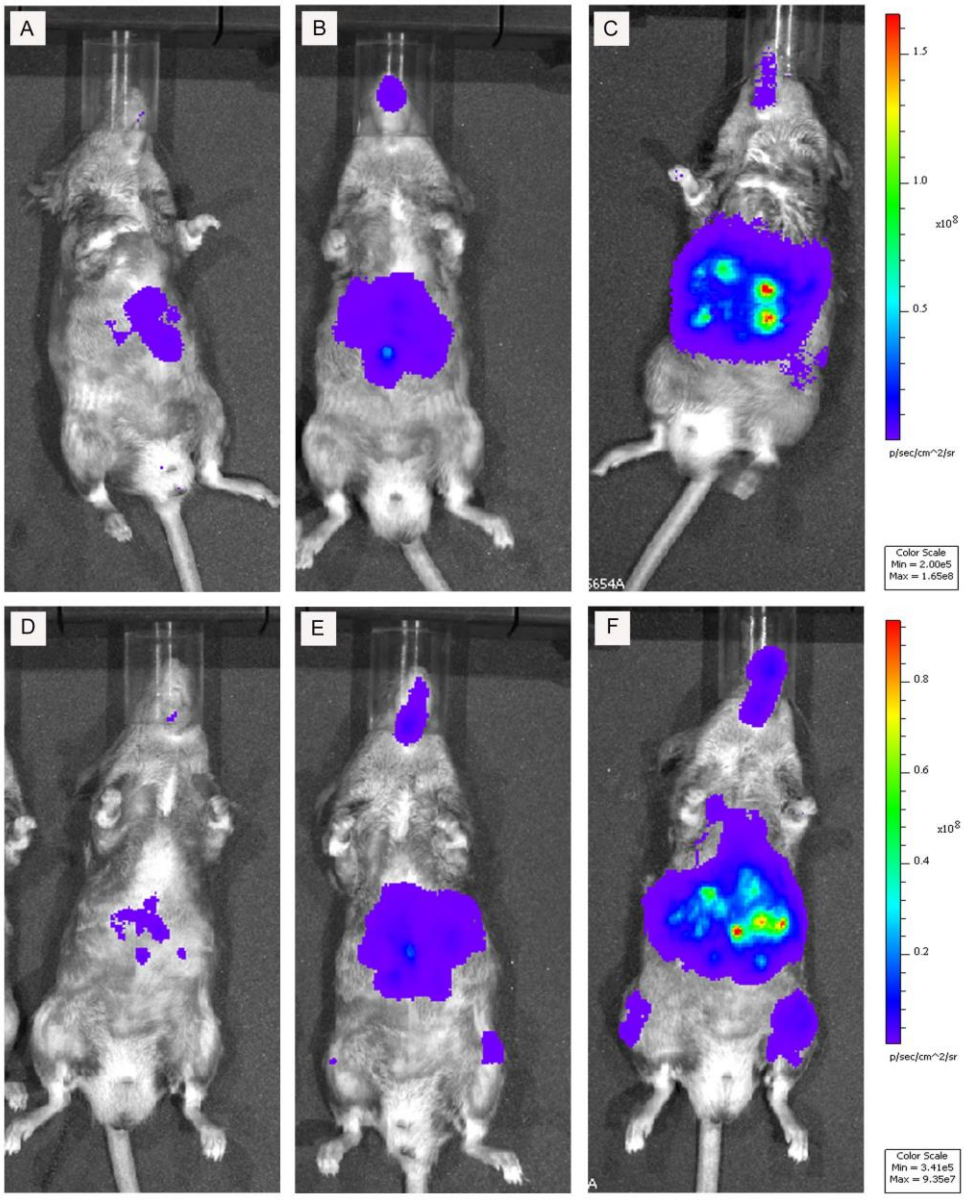

Figure 4-8: In-vivo imaging of the bioluminescence study group.
Animals from the bioluminescence study group were imaged every seven days beginning two weeks post intra-cardiac injection of the TRAMP tumour derived TM2-luc15 bioluminescent tagged cell line, for three weeks (weeks 2, 3 and 4). Images were taken on the IVIS Lumina imager 9 mins post injection of D-luceferin with medium binning and normalised for photons to allow comparison across images of the mice over the three weeks (detailed 2.3.5.3.2). Panels A, B and C represent imaging of a *Cd151* wt mouse over the three weeks, while panels D, E and F represent imaging of a *Cd151* KO animal over the three weeks. Analysis was performed using regions of interest encompassing the whole of the mouse body and normalised between groups to photons/second to allow comparison, using the living image software (Caliper).

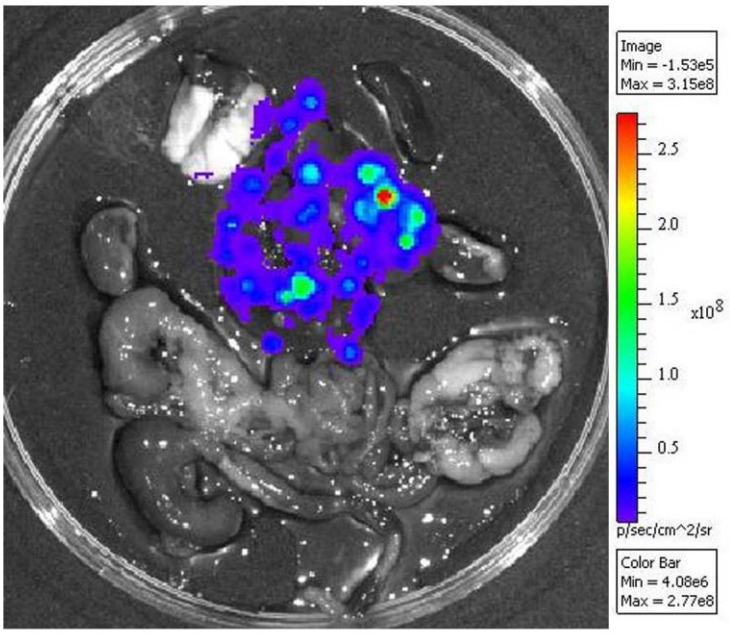

Figure 4-9: *Ex-vivo* bioluminescence imaging of organs.
After the animals from the bioluminescence group had been *in-vivo* imaged for 3 weeks they were culled and organs were dissected and imaged *ex-vivo* for confirmation of location of tumour foci by bioluminescence, which was mainly in the liver as shown. The analysis was semi–quantitative due to the varying time lag from *in-vivo* imaging, culling and dissection of animals along with having to pipette varying amounts of D-luciferin directly onto the non-circulating *ex vivo* organs to get a bioluminescence signal, which excluded making extensive comparison between animals. Analysis was performed using regions of interest encompassing specific organs and normalised between groups to photons/second to allow semi-quantitive comparison, using the living image software (Caliper).

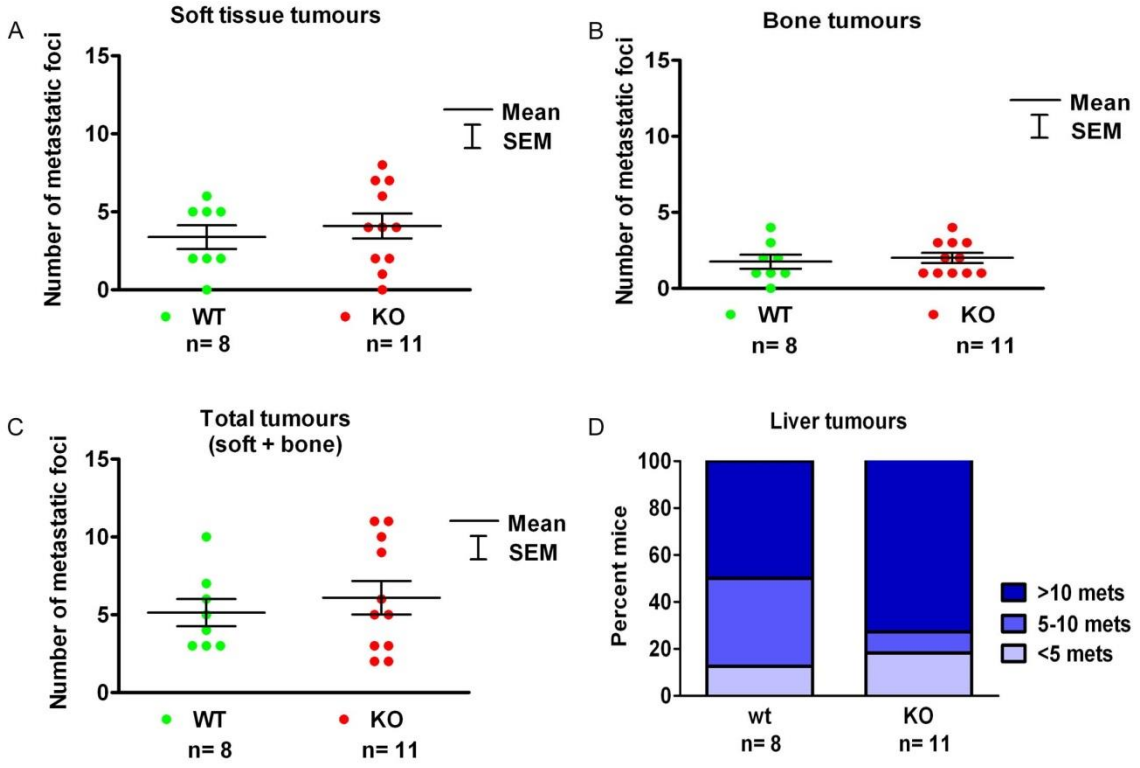

Figure 4-10: Analysis of metastatic foci from the bioluminescence images.
Once the *in-vivo* images of the animals had been acquired the bioluminescence "hotspots" in the images from the 4 week post injection cull point could be manually counted to semi-quantitatively determine the total number of metastatic foci in the soft tissue (A), bone (B) and liver, which was quantified separately as the majority of foci were seen here as shown in Figure 4-8 (C and F). The Mann-Whitney test revealed no significant differences in the number of metastatic foci between the wt and *Cd151* KO groups (p> 0.798).

4.2.2.2 Histopathology analysis of liver metastasis

Once all the animals were imaged at 4 weeks post intracardiac injection they were culled. As an extension of the *in vivo* and *ex vivo* imaging analyses, the livers from each animal were processed into FFPE blocks and sectioned as described in 2.3.6. The foci in the livers were identified and analysed by histopathology (Figure 4-11 A and B). The cancerous foci in the liver were partly characterized by immunohistochemistry and shown to express the TRAMP SV40 T-ag protein from the injected TM2-Luc15 TRAMP cells, specific to the foci and not the surrounding normal liver tissue (Figure 4-11 C and D). The Aperio digital pathology system was used to analyse the number and total area of metastatic foci in the livers of each

animal (detailed in 2.3.14). No differences in number of metastatic foci or total area of metastatic foci were seen between the wt and *Cd151* KO groups Figure 4-12.

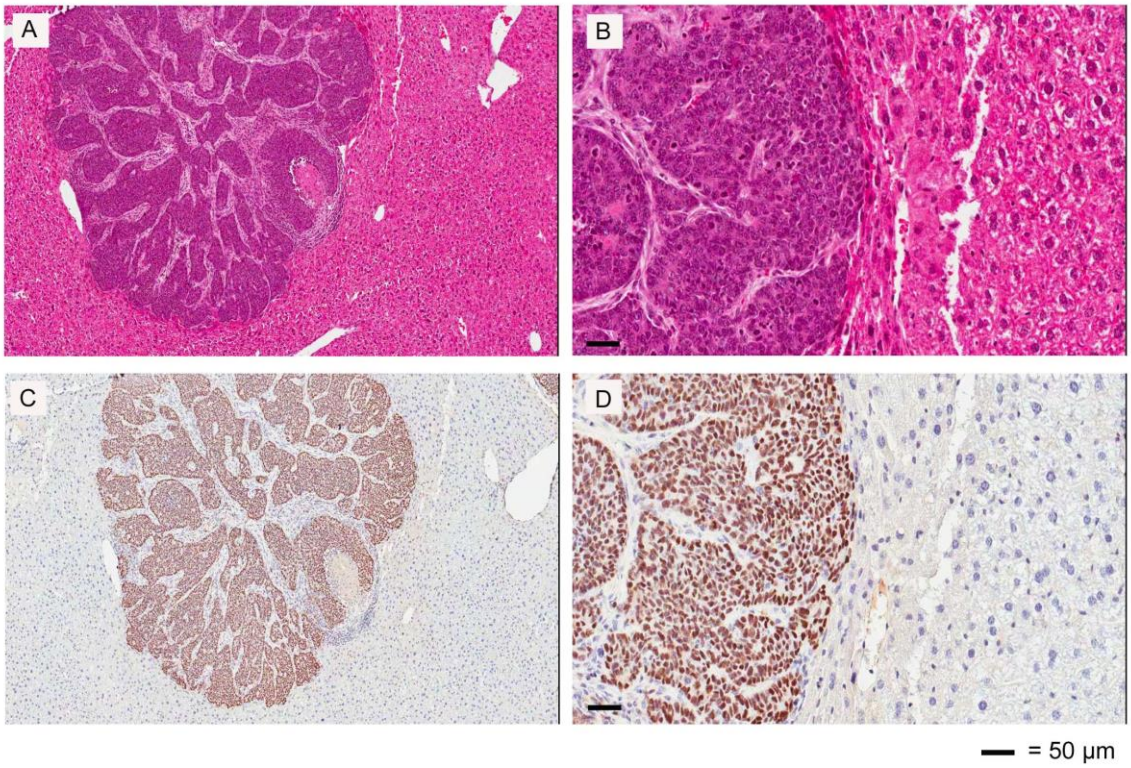

Figure 4-11: Histopathology analysis of the liver metastases of the bioluminescence animals. Once the animals from the bioluminescence study group were culled, 4 weeks post intra-cardiac injection; livers were removed, processed and 5 µm FFPE sections were analysed by histopathology to determine metastatic foci (A and B). Serial sections were stained via indirect peroxidase IHC using DAB as the chromagen with the anti SV40 T-ag antibody (Table 2-7) for characterisation (C and D). The metastatic foci did express the transgene SV40 T-ag protein while the surrounding normal liver tissue did not.

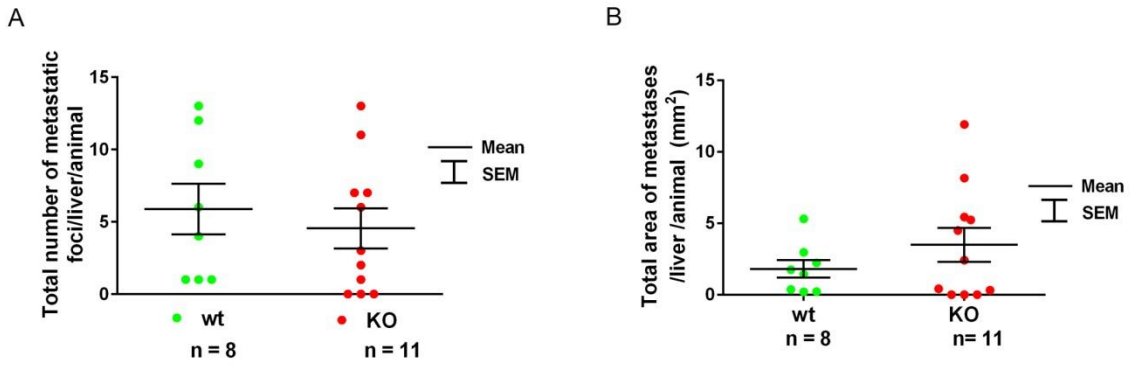

Figure 4-12: Total number and area of the metastatic foci in liver of the bioluminescence study group animals.
Analysis of the livers by histopathology as shown in Figure 4-11 via H&E stain was visualised with the Aperio digital pathology software and areas of metastases were annotated as regions of interest. The software automates a total number and total area of metastatic foci per liver section, per animal. No significant difference was seen between the wt and *Cd151* KO groups in number or total area of metastatic foci to the liver using the Mann-Whitney test (p=0.501 and p=0.712, respectively).

4.3 *Discussion*

In this chapter we have analysed the influence of endogenous CD151 on initiation and progression of prostate cancer by using a *Cd151* KO murine model crossed with the transgenic TRAMP model of spontaneously forming prostate cancer.

Almost all the experimental mice in the endpoint cohort developed palpable tumours by 40 weeks of age. The onset of primary prostate tumours (time to palpable tumour) was not affected by the ablation of *Cd151* in this model (Figure 4-1). It is possible that if the more sensitive *in vivo* imaging monitoring method was successful (2.3.5.1.1) it might have revealed more subtle differences. Mice were euthanased as soon as palpable tumours were detected. Consistent with the lack of effect of *Cd151* deletion on primary tumour growth, there were no significant differences between groups in regards to tumour weights or in their proportion of mitotic or apoptotic cells (Ki67- or activated caspase-3 positive respectively; Figure 4-3).

In vivo grafting experiments have been used by others to investigate the influence of CD151 on tumour growth at the primary site. Studies with syngeneic tumours grafted into *Cd151* wt and KO mice have given variable results. Subcutaneous growth of Lewis Lung Carcinoma (LLC), but not B16 melanoma cells, was reduced in *Cd151* KO mice (Takeda, Kazarov et al. 2007, Takeda, Li et al. 2011). This may be associated with an effect on tumour vascularisation which was not seen in the case of B16 tumours (Takeda, Li et al. 2011) or in primary tumours in our study. This is discussed further below. Xenografts of tumour cells with or without CD151 knockdown (KD) by RNA interference into immunocompromised mice have shown reduced growth as a result of CD151 KD. Using MDA-MB-231 human breast cancer cells injected subcutaneously or into the mammary fat pad, Yang *et al.* (2008) showed that KD of tumour cell CD151 substantially delayed tumour appearance although no difference in growth *in vitro* was observed. Also using MDA-MB-231 cells Sadej *et al.* (2009) demonstrated reduced growth of CD151 KD sub-cutaneous xenografts in mice although, again, no intrinsic differences in growth *in vitro* were seen. Differences in the pattern of vascularisation of CD151 KD tumours were noted (Sadej, Romanska et al. 2009). Taken together, the results indicate that CD151 on both the tumour cells and in the host environment can be involved in interactions promoting the growth of grafted tumours at the primary site. It will be important to examine further examples of *de novo* tumour development.

Upon dissection of animals with palpable prostate tumours we frequently noticed macro- metastases to the liver and therefore collected liver as well as lungs from all animals. The original TRAMP characterisation papers did not commonly report liver metastases and seem to have set a trend to only examine the lungs for metastases in research involving this model (Gingrich, Barrios et al. 1996, Gingrich, Barrios et al. 1999). We suggest that liver should be included in future studies that use the TRAMP model to analyse metastasis. Even though we saw

frequent metastatic lesions in the liver, the ablation of *Cd151* did not have a significant effect on the incidence of metastases to this organ. However, the ablation of *Cd151* did have a significant effect on metastasis to the lungs of the animals, specifically reductions in incidence, number and total area of metastatic foci. The individual area of the foci in the lungs were not significantly different between the *Cd151* wt, heterozygous and KO animals. This suggests that ablation of *Cd151* did not affect the growth of the foci once metastatic cells were recruited to the lungs. Overall these data are consistent with the view that CD151 is primarily a metastasis promoter (reviewed in Zoller 2009).

Multiple studies have demonstrated that CD151 on tumour cells promotes their adhesion to basement membrane components, migration and invasion *in vitro* (Kohno, Hasegawa et al. 2002, Yang, Richardson et al. 2008, Sadej, Romanska et al. 2009) all of which are important in metastasis. Adhesion strengthening via laminin-binding integrins has been shown to depend on CD151 (Lammerding, Kazarov et al. 2003).The pro-migratory role of CD151 may depend in part on its regulation of integrin internalisation and trafficking (Winterwood, Varzavand et al. 2006, Liu, He et al. 2007). Sadej *et al.* (2010) reported that KD of CD151 depleted TGF-β-induced scattering of breast cancer cells in 3D culture.

The role of tumour cell CD151 *in vivo* has been investigated in models of spontaneous metastasis. Testa and colleagues (1999) studied metastasis to the lung from cells of a human epithelial line placed onto the chorioalantoic membrane of chick embryos and were the first to show that CD151 is a potential metastasis enhancer protein. They showed that a CD151 antibody, 1A5, did not affect proliferation of the tumour cells or primary tumour size but did significantly reduce metastasis. This group then went on to show that the CD151 antibody reduced metastasis by inhibition of cell detachment from the primary tumour and hence entry into the vascular system (intravasation) (Zijlstra, Lewis et al. 2008). Interestingly they showed no difference in the recruitment of cancer cells to the

lungs whether CD151 antibody was used or not. This result appears to be at odds with other data which indicate involvement of CD151 at multiple steps of the metastatic cascade (see below), but may be explained by the different models used as well as the different modality of the CD151 interference. It is not clear precisely how mAb 1A5 is working, but it appears not to simply block CD151 function since *Cd151* $^{-/-}$ mouse embryo fibroblasts and tumour cells with knockdown of CD151 did not exhibit the same detachment defect. Rather, it is proposed that binding of mAb 1A5 mediates its effect by acting on CD151-containing complexes in the cell membrane (Zijlstra, Lewis et al. 2008).

In an earlier CD151 over-expression study Kohno *et al*. (2002) showed that CD151 promoted cell migration *in vitro* and metastasis to the lungs in mice following injection of cells via the orbital vein. Lung metastasis was markedly inhibited by pretreatment of the cells with a CD151 mAb. More recent studies have used tumour cells with KD of CD151. Sadej and colleagues (2010) injected wt and CD151 KD MDA-MB-231 breast cancer cells into mice via the tail vein. The CD151 KD cells were shown to form less and smaller lung metastatic foci in comparison to the CD151 wt cells. The group then went on to investigate early recruitment of the *Cd151* wt and KD cells to the lungs and liver over a 1 hour period by intravital microscopy. They found a reduction in recruitment of the CD151 KD cells relative to wt cells to the lungs but, interestingly, not to the liver, which is in accord with our result on spontaneous metastasis. These findings indicate that CD151 on the primary tumour can influence metastasis by altering homing to secondary sites and also may account in part for the organ site specificity.

The studies reviewed above clearly demonstrate that tumour cell CD151 plays a major role in metastasis. The model used in our experiments had *Cd151* knocked out in every cell of the animal, which included the environment (host) and the *de-novo* forming prostate tumour itself. Therefore we cannot delineate whether the KO of *Cd151* in the host or tumour (or both) was responsible for the effects on

metastasis we observed. CD151 is widely expressed in tissues, including vascular endothelium, and reports using tumour grafts have indicated its importance in the host environment in regulating metastasis. Several of these have indicated effects on development of tumour vasculature. Although no vascular defects have been reported in unperturbed *Cd151* KO mice (Wright, Geary et al. 2004, Sachs, Kreft et al. 2006) a mAb to CD151 was previously shown to modify migration and *in vitro* tube formation of primary human endothelial cells (Sincock, Fitter et al. 1999).

Experiments using grafting of syngeneic tumours into wt and *Cd151* KO C57BL/6 mice have demonstrated effects mediated by CD151 in non-tumour tissues. Using Lewis Lung Carcinoma (LLC) cells injected subcutaneously, Takeda *et al*. (2007) demonstrated reduced tumour growth and microvessel density in the *Cd151* KO animals indicating an effect on angiogenesis. This study included extensive characterization of endothelial cell function in wt and *Cd151* KO mice *in vitro* and *in vivo* and demonstrated that lack of CD151 resulted in impairment in several functions relevant to angiogenesis. The effect on tumour angiogenesis may be somewhat specific to different tumours since this group did not see an effect on subcutaneous growth or angiogenesis of another syngeneic tumour, B16 melanoma (Takeda, Li et al. 2011). Similarly we did not see differences in blood vessel density in the primary prostate tumours in our experiments; however more subtle differences in the tumour vasculature, possibly in tumour margins, may occur and might be detected by more detailed analysis. Importantly, the study by Takeda *et al*. (2011) demonstrated marked reduction in the number of lung metastases resulting from intravenous injection of both LLC and B16 melanoma cells in mice lacking CD151. Further experiments showed reduced tumour-endothelial adhesion and transendothelial migration as the likely mechanism. The results of these two studies clearly demonstrate the important role of endothelial cell CD151 in tumour growth and metastasis.

Studies with *Cd151* KO mice have indicated that the protein plays important roles in platelet function and antigen presentation to T cells by dendritic cells (Wright, Geary et al. 2004, Orlowski, Chand et al. 2009, Sheng, van Spriel et al. 2009), both of which have the potential to affect metastasis (reviewed in Gay and Felding-Habermann 2011). Takeda *et al*. (2011) did not see any difference in aggregation of B16 melanoma cells between *Cd151* wt and KO mice, however the model may not accurately reflect the process of spontaneous metastasis. Nor did preliminary investigations reveal any differences in anti-tumour immunity. In both cases further studies are required.

From published studies reviewed above it appears that CD151 on both the tumour cells and the host are involved in regulating tumour growth and metastasis. CD151 on the tumour cells may regulate cell-cell attachment and release from the primary tumour mass (Zijlstra, Lewis et al. 2008, Johnson, Winterwood et al. 2009) and influence extravasation through its well-established influence on adhesion and migration. In some systems CD151 on tumour cells appears to regulate angiogenesis which is likely to promote primary tumour growth as well as metastasis (Sadej, Romanska et al. 2009). Studies with CD151-ablated mice indicated that, at least in some instances, angiogenesis is also regulated by CD151 expression on the vascular endothelium of the host animal (Takeda, Kazarov et al. 2007). Many additional steps in the metastatic cascade including cell binding to the vascular endothelium in the target organ and transmigration into the tissue involve interactions with the vascular endothelium. Although vasculogenesis appears normal in *Cd151*-null mice, multiple assays showed endothelial functional defects which may influence pathological angiogenesis as well as tumour cell homing to secondary sites (Takeda, Kazarov et al. 2007). Indeed, the lack of CD151 in host mice led to reduced tumour cell attachment to endothelial cells, transmigration and metastasis to the lungs (Takeda, Li et al. 2011). Thus CD151 status of both tumour cells and environment is important for tumour growth and metastasis.

In our experiments, we found that deletion of CD151 on both the tumour and the host led to reduced spontaneous metastasis to lung but not the liver. In an attempt to clarify the role of tumour versus environmental CD151, we conducted a preliminary experiment in which cells of a luciferase-transduced C57BL/6 TRAMP cell line (TM2-Luc15) were injected via the heart into (C57BL/6 x FVB/N) F_1 wt and *Cd151* KO mice (detailed in 2.3.5.2). Animals were monitored by *in vivo* bioluminescence imaging over 4 weeks. The results were inconclusive because metastasis was predominantly to the liver, with some to bone, but few lung metastases were observed. No significant difference in the frequency of metastases to liver between groups was observed. Further experiments using cultured primary tumour cells and different routes of injection need to be carried out (discussed further in 7.1).

In summary, here for the first time we report the effects of ablation of *Cd151* in a spontaneously developing model of prostate cancer. It was shown that the ablation of *Cd151* did not affect *de-novo* primary tumour growth or angiogenesis; however it did significantly reduce the incidence, frequency and total area of spontaneously forming metastatic foci to the lungs.

Chapter 5: Effects of the genetic ablation of the tetraspanin *Cd9* on prostate cancer initiation and progression in the TRAMP model

5.1 *Introduction*

As previously mentioned, the two KO models used in this study were obtained from different parental lineages. They were both independently crossed with the TRAMP model to create two distinct cohorts to allow each cohort to have its own specific littermate controls. Accordingly, results from the two cohorts have been divided into separate chapters with results from the CD151/TRAMP animals reported in chapter 4 and results pertaining to the CD9/TRAMP cohort reported here. The results from this chapter have been published in a peer reviewed scientific journal (Copeland, Bowman et al. 2013b).

The tetraspanin CD9 is widely expressed in human tissues and on many cell types including platelets, epithelial and vascular endothelial cells (Sincock, Mayrhofer et al. 1997). It is also known as motility related protein 1 (MRP-1) and the gene is located on human chromosome 12p13.3 (Boucheix, Nguyen-van et al. 1985). Sequence data published by three different groups in 1991 indicated the identity of MRP-1 and CD9 clones (Boucheix, Benoit et al. 1991, Lanza, Wolf et al. 1991, Miyake, Kovama et al. 1991).

Clinical studies have shown a correlation between decreased CD9 expression and progression and/or poorer prognosis in a variety of cancers, including prostate (Chuan, Pang et al. 2005, Wang, Begin et al. 2007), breast (Miyake, Nakano et al. 1995, Miyake, Nakano et al. 1996), lung (Higashiyama, Taki et al. 1995, Higashiyama, Doi et al. 1997), liver (Mori, Mimori et al. 1998), colon (Cajot, Sordat et al. 1997, Mori, Mimori et al. 1998, Hashida, Takabayashi et al. 2002), oral squamous cell carcinoma (Kusukawa, Ryu et al. 2001), head and neck (Erovic, Pammer et al. 2003, Mhawech, Dulguerov et al. 2004), urothelial bladder (Mhawech, Herrmann et al. 2003), multiple myeloma (De Bruyne, Bos et al. 2008) and gall bladder (Zou, Xiong et al. 2012). One study that found an inverse correlation of CD9 expression with progressive cervical cancer, also reported strong CD9 expression within specific regions of tumour invasion into

lymphovascular spaces (Sauer, Windisch et al. 2003). This suggests that CD9 may differentially affect particular aspects of tumour growth and progression. In contrast to the majority of findings reporting inverse correlations of CD9 expression and cancer progression there have been two independent reports of a correlation between increased CD9 expression and progression in gastric cancers (Hori, Yano et al. 2004, Soyuer, Soyuer et al. 2010), while two other clinical studies saw no correlation of CD9 expression with prognosis in progressive osteosarcoma (Kubista, Erovic et al. 2004) or with tumour grade (Gleason score) in prostate cancer (Chuan, Pang et al. 2005).

Cancer related experimental studies involving CD9 have thus far mainly focused on *in vitro* systems and have mostly shown that CD9 expression levels are inversely correlated with cell motility, migration, adhesion and platelet activation (reviewed in Zoller 2009, Powner, Kopp et al. 2011, Zhang, Dong et al. 2012). One study conversely reported that increased CD9 expression levels increased invasiveness of prostate cancer cells *in vitro*, the overexpressing CD9 cells did not have increased metastatic potential *in vivo* after orthotopic grafting (Zvieriev, Wang et al. 2005).
The discrepancies between clinical studies with respect to correlation to expression and cancer progression/prognostic significance along with variable effects of CD9 manipulation in experimental studies relevant to tumour invasion and metastasis warrant further investigation into the role of CD9 in cancer. Furthermore, there have been no reports of the effects of CD9 manipulation in models of de novo tumour development and spontaneous metastases.

As previously described we crossed the *Cd9* KO murine model (detailed in 1.9.2.3) onto the TRAMP murine model (detailed in 1.9.2.1) that develops *de novo* prostate cancer and spontaneously forms metastatic lesions, to analyse the effects of the ablation of *Cd9* on the development and progression of prostate cancer. We report for the first time that the genetic ablation of *Cd9* in the TRAMP model did not affect

the onset of *de novo* primary prostate tumour development but did significantly increase the incidence of spontaneous metastases.

It has been previously reported that CD9 expression can be induced by androgens in humans (Chuan, Pang et al. 2005) and therefore may also be affected by androgens in murine models. However, in the *Cd9* KO animals the expression of *Cd9* is completely ablated through cre/lox technology rendering any subsequent up-regulation of *Cd9* impossible, as may be possible in other systems such as siRNA knockdown models where low Cd9 expression levels may still exist.

Preliminary studies describing Cd9 expression in mouse prostate tissue and TRAMP tumours as well as the time course of tumour progression are described in chapter 3. All of the results in this chapter relate to animals in the “end-point” cohort, where the animals were monitored for development of palpable tumours up to 40 weeks of age (detailed in section 2.3.5.1).

5.2 *Results*

5.2.1 Effects of ablation of Cd9 on primary prostate tumour development

Experimental animals were palpated blind in regards to genotype and once they developed a palpable prostate tumour they were culled and the tumour and lower urogenital tract removed and weighed (detailed in 2.3.5.1.2.2). No significant difference was seen between the wt, heterozygous and *Cd9* KO groups for tumour weights as seen in Figure 5-1 (Mann-Whitney test; $p > 0.18$). Animals were also analysed for age of onset of the palpable tumours as shown in Figure 5-2. The number of animals that developed palpable prostate tumours in each group were 28/32 (88%) wt, 24/25 (96%) heterozygous and 30/35 (86%) for the *Cd9* KO group. Again no significant difference was seen between the wt, heterozygous and *Cd9* KO group for time to palpable prostate tumour ($p > 0.262$, Mantel-Cox log rank test).

All TRAMP positive animals without a palpable tumour were culled at 40 weeks and all were found to have varying degrees of neoplasia of the prostate. However, since they did not meet the experimental criteria of the development of a palpable prostate tumour they did not have their tumours weighed. In addition 10 animals (4 wt, 3 het and 3 KO) were not weighed upon dissection as protocols were developed. However, all these animals were included in the survival analysis, as appropriate.

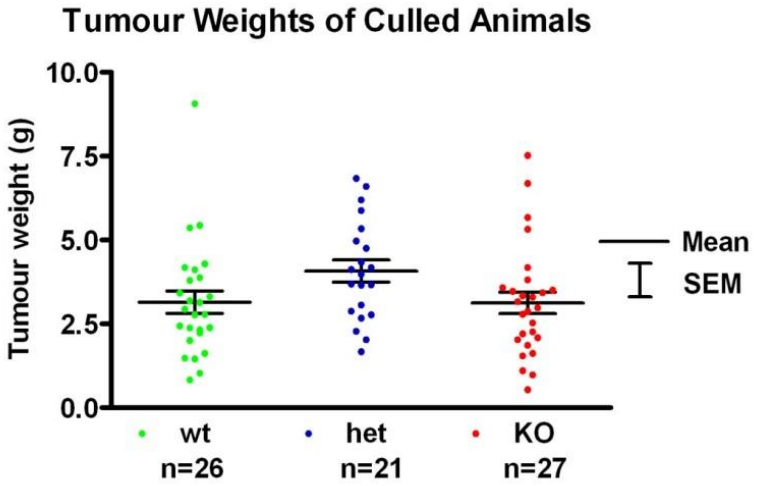

Figure 5-1: Tumour weights of *Cd9* animals at time of palpable tumour detection.
Once CD9/TRAMP animals had a palpable prostate tumour, they were culled and urogenital tracts/prostate tumours were dissected and weighed (as detailed 2.3.5.1.2). The weights of the tumours were not statistically different among the wt, heterozygous, or *Cd9* KO groups (Mann–Whitney rank sum test done individually between two groups at a time; p> 0.18)

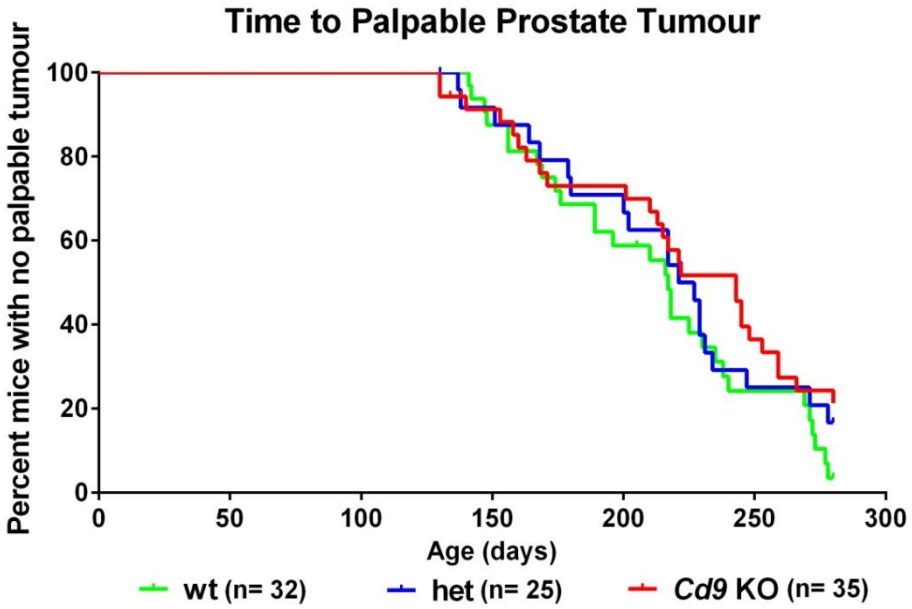

Figure 5-2: Survival curves of wt, heterozygous and *Cd9* KO animals.
CD9/TRAMP animals were monitored, blind with respect to their genotype, for onset of a palpable prostate tumour. Once animals had palpable prostate tumours they were culled and time to palpable tumour was plotted in Kaplan–Meier survival curves and found not to be statistically different through analysis carried out by the log-rank (Mantel–Cox) test (p=0.262).

5.2.2 Effects of Cd9 on proliferation, apoptosis and angiogenesis in cells in the primary prostate tumour

The harvested primary prostate tumours were characterised by IHC for markers of proliferation (anti-KI67), angiogenesis (anti-CD31) and apoptosis (anti-active caspase-3) as detailed in section 2.3.11. Labeling of the antibodies on the poorly differentiated primary prostate tumour sections is represented in, panels A, D and G. The Aperio™ automated algorithms were used to quantitate the IHC labeling based on intensity and a pseudo markup of positive labeling is represented in panels B, E and H and graphical representation of the quantitation is shown in panels C, F and I. There were no significant differences between the *Cd9* wt, heterozygous and KO groups for labeling of any of the three markers. All *p values* between wt/heterozygous, wt/KO, heterozygous/KO generated from the non-parametric Mann-Whitney test were greater than 0.23 (active caspase-3; heterozygous/KO).

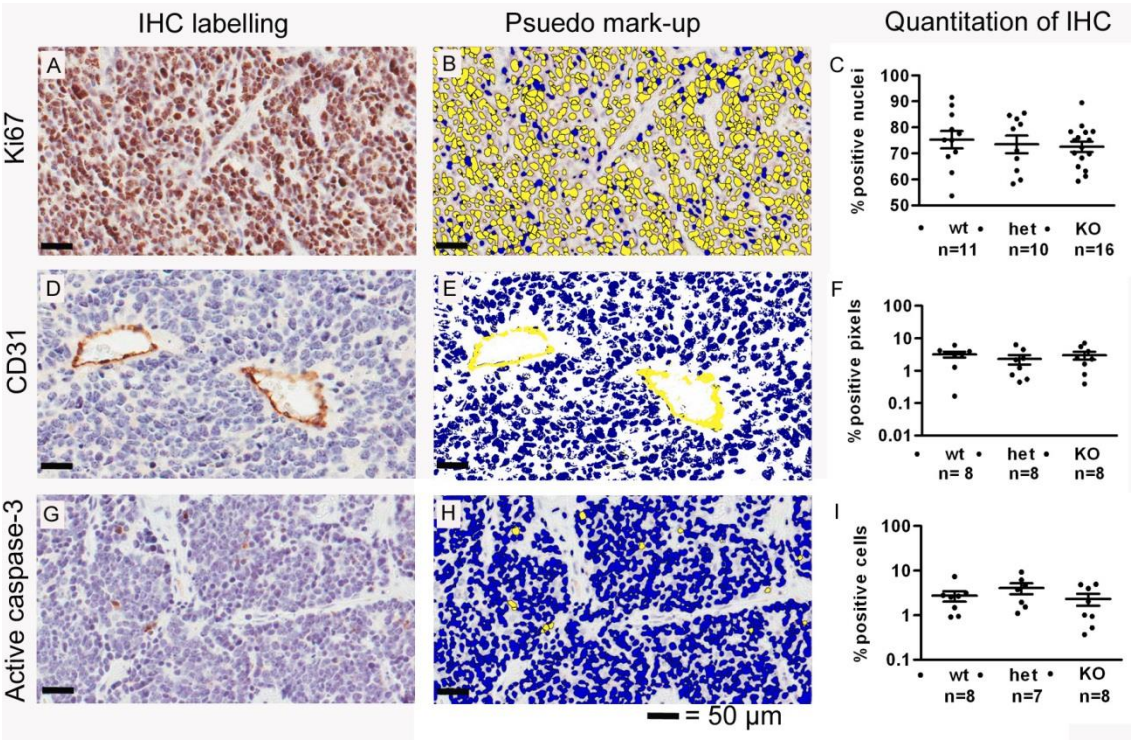

Figure 5-3: Representative IHC labelling and automated algorithm analysis of TMAs. FFPE primary prostate tumour sections were labelled by indirect peroxidase IHC using DAB as the chromagen using primary antibodies, anti-ki67 (clone SP6; Panel A), anti-CD31 (clone SZ31; panel D) and anti-active caspase-3 (clone ASP 175; Panel G) detailed in Table 2-7. Ki67 and active caspase-3 staining was analysed for percentage positive staining using the Aperio nuclear algorithm (B and H respectively) where the positive cells are marked in a yellow and negative cells are blue. CD31 staining was analysed using the positive pixel algorithm for percentage positive pixels, marked in yellow to negative pixels, marked in blue (panel E), described in detail in section 2.3.14.4. The percentage of positive staining for each of the markers was not statistically different among the wt, heterozygous, or KO groups, panels C, F and I (Mann–Whitney rank sum test done individually between two groups at a time, e.g. wt and KO with the p value always > 0.23).

5.2.3 Effects of Cd9 on metastases

Mice that were culled due to development of primary prostate tumours also had their liver and lungs removed as previously described in section 2.3.5.1.2.4. The liver and lungs were processed and analysed for presence of metastatic foci, which were previously shown to be derived from the primary prostate tumours (section 3.2.6). From the mice that developed primary prostate tumours, the number of mice that progressed to have secondary metastatic lesions is displayed below. Incidences of liver and lung metastases are shown in the contingency tables in

Table 5-1 and Table 5-2, respectively. Statistical analysis was performed via the Fisher's exact test and revealed that ablation of *Cd9* significantly increased the incidence of metastasis in the liver in comparison to wt animals (p =0.004) as shown in Figure 5-4, A. The heterozygous *Cd9* group had an intermediate frequency of metastasis but the difference was not significant, p=0.454 for wt compared to heterozygous while the *p value* for heterozygous compared to KO was 0.125. In contrast, the frequency of animals with lung metastasis was not altered by CD9 ablation with the *p value* always >0.86 (wt v's KO; Figure 5-4, B).

The discrepancy of *n* between total number of animals that developed primary tumours (5.2.1) and *n* stated for the number of animals included here was due to technical difficulties in fixing, processing, or sectioning of liver and/or lungs from a small number of animals for analysis of metastases. Exclusion was done with no knowledge of the donor animals' genotype or presence or absence of metastases within those samples.

Table 5-1: Contingency table showing incidence of metastatic lesions to the liver in *Cd9* animals.
When animals were culled for palpable primary prostate tumour their liver and lungs were dissected and analysed by histopathology for presence of metastatic lesions. Since the metastatic incidence data was binominal, in that each animal either had metastases or not, the data was placed into the two 2 x 2 contingency tables, the first for metastatic incidence to the liver and the second for lung metastatic incidence. This allowed statistical analysis via the stringent Fisher's exact test. A statistical difference was only seen in the incidence of metastases to the liver between the *Cd9* wt and *Cd9* KO animal. The resultant p-values are shown in the graph below (Figure 5-4, A).

Incidence of metastasis to the liver in *Cd9* wt and KO mice	Number of animals with NO metastases (Total number and % of mice)	Number of animals with metastases (Total number and % of mice)	**Total animals**
Cd9 wt animals	**19 (83%)**	**4 (17%)**	23
Cd9 KO animals	**12 (43%)**	**16 (57%)**	28
Total animals	31	20	51

Table 5-2: Contingency table showing incidence of metastatic lesions to the lung in *Cd9* animals.

Incidence of metastasis to the lung in *Cd9* wt and KO mice	Number of animals with NO metastases (Total number and % of mice)	Number of animals with metastases (Total number and % of mice)	**Total animals**
Cd9 wt animals	**18 (78%)**	**5 (22%)**	23
Cd9 KO animals	**22 (79%)**	**6 (21%)**	28
Total animals	40	11	51

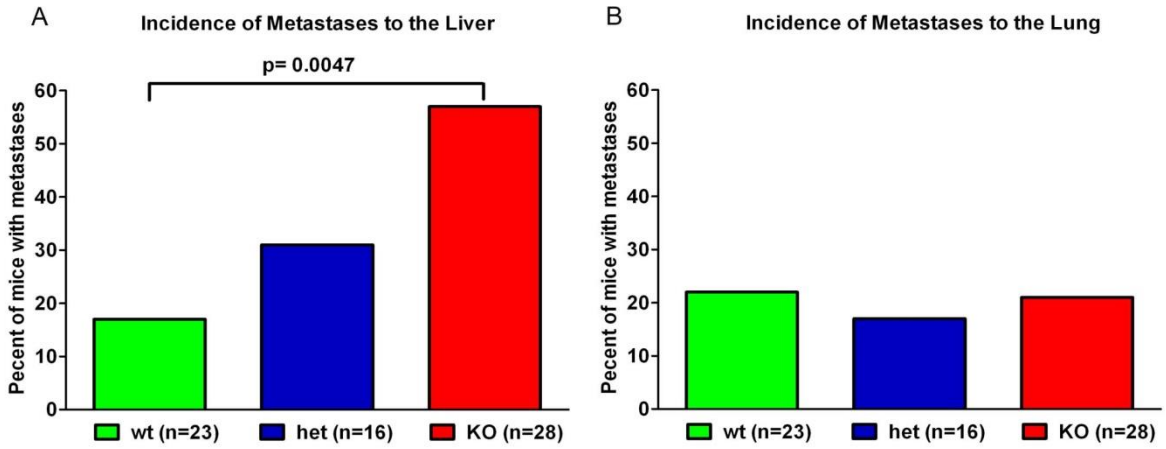

Figure 5-4: Incidence of metastasis to the liver (A) and lung (B) in *Cd9* wt, heterozygous and KO animals.

When animals were culled for palpable primary prostate tumour their liver and lungs were dissected and analysed by histopathology for presence of metastatic lesions. Incidence of metastases (graphed as a percentage of the total animals with metastases present for each genotype) in *Cd9* wt, heterozygous and KO animals to the liver, A; and to the lung, B; are shown. The p-values were determined by the Fishers exact test. Incidence of metastases to the liver was significantly increased in the *Cd9* KO cohort compared to the wt cohort. No significant differences were seen between the groups in regards to metastases to the lung with all p values >0.86.

The ablation of *Cd9* also significantly increased the total number and total area of metastases in the liver in comparison to wt animals (*p*= 0.008 and 0.017 respectively; Figure 5-5 A and C). Again an intermediate effect was seen in the *Cd9* heterozygous animals. No significant differences were seen between the *Cd9* wt, heterozygous and KO animals in regards to number or total area of foci to the lung, with all *p values* larger than 0.233 (Figure 5-5 B and D). The average areas of the individual metastatic foci in each organ in each animal were also analysed (Figure 5-6). Statistical analysis revealed no significant difference in the average foci area between wt, heterozygous and *Cd9* KO groups in the liver or the lung; p=0.478 and p=0.432, respectively.

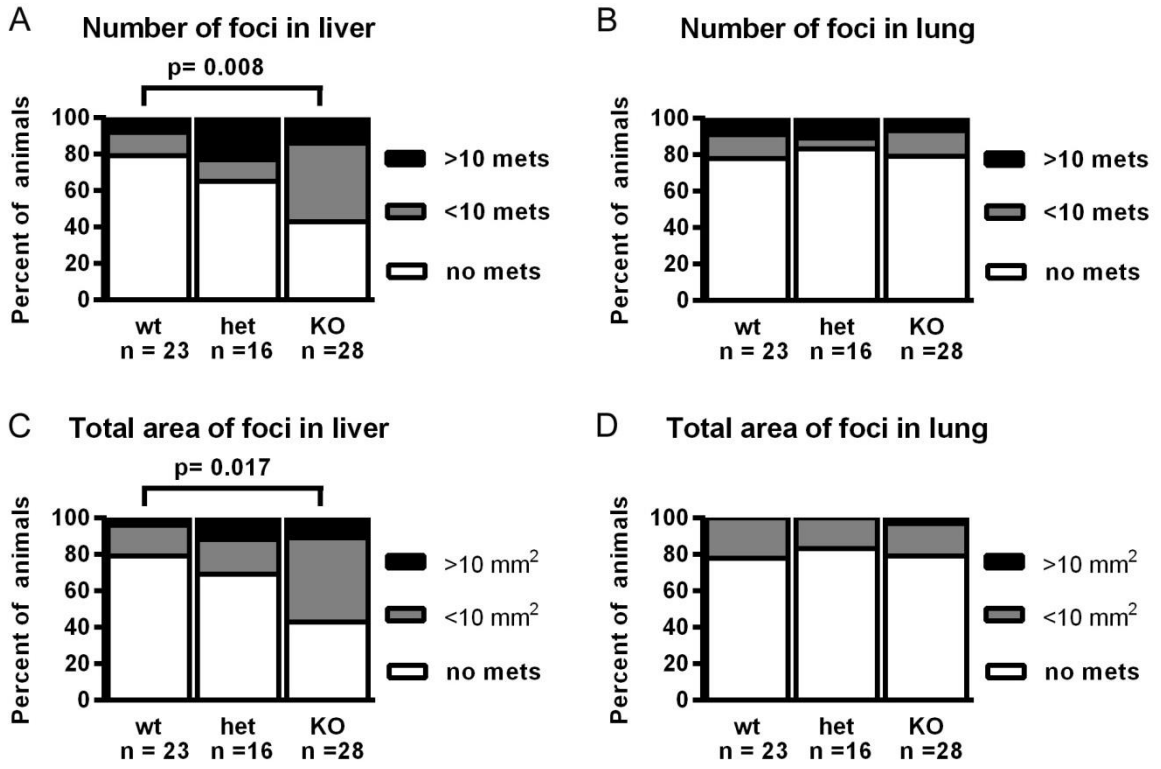

Figure 5-5: Number of metastatic foci to the liver in *Cd9* wt, heterozygous and KO animals. The liver and lung sections previously detailed in Figure 5-4 were viewed in Imagescope at 200x magnification and metastatic foci were manually annotated to produce an automated output of number of metastatic foci and total area of metastatic foci for each organ for each animal. The raw count data were statistically analysed using the Mann-Whitney-U (rank sum) test to obtain p values. Due to the many zero counts (animals with no metastases) making the graphs difficult to distinguish, data were grouped arbitrarily into 3 subsets for graphing, animals with no metastases, less than 10 metastatic lesions and more than 10 metastatic lesions in the liver (**A**) and lungs (**B**) for each of the wt, heterozygous and KO genotype groups. Similarly data on the total area of metastatic lesions were grouped according to no lesions, less than 10 mm^2 total area of metastatic lesions and animals with more than 10 mm^2 total area of metastatic lesions in the liver (**C**) and lungs (**D**) for each of the wt, heterozygous and KO genotype groups. No statistical difference was seen between the wt, heterozygous or KO groups in the number or total area of metastatic lesions in the lungs ($p>0.445$). The number of metastatic foci and total area of metastatic lesions in the liver were significantly increased in the *Cd9* KO cohort of animals compared to the wt cohort.

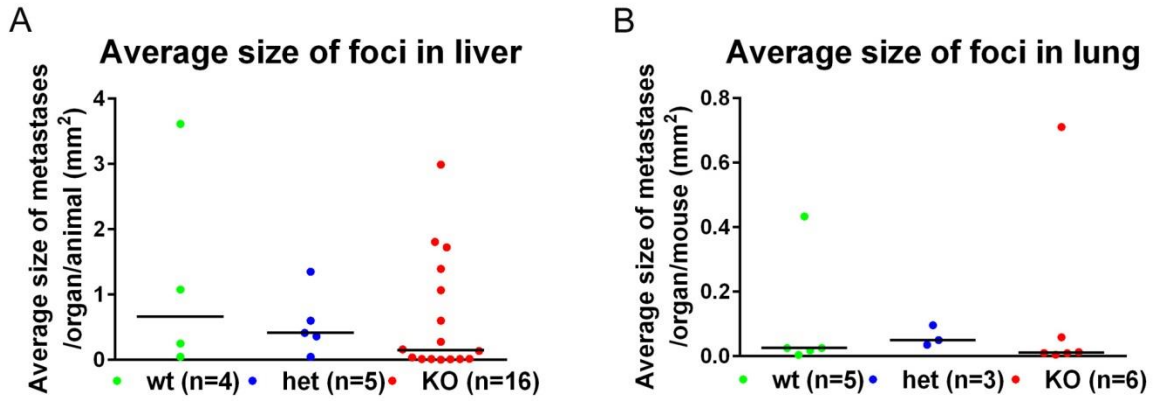

Figure 5-6: Average size of metastatic foci.
The liver and lung sections previously detailed in Figure 5-4 were viewed in Imagescope at 200x magnification and metastatic foci were manually annotated to produce an automated output of total area of metastatic foci for each organ for each animal. The average area for the metastatic foci was calculated and plotted for the wt, heterozygous and *Cd9* KO groups for both the liver and lung. Statistical analysis was performed by the non-parametric Kruskal-Wallis one way analysis of variance test. No significant differences in total metastatic foci in either the liver or lung were seen between the genetic groups (p=0.478 for liver and p=0.432 for lung were the lowest values).

5.3 *Discussion*

This is the first report demonstrating the effect of the genetic ablation of *Cd9* in a *de novo* model of prostate cancer development and spontaneous metastasis.

The *TRAMP* positive experimental animals showed progressive onset of prostate cancer and by the 40-week endpoint 92% (85/92) of the total animals (wt, *Cd9* heterozygous and *Cd9* KO) had developed palpable primary tumours. The onset of primary prostate tumours (time to palpable tumour) was not affected by the ablation of *Cd9* in this model (Figure 5-2). Furthermore, ablation of *Cd9* did not affect the weight of these tumours (Figure 5-1) or their proliferation or apoptotic rates (Figure 5-3).

However the loss of *Cd9* did significantly increase the incidence (Figure 5-4), number and total area of the metastatic foci to the liver (Figure 5-5). While metastases were frequently found in the lungs of the animals, the ablation of *Cd9* did not affect the incidence (Figure 5-4), number or average size of the metastatic foci to the lungs (Figure 5-5). The average size of the individual metastases in both

the liver and lungs were not significantly different between the genetic groups (Figure 5-6).

In this model *Cd9* was ablated in the tumor initiating cells as well as in all other cells in the animal. Therefore we cannot delineate whether the increase in metastasis was due to loss of *Cd9* on the tumour itself and/or the host environment. Changes in metastasis were not due to differences in the size of primary tumours which was unaffected by *Cd9* deletion. Importantly, the increase in metastasis was site-specific; the lack of effect on lung metastasis implies that altered release of tumour cells from the primary site was not a major mechanism. Furthermore, because the average area of the individual metastatic foci was also not affected, it appears that once the circulating metastatic cells lodged in the liver their subsequent expansion was not altered by the ablation of *Cd9*. This suggests that the *Cd9* dependent differences in metastatic incidence were due to effects on intermediate steps of the metastatic cascade.

Metastasis is a multistep process that includes cell dissemination from the primary tumour, intravasation, evasion of immune-surveillance, extravasation and lodgment in distal sites with subsequent foci expansion that includes angiogenesis, with each of these steps involving a multitude of processes (Valastyan and Weinberg 2011). Cell motility is required for all these steps. Multiple studies have demonstrated effects of CD9 over-expression or knockdown on cell motility *in vitro* (reviewed by Powner, Kopp et al. 2011). For example, one group transfected three tumour cell lines with CD9 and saw reduced motility in all lines which inversely correlated to CD9 expression (Ikeyama, Koyama et al. 1993). Knockdown of CD9 in MDA-MB-231 cells increased migration on fibronectin *in vitro*, but did not alter attachment to various other matrices (Powner, Kopp et al. 2011), while siRNA knockdown and blocking antibodies to CD9 in melanocytes both caused increased cell motility (García-López, Barreiro et al. 2005).

The functional role of CD9 in motility has been postulated to result from the known lateral association with the motility related integrins, particularly β1 (Berditchevski

2001). Tetraspanins are proposed to exert their effect on integrins by either inducing conformational changes or deregulating integrin-dependent signaling pathways such as phosphoinositide 3-kinase and p130Cas (Kotha, Longhurst et al. 2008). CD9 related effects on motility may also be mediated by other CD9 motility related partner molecules such as epidermal growth factor receptor (Murayama, Shinomura et al. 2008), CD9P-1/EWI-F, FPRP/EWI-2 (Stipp, Kolesnikova et al. 2001, Stipp, Orlicky et al. 2001) and intercellular adhesion molecule 1 (Barreiro, Zamai et al. 2008). Furthermore, CD9 is one of the only tetraspanins reported to directly bind ligands, specifically pregnancy-specific glycoprotein 17 (Waterhouse, Ha et al. 2002) and more relevant to cancer progression, fibronectin (Longhurst, Jacobs et al. 2002). The *in vitro* experiments reviewed above solidly suggest that CD9 has anti-migratory properties which could account in part for the increase in metastases when *Cd9* is ablated. The conflicting reports of CD9 mediated functional effects have been rationalised as effects of the CD9 partner molecules within the dynamic TEMs and furthermore CD9 may only inhibit specific steps within the metastatic process (reviewed by Zoller 2009).

CD9 has also been implicated in other processes associated with metastasis. For instance transfection of CD9 into various human lung and colorectal cancer cell lines inhibited epithelial-mesenchymal transition (EMT) through downregulation of the cell transforming Wnt family genes (Huang, Liu et al. 2004). CD9 has also been shown to inhibit platelet –tumour cell aggregation mediated by the aggrus/podoplanin protein. Over-expression of CD9 in HT1080 human fibrosarcoma cells inhibited platelet aggregation and metastasis of the cells to the lung following tail vein injection in mice (Nakazawa, Sato et al. 2008). Reduced survival of tumour cells in circulation and reduced lung retention were suggested mechanisms. CD9 has also been implicated in angiogenesis which is important for both tumour growth and access of tumour cells to the circulation. Knocking down CD9 was reported to inhibit endothelial cell migration and invasiveness coupled with a reduction in angiogenesis in *in vivo* models (Kamisasanuki, Tokushige et al. 2011). Though in this study we saw no overall effect from the ablation of *Cd9* on

primary tumour angiogenesis, regional effects (e.g. at tumour margins) may be seen with more detailed analysis. Furthermore, we did not observe differences in the growth of either primary tumours or individual metastatic foci as a result of *Cd9*-KO.

CD9 has been shown to be important in the interaction of tumour cells with the vascular endothelium. CD9 inhibited tumour cell trans-endothelial migration via association with β1 integrins (Longo, Yáñez-Mó et al. 2001) which may explain the increased incidence and frequency of liver metastases we observed when *Cd9* was ablated. However another study conversely reported that even though overall CD9 expression was decreased in correlation with cervical cancer progression, its expression was increased at sites of tumour infiltration into lymph and blood vessels (Sauer, Windisch et al. 2003) suggesting that in some cases CD9 may promote egress of tumour cells into the circulation.

In vivo models of investigating the role of CD9 in tumour progression have strongly implicated CD9 as a tumour suppressor. There have been a number of reports of orthotopic and ectopic grafting studies in syngeneic mice using cells that have had CD9 expression levels manipulated. One of the groups that originally discovered CD9, has done extensive *in vivo* experiments, including showing that lung metastasis after intravenous injection of murine melanoma cells was significantly inhibited by Cd9 over-expression (Ikeyama, Koyama et al. 1993). In another study the group saw a 73.7% reduction in lung metastases when murine melanoma cells grafted into the foot pad of mice were subsequently transduced with Cd9 adenovirus via intra-tumour injection, with no effect on primary tumour growth (Miyake, Inufusa et al. 2000). They subsequently developed an orthotopic lung tumour model by implanting Lewis Lung Carcinoma (LLC) cells in the lungs of C57BL/6 mice that progressed to develop lymph node metastases. They showed that adenoviral Cd9 transduction of LLC prior to implantation or intratracheal delivery of the CD9 adenovirus post LLC implantation reduced metastases, again importantly with no effect on primary tumour growth (Takeda, Hattori et al. 2007).

The results of these studies are in agreement with our finding that *Cd9* functions to inhibit metastasis without affecting primary tumour growth.

Other studies have used xenografts of human tumour cells in immunocompromised mice. Reduction in metastasis to the lung and liver by intravenously introduced fibrocarcinoma and small cell lung cancer cells following CD9 overexpression has been reported (Zheng, Yano et al. 2005, Nakazawa, Sato et al. 2008). Another study reported that tumour lesion volumes from subcutaneous human gastric cancer cells were reduced by intravenous injection of a blocking CD9 antibody apparently due to anti-proliferation/apoptotic and angiogenic effects (Nakamoto, Murayama et al. 2009). It is notable that the function of CD9 in gastric cancer appears atypical in that a positive correlation of CD9 expression with progression has been found in clinical studies (Hori, Yano et al. 2004, Soyuer, Soyuer et al. 2010). In contrast, no effect on tumourigenesis or metastasis from orthotopic injection of prostate cancer cells overexpressing CD9 was observed (Zvieriev, Wang et al. 2005). Again, the divergent results between different systems may be due to the major role of CD9 partner molecules in its functional effects. As Zvieriev *et al*. (2005) suggest, simply overexpressing CD9 without these partner molecules may explain their contrasting results. Furthermore it has been shown that CD9 and CD81 have similar functions and can both associate with the EWI family of proteins. These similarities coupled with the fact that, even though *Cd9* is ubiquitously expressed, most cell types in the *Cd9* KO display minimal phenotypes suggests that there may be some compensation between these tetraspanins (reviewed by Rubinstein 2011). Such compensation may also explain conflicting outcomes in various *in vitro* and *in vivo* systems; especially in studies where CD9 expression is reduced. In CD9 overexpression studies, basal levels in the parental cells may be sufficient to exert functional effects masking significant experimental outcomes. Furthermore, the individual CD9 related processes that make up the metastatic cascade such as motility, EMT, adhesion and trans-endothelial migration are not uni–directional and are dynamic throughout various stages of

metastasis. Therefore CD9 likely plays various roles at different stages within individual model systems which may help explain conflicting data.

In conclusion we have reported in this chapter for the first time that the genetic ablation of *Cd9* in the TRAMP model does not affect *de novo* prostate cancer development, but does significantly increase spontaneous metastasis to the liver.

Chapter 6: Evaluation of tetraspanins as prognostic biomarkers for prostate cancer in humans

6.1 *Introduction*

Prostate cancer is the most commonly diagnosed cancer in developed countries and one of the leading causes of cancer related deaths in males. However PCa is a very heterogeneous disease. Some patients diagnosed with PCa will follow an indolent course and never have their life expectancy threatened by the disease. Other patients will progress to the metastatic form of the disease for which current treatment options are basically palliative (Siegel, Naishadham et al. 2012). One of the major unmet needs in treatment of PCa is prognostic biomarkers that can stratify these patients. This would allow better assignment of treatment modalities to benefit patient outcomes and reduce unnecessary side effects.

The tetraspanin group of membrane bound proteins (detailed in section 1.8) have been investigated in clinical studies in a variety of cancers. Clinical studies involving CD151, Tspan8, CD9 and CD82 have been extensively reviewed previously in this thesis in section 1.8.4.1 and elsewhere (Berditchevski and Rubinstein 2013). Briefly, high expression levels of CD151 and Tspan8 have been mostly positively correlated to cancer progression and poorer patient outcomes. In contrast to this, reduced expression of CD9 and CD82 has been mostly negatively correlated with cancer progression and poor prognosis in a variety of cancers. A previous study reported CD151 to have prognostic significance in PCa that outperformed the classical Gleason grading system, especially in early stage PCa (Ang, Lijovic et al. 2004). This is significant as, since the advent of PSA testing, approximately 90% of patients still have the cancer confined to the prostatic capsule at diagnosis (Jemal, Siegel et al. 2008). A biomarker that could give prognostic information for these patients could allow prescription of aggressive treatment to those who required it, while allowing for the non-invasive “watchful waiting” approach to those with indolent cancer avoiding unnecessary deleterious side effects (detailed in section 1.4).

In this chapter we have extended on from the previous clinical study of CD151 to include IHC analysis on an additional CD151 antibody clone along with other potential prognostic tetraspanins Tspan8, CD9 and CD82 on an independent cohort of PCa tissue samples, while evaluating automated IHC analysis in an effort to standardise IHC scoring.

6.2 *Results*

6.2.1 IHC staining of TMAS

TMAs were sourced from the Australian Prostate Cancer Collaboration (APCC). Initially FFPE pilot TMAs that contained 10 various patient prostate cancer samples were used to optimise the IHC for the primary antibodies (detailed in section 2.4.1.2). Once this was satisfactorily achieved APCC supplied FFPE serial sections of the “Gleason progression” TMAs (section 2.4.1.3). These TMAs each consisted of human prostate tissue samples with BPH, various stages of prostate cancer along with some matched normal prostate tissue samples from over 150 patients. IHC was performed on the sections as explained in 2.4.2 using the primary antibodies, anti-CD151 (clone 11B1), anti-Tspan8 (clone Ts29.1), anti-CD9 (clone 72F6) and anti-CD82 (clone G-2) along with matched isotype primary antibody controls as detailed in section 2.4.2. IHC staining with the anti-CD151 (clone RLM30) was optimised and performed on an autostainer at the Garvan Institute as explained in section 2.4.2. Representative labelling of the antibodies is shown in Figure 6-1. The labelling of all the tetraspanins was shown to be specific to the membrane and cytoplasm of the basal and secretory epithelial cells of the prostate glands, with limited background staining. There also was some specific staining of vasculature, especially with CD151 and also sporadic staining of muscle cells. No background staining was seen in the matched isotype controls as shown in Figure 6-1, K-N.

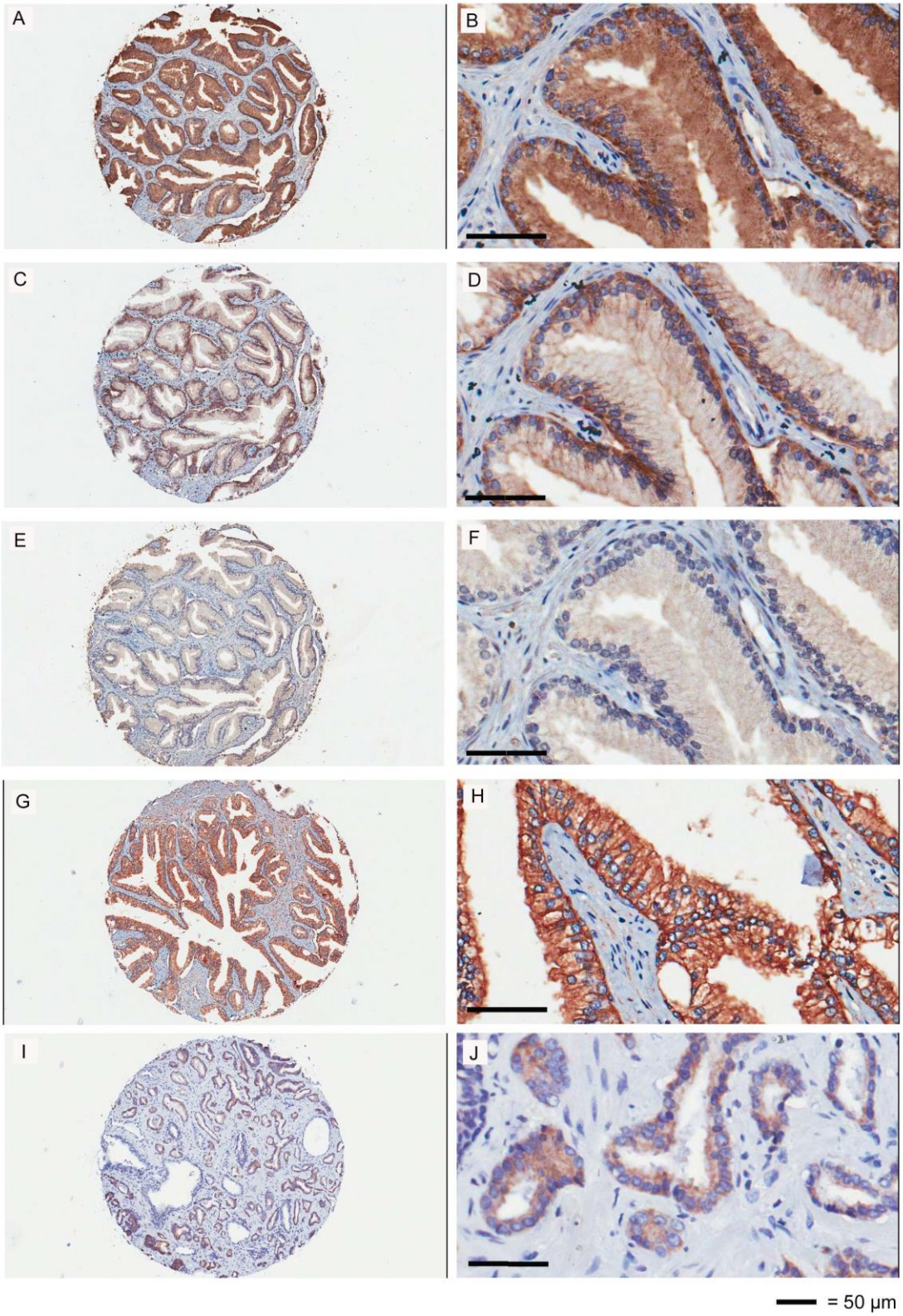
A
B
C
D
E
F
G
H
I
J
= 50 µm

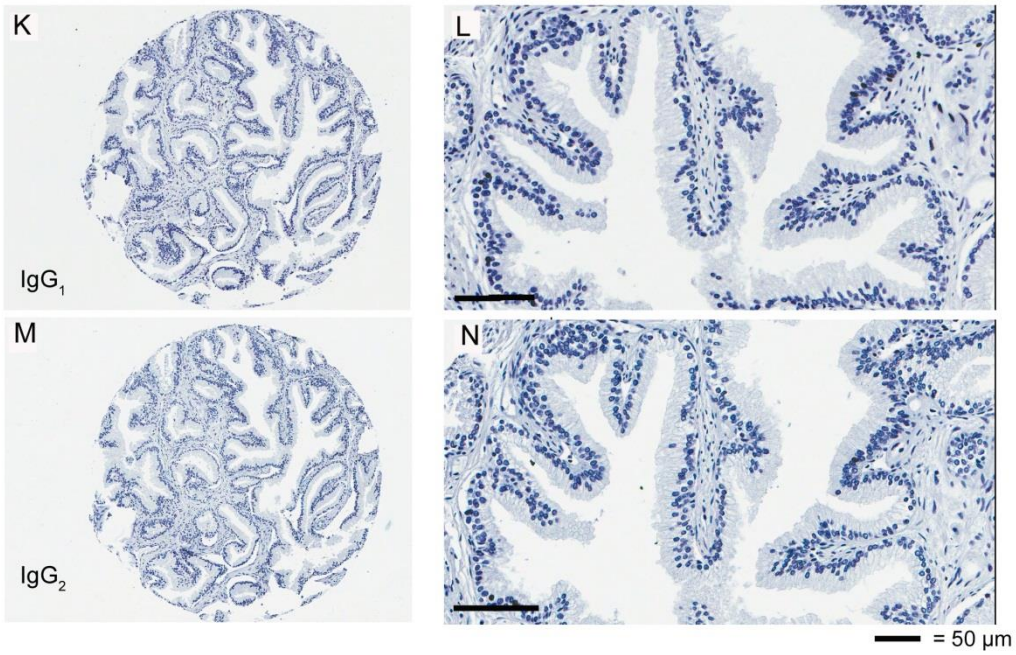

Figure 6-1: Representative IHC labelling on the TMAs.
The 5µm FFPE TMA sections were labelled by indirect peroxidase IHC using DAB as the chromagen (2.4.2) and the primary antibodies, anti-CD9 (clone 72F6, A and B), anti-CD151 (clone RLM30, C and D), anti-CD151 (clone 11B1.G4, E and F), anti-CD82 (clone G-2, G and H), anti-Tspan8 (clone Ts29.1, I and J) and the isotype matched negative control antibodies (K, L, M and N) as detailed in 2.4.2.

6.2.2 Analysis of protein expression on TMAs

The stained TMAs on glass slides were scanned in to high resolution digital virtual slides at 400x magnification using the Aperio digital pathology image capture system (section 2.3.14.2) and viewed using the adjunct ImageScope software. Due to the highly heterogeneous nature of prostate tissue samples, regions of interest (characterised by a pathologist) were selected by manual annotation for each individual spot on each TMA for each of the five different antibodies, as represented in Figure 6-2. The regions of interest were then used to analyse protein expression through the staining intensity by two different methodologies: the Aperio digital automated algorithms (section 2.4.3.4) and the classical pathological manual scoring system (section 2.4.3.5).

.

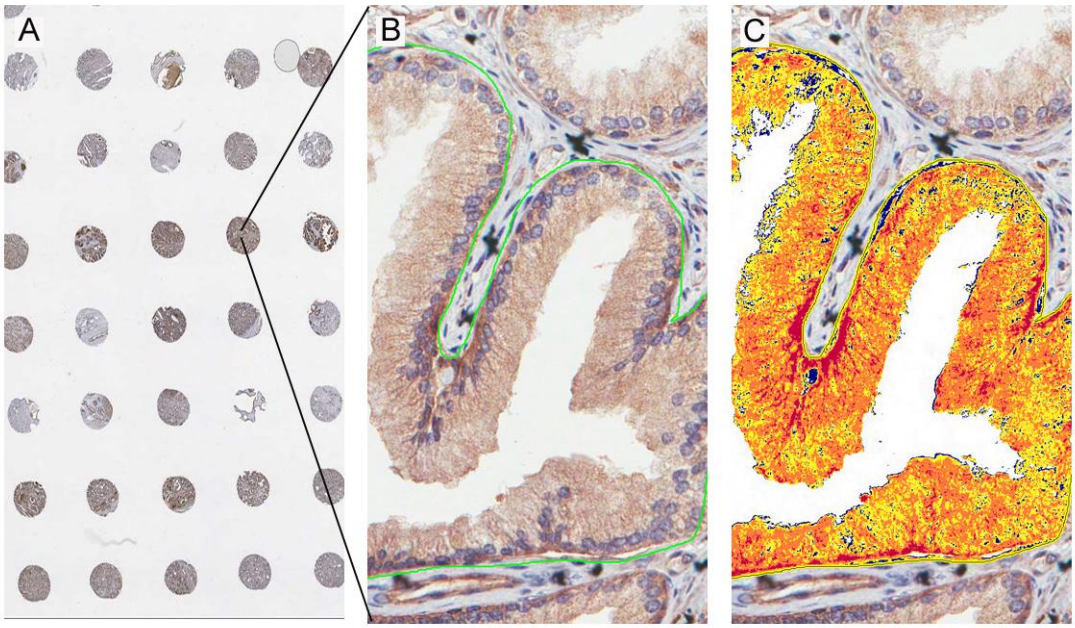

Figure 6-2: Representation of the annotations to select regions of interest in the TMA spots. The stained TMAs (A; CD151 11B1) were annotated to select regions of interest (ROI) in each of the TMA spots to reduce heterogeneous cell populations, as represented by the green line surrounding the gland in panel B. The colour deconvolution algorithm was then optimised to quantitate staining intensities for each antibody within the ROI. The staining intensities are calculated only on stained material and are displayed as a overlayed pseudo colour mark-up as negative (blue), weak (yellow), medium (orange) and strong (red) staining intensities(C). The results are given for each of the staining intensities as a percentage of the total area and/or pixels within the ROI in each case excluding any unstained areas, for subsequent graphing and analysis as shown in Figure 6-3.

6.2.2.1 Analysis by Aperio automated digital pathology algorithms

In an effort to standardise IHC scoring, analysis on the ROI was performed utilising the Aperio digital pathology system as detailed in 2.3.14. The automated colour deconvolution algorithm was optimised for each antibody and then used to quantitate the IHC labelling intensity on all spots on the TMAs (detailed in section 2.4.3). The intensity of the IHC determined by the algorithm is represented as a pseudo colour mark-up as shown in Figure 6-2, C, where blue is negative, yellow is low weak, orange is medium and red is strong staining as described in 2.4.3.4.2. From these staining intensities a “score” was produced for each tissue sample with each antibody as explained in section 2.4.3.4.2. Some of the patients had more

than one tumour sample on the TMA, if the tumour samples were the same Gleason grade an average of the IHC scores was used. If they were different grades, they were both used independently. The automated IHC scores were graphed for each of the five antibodies in three different ways: as a comparison of all the tumour and normal samples, as a pairwise comparison of the matched tumour and normal samples and lastly as a comparison between each of the various normal and Gleason score cancer subgroups as shown in Figure 6-3.

CD151 expression with both antibody clones (RLM30 and 11B1) was not altered when comparing all normal and tumour samples (RLM30 p=0.286 and 11B1 p=0.645, Figure 6-3; A and D) or normal/BPH samples to PCa grades (RLM30 p>0.0708 and 11B1 p=>0.421; panel C and F). CD151 expression was also not altered when comparing matched tumour and normal samples with the RLM30 antibody (p=0.4; panel B). However, CD151 (11B1) expression was upregulated in tumour samples compared to matched normal samples (p= 0.0314; panel E). Expression of the two CD151 antibodies did not correlate with each other (data not shown) as is deliberated in the discussion.

Tspan8 expression was not different between all tumour and normal samples (p=0.1761; G) or matched tumour and normal samples (p=0.0690; panel H). Tspan8 was shown to be upregulated in low grade PCa (all Gleason 2 and Gleason 3 samples combined) compared to BPH (p=0.0345; panel I).

Expression of CD9 and CD82 were both decreased in tumour relative to normal prostate when all samples were compared (p<0.0001; panel J and M) and also decreased in tumour compared to matched normal samples (p<0.0001; panel K and N). CD9 and CD82 expression was decreased in low grade (all Gleason 2 and Gleason 3 samples combined) and high grade PCa (all Gleason 4 and Gleason 5 samples combined) compared to BPH (CD9, p=0.0004 and p=0.0304; panel L and CD82 p<0.0001 and p=0.0022; panel O).

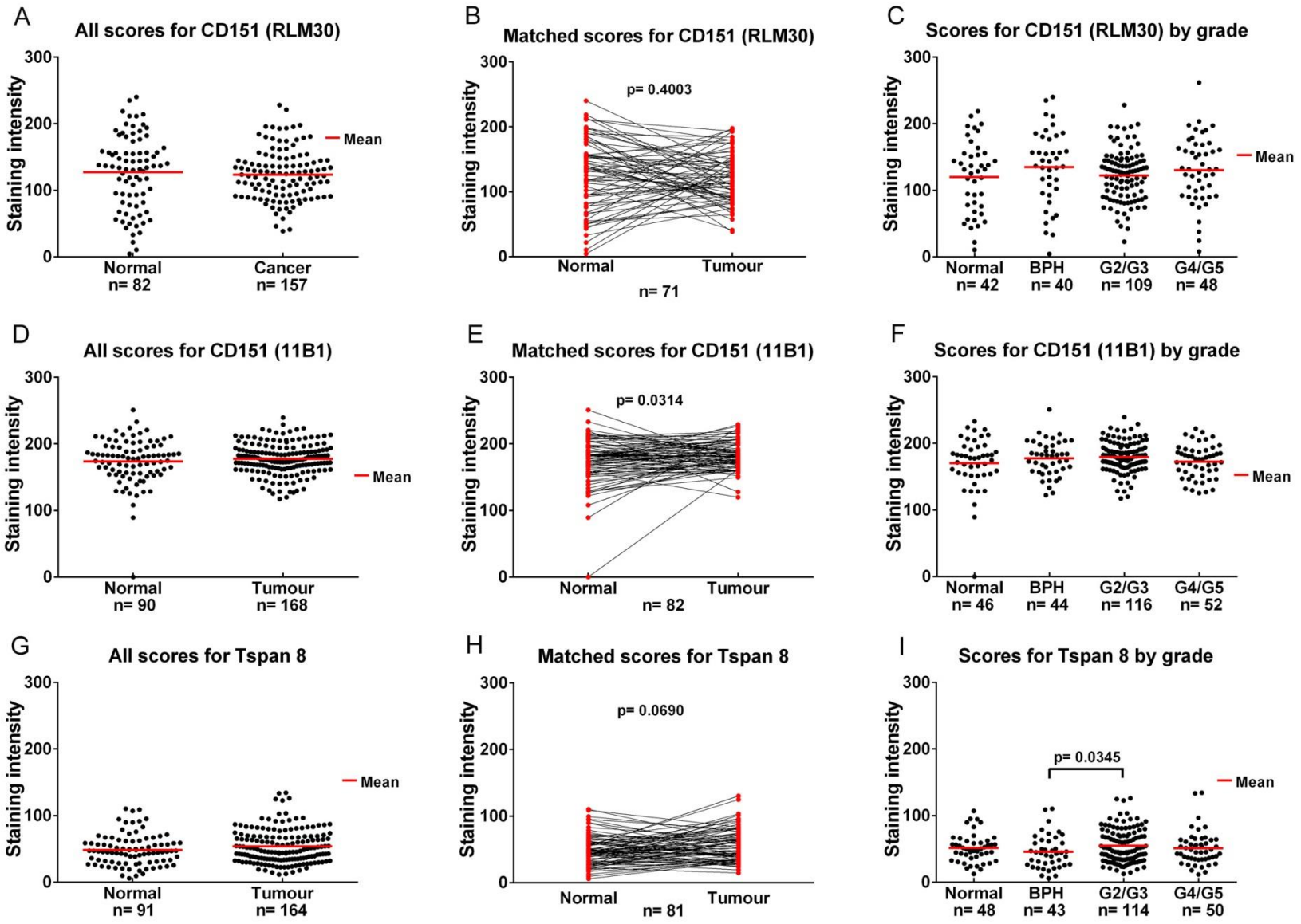
A
All scores for CD151 (RLM30)
Staining intensity
300
200
100
0
Mean
Normal
n= 82
Cancer
n= 157
B
Matched scores for CD151 (RLM30)
p= 0.4003
Normal
Tumour
n= 71
C
Scores for CD151 (RLM30) by grade
Normal
n= 42
BPH
n= 40
G2/G3
n= 109
G4/G5
n= 48
D
All scores for CD151 (11B1)
Normal
n= 90
Tumour
n= 168
E
Matched scores for CD151 (11B1)
p= 0.0314
Normal
Tumour
n= 82
F
Scores for CD151 (11B1) by grade
Normal
n= 46
BPH
n= 44
G2/G3
n= 116
G4/G5
n= 52
G
All scores for Tspan 8
Normal
n= 91
Tumour
n= 164
H
Matched scores for Tspan 8
p= 0.0690
Normal
Tumour
n= 81
I
Scores for Tspan 8 by grade
p= 0.0345
Normal
n= 48
BPH
n= 43
G2/G3
n= 114
G4/G5
n= 50

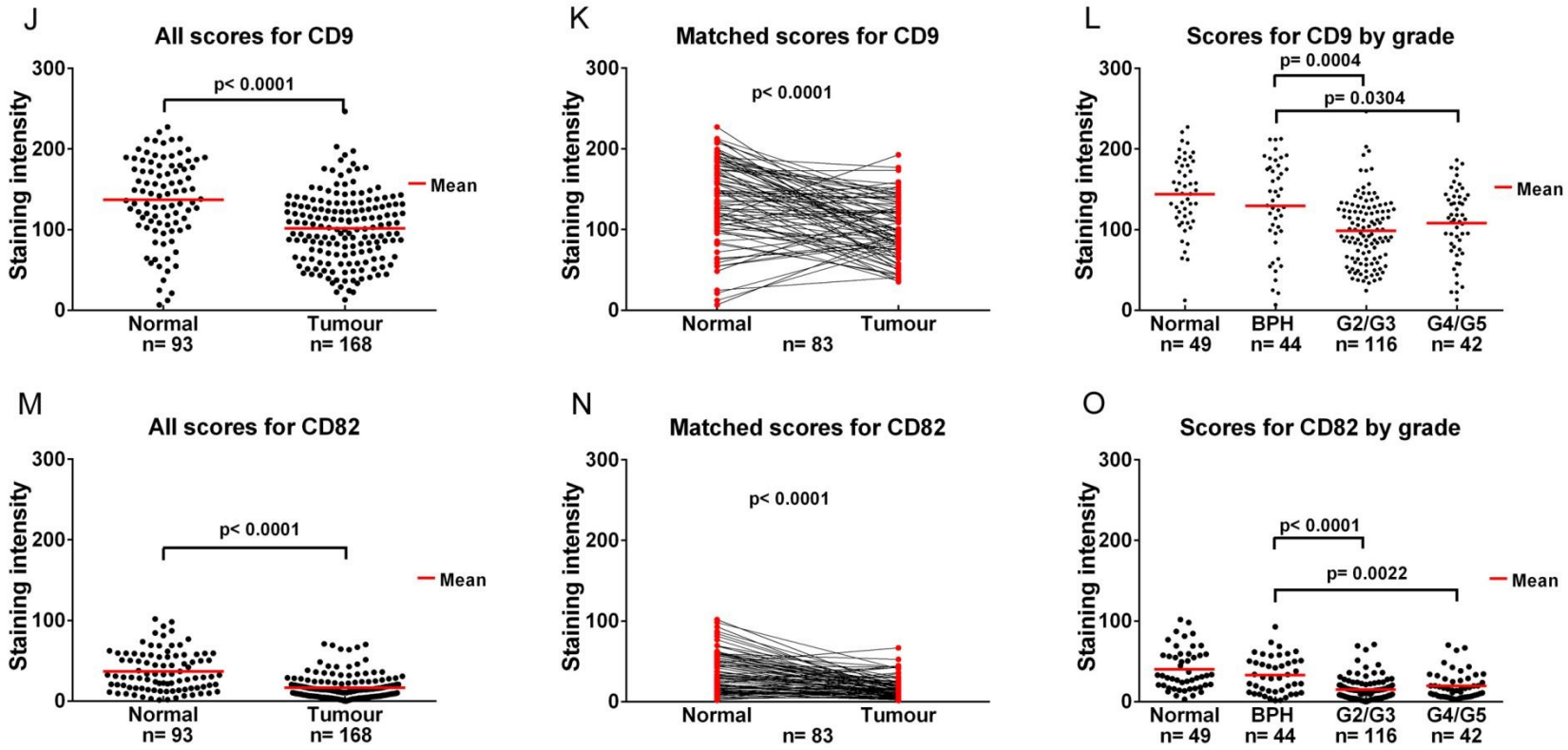

Figure 6-3: IHC quantitation using the Aperio automated algorithms.
Quantitation of staining intensity was assessed using the Aperio digital pathology system. The algorithm results are based on staining intensities and converted to a "score" to produce linear data in the range of 0-300 (detailed in 2.4.3.4 and Figure 6-2). The scores for all samples stained with the five primary antibodies CD151 (RLM30; A, B and C), CD151 (11B1; D, E and F), Tspan8 (G, H and I), CD9 (J, K and L) and CD82 (M, N and O) are shown (detailed in 2.4.2). IHC staining intensities were analysed for each antibody in regard to comparison of all tumour (Gleason grade 2 to Gleason grade 5 [G2 to G5]) and normal samples, matched tumour normal samples (NB: normal also includes the BPH samples) and the normal, BPH and low grade (all G 2 and G3 samples) and high (all G4 and G5 samples) grade PCa. Statistical analysis was performed using the Mann-Whitney U-test for comparison between individual groups and the Wilcoxon signed rank test for matched tumour and normal samples, with all significant p-values displayed in the appropriate graphs.

6.2.2.2 Analysis by manual scoring

The stained TMAs were viewed at 400x magnification using the ImageScope software. The same annotated regions of interest used in the automated analysis were analysed again by manual scoring, based on scores of 0, 1, 2 and 3 representing increasing staining intensity as described in 2.4.3.5. The IHC scores were graphed for each of the five antibodies, in three ways firstly, a comparison of all the tumour and normal samples, secondly a pairwise comparison of the matched tumour and normal samples and lastly to compare normal and BPH with the various PCa Gleason score subgroups (Figure 6-4).

Both the CD151 antibodies (RLM30 and 11B1) showed CD151 expression was upregulated in tumour samples compared to normal samples (RLM30 $p=0.002$ and 11B1 $p<0.0001$, Figure 6-4; panel A and D). CD151 was also upregulated in tumour tissue compared to matched normal samples (RLM30 $p=0.0167$; B and 11B1 $p<0.0001$; panel E). When comparing CD151 expression by stages of PCa, CD151 was upregulated in high grade PCa (all Gleason 4 and 5 samples combined) compared to BPH (RLM30 $p=0.0002$; panel C and 11B1 $p<0.001$; panel F). Furthermore CD151 (11B1) was also upregulated in low grade PCa (all Gleason 2 and Gleason 3 samples combined) compared to BPH ($p<0.0001$; panel F). Tspan8 expression was also upregulated in cancer samples when comparing all normal and tumour samples and matched tumour and normal samples both $p<0.0001$, Figure 6-4; panels G and H). When comparing PCa grades to normal and BPH Tspan8 was upregulated in low grade PCa and high grade PCa in comparison to BPH (both $p<0.0001$;panel I).

In contrast to CD151 and Tspan8, expression of CD9 and CD82 were both significantly decreased in tumour tissue compared to normal tissue when all samples were compared (both $p<0.0001$; panels J and M) and also decreased in tumour compared to matched normal samples (both $p<0.0001$; panels K and N).

CD9 and CD82 expression was also significantly decreased in both low grade and high grade PCa in comparison to BPH (both $p<0.0001$; panels L and O).

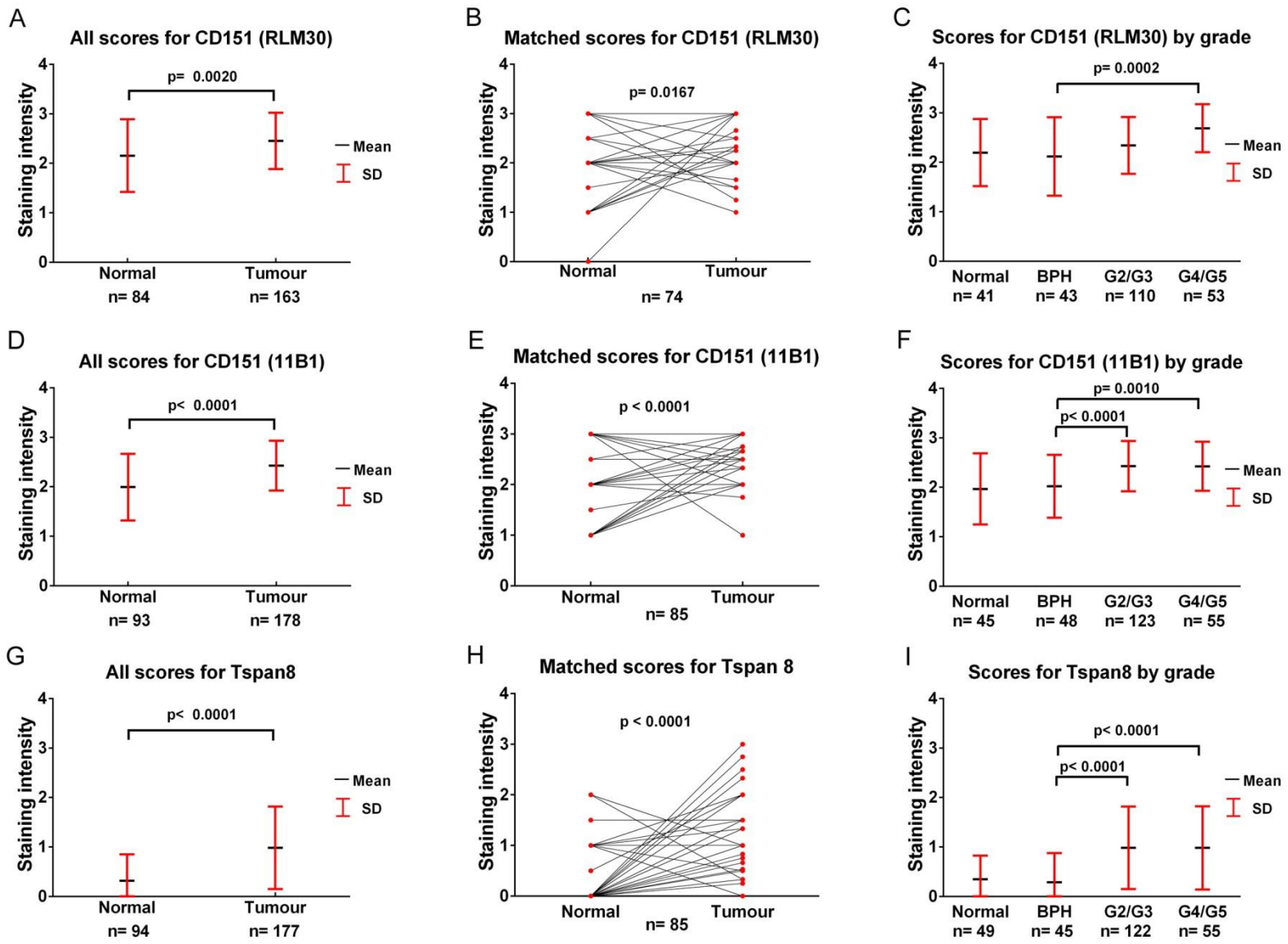
A
All scores for CD151 (RLM30)
p= 0.0020
Staining intensity
Mean
SD
Normal
n= 84
Tumour
n= 163
B
Matched scores for CD151 (RLM30)
p= 0.0167
Staining intensity
Normal
Tumour
n= 74
C
Scores for CD151 (RLM30) by grade
p= 0.0002
Staining intensity
Mean
SD
Normal
n= 41
BPH
n= 43
G2/G3
n= 110
G4/G5
n= 53
D
All scores for CD151 (11B1)
p< 0.0001
Staining intensity
Mean
SD
Normal
n= 93
Tumour
n= 178
E
Matched scores for CD151 (11B1)
p < 0.0001
Staining intensity
Normal
Tumour
n= 85
F
Scores for CD151 (11B1) by grade
p= 0.0010
p< 0.0001
Staining intensity
Mean
SD
Normal
n= 45
BPH
n= 48
G2/G3
n= 123
G4/G5
n= 55
G
All scores for Tspan8
p< 0.0001
Staining intensity
Mean
SD
Normal
n= 94
Tumour
n= 177
H
Matched scores for Tspan 8
p < 0.0001
Staining intensity
Normal
Tumour
n= 85
I
Scores for Tspan8 by grade
p< 0.0001
p< 0.0001
Staining intensity
Mean
SD
Normal
n= 49
BPH
n= 45
G2/G3
n= 122
G4/G5
n= 55

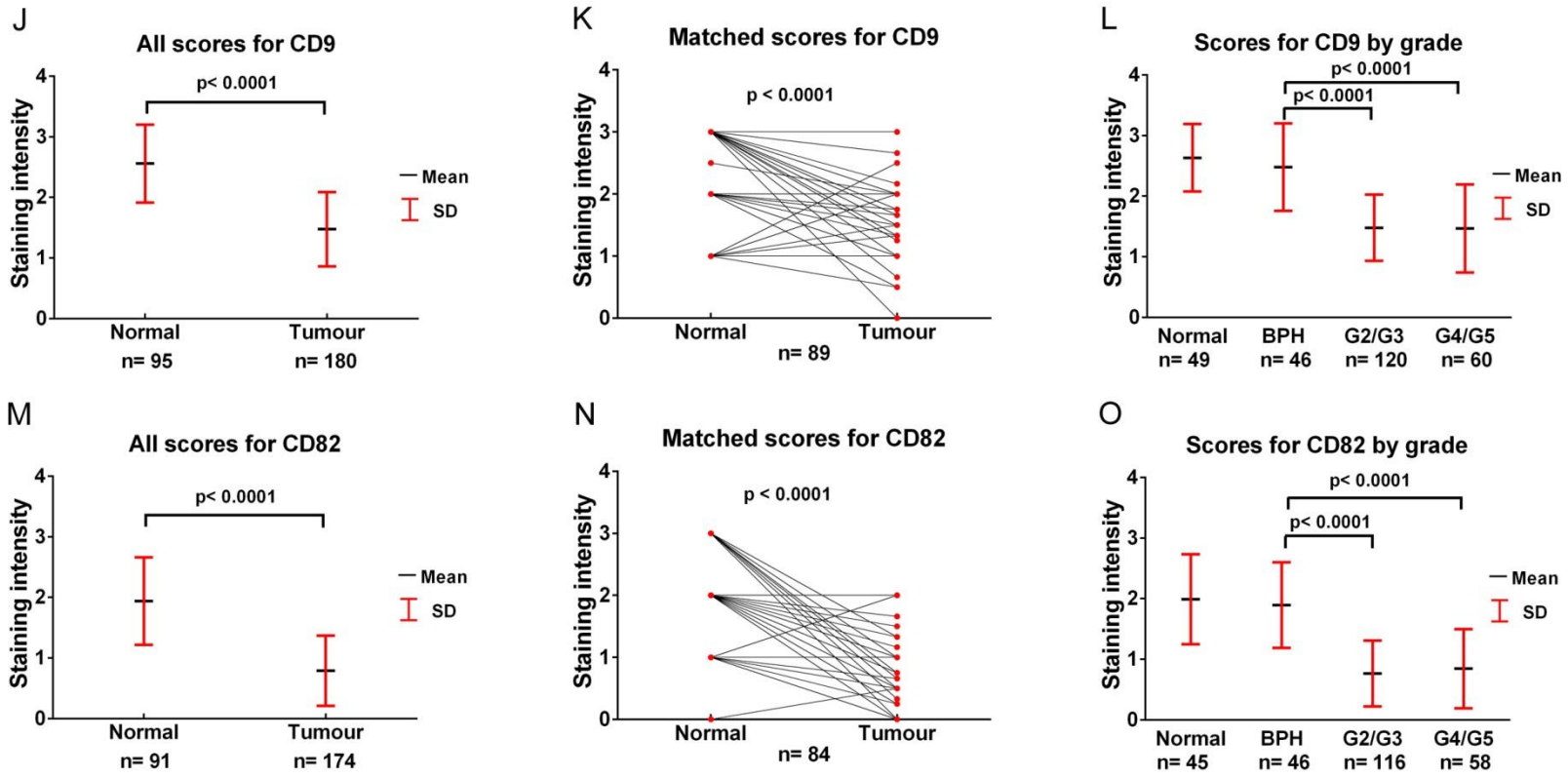

Figure 6-4: IHC quantitation using the manual pathological scoring method.
TMAs were stained by IHC (2.4.2) with the primary antibodies CD151 (RLM30; A, B and C), CD151 (11B1; D, E and F), Tspan8 (G, H and I), CD9 (J, K and L) and CD82 (M, N and O) as detailed in 2.4.2 and quantitated by manual scoring based on IHC staining intensity (2.4.3.5). The average scores for staining intensities were analysed based on the predetermined Gleason scores (G2-G5) for comparison between all normal and tumour samples, normal compared to matched tumour samples (normal includes the BPH samples) and comparison of the normal, BPH, low (all G2 and G3 samples) and high (all G4 and G5 samples) grade PCa. Statistical analysis was performed using the Mann-Whitney U-test for comparison between individual groups and the Wilcoxon signed rank test for matched tumour and normal samples, with all significant p-values displayed in the appropriate graphs.

6.2.2.3 Clinical data analysis

The IHC staining results from the manual pathological scoring were further analysed in regards to patient follow up data. The manual scoring results were chosen as they were more significantly varied between normal and tumour samples in comparison to the automated analysis.

As previously mentioned, the TMAs occasionally contained more than one tumour tissue sample per patient. Sometimes the additional tumour samples from the same patient were pathologically classified as a different Gleason grade. Therefore, the resultant staining intensities for cancer samples were grouped in 3 main ways; average cancer score per patient, average cancer score per patient categorised as low or high (CD151, low 0-2, high >2-3; CD9, low <1.5, high >1.5 and CD82, low <1, high >1) and highest cancer score per patient.

The clinical-pathological data (summarised in Table 6-1) is held by the APCC and due to ethical constraints cannot be distributed, therefore analysis was undertaken at the APCC affiliated, Garvan Institute by Dr Karen Chiam. The clinical and pathological parameters used in the analysis were age at diagnosis, pre-operative PSA levels, pathological cancer stage, extra-prostatic extension, primary, secondary and combined Gleason score, clinical stage, seminal vesicle invasion, margin status, perineural invasion, survival and relapse. Spearman's test was used to examine correlation of IHC staining to clinical parameters. Association of IHC intensity to survival and relapse was analysed by Kaplan-Meier plots while association to other clinical-pathological parameters were examined with univariate and multivariate Cox regression analysis.

Highest cancer score per patient for CD151 (RLM30) expression was significantly positively correlated with Gleason score ($p=0.038$) and there was a trend towards positive correlation with highest cancer score for CD151 (RLM30) expression and relapse ($p=0.060$; Kaplan-Meier plot not shown).

Average score of CD9 expression showed a trend towards a negative correlation with relapse of patients in a univariate Cox regression analysis (p=0.056). CD82 expression when analysed as average and highest cancer score per patient were negatively correlated with age at diagnosis (p=0.009 and p=0.003, respectively). Also average CD82 expression was negatively correlated with Gleason score by Spearman's test (p=0.003), while highest cancer score of CD82 expression was negatively associated with relapse (p=0.049).

Table 6-1: Summary of the clinical and pathological parameters of the patient cohort used for clinical analysis for the IHC staining intensity results.

Age at diagnosis, years		Patients (n)
	Mean age (range)	63.4 (48.4-75.7)
	≤65	54
	>65	42
Follow-up duration (months)		
	Mean (range)	149.5 (27.7-258.5)
PreOperative PSA, ng/mL		
	Mean (range)	9.5 (2-33.2)
	≤10	54
	>10	38
pT Stage		
	≤pT2C	54
	>pT2C	41
Clinical stage		
	T1	36
	T2	59
Extraprostatic Extension		
	Absent	57
	Present	38
Pathological Gleason Sum		
	≤6	57
	7	34
	≥8	4
Primary Gleason Grade		
	2	11
	3	64
	4	10
Secondary Gleason Grade		
	2	11
	3	44
	4	27
	5	3
Seminal Vesicle Invasion		
	Absent	87
	Present	8
Surgical Margin Status		
	Negative	49
	Positive	46
Perineural invasion		
	Absent	22
	Present	43
	Not Reported	29
Overall Outcome		
	Nil Relapse	51
	PSA	36
	Death	13
	- prostate cancer	3
	RP Not Curative	3

6.2.3 Discussion

The experiments in this chapter were initially designed as a follow on from earlier work that reported CD151 as a potential biomarker in PCa. Specifically CD151 was reported to be a better prognostic marker than the classical Gleason grading system in earlier stage PCa (Ang, Lijovic et al. 2004). The chapter moves forward from the previous experiments in that it is an independent study with a larger cohort analysing not just CD151 using the monoclonal antibody 11B1 as previously, but also a second commercially available CD151 antibody (RLM30) as well as examining other tetraspanin molecules Tspan8, CD9 and CD82. Furthermore the classical IHC manual pathological scoring method was used alongside the automated analysis using the Aperio digital imaging system algorithms for analysis of IHC staining intensity.

In regards to the previous paper and the current study, the spatial expression patterns of CD151 (both antibodies) in the cytoplasm and membrane of the epithelial cells of prostate glands were recapitulated. The current study showed a positive correlation of manually scored CD151 expression and PCa progression, which was in agreement with the previous report and many other studies involving CD151 in various cancers as detailed in 1.8.4.1.1. However, in this study the CD151 expression was not sufficiently different between the normal and cancer groups to be of clinical use (Figure 6-4). Also in regards to expression of CD151, the two CD151 antibodies used in this study were compared. It was shown that the staining intensities of the two CD151 antibodies were not significantly correlated (data not shown). A possible explanation for this is that the two antibodies recognise different epitopes of the CD151 antigen. The epitope for the 11B1 clone is known (Yamada, Tamura et al. 2008), while to the best of the authors knowledge, the epitope for the RLM30 clone is not. Varying epitope recognition, resulting in different staining patterns has been previously shown in a study that analysed a panel of six different CD151 antibodies that included 11B1, but unfortunately not the RLM30 clone (Geary, Cambareri et al. 2001). In the previous study evidence was presented to show that the variations in binding of different

antibodies was due to the masking of some epitopes, which was dependent of the nature of the complexes that CD151 forms with partner molecules in TEMs. The CD151 staining in this study and the previous study (Ang, Lijovic et al. 2004) was shown to be heterogeneous in PCa samples. This staining heterogeneity may be exacerbated by sampling handling and IHC methodology which could also affect the epitope masking and/or stability. Further characterisation of these and other CD151 antibodies needs to be investigated (discussed in 7.1).

This study was unable to replicate the prognostic importance of CD151 expression in PCa as shown previously and in other reports of various cancers (see section 1.8.4.1.1). Furthermore, the other tetraspanins (Tspan8, CD9 and CD82) did show limited prognostic value, but were disappointing compared to previous reports (see section 1.8.4.1). The meagre results may be attributed to a number of factors. The previous study by Ang et al. (2004) used PCa specimens collected from and processed in a single institute while this study used tissue gathered from multiple sites. The inherent variations in specimen handling between different institutions could affect epitope stability and IHC staining. Furthermore, in the current study, although expression of CD82 and CD9 were significantly inversely correlated to cancer progression, they only had limited clinical value. Notably CD82 which is now widely accepted to have adjunct prognostic significance in a number of cancers (see section 1.8.4.1.3) was not correlated to survival and only was just significantly correlated to patient relapse. The limited clinical follow-up data available in this study may have contributed to this lack of correlation with clinical outcome parameters. Nevertheless, it must be conceded that the differences of tetraspanin expression between normal and tumour in this study may be too small to be of clinical prognostic importance. However in light of the significant correlation of expression and PCa progression and the associated literature, future studies addressing the issues highlighted above are warranted and are discussed further in section 7.1.

In an effort to standardise IHC analysis this study also examined correlation between the Aperio algorithms for automated analysis of the IHC staining intensities and cancer progression as detailed in 2.4.3.4. Unexpectedly, the automated analysis showed that there was no change in expression of CD151 (RLM30 and 11B1) in tumour compared to normal samples. However in agreement with previous studies CD151 (11B1) was upregulated in tumour compared to matched normal samples (detailed in 1.8.4.1.1). CD82 and CD9 were both downregulated in tumour samples when compared to all normal samples and matched normal samples and also downregulated in low and high grade PCa compared to BPH. The results are in agreement with results from the manual scoring and previously published reports (reviewed in 1.8.4.1). Tspan8 was upregulated in tumour compared to matched normal samples and in low grade PCa compared to BPH. This also is in agreement with the manual scoring reported here and similar studies as described in section 1.8.4.1.2.

Due to the automated analysis data being less significantly correlated to cancer progression than the manual scoring analysis, it was not further analysed against the patient clinical data. This discrepancy of the automated data from the manually analysed data most likely stems from the inherent issue of the analysis software not being able to differentiate between the heterogeneous cell types characteristic in PCa. Therefore, even though each single tissue sample was laboriously manually annotated, as best as possible with regions of interest, the automated analysis results may have been skewed by inclusion of non-specific material. A possible way to alleviate this problem is by implementation of software from Aperio called “GENetic Imagery Exploration” (Genie) that is designed to recognise various cell types. The Genie software is proposed to allow the system to recognise only epithelial cells of the prostate gland. The subsequent automated analysis could then score only the cells of interest. This has been shown to be beneficial in a number of studies dealing with heterogeneous cell populations (see section 7.1 for more details). The software was only developed during the course of this project

and the cost of this proprietary software precluded its use. However possible future experiments using this are discussed in section 7.1.

Based on the urgent need for biomarkers that can stratify patients in regards to outcomes when diagnosed with PCa and the significant correlation of tetraspanins and disease progression in this and other studies, further clinical analysis of tetraspanins is warranted with appropriate patient cohorts containing suitable follow-up data and with revised analysis methodologies (further discussed in section 7.1).

Chapter 7: General discussion and future directions

7.1 *General discussion and future directions*

This project has tried to address two major unmet needs in the field of PCa. Firstly, PCa is a very heterogeneous disease in terms of progression. There are currently no reliable prognostic markers to predict which patients' cancer will remain indolent and have limited health impacts on their natural life and which patients will go on to more advanced, untreatable disease. Tetraspanins have shown promise as prognostic markers in a variety of cancers. We have shown here that expression of CD151 and Tspan8 were positively correlated to PCa progression. Conversely, CD9 and CD82 were downregulated in correlation to PCa progression, all in agreement with other studies in various cancers (reviewed in section 1.8.4.1). Even though there were significant differences of tetraspanin expression between the cancer stages, there was overlap and no clear segregated groupings to make the correlation data clinically useful. Additionally the IHC expression results for the two CD151 antibodies did not correlate with each other, suggesting the antibodies may recognise different epitopes as previously shown for other CD151 antibodies (Geary, Cambareri et al. 2001). Further studies on the various CD151 antibodies need to be investigated. Specifically, a panel of tetraspanin antibodies with multiple clones for each tetraspanin on a range of TMAs from different sources may elucidate both the epitope binding efficacies of various antibody clones and also the epitope masking effects caused by various tissue handling procedures. This would further allow future similar clinical studies to have a benchmark to compare with.

In regards to patient outcome data, this study has also shown that CD151 was positively correlated to Gleason score and patient relapse. Conversely CD82 was negatively correlated to Gleason score and patient relapse. While these prognostic results are in agreement with other studies, they are much less clear cut than previously shown (Ang, Lijovic et al. 2004). This may suggest that the low amounts of clinical outcome data that were available in this study may have been one of the limiting factors. Furthermore, the APCC TMA cohort used in this study consisted mostly of early stage PCa samples that were pathologically characterised as

Gleason 3 (n=~206) and only a handful of the more advanced Gleason 5 samples (n=~14). Also the *in vivo* work described in chapters 4 and 5 found that the ablation of *Cd151* or *Cd9* had no effect on the primary PCa but did influence metastases. Therefore, future biomarker experiments incorporating cohorts with greater numbers of later stage PCa samples known to go on to metastasise, and greater amounts of patient follow up data may reveal tetraspanin expression levels that correlate not only to cancer stage but also to related patient outcomes.

In an effort to try to reduce subjectivity and create a standardised IHC scoring system that may be used across institutions, automated IHC analysis methods from Aperio (section 2.4.3.4) were used alongside the more traditional manual scoring methods. The analyses by automated algorithms showed the same general correlation trends of tetraspanin expression with cancer progression as the manual scoring. However, the results were less significant compared to manual analysis, which is in contrast to other reports comparing the two IHC analysis methods (Neltner, Abner et al. 2012, Alvarenga, Coutinho-Camillo et al. 2013). Therefore, the automated IHC data was not followed up with analysis against patient outcomes.

The poor results obtained from the Aperio automated analysis may have been due to an inherent flaw in the software of not being able to recognise and analyse specific cell population within the heterogeneous cell populations, characteristic of PCa. The software developer has recently tried to resolve this issue by developing adjunct software that will purportedly perform this task. The “Genie” software program enables the user to train the software to distinguish between cell types. The software has successfully been utilised in other biomarker discovery projects to identify specific cell populations within heterogeneous populations such as breast cancer samples (Laurinavicius, Laurinaviciene et al. 2012, Tanaka, Kuraoka et al. 2012). Future experiments could involve validating the Genie software package on the same set of PCa TMAs used in this study to specifically identify epithelial cells of the prostate glands in the normal tissue samples and only tumour

cells in the cancer tissue samples to eliminate any unwanted tissue such as stroma and vasculature. Subsequently the same previously used automated algorithms could be utilsed to quantitate IHC intensities on the specific homogenous cell populations. We are currently negotiating with Aperio (who have recently been purchased by Leica) to obtain a trial version of the software.

The second major unmet need in prostate cancer research, due to the majority of deaths from prostate cancer resulting from largely untreatable late stage metastatic forms of the disease, is understanding molecules involved in the metastatic cascade. Here we have reported that the ablation of *Cd151* and *Cd9* did not affect primary tumour onset, however ablation of *Cd151* was shown to decrease metastatic incidence to the lung while ablation of *Cd9* increased metastatic incidence to the liver. Hence we have shown for the first time in a truly *de novo* model of PCa that *Cd151* is a metastatic enhancer gene while *Cd9* is a metastatic suppressor gene. Two immediate questions have arisen from the *in vivo* experiments. Firstly, is the ablation of *Cd151* and *Cd9* in the tumour cell or the host (environment) exerting the effects on metastasis? Secondly, why are the opposing metastatic effects of *Cd151* and *Cd9*, organ specific in the TRAMP model?

The fact that the ablation of the tetraspanins had no effect on the primary tumour or on the expansion of individual metastatic foci once lodged at distant sites (see chapters 4 and 5) indicates an effect on one or more of the intermediate steps of the metastatic cascade. The association of tetraspanins with integrins has long been established. The widely held theory is that tetraspanins act as molecular facilitators that are able to laterally arrange these molecules in spatial and temporal arrangements within tetraspanins enriched microdomains (TEMs) that have subsequent functional effects relevant to metastasis, such as adhesion and motility (reviewed by Hemler 2008, Stipp 2010, Detchokul, Williams et al. 2013). One of the most studied tetraspanin partner associations is that of CD151 and the laminin binding integrin subfamily, which have been shown to play a role in aforementioned metastatic functions (Zevian, Winterwood et al. 2010). Loss of CD151 has been

shown to inhibit recruitment of integrins into TEMs (Winterwood, Varzavand et al. 2006, Yang, Richardson et al. 2008), while CD151 has also been shown to regulate the internalisation and trafficking of integrins (Winterwood, Varzavand et al. 2006, Liu, He et al. 2007). Furthermore, CD9 association with integrins has been shown to inhibit tumour cell trans-endothelial migration *in vitro* (Longo, Yáñez-Mó et al. 2001). In contrast knockdown of CD151 was shown to reduce trans-endothelial migration (Deng, Li et al. 2012).The tetraspanin dependent recruitment of integrins into ordered structural TEMs may help explain the tetraspanin dependent functional effects such as motility and adhesion on the metastatic cascade.

Tetraspanins have also been shown to be associated with the matrix metalloproteinase (MMP) enzymes. For example, CD151 has been shown to be co-localised with MMP-7, with increased CD151 expression correlated to increased expression of MMP-7, MMP-2 and MMP-9 (Hong, Jin et al. 2006, Hasegawa, Furuya et al. 2007). A recent paper has shown that the pro-invasive functions of CD151 is partly attributed to the activation of MMP9 and MMP13 (Yue, Mu et al. 2013) Conversely increased CD82 and CD9 expression was shown to down regulate MMP-9 (Hong, Jin et al. 2006) and MMP-26 (Yamamoto, Vinitketkumnuen et al. 2004) expression, respectively. The tetraspanin dependent effects on the ability of the various MMPs ability to degrade extracellular matrix, which is required for the intermediate steps of the metastatic cascade, have to be considered.

The conundrum of either the host or tumour cell tetraspanin expression exerting metastatic effects may possibly be addressed by two different sets of experiments. The primary prostate tumours from wt and *Cd151* /*Cd9* KO animals could be used to produce primary cell cultures. The *Cd151* and *Cd9* wt and KO cell cultures could be grafted back into animals of matching and opposing genotypes. Another way to clarify this problem would be to use our *Cd151* and *Cd9* KO animals along with cre-lox techniques to develop models that would allow inducible KO of the tetraspanins, specific to the prostate. This would allow endogenous *Cd151* and

Cd9 to still be expressed in the rest of the host environment including the metastatic sites of the lungs and liver. These experiments may help show whether the ablation of *Cd151* and *Cd9* on the tumour cell or in the environment (or most likely both) influenced metastatic incidences *in vivo*. Similar models have been recently developed where the KO of *Cd151* was specific to the epidermal tissue of mice (Sachs, Secades et al. 2013).

While the aforementioned experiments may explain the tetraspanin influence on metastases in this model, they do not explain the organ specific effects where *Cd151* ablation decreased metastasis to the lung but not the liver, while conversely *Cd9* ablation increased metastasis to the liver but not the lungs. It has long been established that metastasising cells show preference for organs to seed and establish secondary metastatic tumour sites in humans, such as the propensity for primary prostate cancer cells to metastasise to bone. Stephen Paget's seminal 1989 paper describing the original "seed and the soil" hypothesis was used to explain the concept (Paget 1989) and is still the foundation for many theories to this day, while others have attributed the selective organ tropism to the anatomical/mechanical hypothesis. Both theories were discussed in a recent review by Langley and Fiddler (2011), leaders in the field of cancer metastasis. While there is no definitive functional data to explain these effects in humans, there has been even less investigation with animal models. However, the organ specific effects seen in this project, while unexpected, are most intriguing and therefore warrant follow up with further investigation.

Our results of a reduction in metastasis to the lungs but not the liver in the *Cd151* KO animals somewhat recapitulated results of a previous independent experiment where the knockdown of CD151 on breast cancer tumour cells resulted in reduced recruitment of the KD cells to the lungs in comparison to the wt cells, while no difference was seen in recruitment to the liver (Sadej, Romanska et al. 2010). As previously stated CD151 and CD9 have been shown to have opposing effects at sites of vascular epithelial interaction. Tetraspanins may have tissue specific

effects on interaction of tumour cells with the vascular endothelium and subsequent transmigration into specific secondary sites. Furthermore, functional tetraspanins have been shown to be enriched in exosomes (reviewed by Zoller 2009). These exosomes have been shown to facilitate long distance cell signaling, and furthermore the tetraspanins within the exosomes have been shown to affect target cell selection of exosomes (Rana, Yue et al. 2012). The enriched exosomes may have the ability to set up pre-metastatic niches in specific tissues. The ablation of tetraspanins may disrupt this pre-metastatic niche, causing organ tropism and/or embedding to be affected. A recent paper has shown that the tetraspanins CD151 and Tspan8 exert their pro-metastatic functional effects through differing mechanisms, where CD151 effects were attributed to association with MMPs and Tspan8 functional effects were attributed to the associated motility FAK and paxillin molecules (Yue, Mu et al. 2013). If this holds true for other tetraspanins, the varying subsequent organ specific effects of *Cd151* and *Cd9* ablation may not be so bewildering.

Following on from the previously explained work (section 4.3) by Sadej and colleagues (2009), grafting studies involving intravital microscopy to track tagged *Cd151* and *Cd9* wt and KO cells in various *in vivo* models to elucidate recruitment and subsequent seeding rates in the various organs may also help explain this interesting result. Finally quantitating tetraspanin expression levels to see if there are variations between the different organs may help to explain the site specificity through the interactions of tetraspanins and their partner molecules allowing seeding and establishment of secondary tumour sites by cells disseminated from the primary tumour foci.

In conclusion, we have shown for the first time in a truly *de novo* model of PCa that *Cd151* is a metastatic enhancer gene. Conversely, we have shown that *Cd9* is a metastatic suppressor gene. This is in agreement with the project's first hypothesis that "tetraspanin proteins influence prostate cancer progression". This project also showed that tetraspanin expression was correlated with PCa progression.

However, the studies with patients' specimens did not support the second hypothesis that "tetraspanins can also be used as prognostic markers as an adjunct to classical grading methods". This hypothesis requires further testing using additional material and follow-up data as well as improved analytical techniques.

Appendix

8.1 *Buffers and reagents for IHC*

8.1.1 10X PBS stock solution

425.0 g of NaCl (sodium chloride); 71.5 g of K_2HPO_4 (di-potassium hydrogen orthophosphate) and 12.5 g of KH_2PO_4 (potassium di-hydrogen orthophosphate), make up to 5 L with ddH_20.

8.1.2 1X PBS working solution

100 ml of 10X PBS to 900 ml of ddH_20 and mix well.

8.1.3 PBT working Buffer

1X PBS; 1% Bovine Serum Albumin (w/v) and 0.1% tween 20 (v/v). Vortex and store at 4 ºC for a maximum of two weeks.

8.1.3.1 Scott's tap water substitute

1g $NaHCO_3$ (sodium hydrogen carbonate), 20.47g of $MgSO_4$ (magnesium heptahydrate), make up to 500 mL with ddH_20.

References

Abate-Shen, C., W. A. Banach-Petrosky, X. Sun, et al. (2003). "Nkx3.1; Pten Mutant Mice Develop Invasive Prostate Adenocarcinoma and Lymph Node Metastases." Cancer Research **63**(14): 3886-3890.

Abate-Shen, C. and M. M. Shen (2002). "Mouse models of prostate carcinogenesis." Trends in Genetics **18**(5): S1-S5.

Abrahamsson, P. (1999). "Neuroendocrine Differentiation in Prostatic Carcinoma." Prostate **39**: 135-148.

Adhami, V. M., I. A. Siddiqui, S. Sarfaraz, et al. (2009). "Effective Prostate Cancer Chemopreventive Intervention with Green Tea Polyphenols in the TRAMP Model Depends on the Stage of the Disease." Clinical Cancer Research **15**(6): 1947-1953.

Agarwal, N., G. Sonpavde and O. Sartor (2011). "Cabazitaxel for the treatment of castration-resistant prostate cancer." Future Oncology **7**(1): 15-24.

Ahlgren, G., K. Pedersen, S. Lundberg, et al. (2000). "Regressive changes and neuroendocrine differentiation in prostate cancer after neoadjuvant hormonal treatment." The Prostate **42**(4): 274-279.

Ahmad, I., O. Sansom and H. Leung (2008). "Advances in mouse models of prostate cancer." Expert reviews in molecular medicine **10**(16): 1-12.

AIHW (2010). "Cancer in Australia: an overview, 2010." Australian Institute of Health and Welfare & Australasian Association of Cancer Registries 2010 **60**(60).

Alam, N., H. L. Goel, M. J. Zarif, et al. (2007). "The integrin - growth factor receptor duet." Journal of Cellular Physiology **213**(3): 649-653.

Alcaraz, A., P. Hammerer, A. Tubaro, et al. (2009). "Is There Evidence of a Relationship between Benign Prostatic Hyperplasia and Prostate Cancer? Findings of a Literature Review." European Urology **55**(4): 864-875.

Alvarenga, A. W., C. M. Coutinho-Camillo, B. R. Rodrigues, et al. (2013). "A Comparison between Manual and Automated Evaluations of Tissue Microarray Patterns of Protein Expression." Journal of Histochemistry & Cytochemistry **61**(4): 272-282.

Ammirante, M., J.-L. Luo, S. Grivennikov, et al. (2010). "B-cell-derived lymphotoxin promotes castration-resistant prostate cancer." Nature **464**(7286): 302-305.

Andriole, G. L., E. D. Crawford, R. L. Grubb, et al. (2012). "Prostate Cancer Screening in the Randomized Prostate, Lung, Colorectal, and Ovarian Cancer Screening Trial: Mortality Results after 13 Years of Follow-up." Journal of the National Cancer Institute **104**(2): 125-132.

Andriole, G. L., E. D. Crawford, R. L. Grubb, III, et al. (2009). "Mortality Results from a Randomized Prostate-Cancer Screening Trial." N Engl J Med **360**(13): 1310-1319.

Ang, J., B. Fang, L. K. Ashman and A. G. Frauman (2010). "The migration and invasion of human prostate cancer cell lines involves CD151 expression." Oncology reports **24**(6): 1593-1597.

Ang, J., M. Lijovic, L. K. Ashman, et al. (2004). "CD151 Protein Expression Predicts the Clinical Outcome of Low-Grade Primary Prostate Cancer Better than Histologic Grading: A New Prognostic Indicator?" Cancer Epidemiol Biomarkers Prevention **13**(11): 1717-1721.

Ashman, L. K. (2013). "Renal disease as a potential compounding factor in carcinogenesis experiments with Cd151-null mice." Oncogene.

Ashman, L. K., G. W. Aylett, P. Mehrabani, A, et al. (1991). "The murine monoclonal antibody, 14A2.H1, identifies a novel platelet antigen." British Journal of Haematology **79**: 263-270.

Ashman, L. K., S. Fitter, P. M. Sincock, et al. (1997). CD151 (PETA-3) Workshop Summary Report. Leucocyte Typing VI. T. Kishimoto, H. Kikutani, A. von dem Borne et al. New York and London, Garland**:** 681-683.

Bahl, A., J. Bellmunt and S. Oudard (2012). "Practical aspects of metastatic castration-resistant prostate cancer management: patient case studies." BJU International **109**: 14-19.

Baleato, R., P. Guthrie, M.-C. Gubler, et al. (2008). "Deletion of CD151 results in a Strain dependent Glomerular Disease Due to Severe Alterations of the Glomerular Basement Membrane." The American Journal of Pathology **173**(4): 927-937.

Bandyopadhyay, S., R. Zhan, A. Chaudhuri, et al. (2006). "Interaction of KAI1 on tumor cells with DARC on vascular endothelium leads to metastasis suppression." Nature Medecine **12**: 933-938.

Barkin, J. (2008). "Management of benign prostatic hyperplasia by the primary care physician in the 21st century: the new paradigm." The Canadian Journal of Urology **15**: 21-30.

Barreiro, O., M. Zamai, M. Yanez-Mo, et al. (2008). "Endothelial adhesion receptors are recruited to adherent leukocytes by inclusion in preformed tetraspanin nanoplatforms." The Journal of Cellular Biology **183**(3): 527-542.

Beekman, K. W. and M. Hussain (2008). "Hormonal approaches in prostate cancer: Application in the contemporary prostate cancer patient." Urologic Oncology: Seminars and Original Investigations **28**: 415-419.

Bellmunt, J., G. Attard, A. Bahl, et al. (2012). "Advances in the management of high-risk localised and metastatic prostate cancer." BJU International **109**: 8-13.

Berditchevski, F. (2001). "Complexes of tetraspanins with integrins: more than meets the eye." Journal of Cell Science **114**: 4143-4151.

Berditchevski, F., E. Odintsova, S. Sawada and E. Gilbert (2002). "Expression of the Palmitoylation-deficient CD151 Weakens the Association of α3β1 Integrin with the Tetraspanin-enriched Microdomains and Affects Integrin-dependent Signaling." Journal of Biological Chemistry **277**(40): 36991-37000.

Berditchevski, F. and E. Rubinstein, Eds. (2013). Proteins and Cell Regulation. Tetraspanins. The Netherlands, Springer.

Berman-Booty, L. D., A. M. Sargeant, T. J. Rosol, et al. (2011). "A Review of the Existing Grading Schemes and a Proposal for a Modified Grading Scheme for Prostatic Lesions in TRAMP Mice." Toxicologic Pathology **40**(1): 5-17.

Bhatia-Gaur, R., A. A. Donjacour, P. J. Sciavolino, et al. (1999). "Roles for Nkx3.1 in prostate development and cancer." Genes & Development **13**(8): 966-977.

Billis, A., M. S. Guimaraes, L. L. L. Freitas, et al. (2008). "The Impact of the 2005 International Society of Urological Pathology Consensus Conference on Standard Gleason Grading of Prostatic Carcinoma in Needle Biopsies." The Journal of Urology **180**: 548-553.

Bono, A. (2004). "Overview of Current treatment Strategies in Prostate Cancer." European Urology Supplements **3**: 2-7.

Boucheix, C., P. Benoit, P. Frachet, et al. (1991). "Molecular cloning of the CD9 antigen. A new family of cell surface proteins." J. Biol. Chem. **266**(1): 117-122.

Boucheix, C., C. Nguyen-van, J. Perrot, et al. (1985). "Assignment to chromosome 12 of the gene coding for the human cell surface antigen CD9(p24) using the monoclonal antibody ALB6." Annales de génétique **28**(1): 19-24.

Boucheix, C. and E. Rubinstein (2001). "Tetraspanins." Cellular and Molecular Life Sciences **58**: 1189-1205.

Bradford, T. J., S. A. Tomlins, X. Wang and A. M. Chinnaiyan (2006). "Molecular markers of prostate cancer." Urologic Oncology: Seminars and Original Investigations **24**(6): 538-551.

Bredel, M., C. Bredel, D. Juric, et al. (2005). "Functional Network Analysis Reveals Extended Gliomagenesis Pathway Maps and Three Novel MYC-Interacting Genes in Human Gliomas." Cancer Research **65**(19): 8679-8689.

Cajot, J., I. Sordat, T. Silvestre and B. Sordat (1997). "Differential display cloning identifies motility-related protein (MRP1/CD9) as highly expressed in primary compared to metastatic human colon carcinoma cells." Cancer Research **57**: 2593-2597.

Calhoun, M. E., D. Kurth, A. L. Phinney, et al. (1998). "Hippocampal neuron and synaptophysin-positive bouton number in aging C57BL/6 mice." Neurobiology of Aging **19**(6): 599-606.

Charrin, S., S. Maine, M. Oualid, et al. (2002). "Differential stability of tetraspanin/tetraspanin interactions: role of palmitoylation." FEBS Letters **516**( ): 139-144.

Charrin, S., F. Naour, O. Silvie, et al. (2009). "Lateral organization of membrane proteins: tetraspanins spin their web." Biochemical Journal **420**(2): 133-154.

Chattopadhyay, N., Z. Wang, L. K. Ashman, et al. (2003). "α3β1 integrin–CD151, a component of the cadherin–catenin complex, regulates PTPμ expression and cell–cell adhesion." The Journal of Cell Biology **163**(6): 1351-1362.

Chiaverotti, T., S. S. Couto, A. Donjacour, et al. (2008). "Dissociation of Epithelial and Neuroendocrine Carcinoma Lineages in the Transgenic Adenocarcinoma of Mouse Prostate Model of Prostate Cancer." The American Journal of Pathology, **172**(1): 236-247.

Chien, C. W., S. C. Lin, Y. Y. Lai, et al. (2008). "Regulation of CD151 by Hypoxia Controls Cell Adhesion and Metastasis in Colorectal Cancer." Clin Cancer Res **14**(24): 8043-8051.

Christgen, M., H. Bruchhardt, M. Ballmaier, et al. (2008). "KAI1/CD82 is a novel target of estrogen receptor-mediated gene repression and downregulated in primary human breast cancer." International Journal of Cancer **123**(10): 2239-2246.

Chuan, Y., S. Pang, A. Bergh, et al. (2005). "Androgens induce CD-9 in human prostate tissue." International Journal of Andrology **28**(5): 291-296.

Claas, C., K. Herrmann, S. Matzku, et al. (1996). "Developmentally regulated expression of metastasis-associated antigens in the rat." Cell Growth Differ **7**(5): 663-678.

Class, C., J. Wahl, D. Orlicky, et al. (2005). "The tetraspanin D6.1A and its molecular partners on rat carcinoma cells." The Biochemical Journal **389**(1): 99-110.

Collins, A. T. and N. J. Maitland (2006). "Prostate cancer stem cells." European Journal of Cancer **42**(9): 1213-1218.

Copeland, B. T., M. J. Bowman and L. K. Ashman (2013a). "Genetic Ablation of the Tetraspanin CD151 Reduces Spontaneous Metastatic Spread of Prostate Cancer in the TRAMP Model." Molecular Cancer Research **11**(1): 95-105.

Copeland, B. T., M. J. Bowman, C. Boucheix and L. K. Ashman (2013b). "Knockout of the tetraspanin Cd9 in the TRAMP model of de novo prostate cancer increases spontaneous metastases in an organ-specific manner." International Journal of Cancer **133**(8): 1803-1812.

Cowin, A. J., D. Adams, S. M. Geary, et al. (2006). "Wound Healing Is Defective in Mice Lacking Tetraspanin CD151." J Invest Dermatol **126**(3): 680-689.

Damber, J.-E. and G. Aus (2008). "Prostate Cancer." The Lancet **371**: 1710-1721.

Darson, M., A. Pacelli, P. Roche, et al. (1997). "Human glandular kallikrein 2 (hK2) expression in prostatic intraepithelial neoplasia and adenocarcinoma: A novel prostate cancer marker." Urology **49**: 857-862.

Dayyani, F., G. E. Gallick, C. J. Logothetis and P. G. Corn (2011). "Novel Therapies for Metastatic Castrate-Resistant Prostate Cancer." Journal of the National Cancer Institute **103**(22): 1665-1675.

De Bruyne, E., T. J. Bos, K. Asosingh, et al. (2008). "Epigenetic Silencing of the Tetraspanin CD9 during Disease Progression in Multiple Myeloma Cells and Correlation with Survival." Clinical Cancer Research **14**(10): 2918-2926.

de la Taille, A., J. Jones and E. Klein (2008). "Open to debate. The motion: at least 18 cores are necessary to make a prostatic biopsy useful." European Urology **53**(3): 659-662.

De Nunzio, C., G. Kramer, M. Marberger, et al. (2011). "The Controversial Relationship Between Benign Prostatic Hyperplasia and Prostate Cancer: The Role of Inflammation." European Urology **60**(1): 106-117.

Delahunt, B., R. J. Miller, J. R. Srigley, et al. (2012). "Gleason grading: past, present and future." Histopathology **60**(1): 75-86.

Deng, X., Q. Li, J. Hoff, et al. (2012). "Integrin-Associated CD151 Drives ErbB2-Evoked Mammary Tumor Onset and Metastasis." Oncogene **14**(8): 678–689.

Detchokul, S. and A. G. Frauman (2011). "Recent developments in prostate cancer biomarker research: therapeutic implications." British Journal of Clinical Pharmacology **71**(2): 157-174.

Detchokul, S., E. D. Williams, M. W. Parker and A. G. Frauman (2013). "Tetraspanins as regulators of the tumour microenvironment: implications for metastasis and therapeutic strategies." British Journal of Pharmacology: DOI: 10.1111/bph.12260.

Devbhandari, R. P., G.-M. Shi, A.-W. Ke, et al. (2011). "Profiling of the Tetraspanin CD151 Web and Conspiracy of CD151/Integrin Î²1 Complex in the Progression of Hepatocellular Carcinoma." PLoS ONE **6**(9): e24901.

Dong, J.-T., P. W. Lamb, C. W. Rinker-Schaeffer, et al. (1994). "KAII, a Metastasis Suppressor Gene for Prostate Cancer on Human Chromosome 1 1 p1 1.2."

Eeles, R. A., A. A. A. Olama, S. Benlloch, et al. (2013). "Identification of 23 new prostate cancer susceptibility loci using the iCOGS custom genotyping array." Nat Genet **45**(4): 385-391.

Engel, P. and T. F. Tedder (1994). "New CD from the B cell section of the Fifth International Workshop on Human Leukocyte Differentiation Antigens." Leukemia and Lymphoma **13**(Supplement 1): 61-64.

Epstein, J., W. J. Allsbrook, M. Amin and L. Egevad (2005). "The 2005 International Society of Urological Pathology (ISUP) Consensus Conference on Gleason Grading of Prostatic Carcinoma." American Journal of Surgical Pathology **29**.

Epstein, J. I. (2010). "An Update of the Gleason Grading System." The Journal of Urology **183**(2): 433-440.

Erovic, B. M., J. Pammer, D. Hollemann, et al. (2003). "Motility-related protein-1/CD9 expression in head and neck squamous cell carcinoma." Head & Neck **25**(10): 848-857.

Fekete, T., E. Raso, I. Pete, et al. (2012). "Meta-analysis of gene expression profiles associated with histological classification and survival in 829 ovarian cancer samples." International Journal of Cancer: n/a-n/a.

Fitter, S., P. M. Sincock, C. N. Jolliffe and L. K. Ashman (1999). "Transmembrane 4 superfamily protein CD151 (PETA-3) associates with beta 1 and alpha IIb beta 3 integrins in haemopoietic cell lines and modulates cell-cell adhesion." Biochem. J. **338**(1): 61-70.

Fitter, S., T. Tetaz, M. Berndt and L. Ashman (1995). "Molecular cloning of cDNA encoding a novel platelet-endothelial cell tetra-span antigen, PETA-3." Blood **86**(4): 1348-1355.

Fitter, S., T. J. Tetaz, M. C. Berndt and L. K. Ashman (1995). "Molecular cloning of cDNA encoding a novel platelet-endothelial cell tetra-span antigen, PETA-3." Blood **86**(4): 1348-1355.

Flint, M., T. von Hahn, J. Zhang, et al. (2006). "Diverse CD81 proteins support hepatitis C virus infection." Journal of Virology **80**: 11331-11342.

García-López, M., O. Barreiro, A. García-Díez, et al. (2005). "Role of tetraspanins CD9 and CD151 in primary melanocyte motility." The Journal of Investigative Dermatology **125**(5): 1001-1009.

Gaugitsch, H. W., E. Hofer, N. E. Huber, et al. (1991). "A new superfamily of lymphoid and melanoma cell proteins with extensive homology to Schistosoma mansoni antigen Sm23." European Journal of Immunology **21**(2): 377-383.

Gay, L. J. and B. Felding-Habermann (2011). "Contribution of platelets to tumour metastasis." Nature Reviews Cancer **11**(2): 123-134.

Geary, S. M., A. C. Cambareri, P. M. Sincock, et al. (2001). "Differential tissue expression of epitopes of the tetraspanin CD151 recognised by monoclonal antibodies." Tissue Antigens **58**: 141-153.

Geary, S. M., A. J. Cowin, B. Copeland, et al. (2008). "The role of the tetraspanin CD151 in primary keratinocyte and fibroblast functions: Implications for wound healing." Experimental Cell Research **314**(11-12): 2165-2175.

Gelmann, E. (2008). "Complexities of prostate-cancer risk." New England Journal of Medicine **358**: 961.

George, D. and J. Moul (2012). "Emerging TreatmentOptions for Patients With Castration-Resistant Prostate Cancer." The Prostate **72**: 338-349.

Gesierich, S., C. Paret, D. Hildebrand, et al. (2005). "Colocalization of the Tetraspanins, CO-029 and CD151, with Integrins in Human Pancreatic Adenocarcinoma: Impact on Cell Motility." Clinical Cancer Research **11**(8): 2840-2852.

Giles, A. (2006). "PCFA policy statement for PSA/DRE testing for early detection of prostate cancer ", 2012, from http://www.prostate.org.au.

Gillatt, D., L. Klotz, C. Lawton, et al. (2007). "Localised and Locally Advanced Prostate Cancer: Who to Treat and How?" European Urology Supplements **6**: 334-343.

Gingrich, J., R. Barrios, B. Foster and N. Greenberg (1999). "Pathologic progression of autochthonous prostate cancer in the TRAMP model." Prostate Cancer and Prostatic Disorders **2**: 70-77.

Gingrich, J. R., R. J. Barrios, B. Foster and N. M. Greenberg (1999). "Pathologic progression of autochthonous prostate cancer in the TRAMP model." **2**(2): 70-75.

Gingrich, J. R., R. J. Barrios, R. A. Morton, et al. (1996). "Metastatic Prostate Cancer in a Transgenic Mouse." Cancer Research **56**(18): 4096-4102.

Gittes, R. F. (1991). "Carcinoma of the Prostate." New England Journal of Medecine **324**: 236-245.

Gleason, D. and G. Mellinger (1974). "Prediction of prognosis for prostatic adenocarcinoma by combined histological grading and clinical staging." The Journal of Urology **111**(58).

Gnanapragasam, V. J., M. D. Mason, G. L. Shaw and D. E. Neal (2012). "The role of surgery in high-risk localised prostate cancer." BJU International **109**(5): 648-658.

Goel, H. L., N. Alam, I. N. S. Johnson and L. R. Languino (2009). "Integrin signaling aberrations in prostate cancer." American Journal of Translational Reserach **1**(3): 211-220.

Goel, H. L., J. Li, S. Kogan and L. R. Languino (2008). "Integrins in prostate cancer progression." Endocr Relat Cancer **15**(3): 657-664.

Gordon-Alonso, M., M. Yañez-Mó, O. Barreiro, et al. (2006). "Tetraspanins CD9 and CD81 modulate HIV-1-induced membrane fusion." Journal of Immunology **177**: 5129-5137.

Greco, C., M.-P. Bralet, N. Ailane, et al. (2010). "E-Cadherin/p120-Catenin and Tetraspanin Co-029 Cooperate for Cell Motility Control in Human Colon Carcinoma." Cancer Research **70**(19): 7674-7683.

Greenberg, N. M., F. DeMayo, M. J. Finegold, et al. (1995). "Prostate cancer in a transgenic mouse." Proceedings of the National Academy of Sciences of the United States of America **92**(8): 3439-3443.

Greenberg, N. M., F. J. DeMayo, P. C. Sheppard, et al. (1994). "The Rat Probasin Gene Promoter Directs Hormonally and Developmentally Regulated Expression of a Heterologous Gene Specifically to the Prostate in Transgenic Mice." Molecular Endocrinology **8**(2): 230-239.

Han, K., D. Seligson, X. Liu, et al. (2004). "Prostate stem cell antigen expression is associated with Gleason score, seminal vesicle invasion and capsular invasion in prostate cancer." Journal of Urology **171**: 1117-1121.

Hao, S., Z. Ye, F. Li, et al. (2006). "Epigenetic transfer of metastatic activity by uptake of highly metastatic B16 melanoma cell-released exosomes." Experimental Oncology **28**(2): 126-131.

Harris, R. and K. N. Lohr (2002). "Screening for Prostate Cancer: An Update of the Evidence for the U.S. Preventive Services Task Force." Ann Intern Med **137**(11): 917-929.

Hasegawa, H., Y. Utsunomiya, K. Kishimoto, et al. (1996). "SFA-1, a novel cellular gene induced by human T-cell leukemia virus type 1, is a member of the transmembrane 4 superfamily." J. Virol. **70**(5): 3258-3263.

Hasegawa, M., M. Furuya, Y. Kasuya, et al. (2007). "CD151 dynamics in carcinoma-stroma interaction: integrin expression, adhesion strength and proteolytic activity." Lab Invest **87**(9): 882-892.

Hashida, H., A. Takabayashi, T. Tokuhara, et al. (2003). "Clinical significance of transmembrane 4 superfamily in colon cancer." British Journal of Cancer **89**: 158-167.

Hashida, H., A. Takabayashi, T. Tokuhara, et al. (2002). "Integrin a3 expression as a prognostic factor in colon cancer:association with MRP-1/CD9 and KAI1/CD82." International Journal of Cancer **97**: 518-525.

Hemler, M. E. (2003). "Tetraspanin proteins mediate cellular penetration, invasion and fusion events and define a novel type of membrane microdomain." Annual Review of Cell and Developmental Biology **19**(1): 397-422.

Hemler, M. E. (2005). "Tetraspanin functions and associated microdomains." Nature Reviews Molecular Cell Biology **6**(10): 801-811.

Hemler, M. E. (2008). "Targeting of tetraspanin proteins - potential benefits and strategies." Nat Rev Drug Discov **7**(9): 747-758.

Hensley, P. J. and N. Kyprianou (2011). "Modeling Prostate Cancer in Mice: Limitations and Opportunities." J Androl **33**(2): 133-134.

Higashiyama, M., O. Doi, K. Kodama, et al. (1997). "Immunohistochemically detected expression of motility-related protein-1 (MRP-1/CD9) in lung adenocarcinoma and its relation to prognosis." International Journal of Cancer **74**(2): 205-211.

Higashiyama, M., T. Taki, Y. Ieki, et al. (1995). "Reduced Motility Related Protein-1 (MRP-1/CD9) Gene Expression as a Factor of Poor Prognosis in Non-Small Cell Lung Cancer." Cancer Res **55**(24): 6040-6044.

Hirano, C., M. Nagata, A. A. Noman, et al. (2009). "Tetraspanin gene expression levels as potential biomarkers for malignancy of gingival squamous cell carcinoma." International Journal of Cancer **124**(12): 2911-2916.

Hong, I.-K., Y.-J. Jin, H.-J. Byun, et al. (2006). "Homophilic Interactions of Tetraspanin CD151 Up-regulate Motility and Matrix Metalloproteinase-9 Expression

of Human Melanoma Cells through Adhesion-dependent c-Jun Activation Signaling Pathways." Journal of Biological Chemistry **281**(34): 24279-24292.

Hood, J. and D. Cheresh (2002). "Role of integrins in cell invasion and migration." Nature Review Cancer **2**: 91-100.

Hori, H., S. Yano, K. Koufuji, et al. (2004). "CD9 expression in gastric cancer and its significance." Journal of Surgical Research **117**(2): 208-215.

Hsieh, C.-L., Z. Xie, J. Yu, et al. (2007). "Non-invasive bioluminescent detection of prostate cancer growth and metastasis in a bigenic transgenic mouse model." The Prostate **67**(7): 685-691.

Hsu, C., S. Joniau, R. Oyen, et al. (2007). "Outcome of surgery for clinical unilateral T3a prostate cancer: a single institution experience." European Urology **51**: 121-128.

Huang, C.-l., N. Kohno, E. Ogawa, et al. (1998). "Correlation of Reduction in MRP-1/CD9 and KAI1/CD82 Expression with Recurrences in Breast Cancer Patients." The American Journal of Pathology **153**(3): 973-983.

Huang, C.-l., D. Liu, D. Masuya, et al. (2004). "MRP-1//CD9 gene transduction downregulates Wnt signal pathways." Oncogene **23**(45): 7475-7483.

Huang, H., J. Groth, K. Sossey-Alaoui, et al. (2005). "Aberrant Expression of Novel and Previously Described Cell Membrane Markers in Human Breast Cancer Cell Lines and Tumors." Clinical Cancer Research **11**(12): 4357-4364.

Huang, X. Y., A. W. Ke, G. M. Shi, et al. (2010). "Overexpression of CD151 as an adverse marker for intrahepatic cholangiocarcinoma patients." Cancer **116**(23): 5440-5451.

Huggins, C. and C. Hodges (1941). "Studies in Prostatic Cancer. 1. The effect of castration, of estrogen and of androgen injection on serum phosphatases in metastatic carcinoma of the prostate." Cancer Research **1**: 293-297.

Humphrey, P. (2003). Grading of prostatic carcinoma. Prostate Pathology. Chicago, ASCP Press**:** 338-374.

Humphrey, P. A. (2004). "Gleason grading and prognostic factors in carcinoma of the prostate." Modern Pathology **17**: 292-306.

Huss, W. J., D. R. Grayy, K. Tavakoli, et al. (2007). "Origin of Androgen-Insensitive Poorly Differentiated Tumors in the Transgenic Adenocarcinoma of Mouse Prostate Model." Neoplasia **9**(11): 938–950.

Hynes, R. (2002). "Integrins: bidirectional, allosteric signaling machines." Cell **110**: 673-687.

Ikeyama, S., M. Koyama, M. Yamaoko, et al. (1993). "Suppression of cell motility and metastasis by transfection with human motility-related protein (MRP-1/CD9) DNA." The Journal of Experimental Medicine **177**(5): 1231-1237.

Israels, S. J. and M. J. McMillian-Ward (2007). "Platelet tetraspanin complexes and their association with lipid rafts." Thrombosis and Haemostasis **98**(5): 1081-1087.

Iwamoto, R. (1994). "Heparin-binding EGF-like growth factor, which acts as a diphtheria toxin receptor, forms a complex with membrane protein DRAP27/CD9, which upregulates functional receptors and diphtheria toxin sensitivity." EMBO J. **13**: 2322-2330.

Janes, S. and F. Watt (2006). "New roles for integrins in squamous-cell carcinoma." Nature Review Cancer **6**: 175-183.

Jeet, V., K. Ow, E. Doherty, et al. (2008). "Broadening of Transgenic Adenocarcinoma of the Mouse Prostate (TRAMP) Model to Represent Late Stage Androgen Depletion Independent Cancer." The Prostate **68**(5): 548-562.

Jeet, V., P. Russell and A. Khatri (2010). "Modeling prostate cancer: a perspective on transgenic mouse models." Cancer and Metastasis Reviews **29**(1): 123-142.

Jemal, A., R. Siegel, E. Ward, et al. (2008). "Cancer Statistics, 2008." A Cancer Journal for Clinicians **58**(2): 71-96.

Jiang, Z., C. Wu, B. Woda, et al. (2004). "Alpha-methylacyl-CoA racemase:A multi-institutional study of a new prostate cancer marker." Histopathology **45**: 218 -225.

Jin, J.-K., F. Dayyani and G. E. Gallick (2011). "Steps in prostate cancer progression that lead to bone metastasis." International Journal of Cancer **128**(11): 2545-2561.

Johnson, J. L., N. Winterwood, K. A. DeMali and C. S. Stipp (2009). "Tetraspanin CD151 regulates RhoA activation and the dynamic stability of carcinoma cell-cell contacts." Journal of Cell Science **122**(13): 2263-2273.

Johnstone, R. M., M. Adam, J. R. Hammond, et al. (1987). "Vesicle formation during reticulocyte maturation. Association of plasma membrane activities with released vesicles (exosomes)." J. Biol. Chem. **262**(19): 9412-9420.

Jones, M. J. and K. S. Koeneman (2008). "Local-regional prostate cancer." Urologic Oncology: Seminars and Original Investigations **26**(5): 516-521.

Jung, T., D. Castellana, P. Klingbeil, et al. (2006). "CD44v6 dependence of premetastatic niche preparation by exosomes." Neoplasia **11**(10): 1093-1105.

Kagan, A., S. Feld, J. Chemke and Y. Bar-Khayim (1988). "Occurrence of hereditary nephritis, pretibial epidermolysis bullosa and beta-thalassemia minor in two siblings with end-stage renal disease." Nephron **49**: 331-332.

Kamisasanuki, T., S. Tokushige, H. Terasaki, et al. (2011). "Targeting CD9 produces stimulus-independent antiangiogenic effects predominantly in activated endothelial cells during angiogenesis: A novel antiangiogenic therapy." Biochemical and Biophysical Research Communications **413**(1): 128-135.

Kaplan-Lefko, P. J., T. M. Chen, M. M. Ittmann, et al. (2003). "Pathobiology of autochthonous prostate cancer in a pre-clinical transgenic mouse model." The Prostate **55**(3): 219-237.

Karamatic-Crew, V., N. Burton, A. Kagan, et al. (2004). "CD151, the first member of the tetraspanin (TM4) superfamily detected on erythrocytes, is essential for the correct assembly of human basement membranes in kidney and skin." Blood **104**: 2217-2223.

Kasper, S., P. Sheppard, Y. Yan, et al. (1998). "Development, progression and androgen-dependence of prostate tumours in probasin-large T antigen transgenic mice: a model for prostate cancer." Laboratory Investigation **78**: 1-15.

Kawana, Y., A. Komiya, T. Ueda, et al. (1997). "Location of KAI1 on the short arm of human chromosome 11 and frequency of allelic loss in advanced human prostate cancer." The Prostate **32**(3): 205-213.

Kim, M. J., R. Bhatia-Gaur, W. A. Banach-Petrosky, et al. (2002). "Nkx3.1 Mutant Mice Recapitulate Early Stages of Prostate Carcinogenesis." Cancer Research **62**(11): 2999-3004.

King, D. L. and G. W. Arendash (2002). "Maintained synaptophysin immunoreactivity in Tg2576 transgenic mice during aging: correlations with cognitive impairment." Brain Research **926**(1-2): 58-68.

King, T. E., S. C. Pawar, L. Majuta, et al. (2008). "The Role of Alpha 6 Integrin in Prostate Cancer Migration and Bone Pain in a Novel Xenograft Model." PLoS ONE **3**(10): e3535.

Kitadokoro, K., D. Bordo, G. Galli, et al. (2001). "CD81 extracellular domain 3D structure: insight into the tetraspanin superfamily structural motifs." EMBO J **20**(1/2): 12-18.

Klezovitch, O., J. Chevillet, J. Mirosevich, et al. (2004). "Hepsin promotes prostate cancer progression and metastasis." Cancer Cell **6**(2): 185-195.

Klingbeil, P., R. Marhaba, T. Jung, et al. (2009). "CD44 Variant Isoforms Promote Metastasis Formation by a Tumor Cell-Matrix Cross-talk That Supports Adhesion and Apoptosis Resistance." Molecular Cancer Research **7**(2): 168-179.

Kohno, M., H. Hasegawa, M. Miyake, et al. (2002). "CD151 enhances cell motility and metastasis of cancer cells in the presence of focal adhesion kinase." International Journal of Cancer **97**(3): 336-343.

Kote-Jarai, Z., A. A. A. Olama, G. G. Giles, et al. (2011). "Seven prostate cancer susceptibility loci identified by a multi-stage genome-wide association study." Nat Genet **43**(8): 785-791.

Kotha, J., C. Longhurst, W. Appling and L. K. Jennings (2008). "Tetraspanin CD9 regulates β1 integrin activation and enhances cell motility to fibronectin via a PI-3 kinase-dependent pathway." Experimental Cell Research **314**(8): 1811-1822.

Kovalenko, O., X. Yang, T. V. Kolesnikova and M. E. Hemler (2004). "Evidence for specific tetraspanin homodimers: inhibition of palmitoylation makes cysteine residues available for cross-linking." Journal of Biological Chemistry **377**: 407-417.

Kubista, B., B. M. Erovic, H. Klinger, et al. (2004). "CD9 expression is not a prognostic factor in human osteosarcoma." Cancer Letters **209**(1): 105-110.

Kundra, V., P. M. Silverman, S. F. Matin and H. Choi (2007). "Imaging in Oncology from The University of Texas M. D. Anderson Cancer Center: Diagnosis, Staging, and Surveillance of Prostate Cancer." Am. J. Roentgenol. **189**(4): 830-844.

Kusukawa, J., F. Ryu, T. Kameyama and E. Mekada (2001). "Reduced expression of CD9 in oral squamous cell carcinoma: CD9 expression inversely related to high prevalence of lymph node metastasis." Journal of Oral Pathology & Medicine **30**(2): 73-79.

Kwon, M. J., S. Park, J. Y. Choi, et al. (2012). "Clinical significance of CD151 overexpression in subtypes of invasive breast cancer." Br J Cancer **106**(5): 923-930.

Kwon, M. J., J. Seo, Y. J. Kim, et al. (2013). "Prognostic significance of CD151 overexpression in non-small cell lung cancer." Lung cancer.

Kyprianou, N. and J. Isaacs (1988). "Activation of programmed cell death in the rat ventral prostate after castration." Endocrinology **122**(2): 552-562.

Lammerding, J., A. R. Kazarov, H. Huang, et al. (2003). "Tetraspanin CD151 regulates α6β1 integrin adhesion strengthening." Proceedings of the National Academy of Sciences **100**(13): 7616-7621.

Langley, R. R. and I. J. Fidler (2011). "The seed and soil hypothesis revisited - the role of tumor-stroma interactions in metastasis to different organs." International Journal of Cancer **128**(11): 2527-2535.

Lanza, F., D. Wolf, C. F. Fox, et al. (1991). "cDNA cloning and expression of platelet p24/CD9. Evidence for a new family of multiple membrane-spanning proteins." J. Biol. Chem. **266**(16): 10638-10645.

Lau, L.-M., J. L. Wee, M. D. Wright, et al. (2004). "The tetraspanin superfamily member CD151 regulates outside-in integrin alphaIIb beta3 signaling and platelet function." Blood **104**(8): 2368-2375.

Laurinavicius, A., A. Laurinaviciene, V. Ostapenko, et al. (2012). "Immunohistochemistry profiles of breast ductal carcinoma: factor analysis of digital image analysis data." Diagnostic Pathology **7**: 27-43.

Lazo, P. (2007). "Functional implications of tetraspanin proteins in cancer biology." Cancer Science **98**(11): 1666-1677.

Le Naour, F., M. Andre, C. Greco, et al. (2006). "Profiling of the tetraspanin web of human colon cancer cells." Molecular and Cellular Proteomics **5**: 845-857.

Le Naour, F., E. Rubinstein, C. Jasmin, et al. (2000). "Severely reduced female fertility in CD9-deficient mice." Science **287**: 319-321.

Levy, S. and T. Shoham (2005). "Protein-Protein Interactions in the Tetraspanin Web." Physiology **20**(4): 218-224.

Li, Q., X. H. Yang, F. Xu, et al. (2012). "Tetraspanin CD151 plays a key role in skin squamous cell carcinoma." Oncogene.

Lilja, H., D. Ulmert and A. J. Vickers (2008). "Prostate-specific antigen and prostate cancer: prediction, detection and monitoring." Nat Rev Cancer **8**(4): 268-278.

Lin, K., R. Lipsitz, T. Miller and S. Janakiraman. (2008, August 5, 2008). "Screening for Prostate Cancer: U.S. Preventive Services Task Force Recommendation Statement." Ann Intern Med Retrieved 3, 149, from http://www.annals.org/cgi/content/abstract/149/3/185

Linton, K. D. and F. C. Hamdy (2003). "Early Diagnosis and Surgical Management of Prostate Cancer." Cancer Treatment Reviews **29**: 151-160.

Liu, L., B. He, W. M. Liu, et al. (2007). "Tetraspanin CD151 Promotes Cell Migration by Regulating Integrin Trafficking." Journal of Biological Chemistry **282**(43): 31631-31642.

Liu, W. M. and X. A. Zhang (2006). "KAI1/CD82, a tumor metastasis suppressor." Cancer Letters **240**(2): 183-194.

Longhurst, C. M., J. D. Jacobs, M. M. White, et al. (2002). "Chinese Hamster Ovary Cell Motility to Fibronectin Is Modulated by the Second Extracellular Loop of CD9:

IDENTIFICATION OF A PUTATIVE FIBRONECTIN BINDING SITE." Journal of Biological Chemistry **277**(36): 32445-32452.

Longo, N., M. a. Yáñez-Mó, M. a. Mittelbrunn, et al. (2001). "Regulatory role of tetraspanin CD9 in tumor–endothelial cell interaction during transendothelial invasion of melanoma cells." Blood **98**(13): 3717-3726.

Lose, F., M. Lawrence, S. Srinivasan, et al. (2012). "The kallikrein 14 gene is down-regulated by androgen receptor signalling and harbours genetic variation that is associated with prostate tumour aggressiveness." Biological Chemistry **393**(5): 403-412.

Luo, J.-L., W. Tan, J. M. Ricono, et al. (2007). "Nuclear cytokine-activated IKK[agr] controls prostate cancer metastasis by repressing Maspin." Nature **446**(7136): 690-694.

Magklara, A., A. Scorilas, W. J. Catalona and E. P. Diamandis (1999). "The Combination of Human Glandular Kallikrein and Free Prostate-specific Antigen (PSA) Enhances Discrimination Between Prostate Cancer and Benign Prostatic Hyperplasia in Patients with Moderately Increased Total PSA." Clin Chem **45**(11): 1960-1966.

Maitland, N. J. and A. T. Collins (2008). "Prostate Cancer Stem Cells: A New Target for Therapy." J Clin Oncol **26**(17): 2862-2870.

Malik, F., A. J. Sanders and W. G. Jiang (2009). "KAI-1/CD82, The molecule and clinical implication in cancer and cancer metastasis." Histology and Histopathology **24**: 519-530.

Martınez-Pineiro, L. (2008). "Does Neoadjuvant and Adjuvant Treatment Improve Outcome in Localised Prostatic Cancer?" European Urology Supplements **7**: 406-409.

Mazzola, C., T. Ghoneim and S. F. Shariat (2011). "Emerging biomarkers for the diagnosis, staging and prognosis of prostate cancer." Progressive Urology **21**(1): 1-10.

McCabe, K. L. and M. Bronner-Fraser (2011). "Tetraspanin CD151 is required for maintenance of trigeminal placode identity." Journal of Neurochemistry **117**(2): 221-230.

McLeod, D. G., P. Iversen, W. A. See, et al. (2006). "Bicalutamide 150 mg plus standard care vs standard care alone for early prostate cancer." BJU International **97**(2): 247-254.

McNeal, J. (1988). "Normal anatomy of the prostate and changes in benign prostatic hypertrophy and carcinoma." Seminars in Ultrasound, CT and MR **9**(5): 329-334.

McNeal, J. (1997). Prostate. Histology for Pathologists. S. Sternberg. Philadelphia, Lippincott-Raven**:** 997-1013.

Mhawech, P., P. Dulguerov, E. Tschanz, et al. (2004). "Motility-related protein-1 (MRP-1//CD9) expression can predict disease-free survival in patients with squamous cell carcinoma of the head and neck." Br J Cancer **90**(2): 471-475.

Mhawech, P., F. Herrmann, M. Coassin, et al. (2003). "Motility-related protein 1 (MRP-1/CD9) expression in urothelial bladder carcinoma and its relation to tumor recurrence and progression." Cancer **98**(8): 1649-1657.

Miller, R. L. (2011). "Transgenic mice: beyond the knockout." American Journal of Physiology - Renal Physiology **300**(2): F291-F300.

Miranti, C. K. (2009). "Controlling cell surface dynamics and signaling: How CD82/KAI1 suppresses metastasis." Cellular Signalling **21**(2): 196-211.

Miyake, M., H. Inufusa, M. Adachi, et al. (2000). "Suppression of pulmonary metastasis using adenovirally motility related protein-1 (MRP-1/CD9) gene delivery." Oncogene **19**(46): 5221-5226.

Miyake, M., M. Kovama, M. Seno and S. Ikeyama (1991). "Identification of the motilityrelated protein (MRP-1), recognized by monoclonal antibody M31-15. which inhibits cell motilily." Journal of Experimental Medicine **174**: 1347-1354.

Miyake, M., K. Nakano, Y. Ieki, et al. (1995). "Motility Related Protein 1 (MRP-1/CD9) Expression: Inverse Correlation with Metastases in Breast Cancer." Cancer Res **55**(18): 4127-4131.

Miyake, M., K. Nakano, S. Itoi, et al. (1996). "Motility related protein-1 (MRP-1/CD9) reduction as a factor of poor prognosis in breast cancer." Cancer Research **56**: 1244-12249.

Mollinedo, F., G. Fontan, I. Barasoain and P. Lazo (1997). "Recurrent infectious diseases in human CD53 deficiency." Clinical and Diagnostic Laboratory Immunology **4**: 229-231.

Mori, M., K. Mimori, T. Shiraishi, et al. (1998). "Motility related protein 1 (MRP1/CD9) expression in colon cancer." Clinical Cancer Research **4**(6): 1507-1510.

Mosig, R., L. Lin, E. Senturk, et al. (2012). "Application of RNA-Seq transcriptome analysis: CD151 is an Invasion/Migration target in all stages of epithelial ovarian cancer." Journal of Ovarian Research **5**(1): 4.

Munshi, H. G. and M. S. Stack (2006). "Reciprocal interactions between adhesion receptor signaling and MMP regulation
" Cancer Metastasis Reviews **25**: 45-56.

Murayama, Y., Y. Shinomura, K. Oritani, et al. (2008). "The tetraspanin CD9 modulates epidermal growth factor receptor signaling in cancer cells." Journal of Cellular Physiology **216**(1): 135-143.

Murphy, G., G. Kenny, H. Ragde, et al. (1998). "Measurement of serum prostate-specific membrane antigen, a new prognostic marker for prostate cancer." Urology **51**: 89 -97.

N.H.S. (2009). "National Health Services Screening Programmes." from www,cancerscreening.nhs.uk/prostate/index.html

Nakamoto, T., Y. Murayama, K. Oritani, et al. (2009). "A novel therapeutic strategy with anti-CD9 antibody in gastric cancers." Journal of Gastroenterology **44**(9): 889-896.

Nakazawa, Y., S. Sato, M. Naito, et al. (2008). "Tetraspanin family member CD9 inhibits Aggrus/podoplanin-induced platelet aggregation and suppresses pulmonary metastasis." Blood **112**(5): 1730-1739.

Nelson, E., A. Cambio, J. Yang, et al. (2007). "Clinical implications of neuroendocrine differentiation in prostate cancer." Prostate Cancer and Prostatic Diseases **10**(1): 6-14.

Neltner, J. H., E. L. Abner, F. A. Schmitt, et al. (2012). "Digital Pathology and Image Analysis for Robust High-Throughput Quantitative Assessment of Alzheimer Disease Neuropathologic Changes." Journal of Neuropathology & Experimental Neurology **71**(12): 1075-1085 1010.1097/NEN.1070b1013e3182768de3182764.

Nguewa, P. A. and V. Calve (2010). "Use of transgenic mice as models for prostate cancer chemoprevention." Current Molecular Medicine **10**(8): 705-718.

NHMRC (2002). Clinical Practice Guidelines: Evidence-based information and recommendations for the management of localised prostate cancer. A report of the Australian Cancer Network Working Party on Management of Localised Prostate Cancer.

Novitskaya, V., H. Romanska, M. Dawoud, et al. (2010). "Tetraspanin CD151 Regulates Growth of Mammary Epithelial Cells in Three-Dimensional Extracellular Matrix: Implication for Mammary Ductal Carcinoma In situ." Cancer Research **70**(11): 4698-4708.

O'Connor, C. G. and L. K. Ashman (1982). "Application of the nitrocellulose transfer technique and alkaline phosphatase conjugated anti-immunoglobulin for determination of the specificity of monoclonal antibodies to protein mixtures." Journal of Immunological Methods **54**(2): 267-271.

O'Rourke, M. E. (2011). "The Prostate-Specific Antigen Screening Conundrum: Examining the Evidence." Seminars in Oncology Nursing **27**(4): 251-259.

Odintsova, E., T. Sugiura and F. Berditchevski (2000). "Attenuation of EGF receptor signaling by a metastasis suppressor tetraspanin KAI-1/CD82." Curr Biol **10**: 1009-1012.

Oren, R., S. Takahashi, C. Doss, et al. (1990). "TAPA-1. the target of an antiproliferative antibody, defines a new family of transmembrane proteins." Molecular and Cellular Biology **10**: 4007-4015.

Orlowski, E., R. Chand, J. Yip, et al. (2009). "Platelet tetraspanin superfamily member, CD151 is required for regulation of thrombus growth and stability in vivo." Journal of Thrombosis and Haemostasis **7**: 2074-2084.

Osanto, S. and H. Van Poppel (2012). " Emerging novel therapies for advanced prostate cancer " Therapeutic Advances in Urology **4**(1): 3-12.

Paget, S. (1989). "The distribution of secondary growths in cancer of the breast." Cancer Metastasis Reviews **8**(2): 98-101.

Peng, W. M., C. F. Yu, W. Kolanus, et al. (2010). "Tetraspanins CD9 and CD81 are molecular partners of trimeric FcεRI on human antigen-presenting cells." Allergy **66**(5): 605-611.

Petrylak, D., C. Tangen and M. Hussain (2004). "Docetaxel and estramustine compared with mitoxantrone and prednisone for advanced refractory prostate cancer." New England Journal of Medecine **351**: 1513-1520.

Powner, D., P. Kopp, S. Monkley, et al. (2011). "Tetraspanin CD9 in cell migration." Biochemical Society Transactions **39**(2): 563-567.

Protzel, C., C. Kakies, B. Kleist, et al. (2008). "Down-regulation of the metastasis suppressor protein KAI1/CD82 correlates with occurrence of metastasis, prognosis and presence of HPV DNA in human penile squamous cell carcinoma." Virchows Archiv **452**(4): 369-375.

Ramakrishnan, K. and R. C. Salinas (2010). "Prostatitis: Acute and Chronic." Primary Care: Clinics in Office Practice **37**(3): 547-563.

Rana, S., S. Yue, D. Stadel and M. Zöller (2012). "Toward tailored exosomes: The exosomal tetraspanin web contributes to target cell selection." The International Journal of Biochemistry & Cell Biology **44**(9): 1574-1584.

Risbridger, G. P., I. D. Davis, S. N. Birrell and W. D. Tilley (2010). "Breast and prostate cancer: more similar than different." Nat Rev Cancer **10**(3): 205-212.

Risbridger, G. P. and R. A. Taylor (2011). "The complexities of identifying a cell of origin for human prostate cancer." Asian J Androl **13**(1): 118-119.

Romanska, H. M. and F. Berditchevski (2011). "Tetraspanins in human epithelial malignancies." The Journal of Pathology **223**(1): 4-14.

Roobol, M. J., F. H. Schroder, P. van Leeuwen, et al. (2010). "Performance of the Prostate Cancer Antigen 3 (PCA3) Gene and Prostate-Specific Antigen in Prescreened Men: Exploring the Value of PCA3 for a First-line Diagnostic Test." European Urology **58**(4): 475-481.

Ru, P., R. Steele, P. V. Nerurkar, et al. (2011). "Bitter Melon Extract Impairs Prostate Cancer Cell-Cycle Progression and Delays Prostatic Intraepithelial Neoplasia in TRAMP Model." Cancer Prevention Research **4**(12): 2122-2130.

Rubin, M. A. (2008). "Targeted therapy of cancer: new roles for pathologists in prostate cancer." Mod Pathol **21**(S2): S44-S55.

Rubinstein, E. (2011). "The complexity of tetraspanins." Biochemical Society Transactions **39**(2): 501-505.

Rubinstein, E., F. Le Naour, C. Lagaudrière-Gesbert, et al. (1996). "CD9, CD63, CD81, and CD82 are components of a surface tetraspan network connected to HLA-DR and VLA integrins." European Journal of Immunology **26**(11): 2657-2665.

Rubinstein, E., A. Ziyyat, M. Prenant, et al. (2006). "Reduced fertility of female mice lacking CD81." Developmental Biology **290**: 351-358.

Ruijter, E., C. van de Kaa and J. Schalken (1996). "Histological grade heterogeneity in multifocal prostate cancer; Biological and clinical implications." Journal of Pathology **180**: 295-299.

Rundhaug, J. E. (2003). "Matrix Metalloproteinases, Angiogenesis, and Cancer." Clinical Cancer Research **9**(2): 551-554.

Sachs, N., M. Kreft, M. A. van den Bergh Weerman, et al. (2006). "Kidney failure in mice lacking the tetraspanin CD151." J. Cell Biol. **175**(1): 33-39.

Sachs, N., P. Secades, L. van Hulst, et al. (2013). "Reduced Susceptibility to Two-Stage Skin Carcinogenesis in Mice with Epidermis-Specific Deletion of Cd151." J Invest Dermatol.

Sadej, R., H. Romanska, G. Baldwin, et al. (2009). "CD151 Regulates Tumorigenesis by Modulating the Communication between Tumor Cells and Endothelium." Molecular Cancer Research **7**: 787-798.

Sadej, R., H. Romanska, D. Kavanagh, et al. (2010). "Tetraspanin CD151 Regulates Transforming Growth Factor Beta Signaling: Implication in Tumor Metastasis." Cancer Research **70**(14): 6059-6070.

Sagnak, L., H. Topaloglu, U. Ozok and H. Ersoy (2011). "Prognostic Significance of Neuroendocrine Differentiation in Prostate Adenocarcinoma." Clinical Genitourinary Cancer **9**(2): 73-80.

Sala-Valdés, M., N. Ailane, C. Greco, et al. (2012). "Targeting tetraspanins in cancer." Expert Opinion on Therapeutic Targets **16**(10): 985-997.

Salagierski, M. and J. A. Schalken (2012). "Molecular Diagnosis of Prostate Cancer: PCA3 and TMPRSS2:ERG Gene Fusion." The Journal of Urology **187**(3): 795-801.

Sanjmyatav, J., T. Steiner, H. Wunderlich, et al. (2011). "A Specific Gene Expression Signature Characterizes Metastatic Potential in Clear Cell Renal Cell Carcinoma." The Journal of Urology **186**(1): 289-294.

Sartor, A. O. (2011). "Progression of metastatic castrate-resistant prostate cancer: impact of therapeutic intervention in the post-docetaxel space." Journal of Hematology & Oncology **4**(1): 18.

Sauer, B. and N. Henderson (1989). "Cre-stimulated recombination at loxP-containing DNA sequences placed into the mammalian genome." Nucleic Acids Research **17**(1): 147-161.

Sauer, G., J. Windisch, C. Kurzeder, et al. (2003). "Progression of Cervical Carcinomas Is Associated with Down-Regulation of CD9 But Strong Local Re-expression at Sites of Transendothelial Invasion." Clinical Cancer Research **9**(17): 6426-6431.

Scheffer, K. D., A. Gawlitza, G. A. Spoden, et al. (2013). "Tetraspanin CD151 Mediates Papillomavirus Type 16 Endocytosis." Journal of Virology **87**(6): 3435-3446.

Schröder, F. H. (2008). "Screening for prostate cancer; an update on recent findings of the European Randomized Study of Screening for Prostate Cancer (ERSPC)." Urologic Oncology: Seminars and Original Investigations **26**(5): 533-541.

Schroder, F. H., J. Hugosson, M. J. Roobol, et al. (2009). "Screening and Prostate-Cancer Mortality in a Randomized European Study." N Engl J Med **360**(13): 1320-1328.

Schröder, F. H., J. Hugosson, M. J. Roobol, et al. (2012). "Prostate-Cancer Mortality at 11 Years of Follow-up." New England Journal of Medicine **366**(11): 981-990.

Schroder, F. H., P. van der Maas, P. Beemsterboer, et al. (1998). "Evaluation of the digital rectal examination as a screening test for prostate cancer. Rotterdam section of the European Randomized Study of Screening for Prostate Cancer." J. Natl. Cancer Inst. **90**(23): 1817-1823.

Segawa, N., I. Mori, H. Utsunomiya, et al. (2001). "Prognostic significance of neuroendocrine differentiation, proliferation activity and androgen receptor expression in prostate cancer." Pathology International **51**(6): 452-459.

Seigneuret, M., A. Delaguillaumie, C. Lagaudriere-Gesbert and H. Conjeaud (2001). "Structure of the Tetraspanin Main Extracellular Domain: a partially conserved fold with a structurally viable domain insertion." J. Biol. Chem. **276**(43): 40055-40064.

Sela, B., Z. Stwplewski and H. Koprowski (1989). "Colon Carcinoma-Associated Glycoproteins Recognized by Monoclonal Antibodies CO-029 and GA22-2." Hybridoma **8**(4): 481-491.

Shappell, S. B., G. V. Thomas, R. L. Roberts, et al. (2004). "Prostate Pathology of Genetically Engineered Mice: Definitions and Classification. The Consensus Report from the Bar Harbor Meeting of the Mouse Models of Human Cancer Consortium Prostate Pathology Committee." Cancer Res **64**(6): 2270-2305.

Sheng, K.-C., A. B. van Spriel, K. H. Gartlan, et al. (2009). "Tetraspanins CD37 and CD151 differentially regulate Ag presentation and T-cell co-stimulation by DC." European Journal of Immunology **39**(1): 50-55.

Shi, W., H. Fan, L. Shum and R. Derynck (2000). "The tetraspanin CD9 associates with transmembrane TGF-α and regulates TGF-α-induced EGF receptor activation and cell proliferation." Journal of Cell Biology **148**: 591-602.

Shiomi, T., I. Inoki, F. Kataoka, et al. (2005). "Pericellular activation of proMMP-7 (promatrilysin-1) through interaction with CD151." Lab Invest **85**(12): 1489-1506.

Siegel, R., D. Naishadham and A. Jemal (2012). "Cancer statistics, 2012." A Cancer Journal for Clinicians **62**(1): 10-29.

Silvie, O., E. Rubinstein, J. Franetich, et al. (2003). "Hepatocyte CD81 is required for Plasmodium falciparum and Plasmodium yoelii sporozoite infectivity." Nature Medecine **9**: 93-96.

Sincock, P. M., S. Fitter, R. G. Parton, et al. (1999). "PETA-3/CD151, a member of the transmembrane 4 superfamily, is localised to the plasma membrane and endocytic system of endothelial cells, associates with multiple integrins and modulates cell function." Journal of Cell Science **112**(6): 833-844.

Sincock, P. M., G. Mayrhofer and L. K. Ashman (1997). "Localization of the Transmembrane 4 Superfamily (TM4SF) Member PETA-3 (CD151) in Normal

Human Tissues: Comparison with CD9, CD63, and alpha5 beta1 Integrin." J. Histochem. Cytochem. **45**(4): 515-526.

Singer, S. J. and G. L. Nicolson (1972). "The fluid mosaic model of the structure of cell membranes." Science **175**(4023): 720-731.

Singethan, K., E. Topfstedt, S. Schubert, et al. (2006). "CD9-dependent regulation of Canine distemper virus-induced cell-cell fusion segregates with the extracellular domain of the haemagglutinin." The Journal of General Virology **87**: 1635-1642.

Sobel, R. E. and M. D. Sadar (2005). "Cell Lines Used in prostate cancer research: A Compendium of Old and New Lines-Part 1." The Journal of Urology **173**(2): 342-359.

Sobel, R. E. and M. D. Sadar (2005). "Cell Lines Used in prostate cancer research: A Compendium of Old and New Lines-Part 2." The Journal of Urology **173**(2): 360-372.

Soulie, M. (2008). "What is the Role of Surgery for Locally Advanced Disease?" European Urology Supplements **7**: 400-405.

Soyuer, S., I. Soyuer, D. Unal, et al. (2010). "Prognostic significance of CD9 expression in locally advanced gastric cancer treated with surgery and adjuvant chemoradiotherapy." Pathology - Research and Practice **206**(9): 607-610.

Spoden, G., L. Kühling, N. Cordes, et al. (2013). "The Human Papillomaviruses Type 16, 18, and 31 share similar endocytic requirements for entry." Journal of Virology.

Stamey, T., N. Yang, A. Hay, et al. (1987). "Prostate-specific antigen as a serum marker for adenocarcinoma of the prostate." The New England Journal of Medicine.

Staubach, S. and F.-G. Hanisch (2011). "Lipid rafts: signaling and sorting platforms of cells and their roles in cancer." Expert Review of Proteomics **8**(2): 263-277.

Steigler, A., J. Denham, D. Lamb, et al. (2012). "Risk Stratification after Biochemical Failure following Curative Treatment of Locally Advanced Prostate Cancer: Data from the TROG 96.01 Trial." Prostate Cancer **doi: 10.1155/2012/814724**(Epub 2012 Dec 24.).

Stephens, F. (2000). All About Prostate Cancer, Oxford University Press.

Sterk, L. M. T., C. A. W. Geuijen, J. G. van den Berg, et al. (2002). "Association of the tetraspanin CD151 with the laminin-binding integrins alpha3beta1, alpha6beta1, alpha6beta4 and alpha7beta1 in cells in culture and in vivo." Journal of Cell Science **115**(6): 1161-1173.

Stipp, C. S. (2010). "Laminin-binding integrins and their tetraspanin partners as potential antimetastatic targets." Expert Reviews in Molecular Medicine **12**(3).

Stipp, C. S., T. V. Kolesnikova and M. E. Hemler (2001). "EWI-2 Is a Major CD9 and CD81 Partner and Member of a Novel Ig Protein Subfamily." Journal of Biological Chemistry **276**(44): 40545-40554.

Stipp, C. S., D. Orlicky and M. E. Hemler (2001). "FPRP, a Major, Highly Stoichiometric, Highly Specific CD81- and CD9-associated Protein." Journal of Biological Chemistry **276**(7): 4853-4862.

Stricker, P. (2001). "Prostate cancer; Part 1. Issues in screeing and diagnosis." Medicine Today(July): 1-6.

Suva, L. J., C. Washam, R. W. Nicholas and R. J. Griffin (2011). "Bone metastasis: mechanisms and therapeutic opportunities." Nat Rev Endocrinol **7**(4): 208-218.

Suwa, T., A. Nyska, J. K. Haseman, et al. (2002). "Spontaneous Lesions in Control B6C3F1 Mice and Recommended Sectioning of Male Accessory Sex Organs." Toxicologic Pathology **30**(2): 228-234.

Suzuki, S., T. Miyazaki, N. Tanaka, et al. (2010). "Prognostic Significance of CD151 Expression in Esophageal Squamous Cell Carcinoma with Aggressive Cell Proliferation and Invasiveness." Annals of Surgical Oncology: 1-6.

Szala, S., Y. Kasai, Z. Steplewski, et al. (1990). "Molecular cloning of cDNA for the human tumor-associated antigen CO-029 and identification of related transmembrane antigens." Proceedings of the National Academy of Sciences **87**(17): 6833-6837.

Szmulewitz, R. Z. and E. M. Posadas (2007). "Antiandrogen therapy in prostate cancer." Update on Cancer Therapeutics **2** 119-131.

Taft, R. A., M. Davisson and M. V. Wiles (2006). "Know thy mouse." Trends in Genetics **22**(12): 649-653.

Takeda, T., N. Hattori, T. Tokuhara, et al. (2007). "Adenoviral Transduction of MRP-1/CD9 and KAI1/CD82 Inhibits Lymph Node Metastasis in Orthotopic Lung Cancer Model." Cancer Research **67**(4): 1744-1749.

Takeda, Y., A. R. Kazarov, C. E. Butterfield, et al. (2007). "Deletion of tetraspanin Cd151 results in decreased pathologic angiogenesis in vivo and in vitro." Blood **109**(4): 1524-1532.

Takeda, Y., Q. Li, A. R. Kazarov, et al. (2011). "Diminished metastasis in tetraspanin CD151 knockout mice." Blood **118**: 464-472.

Tanaka, M., K. Kuraoka, J. Sakane, et al. (2012). "Auto-analysis of immunohistochemical findings for breast cancer using specified software and virtual microscopy." Journal of Clinical Pathology **60**(3): 206-211.

Tang, Y., L. Wang, O. Goloubeva, et al. (2008). "Divergent Effects of Castration on Prostate Cancer in TRAMP Mice: Possible Implications for Therapy." Clinical Cancer Research **14**(10): 2936-2943.

Tang, Y., L. Wang, O. Goloubeva, et al. (2009). "The relationship of neuroendocrine carcinomas to anti-tumor therapies in TRAMP mice." The Prostate **69**(16): 1763-1773.

Tannock, I., R. de Wit and W. Berry (2004). " Docetaxel plus prednisone or mitoxantrone plus prednisone for advanced prostate cancer." New England Journal of Medecine **351**: 1502-1512.

Taylor, B. S., N. Schultz, H. Hieronymus, et al. (2010). "Integrative Genomic Profiling of Human Prostate Cancer." Cancer cell **18**(1): 11-22.

Testa, J. E., P. C. Brooks, J.-M. Lin and J. P. Quigley (1999). "Eukaryotic Expression Cloning with an Antimetastatic Monoclonal Antibody Identifies a Tetraspanin (PETA-3/CD151) as an Effector of Human TumorCell Migration and Metastasis." Cancer Research **59**(15): 3812-3820.

Tokuhara, T., H. Hasegawa, N. Hattori, et al. (2001). "Clinical significance of CD151 gene expression in non-small cell lung cancer." Clinical Cancer Research **7**: 4109-4114.

Tomita, K., A. van Bokhoven, G. J. L. H. van Leenders, et al. (2000). "Cadherin Switching in Human Prostate Cancer Progression." Cancer Research **60**(13): 3650-3654.

Tonoli, H. and J. C. Barrett (2005). "CD82 metastasis suppressor gene: a potential target for new therapeutics?" Trends in Molecular Medicine **11**(12): 563-570.

Tracey, E., D. Baker, W. Chen, et al. (2007). Cancer in New South Wales: Incidence, Mortality and Prevalence Report 2005. Sydney, New South Wales Department of Health.

Trotman, L., M. Niki, Z. Dotan, et al. (2003). "Pten dose dictates cancer progression in the prostate." PLoS Biology **1**(3): E59.

Trusolino, L. and P. Comoglio (2002). "Scatter-factor and semaphorin receptors: cell signalling for invasive growth." Nature Review Cancer **2**: 289-300.

Tsai, Y. C. and A. M. Weissman (2011). "Dissecting the diverse functions of the metastasis suppressor CD82/KAI1." FEBS Letters **585**(20): 3166-3173.

Tsujino, K., Y. Takeda, T. Arai, et al. (2012). "Tetraspanin CD151 Protects against Pulmonary Fibrosis by Maintaining Epithelial Integrity." American Journal of Respiratory and Critical Care Medicine **2**(186): 170-180.

Unternaehrer, J., A. Chow, M. Pypaert, et al. (2007). "The tetraspanin CD9 mediates lateral association of MHC class II molecules on the dendritic cell surface." Proceedings of the National Academy of Sciences **104**: 234-239.

Valastyan, S. and Robert A. Weinberg (2011). "Tumor Metastasis: Molecular Insights and Evolving Paradigms." Cell **147**(2): 275-292.

Valkenburg, K. and B. Williams (2011). "Mouse Models of Prostate Cancer." Prostate Cancer: 22.

van der Flier, A. and A. Sonnenberg (2001). "Function and interaction of integrins." Cell and Tissue Research **305**: 285-298.

van Oort, I. M., K. Tomita, A. van Bokhoven, et al. (2007). "The prognostic value of E-cadherin and the cadherin-associated molecules α-, β-, γ-catenin and p120ctn in prostate cancer specific survival: A long-term follow-up study." The Prostate **67**(13): 1432-1438.

Van Poppel, H., S. Joniau and K. Haustermans (2005). "Surgery alone for advanced prostate cancer?": 157-169.

van Soest, S., A. Westerveld, P. de Jong, et al. (1999). "Retinitis pigmentosa: defined from a molecular point of view." Survey of Ophthalmology **43**: 321-334.

Veenbergen, S. and A. B. van Spriel (2011). "Tetraspanins in the immune response against cancer." Immunology Letters **138**(2): 129-136.

Vogelstein, B. and K. Kinzler (2004). "Cancer genes and the pathways they control." Nature Medicine **10**: 789-799.

Voss, M. A., N. Gordon, S. Maloney, et al. (2011). "Tetraspanin CD151 is a novel prognostic marker in poor outcome endometrial cancer." Br J Cancer **104**(10): 1611-1618.

Wang, J.-C., L. R. Begin, N. G. Berube, et al. (2007). "Down-Regulation of CD9 Expression during Prostate Carcinoma Progression Is Associated with CD9 mRNA Modifications." Clinical Cancer Research **13**(8): 2354-2361.

Wang, Z. A. and M. M. Shen (2011). "Revisiting the concept of cancer stem cells in prostate cancer." Oncogene **30**(11): 1261-1271.

Waterhouse, R., C. Ha and G. S. Dveksler (2002). "Murine CD9 Is the Receptor for Pregnancy-specific Glycoprotein 17." The Journal of Experimental Medicine **195**(2): 277-282.

Wilt, T. J. (2012). "The Prostate Cancer Intervention Versus Observation Trial:VA/NCI/AHRQ Cooperative Studies Program #407 (PIVOT): Design and Baseline Results of a Randomized Controlled Trial Comparing Radical Prostatectomy With Watchful Waiting for Men With Clinically Localized Prostate Cancer." JNCI Monographs **2012**(45): 184-190.

Winterwood, N. E., A. Varzavand, M. N. Meland, et al. (2006). "A Critical Role for Tetraspanin CD151 in alpha3beta1 and alpha6beta4 Integrin-dependent Tumor Cell Functions on Laminin-5." Molecular Biology of the Cell **17**(6): 2707-2721.

Wright, M. and M. Tomlinson (1994). "The ins and outs of the transmembrane 4 superfamily." Immunology Today **15**: 588-594.

Wright, M. D., S. M. Geary, S. Fitter, et al. (2004). "Characterization of Mice Lacking the Tetraspanin Superfamily Member CD151." Molecular Cell Biology **24**(13): 5978-5988.

Wright, M. D., K. J. Henkle and G. F. Mitchell (1990). "An immunogenic *M*, 23,000 intergral membrane protein of Schistosoma mansoni worms that closely resembles a human tumour associated protein." Journal Immunology **144**: 3195-3200.

Yamada, M., Y. Tamura, N. Sanzen, et al. (2008). "Probing the interaction of tetraspanin CD151 with integrin α3β1 using a panel of monoclonal antibodies with distinct reactivities toward the CD151–integrin α3β1 complex." Biochem J **415**(3): 417-427.

Yamamoto, H., A. Vinitketkumnuen, Y. Adachi, et al. (2004). "Association of matrilysin-2 (MMP-26) expression with tumor progression and activation of MMP-9 in esophageal squamous cell carcinoma." Carcinogenesis **25**(12): 2353-2360.

Yanez-Mo, M., R. Tejedor, P. Rousselle and F. Sanchez-Madrid (2001). "Tetraspanins in intercellular adhesion of polarized epithelial cells: spatial and functional relationship to integrins and cadherins." Journal of Cell Science **114**: 577-587.

Yang, W., P. Li, J. Lin, et al. (2012). "CD151 promotes proliferation and migration of PC3 cells via the formation of CD151-integrin α3/α6 complex." Journal of Huazhong University of Science and Technology -- Medical Sciences -- **32**(3): 383-388.

Yang, X., C. Claas, S. Kraeft, et al. (2002). "Palmitoylation of tetraspanin proteins:modulation of CD151 lateral interacts, subcellular distribution, and integrin-dependent cell morphology." Molecular Biology of the Cell **13**: 767-781.

Yang, X., O. V. Kovalenko, W. Tang, et al. (2004). "Palmitoylation supports assembly and function of integrins-tetraspanin complexes." The Journal of Cell Biology **167**(6): 1231-1240.

Yang, X. H., A. L. Richardson, M. I. Torres-Arzayus, et al. (2008). "CD151 Accelerates Breast Cancer by Regulating Alpha 6 Integrin Function, Signaling, and Molecular Organization." Cancer Research **68**(9): 3402-3213.

Yang, Y.-M., Z.-W. Zhang, Q.-M. Liu, et al. (2013). "Overexpression of CD151 Predicts Prognosis in Patients with Resected Gastric Cancer." PLoS ONE **8**(3).

Yauch, R., A. Kazarov, B. Desai, et al. (2000). "Direct extracellular contact between integrin alpha 3 beta 1 and TM4SF protein CD151." Journal of Biological Chemistry **275**: 9230-9238.

Yauch, R. L. and M. E. Hemler (2000). "Specific interactions among transmembrane 4 superfamily (TM4SF) proteins and phosphoinositide 4-kinase." Biochem. J. **351**(3): 629-637.

Yoo, S. H., K. Lee, J. Y. Chae and K. C. Moon (2011). "CD151 expression can predict cancer progression in clear cell renal cell carcinoma." Histopathology **58**(2): 191-197.

Yue, S., W. Mu and M. Zöller (2013). "Tspan8 and CD151 promote metastasis by distinct mechanisms." European Journal of Cancer.

Yunta, M. and P. A. Lazo (2003). "Tetraspanin proteins as organisers of membrane microdomains and signalling complexes." Cellular Signalling **15**(6): 559-564.

Zemni, R., T. Bienvenu, M. Vinet, et al. (2000). "A new gene involved in X-linked mental retardation identified by analysis of an X;2 balanced translocation." Nature Genetics **24**: 167-170.

Zevian, S., N. E. Winterwood and C. S. Stipp (2010). "Structure-Function Analysis of Tetraspanin CD151 Reveals Distinct Requirements for Tumor Cell Behaviors Mediated by Î±3Î²1 versus Î±6Î²4 Integrin." Journal of Biological Chemistry **286**(9): 7496-7506.

Zhang, J., J. Dong, H. Gu, et al. (2012). "CD9 Is Critical for Cutaneous Wound Healing through JNK Signaling." J Invest Dermatol **132**(1): 226-236.

Zhang, X. A., A. L. Bontrager and M. E. Hemler (2001). "Transmembrane-4 Superfamily Proteins Associate with Activated Protein Kinase C (PKC) and Link PKC to Specific beta 1 Integrins." J. Biol. Chem. **276**(27): 25005-25013.

Zhang, X. A., A. R. Kazarov, X. Yang, et al. (2002). "Function of the Tetraspanin CD151–α6β1 Integrin Complex during Cellular Morphogenesis." Molecular Biology of the Cell **13**(1): 1-11.

Zhang, X. A., W. S. Lane, S. Charrin, et al. (2003). "EWI2/PGRL Associates with the Metastasis Suppressor KAI1/CD82 and Inhibits the Migration of Prostate Cancer Cells." Cancer Research **63**(10): 2665-2674.

Zhang, Z., L. Zhang, Y. Hua, et al. (2010). "Comparative proteomic analysis of plasma membrane proteins between human osteosarcoma and normal osteoblastic cell lines." BMC Cancer **10**(1): 206.

Zheng, R., S. Yano, H. Zhang, et al. (2005). "CD9 overexpression suppressed the liver metastasis and malignant ascites via inhibition of proliferation and motility of small-cell lung cancer cells in NK cell-depleted SCID mice." Oncology research **15**(7-8): 365-372.

Zhu, G.-H., C. Huang, Z.-J. Qiu, et al. (2010). "Expression and Prognostic Significance of CD151, c-Met, and Integrin alpha3/alpha6 in Pancreatic Ductal Adenocarcinoma." Digestive Diseases and Sciences: 1-9.

Zijlstra, A., J. Lewis, B. DeGryse, et al. (2008). "The Inhibition of Tumor Cell Intravasation and Subsequent Metastasis via Regulation of In Vivo Tumor Cell Motility by the Tetraspanin CD151." Cancer Cell **13**(3): 221-234.

Zoller, M. (2009). "Tetraspanins: push and pull in suppressing and promoting metastasis." Nat Rev Cancer **9**(1): 40-55.

Zou, Q., L. Xiong, Z. Yang, et al. (2012). "Expression levels of HMGA2 and CD9 and its clinicopathological significances in the benign and malignant lesions of the gallbladder." World Journal of Surgical Oncology **10**(1): 92.

Zvieriev, V., J.-C. Wang and M. Chevrette (2005). "Over-expression of CD9 does not affect in vivo tumorigenic or metastatic properties of human prostate cancer cells." Biochemical and Biophysical Research Communications **337**(2): 498-504.